Evidence-Based Complementary and Alternative Medicine

Toxic versus Therapeutic Effects of Natural Products on Reproductive Disorders

Lead Guest Editor: Arielle Cristina Arena
Guest Editors: Candida Kassuya, Glaura Fernandes, and Wellerson Scarano

Toxic versus Therapeutic Effects of Natural Products on Reproductive Disorders

Evidence-Based Complementary and Alternative Medicine

Toxic versus Therapeutic Effects of Natural Products on Reproductive Disorders

Lead Guest Editor: Arielle Cristina Arena
Guest Editors: Candida Kassuya, Glaura Fernandes, and Wellerson Scarano

Editorial Board

Contents

Hindawi
Evidence-Based Complementary and Alternative Medicine
Volume 2019, Article ID 9791506, 2 pages
https://doi.org/10.1155/2019/9791506

Editorial

Toxic versus Therapeutic Effects of Natural Products on Reproductive Disorders

Arielle Cristina Arena,[1] **Cândida Aparecida Leite Kassuya**,[2] **Glaura Scantamburlo Alves Fernandes**,[3] **and Wellerson Rodrigo Scarano**[1]

[1]*Universidade Estadual Paulista, São Paulo, Brazil*
[2]*Universidade Federal da Grande Dourados, Dourados, Brazil*
[3]*Universidade Estadual de Londrina, Londrina, Brazil*

Correspondence should be addressed to Arielle Cristina Arena; arielle.arena@unesp.br

Received 5 November 2019; Accepted 6 November 2019; Published 18 November 2019

The idea for this special issue emerged from increased interest in alternative therapies, especially the use of products of natural origin, for the prevention and/or treatment of reproductive disorders. However, natural products can also negatively affect male and female reproductive tracts; if the exposure occurs before and after the conception, it can affect parents as well as the offspring. Since studies focusing on the toxic versus therapeutic effects of natural products on reproductive disorders are still scarce, the purpose of this special issue is to show therapeutic effects as well detecting potential reproductive health hazards of natural products. For this special issue, researchers from different countries were invited to contribute with original research and review articles. After the review process, 12 high-quality papers were accepted for publication. The main topics addressed in this special issue include the therapeutic effects of natural products on male or female reproductive disorders, the toxicity of natural products on the male reproductive tract, and embryotoxicity and teratogenic effects of natural products. A summary of all accepted articles is provided below.

Some papers have focused on studying the benefits of natural products to treat male reproductive disorders. J. Wang and colleagues have demonstrated that Shengjing capsules (Chinese herbal medicine) could be an important therapeutic medicine for the treatment of nonobstructive azoospermia (NOA). The authors have proposed a mechanism associated with the PI3K/AKT pathway modulation to activate spermatogonial stem cells in the NOA rats. These findings provide new insights for the treatment of NOA. In another paper, Z. Zhu and colleagues have shown the beneficial effects of a water-soluble polysaccharide extracted from *Morinda officinalis* (MOP) on varicocele rats. The results of this study have demonstrated that MOP treatment improved the sperm parameters in varicocele rats through the angiogenesis inhibition in testes and a relative upregulation of a VEGF (specific mitogen of vascular endothelial cells) and MMP-9 (the primary mediators of extracellular matrix degradation).

S. M. Ezzat and colleagues have studied the mechanisms by which the *Eurycoma longifolia*, a well-recognized aphrodisiac herb, improves the erectile dysfunction, using an in vitro model. The authors have observed that the aqueous extract of *Eurycoma longifolia* inhibited the ROCK-II activity, leading to contraction of smooth muscle. These findings revealed important insights about the role of this species in male sexual disorders. Still, on the same subject, P. M. Kameni and coauthors have investigated the suppressive effect of *Nymphaea lotus* (a species used as an aphrodisiac, astringent, and anti-inflammatory) on erectile dysfunction induced by nitric oxide deficiency in rats. The results revealed that this species could be an excellent candidate for the treatment of erectile dysfunction.

In another paper, S. M. Ezzat and colleagues have studied the in vivo effects of aqueous extract of *Eurycoma longifolia* on male reproductive functions and the brain cortical and

hippocampal content of dopamine, serotonin, and noradrenaline. The authors have confirmed the aphrodisiac and anabolic activities of the extract in male rats, meaning the effects were attributed to an increase of testosterone level as well as enhancement of brain cortical and hippocampal dopamine content.

The paper by J. Park and colleagues has reported that the Aconiti Lateralis Radix Preparata (AL) can be a therapeutic alternative for the treatment of benign prostatic hyperplasia (BPH). In this study, the treatment with AL ameliorated pathological proliferation in the prostate as well as decreased the two main factors associated with the BPH pathogenesis. Additionally, AL effects did not cause testicular apoptosis, a common adverse effect caused by finasteride, a reference drug used to treat BPH. These results suggest AL as a potential therapeutic agent for BPH treatment.

S. Li and colleagues presented some aspects of male reproductive toxicity of natural products. In this review, the authors have reported that several toxic compounds present in natural products could be used for therapeutic purposes. Some substances that are spermatotoxic may be useful for contraception at therapeutic dosage.

Other papers have focused on studying the therapeutic effects of natural products on female reproductive disorders. C. H. Wu and colleagues have investigated the mechanisms by which the herbal formula B401, widely used in Taiwan, may relieve the symptoms associated with menopause. The treatment with herbal formula B401 in ovariectomized mice confirmed the usefulness of this supplement for alleviating discomfort symptoms in middle-aged women. Y. Wang and coauthors have evaluated the effects of the polysaccharides of *Fructus corni* on ovarian functions in naturally aging female mice. The obtained data demonstrated that this compound improved the ovarian function in aging-associated perimenopause symptoms, indicating that this natural product can be a promising therapeutic alternative for symptoms associated with menopause.

In an in vitro study, Q. Zhou and colleagues have studied the efficacy of formononetin, an isolated ingredient from *Astragalus membranaceus*, in improving the tumoricidal effect of everolimus, an inhibitor of serine-threonine kinase mammalian target of rapamycin with broad antitumor activities. The results showed that the combination treatment of formononetin plus everolimus might be an effective approach for breast cancer chemotherapy. In another paper, X. Mao and colleagues have investigated a new alternative for the treatment of cervicitis, a common sexually transmitted disease, in a mouse model. To this end, the Feilin Vaginal Gel (FVG), a Chinese herbal formula, was tested and the obtained results demonstrated that the FVG might be an alternative for the treatment of cervicitis.

A. A. Alafiatayo and colleagues have assessed the effects of *Curcuma longa* extract, a Southeast Asia traditional medicine, on embryotoxicity and teratogenic effects in Zebrafish. The obtained findings showed that the extract has potential specific toxic effects on embryos and larvae development, especially at a higher dosage, indicating that *Curcuma longa* needs further investigation.

We hope that this special issue can be *really special* for scientists studying the effects of natural products as an alternative medicine, as well as their possible adverse effects focusing on the reproductive system.

Conflicts of Interest

The editors declare that they have no conflicts of interest regarding the publication of this special issue.

Acknowledgments

The editors would like to thank all authors who have contributed their original research articles and reviews to this special issue. A special thank is made to the reviewers and to the journal managers and staff.

Arielle Cristina Arena
Cândida Aparecida Leite Kassuya
Glaura Scantamburlo Alves Fernandes
Wellerson Rodrigo Scarano

Hindawi
Evidence-Based Complementary and Alternative Medicine
Volume 2019, Article ID 8494567, 11 pages
https://doi.org/10.1155/2019/8494567

Research Article

Shengjing Capsule Improves Spermatogenesis through Upregulating Integrin $\alpha 6/\beta 1$ in the NOA Rats

Jiamin Wang,[1] Shankun Zhao,[1] Lianmin Luo,[1] Yangzhou Liu,[1] Ermao Li,[2] Zhiguo Zhu,[1] and Zhigang Zhao[1]

[1]*Department of Urology & Andrology, Minimally Invasive Surgery Center, Guangdong Provincial Key Laboratory of Urology, The First Affiliated Hospital of Guangzhou Medical University, Guangzhou, Guangdong, China*
[2]*Research Laboratory for Clinical & Translational Medicine, Medical School, University of South China, Hengyang 421001, China*

Correspondence should be addressed to Zhigang Zhao; zgzhaodr@126.com

Received 16 April 2019; Revised 11 June 2019; Accepted 25 July 2019; Published 22 August 2019

Guest Editor: Arielle Cristina Arena

Objective. To evaluate the therapeutic effect of Shengjing capsules on nonobstructive azoospermia (NOA) in the rat model. *Methods*. Twenty-five male Sprague–Dawley rats were randomly divided into five groups as follows ($n = 5$ per group): normal group, NOA group, and three Shengjing capsule treatment groups (low-dose, medium-dose, and high-dose groups, respectively). HE staining and semen smear were performed to assess sperm quality. The expression levels of PI3K/AKT and integrin $\alpha 6/\beta 1$ were measured by qRT-PCR and western blot analyses. *Results*. In the NOA group, almost all of the seminiferous tubules were vacuolated with a thin layer of basal compartment containing some spermatogonial stem cells. The counts of sperms in the NOA group were strongly lower than those of the normal group ($P = 0.0001$). The expression of PI3K/AKT and integrin $\alpha 6/\beta 1$ was scarcely expressed in the NOA group. All indexes mentioned above were significantly different from those of the medium- and high-dose groups ($P = 0.001$, all). The sperm count of rats treated with Shengjing capsules was significantly higher than that of the NOA group ($P = 0.0001$). The rats of Shengjing capsule groups had more layers of spermatogonial stem cells and spermatocytes, and some had intracavitary sperms. *Conclusions*. Shengjing capsules may be a promising therapeutic medicine for NOA. The underlying mechanisms might involve activating SSCs by upregulating the integrin $\alpha 6/\beta 1$ expression via the PI3K/AKT pathway.

1. Introduction

Infertility hampers about 15% of couples attempting pregnancy, and male factor infertility accounts for approximately half of all the reasons of this impaired fecundity [1]. The incidence of infertility is increasing year by year, and it has grown up to be a global health problem. Azoospermia, the medical condition that men do not have any measurable level of spermatozoa in their semen, is an extremely important contributor to male infertility. And nonobstructive azoospermia (NOA) is a more complicated infertility syndrome, with the azoospermia being secondary to a failure to produce sperm. NOA, commonly referred to as testicular failure, is classified into three subtypes on the basis of histopathological examination of testicular tissue, including hypospermatogenesis (HS), maturation arrest (MA), and Sertoli cell-only (SCO) syndrome [2]. Almost 10% of infertile men suffer from NOA. NOA is one of the most difficult conditions to treat. Microdissection testicular sperm extraction (micro-TESE) is the most common treatment for NOA [3]. However, 50–60% of the micro-TESE treatments failed to retrieve spermatozoa.

In recent years, many techniques, including spermatogonial stem cell (SSC) transplantation, testis tissue transplantation, and induced pluripotent stem cell and gene therapy, have emerged and developed. Intracytoplasmic sperm injection (ICSI) has also been improved, increasing the chances for men to father a child. However, the effective treatment for NOA patients is absent. Thus, it is urgently needed to find an efficient and feasible therapy.

NOA is characterized by severely impaired or nonexistent spermatogenesis [4]. This suggests that the improvement of

NOA can be achieved by improving spermatogenesis. Spermatogenesis is a complex process that requires about 64 days in rats and 74 days in humans [5]. Sperm originates from SSCs, which are vitally crucial for spermatogenesis and male reproduction. SSCs serve as a basis for spermatogenesis throughout adult life by undergoing self-renewal and providing progeny cells that differentiate into spermatozoa [6, 7]. OCT4, MHC I, C-kit, α6-integrin, and β1-integrin are useful immunohistochemical staining markers of cell populations, which are highly expressed in stem cells. Especially, α6-integrin and β1-integrin were recognized as marker molecules on SSCs [8, 9].

The use of traditional Chinese herbal medicine to improve testicular spermatogenesis has been in China for more than 2,000 years. Shengjing capsules are made up of a variety of medicinal materials that improve sperm production, such as ginseng, *Cordyceps sinensis*, *Epimedium*, and medlar [10–14]. *Panax ginseng* extracts have shown significant improvements in sperm concentrations and motility in semen analysis from a randomized controlled trial [10]. Park et al. [11] reported that *Panax ginseng* plays an important role in improving sperm hyperactivation via the cation channel of the sperm protein gene expression. *Lycium barbarum* (*L. barbarum*), also named wolfberry, obviously has the protective effect on the spermatogenesis of rats with the impaired reproduction system induced by cyclophosphamide [12]. Icariin, the most metabolically active extract of *Epimedium*, has been proved to improve endothelial cell function in the penis and promote the formation of NO [13]. Additionally, *Cordyceps militaris* extracts significantly enhanced the sperm production at the end of the first month and peaked it at the second month [14]. Since its introduction in 2005, the Shengjing capsule is widely used clinically to improve male infertility due to poor semen quality [15]. Shengjing capsules also can improve spermatogenesis ability to improve oligozoospermia [16–18]. The safety of this medicine has been confirmed by clinical use. Shengjing capsules do not relieve obstruction in OA patients. In summary, Shengjing capsule can improve the quality of semen in patients with OA, although it can not relieve the obstruction. This requires more research with a higher level of evidence to support.

Shengjing capsules have the potential to improve NOA spermatogenesis, but their mechanism is not yet clear. We have for the first time explained that Shengjing capsules can upregulate the α6/β1 expression by the PI3K pathway to activate SSCs and improve the therapeutic effect of spermatogenic function on NOA rats.

2. Materials and Methods

2.1. Formula and Preparation. Shengjing capsule extracts, provided by Liao Yuan He Tang Pharmaceutical Co., Ltd. (Zunyi, China), were officially approved in the treatment of male infertility and asthenospermia by the State Food and Drug Administration of P.R. China (SFDA) (standard number WS-11457(ZD-1457)-2002-2011Z; national drug approval Z20027672). The Shengjing capsule manufacturer recommends 504 mg/day for pharmacological research in rats. Meanwhile, in the dose conversion between animals and humans, the US Food and Drug Administration guidance for industries [19] recommended the dose conversion coefficient of rats to be 6.2, and after conversion, the dosage for rats was close to 504 mg/day. Thus, based on its relative equivalent dose of 4.8 g/day in a 60 kg man, 504 mg/kg of the Shengjing capsule was selected in this study (4800 mg/60 kg $*$ 6.2$\approx$504 mg/kg·day). The main active principles of Shengjing capsules are displayed in Table 1. In order to ensure the experimental quality, the experimental Shengjing capsule was dissolved in distilled water to prepare the designated Shengjing capsule concentrations.

2.2. Animals and Experimental Design. Twenty-five male SPF Sprague–Dawley rats (weight 120–140 g, 49–51 days old) were purchased from Guangdong Medical Laboratory Animal Center (Laboratory Animal License Number SYXK (Yue) 2013-0093). The animal room was kept under 12-hour light/dark cycles and maintained at $20 \pm 2^{\circ}$C with 45%–65% relative humidity. The animals had free access to food and water. All the rats were randomly divided into five groups (five rats each): (1) the normal group: the rats were treated daily with distilled water (2 ml) by oral gavage; (2) the NOA group: the rats underwent an NOA modeling, which was conducted by intraperitoneally injecting busulfan 10 mg/kg on day 1 and day 21, as reported previously [20]. At 35 days after second busulfan injection, azoospermia was confirmed in these rats. The NOA rats were treated daily with distilled water (2 ml) by gavage; and (3) the three Shengjing treatment groups: the NOA rats were treated daily with a (a) high dose of Shengjing capsules (1008 mg/kg), (b) medium dose of Shengjing capsules (504 mg/kg), or (c) low dose of Shengjing capsules (252 mg/kg) by gavage. The Shengjing capsules were dissolved in distilled water (2 ml). Intragastric gavage was for 8 weeks, and the body weight of each animal was registered every week. After that, the rats were anesthetized. We obtained the specimens from the rats for tests of corresponding indexes. The rat's testes and epididymides were weighted to get their organ indexes.

All experimental protocols were subject to approval by the Institutional Animal Care and Use Committee of the First Affiliated Hospital of Guangzhou Medical University (Guangzhou, China).

2.3. Sperm Count. To determine the sperm morphology, the animals were sacrificed after anesthesia. Then, the cauda epididymides of all animals were quickly transferred, and epididymal fluid was observed in the polarizing microscope. Then, they were minced in 10 mL prewarmed 0.9% normal saline to incubate at 37°C for 10 minutes that allowed sperm to swim out of the lumen of the cauda epididymides for sperm characteristic analysis.

The sperm count was determined using the haemocytometer under light microscope. A cover slip was placed on the haemocytometer before a 10 μl drop of caudal epididymal sperm solution was loaded under the cover slip. The

Table 1: Main active principles of Shengjing capsules.

Formula	Percentage
Lu Rong (Pilose Antler)	10.53
Gou Qi Zi (*Lycium barbarum*)	10.53
Ren Shen (*Panax ginseng*)	10.53
Dong Chong Xia Cao (*Cordyceps sinensis*)	10.53
Yin Yang Huo (*Epimedium* herb)	10.53
Sha Wan Zi (*Astragalus complanatus*)	5.26
Tu Si Zi (Semen Cuscutae)	5.26
Huang Jing (Rhizoma Polygonati)	5.26
He Shou Wu (*Polygonum multiflorum*)	5.26
Sang Shen (mulberry)	2.63
Bu Gu Zhi (*Psoralea corylifolia*)	2.63
Gu Sui Bu (Rhizoma Drynariae)	2.63
Xian Mao (*Curculigo orchioides*)	2.64
Jin Ying Zi (*Rosa laevigata* Michx.)	2.63
Fu Pen Zi (*Rubus chingii*)	2.63
Du Zhong (*Eucommia ulmoides*)	2.63
Da Xue Teng (*Sargentodoxa cuneata*)	2.63
Ma Bian Cao (*Verbena officinalis*)	2.63
Yin Xing Ye (*Ginkgo biloba* leaves)	2.63

haemocytometer was placed under the light microscope and viewed under ×400 magnification. The sperm count was calculated by counting 4×4 squares (horizontally or vertically) [21].

2.4. Histological Examination and Morphological Changes of Seminiferous Tubules. An abdominal incision was made, both sides of testes were dissected out, and part of them were fixed in Bouin's fixative for histological investigations and subsequently embedded in paraffin. The embedded tissues were cut into 4 μm thicknesses. Then, tissue sections were deparaffinized in xylene and hydrated in descending concentrations of ethanol before hematoxylin and eosin (HE) staining. Morphological changes were observed under a microscope, for example, the morphology of convoluted tubules, the presence of vacuolization, and the death and degeneration of SSCs and spermatocytes. For histomorphometric analyses, cells were recorded in 50 random seminiferous tubules to compare the differences in average cell numbers among the five groups.

2.5. Quantitative Reverse Transcription-Polymerase Chain Reaction (qRT-PCR). Expression levels of α6-integrin and β1-integrin mRNA in five groups were assayed by qRT-PCR analysis in accordance with the protocol [22]. The comparative Ct method was utilized to calculate the relative changes on the real-time PCR system. The primer sequences are summarized in Table 2.

2.6. Protein Extraction and Western Blot Analysis. Total protein was extracted from testicular tissue. Western blot analysis was conducted as previously published by our laboratory [22]. The membrane was incubated with Anti-Integrin α6 (1 : 2000 dilution; ab181551, Abcam), Anti-Integrin β1 (1 : 2000 dilution; ab179471, Abcam), phospho-Akt polyclonal rabbit antibody at a dilution of 1 : 2000 (ab81283, Abcam), and phosphoinositide 3-kinase (PI3K) at a dilution of 1 : 2000 (4257, CST) overnight at 4°C and incubated with anti-rabbit IgG horseradish peroxidase conjugated secondary antibodies (1 : 3000 dilution; ab136817, Abcam). The relative protein expression was normalized with GAPDH (1 : 3000 dilution; ab8245, Abcam).

2.7. Immunohistochemistry. Testicular tissue section slides in five groups were heated at 60°C for approximately 1 hour in a hot air oven. Then, they were deparaffinized in xylene and rehydrated using alcohol gradient. The antigen retrieval process was performed. Then, they were cooled to room temperature. The primary antibodies used were p-Akt (ab81283, Abcam) at a 1 : 200 dilution, Anti-Integrin α6 (1 : 200 dilution; ab181551, Abcam), and Anti-Integrin β1 (1 : 500 dilution; ab179471, Abcam). After stained according to the standard immunohistochemical protocol, immunoreactivity was evaluated by assessing positive cell percentages and staining intensities. The percentage scoring of immunoreactive cells was as follows: 0 (0–5%), 1 (6–25%), 2 (26–50%), 3 (51–75%), and 4 (>75%). The staining intensity was visually scored and stratified as follows: 0 (negative), 1 (weak), 2 (moderate), and 3 (strong). A final immunoreactivity score (IRS) was obtained for each case, multiplying the percentage and the intensity score.

2.8. Statistical Analysis. SSPS 13.0 software (SPSS, Chicago, IL, USA) was utilized to analyze the experimental data. All experiments were performed more than three times, the data of this research were described as means standard deviations (SDs), and comparisons were performed using Student's *t*-tests. The one-way ANOVA was done for comparison among different groups. $P < 0.05$ was examined statistically significant.

3. Results

3.1. Body Weights and Tissue Weights of Testis and Epididymis. The initial body weight did not differ significantly among the five groups ($P > 0.05$). After Shengjing capsule treatment, we weighted body, testicular, and epididymal weights to establish the declining trend of spermatogenesis. As shown in Table 3, testicular and epididymal weights of two sides of the rats from the NOA group reduced significantly (48.6% and 62.2%; $P = 0.0001$ for both) in comparison with the normal group. In Shengjing treatment groups, the testicular and epididymal weights in the medium-dose group increased significantly ($P = 0.001$ for all) compared to the NOA group. Similarly, there was a significant improvement in testicular and epididymal weights in the high-dose group compared to the NOA group ($P = 0.0001$ for all). No significant differences were detected in these data between the NOA group and low-dose group ($P = 0.957$ and $P = 0.293$). No obvious difference in body weight was proved among the five groups. The findings

Table 2: Primers used for detection of the mRNA expression by RT-PCR.

Gene	Sequences	
	Forward	Reverse
GAPDH	AGGTCGGTGTGAACGGATTTG	GGGGTCGTTGATGGCAACA
ITGA6	GTTGTGCTTGCTCTACCTGTCC	GCGAGCGAGAAGCCGAAGAG
ITGB1	GAATGGAGTGAATGGGACAGGAG	CAGATGAACTGAAGGACCACCTC
DND1	CTCCCTCTTAGCTTGAACCGACG	ACTCCACAGCCACCTGCTCT

ITGA6 = α6-integrin; ITGB1 = β1-integrin.

Table 3: Organ weight information in different groups.

(g)	Normal group	NOA group	Low-dose group	Medium-dose group	High-dose group
Body weight	515.56 ± 1.77	514.22 ± 13.79	514.43 ± 12.75	513.91 ± 27.61	515.64 ± 27.79
Weights of testis	2.90 ± 0.35	1.49 ± 0.14*	1.60 ± 0.17	2.20 ± 0.40*	2.34 ± 0.22*
Weights of epididymis	1.11 ± 0.07	0.42 ± 0.03**	0.44 ± 0.37	0.80 ± 0.16**	0.82 ± 0.35**

Two sides of testes were weighted together as well as the epididymides (five rats per group). *$P < 0.05$; **$P < 0.01$ (one-way ANOVA for comparison among different groups).

presented here suggested a beneficial effect of Shengjing capsules on spermatogenesis in the NOA rats.

3.2. Sperm Counts and Sperm Quality. We examined sperm counts to evaluate the therapeutic efficacy of Shengjing capsules on spermatogenesis by epididymal fluid smear examination. As shown in Figure 1, under the polarizing microscope, the NOA group had less sperms, while the sperm count of the normal group was all over the horizon. There were a few sperms in the low-dose group, while the sperm counts of the medium-dose group and high-dose group have increased with different degrees. There was a similar trend, as shown in Table 4, when we quantitated the counts of sperms. The counts of sperms in the NOA group were strongly lower than those in the normal group ($P = 0.0001$; Table 4; Figure 1), while the counts in the medium-dose group and high-dose group were significantly higher than those in the NOA group ($P = 0.0001$; Table 4; Figure 1). Sperms in the low-dose group also increased when compared with the NOA group ($P = 0.034$; Table 4; Figure 1).

3.3. Histological Morphology of Spermatogenesis. We analyzed the histology of the seminiferous tubules after Shengjing capsule treatment. In the normal group, layers of germ cells, spermatogonia, and spermatocytes were clearly defined, and sperm cells were observed in the lumen of the tubules. However, after double dose of busulfan, spermatogonia and spermatocytes appeared vacuolated, resulting in disturbed seminiferous tubular layers and disappearance of spermatogonia, spermatocytes, and spermatids. In the NOA group, they were manifested by atrophy and sparse arrangement of contorted seminiferous tubules. Almost all of the seminiferous tubules across the section were vacuolated with a thin layer of basal compartment containing Sertoli cells and some SSCs. In the low-dose group, part of seminiferous tubules across the section had a thin layer of SSCs and spermatocytes without sperm cells. In medium- and high-dose groups, there were more layers of SSCs and spermatocytes, part of which had intracavitary sperms. The incidence of spermatogenesis hypofunction gradually decreased as the dosage of Shengjing capsule increased, which meant that the therapeutic efficacy and dosage were closely interrelated. Fifty seminiferous tubules in the medium-dose group and high-dose group were counted, and there were 214.40 ± 6.69 cells and 219.60 ± 12.64 cells after increase, respectively, compared to 63.20 ± 4.97 cells in the NOA group ($P = 0.0001$ for both; Figure 2).

3.4. Expression of Integrin α6/β1. In this study, quantitative RT-PCR and western blot results showed that α6-integrin and β1-integrin were significantly downregulated in the NOA group compared with the normal group. This finding reflected the loss of spermatozoa and fertility. The PCR results were verified by western blot. The expression of integrin α6/β1 declined significantly in the NOA group compared with the normal group (Figure 3). In Shengjing treatment group, the integrin α6/β1 expression significantly increased in the medium-dose and high-dose groups compared with the NOA group, while there was no statistical significance in the low-dose group (Figures 3(a), 3(b), 3(e), and 3(f); $P < 0.01$ for all). Furthermore, densitometric analysis of the western blotting bands revealed that values of α6-integrin were 0.40, 0.59, 1.23, and 1.27 for NOA and low-, medium-, and high-dose groups, respectively (Figure 3(e)). The expression values of β1-integrin were 0.23, 0.53, 1.02, and 1.11 for NOA and low-, medium-, and high-dose groups, respectively (Figure 3(f)). Compared with the NOA group, the expression level of α6-integrin increased by 2.08-fold and of β1-integrin by 1.92-fold in the medium-dose group ($P < 0.01$ for both; Figure 3). The results of PCR demonstrated that no significant difference was found in the expression level of DND1 among the five groups (Figure 3(c); $P > 0.05$ for all).

Immunohistochemistry was performed to assess the integrin α6/β1 expression in the SSCs (Figures 4 and 5). The mean staining intensity of α6-integrin was significantly lower in the NOA group than that in the normal group (0.00 ± 0.00 versus 10.60 ± 1.95; $P = 0.0001$; Figure 4). The staining intensity was significantly stronger in medium-dose and high-dose groups than that in the NOA group ($P = 0.002$ and $P = 0.0001$). Similar results were presented for β1-integrin (Figure 5).

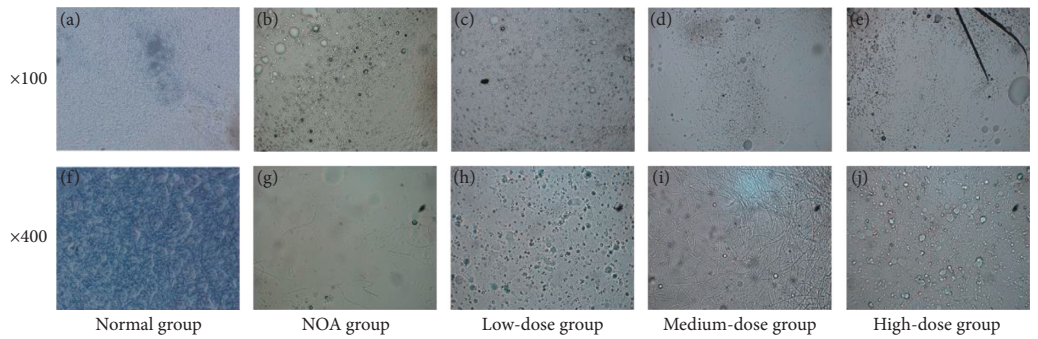

Figure 1: Sperm counts of five groups.

Table 4: Sperm analysis information in different groups.

Sperm analysis	Normal group (10^6/mL)	NOA group (10^2/mL)	Low-dose group (10^2/mL)	Medium-dose group (10^6/mL)	High-dose group (10^6/mL)
Sperm count	63.76 ± 3.22	5.49 ± 1.34	$14.18 \pm 4.17^{*}$	$5.71 \pm 3.81^{***}$	$7.28 \pm 5.32^{***}$

There were five rats per group. $^{*}P < 0.05$; $^{***}P < 0.0001$ (one-way ANOVA for comparison among different groups).

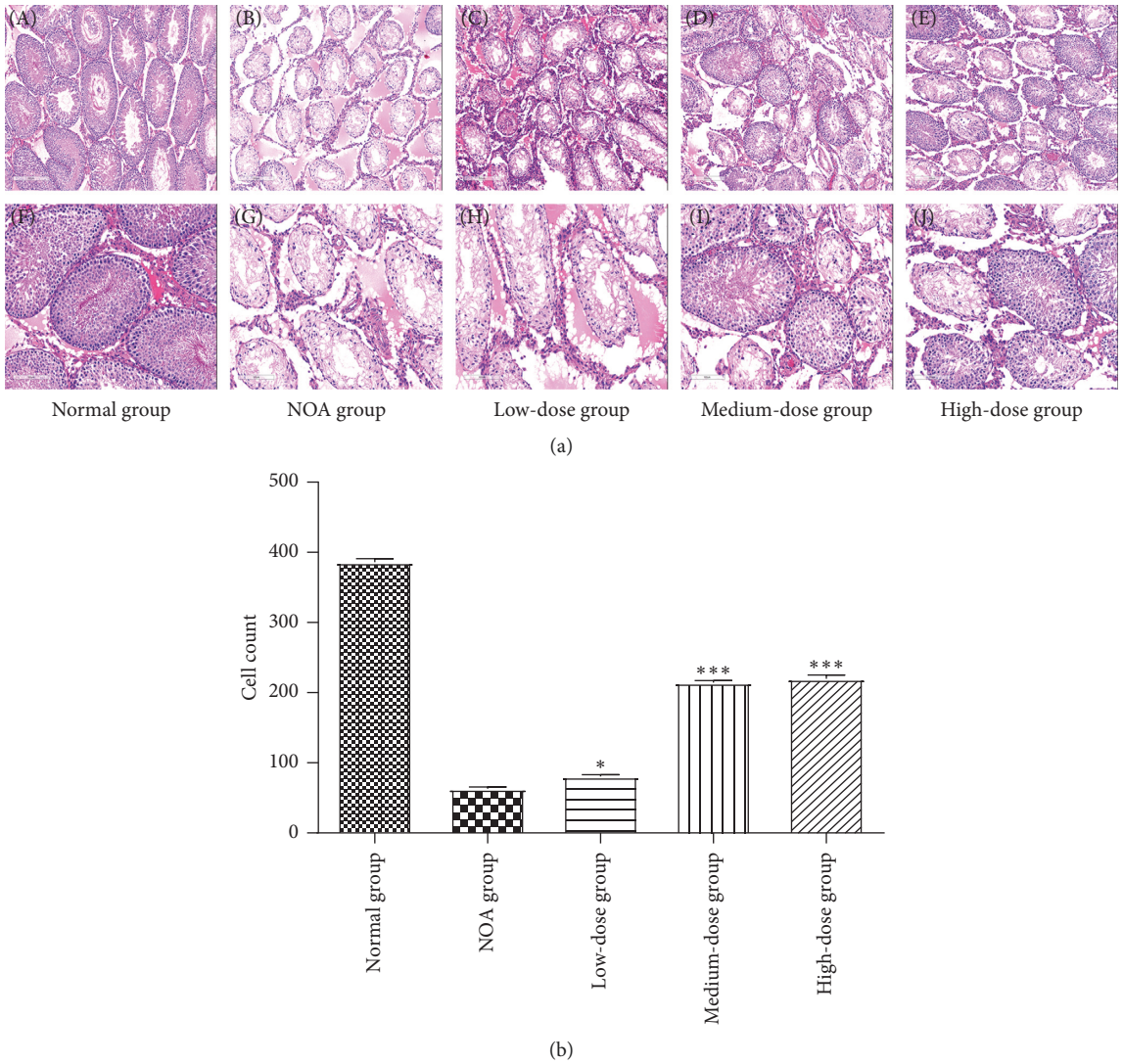

Figure 2: Morphology of seminiferous tubules examined with HE staining. (a) HE-stained sections of testicular tissues from each group. Lower panel: a higher magnification of the upper panel. (b) Average cell counts in 50 seminiferous tubules in each group. $^{*}P < 0.05$ versus the NOA group; $^{***}P < 0.0001$ versus the NOA group.

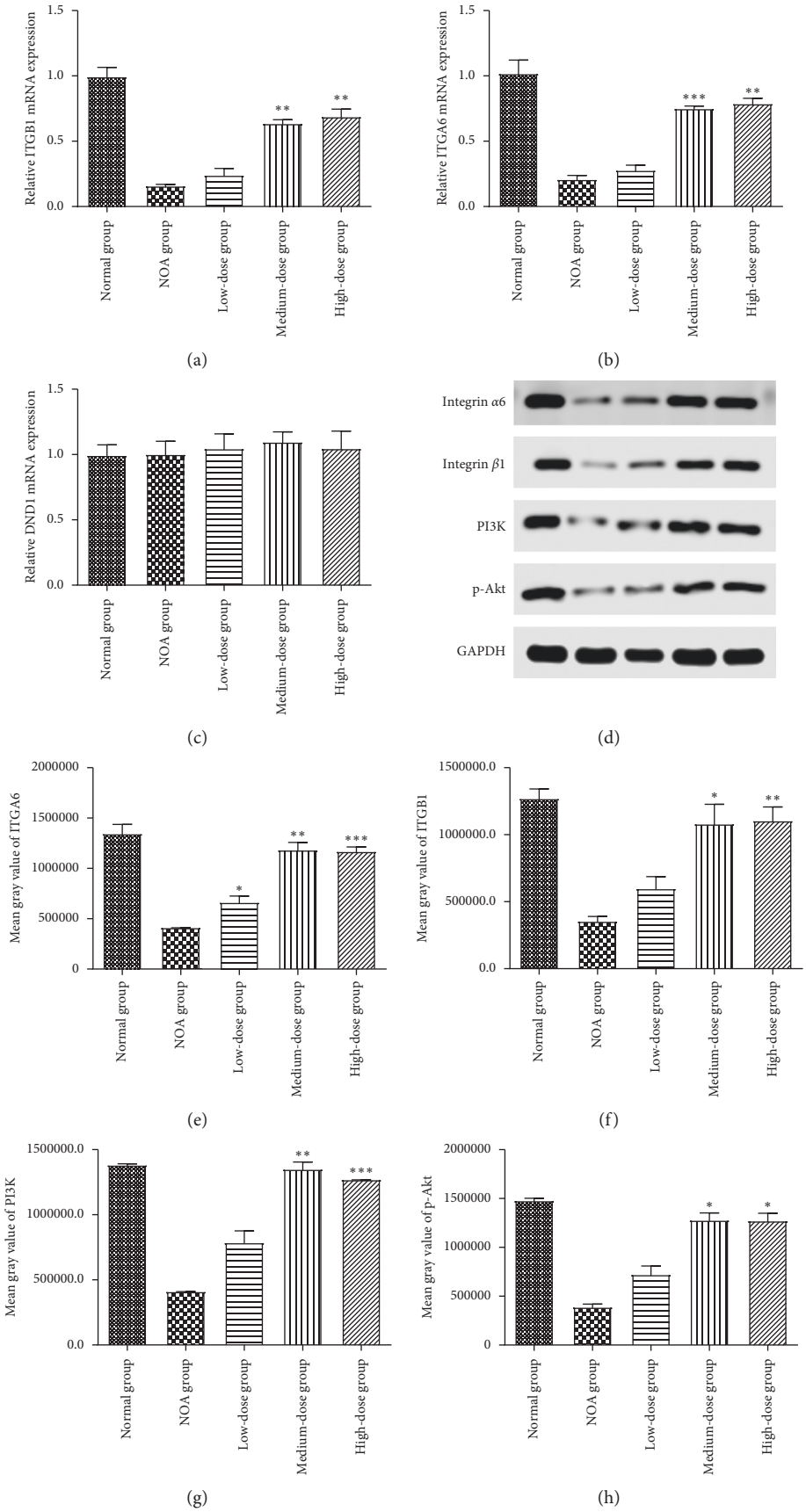

FIGURE 3: (a, b) Expression levels of α6-integrin and β1-integrin mRNA are presented. (c) Expression levels of DND1 mRNA are presented. (d) Western blot analysis showing the protein expression. (e–h) Densitometry and statistical analysis of α6/β1-integrin and PI3K and p-Akt proteins (ratio to GAPDH). qRT-PCR and western blot were conducted three times, and the results are expressed as means ± standard deviations (SDs). $^{*}P < 0.05$ versus the NOA group; $^{**}P < 0.01$ versus the NOA group; $^{***}P < 0.0001$ versus the NOA group.

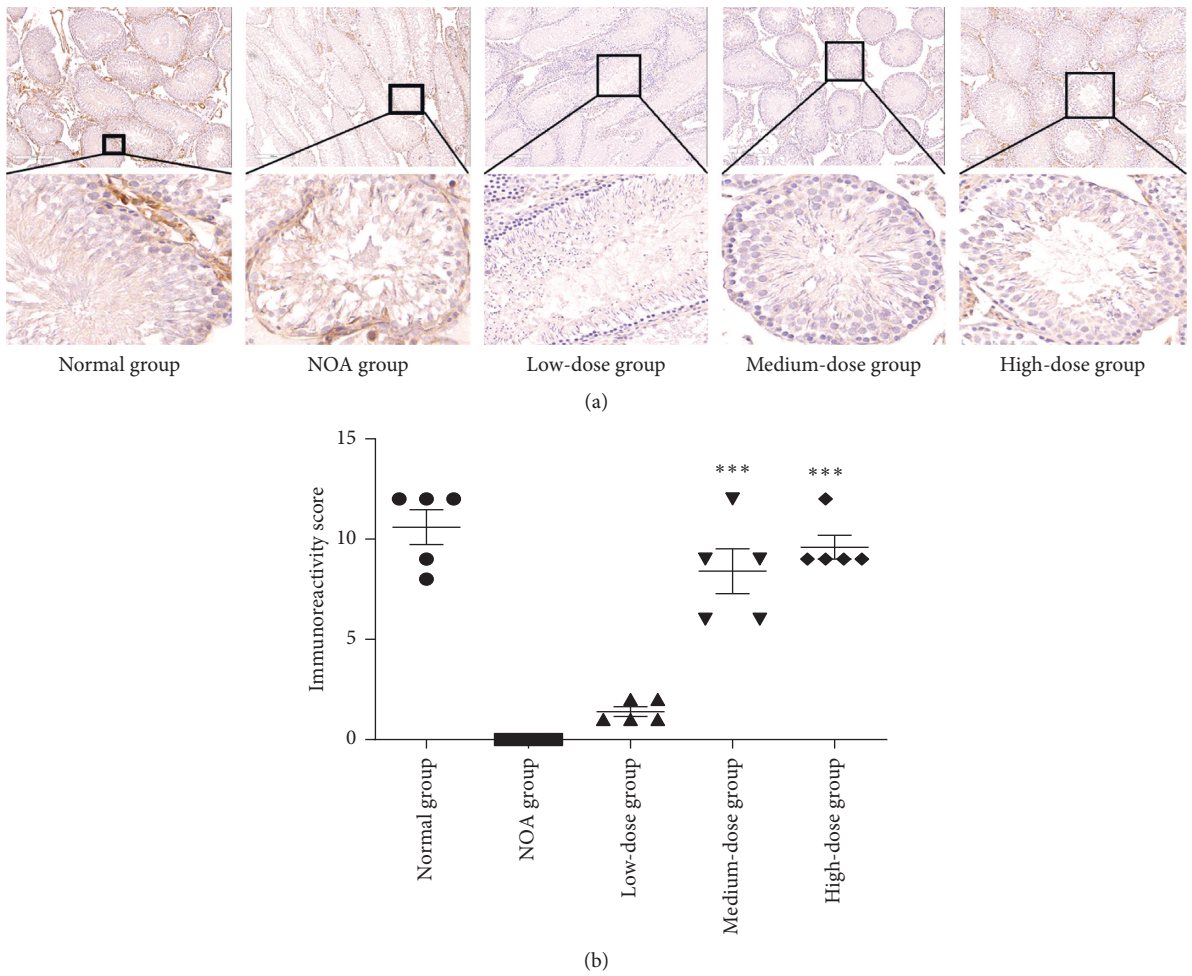

FIGURE 4: Immunohistochemical analysis of the α6-integrin expression in the rat testis. Lower panel: a higher magnification of the upper panel. $^{***}P < 0.0001$ versus the NOA group.

3.5. Shengjing Capsule Upregulated PI3K/AKT Signaling Pathway. The PI3K/AKT pathway is critical to cell proliferation, cell growth, differentiation, and spermatogenesis [6, 7, 23–25]. However, the mechanism remains unknown. The correlation between PI3K/AKT and integrin $\alpha 6/\beta 1$ in spermatogenesis has been unexplored yet.

To detect the expressions of PI3K and Akt in testes, we first confirmed the expression of phosphorylated protein kinase B (p-Akt) by immunohistochemistry. After Shengjing capsule treatment, an evident expression of p-Akt can be observed in the cells near the basal lamina of seminiferous tubules in rat testes, where SSCs are located (Figure 6). The brims of SSCs close to the basal lamina were evidently stained in medium- and high-dose groups compared with the normal group. For the SSCs of seminiferous tubules in the NOA group, they were scarcely stained. Then, we detected the expressions of PI3K and p-Akt through western blotting (Figures 3(d), 3(g), and 3(h)). PI3K and p-Akt expressions increased in medium-dose and high-dose groups, but they scarcely increased in the low-dose group. In quantitative analysis, compared with each respective normal group, the densitometry values of the immunoreactive bands concerning PI3K were 0.43, 0.88, 1.41, and 1.28 for NOA and low-, medium-, and high-dose groups, respectively (Figure 3(g)). Values of p-Akt were 0.44, 0.54, 1.12, and 1.12 for NOA and low-, medium-, and high-dose groups, respectively (Figure 3(h)). p-Akt expression levels also increased significantly in medium- and high-dose groups when compared with the NOA group ($P = 0.0135$ and $P = 0.0206$).

4. Discussion

Patients with azoospermia can achieve pregnancy by extracting sperm from the testicles through assisted reproductive technology [26]. For NOA patients, TESE and testicular sperm aspiration (TESA) are the most common methods for sperm extraction [27]. However, the possibility of finding sperm cells is only about 50% in NOA patients. The disadvantage of this invasive procedure is that testicular tissue may transiently or permanently affect androgen production [28]. Therefore, finding effective and feasible treatments can be an important adjuvant treatment for NOA patients. Traditional Chinese herbal medicines have a history of thousands of years and have the potential to improve sperm production in NOA patients. Shengjing capsules have

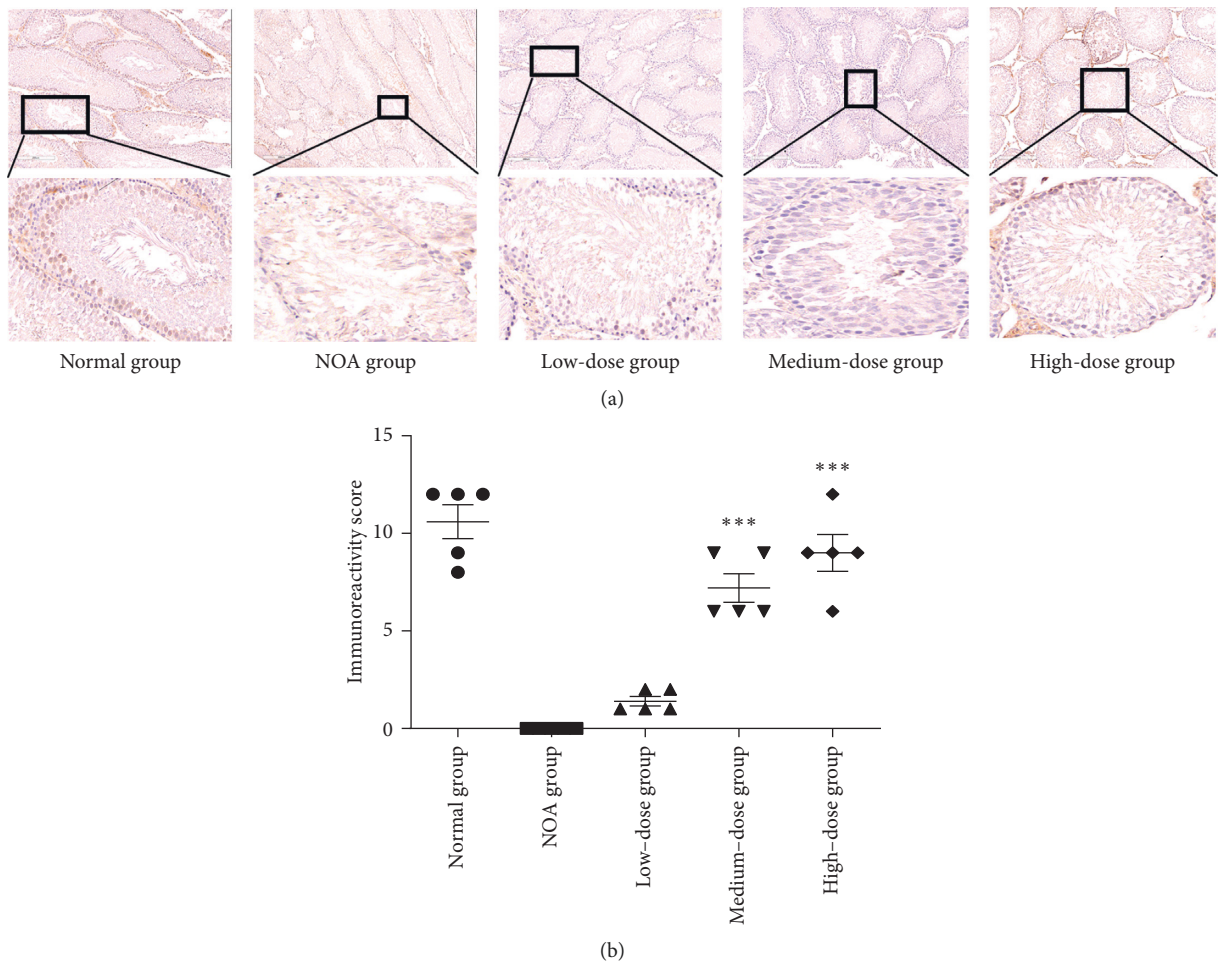

Figure 5: Immunohistochemical analysis of the β1-integrin expression in the rat testis. Lower panel: a higher magnification of the upper panel. $^{***}P < 0.0001$ versus the NOA group.

the potential to improve the sperm production ability of NOA patients. As a noninvasive treatment, the Shengjing capsule is easy to operate and does not cause testicular damage.

In this study, we used HE staining and semen smear to find that the number of spermatogenic epithelial cells was higher in the Shengjing treatment group, and the sperm count was higher than that in the NOA rat group. It showed the disturbance in the seminiferous tubular layers and the disappearance of spermatocytes and spermatids in the NOA group. Almost all the seminiferous tubules across the section were vacuolated with a thin layer of the basal compartment containing Sertoli cells and some SSCs in HE staining. After 8 weeks of Shengjing capsule treatment, the count of the spermatogenic cells, the germ cells, and even the sperms in the medium-dose and high-dose groups was significantly higher than that in the NOA group. These results indicated that the Shengjing capsule could repair the damaged seminiferous epithelium and protect spermatogenesis.

The spermatogenic function of azoospermia rats was improved in the medium- and high-dose spermatogenic capsule groups. However, the spermatogenic function of rats did not increase with the increasing dose of the Shengjing capsule. This is consistent with the clinical use of Shengjing capsules to improve the semen quality of azoospermia patients. These results suggest that Shengjing capsules may have similar effects on improving semen quality in NOA but require more multicenter studies with larger samples.

Spermatogenesis is a complex process that originates with and depends on SSCs. Spermatogonial self-renewal is a critical prerequisite for the maintenance of normal sperm counts. And the disruption in their function has dire consequences on fertility. These primitive cells reside on the basement membrane of the seminiferous tubule and slowly proliferate to provide (a) additional stem cells by self-renewal and (b) progeny cells that undergo significant amplification during the differentiation process to spermatozoa [29]. A single SSC in a rat is capable of producing more than 4,000 sperm, most of which disappear in the normal process by programmed cell death [30].

Stem cells have been reported as a star therapeutic target in a number of cases of busulfan causing NOA model literatures [31]. SSC has a unique self-renewal capacity to maintain the basic number of cell pools from which progenitor cells that are committed to the terminal differentiation pathway are produced [32]. Integrin $\alpha 6/\beta 1$ is an

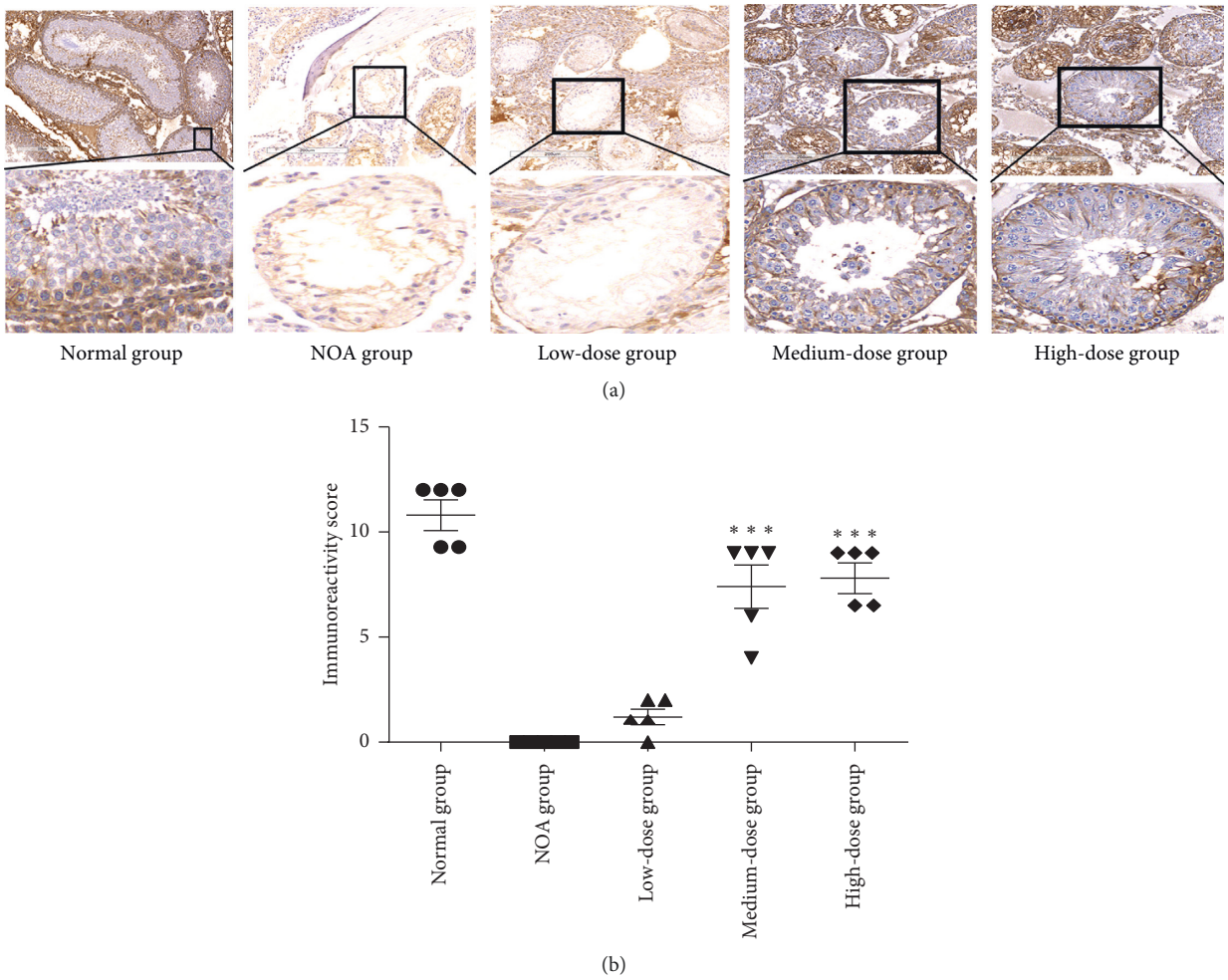

Figure 6: Immunohistochemical analysis of the p-Akt expression in the rat testis. Lower panel: a higher magnification of the upper panel. $^{***}P < 0.0001$ versus the NOA group.

important biomarker of SSCs. These effects make it possible for SSCs to support homeostasis and provide sperm regeneration [33].

In this study, we observe that Shengjing capsules significantly improve the spermatogenesis in the NOA rats. To elucidate the underlying mechanisms, we detect the expression of the specific biomarker of α6-integrin and β1-integrin for SSCs in testicular tissue. We find that the integrin $\alpha 6/\beta 1$ expression is barely expressed in the NOA group. And in medium-dose and high-dose groups, the expression levels of integrin $\alpha 6/\beta 1$ significantly increased compared with the NOA rat group. It means that a significant increase is shown in the numbers of SSCs after Shengjing capsule treatment, though the improvement does not increase with the dose. Since the vertebrate-conserved RNA-binding protein DND1 is necessary for the survival of SSCs, we further examine the DND1 expression. Taken together, these findings reveal that Shengjing capsules might activate SSCs via upregulating integrin $\alpha 6/\beta 1$.

The PI3K/AKT pathway might play an impotent role in male fertility [34]. Male mice with a homozygous mutation of the PI3K pathway are sterile because of a block in spermatogenesis, with initially decreased proliferation and subsequent extensive apoptosis occurring at the SSC level. The findings of De Miguel et al. [35] suggested an important role of AKT/mTOR in mediating primordial germ cell growth, spermatogonial proliferation, and spermatogenesis. In this study, the expression levels of PI3K and p-Akt have a similar trend of integrin $\alpha 6/\beta 1$. Western blotting analysis demonstrated that PI3K and p-Akt expressions apparently enhanced in medium- and high-dose Shengjing capsule groups compared with the normal group. Immunohistochemistry analysis corroborated these results, showing that expressions of PI3K, p-Akt, and integrin $\alpha 6/\beta 1$ were significantly higher in medium-dose and high-dose Shengjing capsule groups than in the NOA group. PI3K/AKT may play an important role in the improvement of azoospermia when using Shengjing capsules for upregulating integrin $\alpha 6/\beta 1$.

The Shengjing capsule comprises 19 ingredients, some of which are used to improve testicular function. For instance, the *Panax ginseng* extract could enhance testicular function by elevating GPx and GST activity, thus resulting in increased glutathione, which prevented LPO in the testis [36].

Kopalli et al. [37] also reported that the *Panax ginseng* extract attenuates H_2O_2-induced spermatocyte oxidative stress in mouse spermatocytes and regulates the expression of antioxidant-related genes, spermatogenesis-related proteins, and sex hormone receptors in aged rats. Ginseng may be a potential natural drug used to protect from or treat stress-induced male infertility. Zhang et al. [38] reported that *Lycium barbarum* could improve sperm density, sperm movement, and the rate of normal sperm morphology. *Lycium barbarum* could also reduce cadmium-induced testicular damage by increasing antioxidant enzyme activity and reducing oxidative stress. It may be a potential adjunct to testicular toxicity. Taken together with the findings presented here, Shengjing capsules, as a Chinese herbal medicine, may activate SSCs into the process of spermatogenesis by upregulating the expression of integrin $\alpha 6/\beta 1$ through the PI3K/AKT signal pathway in the NOA rats.

4.1. Limitations. When evaluating spermatogenic function of rats, only the changes of sperm number were evaluated. No other parameters of sperm quality were compared, such as sperm motility and deformity rate. This is due to the lack of professional evaluation of the rat sperm instrument and cannot carry out effective assessment of rat semen quality. Meanwhile, sperm count is one of the indicators of semen quality, and the increase in the sperm count partly reflects the restoration of spermatogenesis in mice. We did not interbreed rats among the treatment groups to evaluate the fertility achieved by the Shengjing capsules in rats. The restoration of spermatogenesis could theoretically lead to the restoration of fertility in mice. More relevant research is needed to clarify the mechanism of Shengjing capsules in improving spermatogenic function in patients with NOA.

4.2. Strengths. Traditional Chinese medicine for azoospermia enriches the present-day therapies in the field of sexual medicine. To our knowledge, this is the first study to evaluate the therapeutic effect of Shengjing capsules on NOA. We elaborate a possible potential mechanism and provide a new direction for the treatment of NOA, and further research is needed to clarify the possible mechanism of action. It provides evidence for the clinical treatment of NOA patients using Shengjing capsules.

5. Conclusion

This study firstly shows that the Shengjing capsule significantly improves the spermatogenesis in the NOA rats. The underlying mechanisms might involve activating SSCs by upregulating the integrin $\alpha 6/\beta 1$ expression via the PI3K/AKT pathway. Our results suggest Shengjing capsules as a promising therapeutic medicine for NOA.

Data Availability

The data used to support the findings of this study are available from the corresponding author upon request.

Ethical Approval

All experimental protocols were subject to approval by the Institutional Animal Care and Use Committee of the First Affiliated Hospital of Guangzhou Medical University (Guangzhou, China).

Conflicts of Interest

The authors declare no conflicts of interest.

Authors' Contributions

Jiamin Wang, Shankun Zhao, and Lianmin Luo contributed equally to this work.

Acknowledgments

This work was supported by the Science and Technology Planning Project of Guangdong Province (no. 2017B030314108).

References

[1] I. D. Sharlip, J. P. Jarow, A. M. Belker et al., "Best practice policies for male infertility," *Fertility and Sterility*, vol. 77, no. 5, pp. 873–882, 2002.

[2] R. I. McLachlan, E. Rajpert-De Meyts, C. E. Hoei-Hansen, D. M. de Kretser, and N. E. Skakkebaek, "Histological evaluation of the human testis-approaches to optimizing the clinical value of the assessment: mini review," *Human Reproduction*, vol. 22, no. 1, pp. 2–16, 2007.

[3] P. N. Schlegel, "Testicular sperm extraction: microdissection improves sperm yield with minimal tissue excision," *Human Reproduction*, vol. 14, no. 1, pp. 131–135, 1999.

[4] G. D. Palermo, Q. V. Neri, P. N. Schlegel, and Z. Rosenwaks, "Intracytoplasmic sperm injection (ICSI) in extreme cases of male infertility," *PLoS One*, vol. 9, no. 12, Article ID e113671, 2014.

[5] M.-H. Perrard, N. Sereni, C. Schluth-Bolard et al., "Complete human and rat ex vivo spermatogenesis from fresh or frozen testicular tissue," *Biology of Reproduction*, vol. 95, no. 4, p. 89, 2016.

[6] D. D. Sarbassov, A. Guertin David, M. Ali Siraj et al., "Phosphorylation and regulation of Akt/PKB by the rictor-mTOR complex," *Science*, vol. 307, no. 5712, pp. 1098–1101, 2005.

[7] M. A. Deutsch, I. Kaczmarek, S. Huber et al., "Sirolimus-associated infertility: case report and literature review of possible mechanisms," *American Journal of Transplantation*, vol. 7, no. 10, pp. 2414–2421, 2007.

[8] T. Shinohara, M. R. Avarbock, and R. L. Brinster, "1- and 6-integrin are surface markers on mouse spermatogonial stem cells," *Proceedings of the National Academy of Sciences*, vol. 96, no. 10, pp. 5504–5509, 1999.

[9] R. Sá, C. Miranda, F. Carvalho, A. Barros, and M. Sousa, "Expression of stem cell markers: OCT4, KIT, ITGA6, and ITGB1 in the male germinal epithelium," *Systems Biology in Reproductive Medicine*, vol. 59, no. 5, pp. 233–243, 2013.

[10] H. J. Park, S. Choe, and N. C. Park, "Effects of Korean red ginseng on semen parameters in male infertility patients: a randomized, placebo-controlled, double-blind clinical study," *Chinese Journal of Integrative Medicine*, vol. 22, no. 7, pp. 490–495, 2016.

[11] E. H. Park, D. R. Kim, H. Y. Kim, S. K. Park, and M. S. Chang, "Panax ginseng induces the expression of CatSper genes and sperm hyperactivation," *Asian Journal of Andrology*, vol. 16, no. 6, pp. 845–851, 2014.

[12] L. Qian and S. Yu, "Protective effect of polysaccharides from Lycium barbarumon spermatogenesis of mice with impaired reproduction system induced by cyclophosphamide," *American Journal of Reproductive Immunology*, vol. 76, no. 5, pp. 383–385, 2016.

[13] H. Ning, Z.-C. Xin, G. Lin, L. Banie, T. F. Lue, and C.-S. Lin, "Effects of icariin on phosphodiesterase-5 activity in vitro and cyclic guanosine monophosphate level in cavernous smooth muscle cells," *Urology*, vol. 68, no. 6, pp. 1350–1354, 2006.

[14] W.-H. Lin, M.-T. Tsai, Y.-S. Chen et al., "Improvement of sperm production in subfertile boars by Cordyceps militaris supplement," *The American Journal of Chinese Medicine*, vol. 35, no. 4, pp. 631–641, 2007.

[15] Chinese Medical Association Male Science Branch, *Chinese Men's Disease Diagnosis and Treatment Guidelines and Experts Consensus (2016 Version)*, People's Medical Publishing House, Beijing, China, 2017.

[16] S. Zhou, Z. Wen, A. Liang, and S. Zhang, "Experimental research on therapeutic efficacy of traditional Chinese medicine shengjing capsule extracts in treating spermatogenesis impairment induced by oxidative stress," *Medical Science Monitor*, vol. 22, pp. 50–56, 2016.

[17] J. T. Li, X. W. Qu, S. W. Zhang, Z. S. Li, and P. H. Zhang, "Effects of Yishen Shengjing capsules on semen quality and gonadal hormone levels in rats with dibutyl phthalate-induced reproductive function injury," *Zhonghua Nan Ke Xue*, vol. 22, no. 12, pp. 1110–1115, 2016.

[18] F. W. Song and W. D. Zhong, "Clinical efficacy of Shengjing capsule on patients with oligoasthenospermia," *Zhonghua Nan Ke Xue*, vol. 15, no. 8, pp. 762–764, 2009.

[19] US Food and Drug Administration, "Guidance for industry: estimating the maximum safe starting dose in initial clinical trials for therapeutics in adult healthy volunteers," 2005, https://www.fda.gov/media/72309/download.

[20] C. Cakici, B. Buyrukcu, G. Duruksu et al., "Recovery of fertility in azoospermia rats after injection of adipose-tissue-derived mesenchymal stem cells: the sperm generation," *Biomed Research International*, vol. 2013, Article ID 529589, 18 pages, 2013.

[21] S. Parhizkar, M. J. Yusoff, and M. A. Dollah, "Effect of phaleria macrocarpa on sperm characteristics in adult rats," *Advanced Pharmaceutical Bulletin*, vol. 3, no. 2, pp. 345–352, 2013.

[22] R. Kang, S. Zhao, L. Liu et al., "Knockdown of PSCA induces EMT and decreases metastatic potentials of the human prostate cancer DU145 cells," *Cancer Cell International*, vol. 16, no. 1, p. 20, 2016.

[23] L. Asnaghi, P. Bruno, M. Priulla, and A. Nicolin, "mTOR: a protein kinase switching between life and death," *Pharmacological Research*, vol. 50, no. 6, pp. 545–549, 2004.

[24] K. G. Foster and D. C. Fingar, "Mammalian target of rapamycin (mTOR): conducting the cellular signaling symphony," *Journal of Biological Chemistry*, vol. 285, no. 19, pp. 14071–14077, 2010.

[25] J. Rovira, F. Diekmann, M. J. Ramírez-Bajo, E. Bañón-Maneus, D. Moya-Rull, and J. M. Campistol, "Sirolimus-associated testicular toxicity," *Transplantation Journal*, vol. 93, no. 9, pp. 874–879, 2012.

[26] V. Vloeberghs, G. Verheyen, P. Haentjens, A. Goossens, N. P. Polyzos, and H. Tournaye, "How successful is TESE-ICSI in couples with non-obstructive azoospermia?," *Human Reproduction*, vol. 30, no. 8, pp. 1790–1796, 2015.

[27] J. Rajfer, "TESA or TESE: which is better for sperm extraction?," *Reviews in Urology*, vol. 8, no. 3, p. 171, 2006.

[28] S. C. Esteves, "Clinical management of infertile men with nonobstructive azoospermia," *Asian Journal of Andrology*, vol. 17, no. 3, pp. 459–470, 2015.

[29] Y. Clermont, "Kinetics of spermatogenesis in mammals: seminiferous epithelium cycle and spermatogonial renewal," *Physiological Reviews*, vol. 52, no. 1, pp. 198–236, 1972.

[30] D. G. de Rooij and J. A. Grootegoed, "Spermatogonial stem cells," *Current Opinion in Cell Biology*, vol. 10, no. 6, pp. 694–701, 1998.

[31] L. R. Bucci and M. L. Meistrich, "Effects of busulfan on murine spermatogenesis: cytotoxicity, sterility, sperm abnormalities, and dominant lethal mutations," *Mutation Research/Fundamental and Molecular Mechanisms of Mutagenesis*, vol. 176, no. 2, pp. 259–268, 1987.

[32] J. M. Oatley and R. L. Brinster, "The germline stem cell niche unit in mammalian testes," *Physiological Reviews*, vol. 92, no. 2, pp. 577–595, 2012.

[33] P. M. Kluin and D. G. de Rooij, "A comparison between the morphology and cell kinetics of gonocytes and adult type undifferentiated spermatogonia in the mouse," *International Journal of Andrology*, vol. 4, no. 1–6, pp. 475–493, 1981.

[34] P. Blume-Jensen, G. Jiang, R. Hyman, K.-F. Lee, S. O'Gorman, and T. Hunter, "Kit/stem cell factor receptor-induced activation of phosphatidylinositol 3′-kinase is essential for male fertility," *Nature Genetics*, vol. 24, no. 2, pp. 157–162, 2000.

[35] M. P. De Miguel, L. Cheng, E. C. Holland, M. J. Federspiel, and P. J. Donovan, "Dissection of the c-kit signaling pathway in mouse primordial germ cells by retroviral-mediated gene transfer," *Proceedings of the National Academy of Sciences*, vol. 99, no. 16, pp. 10458–10463, 2002.

[36] Y. J. Won, B. K. Kim, Y. K. Shin et al., "Pectinase-treated Panax ginseng extract (GINST) rescues testicular dysfunction in aged rats via redox-modulating proteins," *Experimental Gerontology*, vol. 53, pp. 57–66, 2014.

[37] S. R. Kopalli, K. M. Cha, M. S. Jeong et al., "Pectinase-treated Panax ginseng ameliorates hydrogen peroxide-induced oxidative stress in GC-2 sperm cells and modulates testicular gene expression in aged rats," *Journal of Ginseng Research*, vol. 40, no. 2, pp. 185–195, 2016.

[38] L. Zhang, Q. Li, G. Zheng et al., "Protective effect of Lycium barbarum polysaccharides against cadmium-induced testicular toxicity in male mice," *Food & Function*, vol. 8, no. 6, pp. 2322–2330, 2017.

Hindawi
Evidence-Based Complementary and Alternative Medicine
Volume 2019, Article ID 6369132, 10 pages
https://doi.org/10.1155/2019/6369132

Research Article

Aconiti Lateralis Radix Preparata, the Dried Root of *Aconitum carmichaelii* Debx., Improves Benign Prostatic Hyperplasia via Suppressing 5-Alpha Reductase and Inducing Prostate Cell Apoptosis

Jinbong Park,[1,2] **Dong-Hyun Youn**,[1,2] **and Jae-Young Um**[1,2]

[1]*Department of Pharmacology, College of Korean Medicine, Kyung Hee University, Seoul, Republic of Korea*
[2]*Comorbidity Research Institute, Kyung Hee University, Seoul, Republic of Korea*

Correspondence should be addressed to Jae-Young Um; jyum@khu.ac.kr

Received 5 April 2019; Revised 2 July 2019; Accepted 11 July 2019; Published 31 July 2019

Guest Editor: Arielle Cristina Arena

Benign prostatic hyperplasia (BPH) is a common disease in elderly men which can be characterized by an abnormal enlargement of the prostate associated with lower urinary symptoms. Current medications available for BPH treatment display several adverse effects; thus, the search for effective treatments with less side effects is still ongoing. In this study, we investigated the effect of Aconiti Lateralis Radix Preparata (dried root of *Aconitum carmichaelii* Debx.; AL), which is an herb used to treat extremely cold symptoms in traditional Korean medicine, on BPH using a testosterone propionate- (TP-) induced BPH rat model. Eight-week inguinal injection of TP induced BPH in rats, the prostate of which was displaying an abnormal proliferation. The pathological proliferation of the prostate was ameliorated by AL treatment of 4 weeks. Pathohistological changes in the prostate including epithelial thickness and lumen area were restored in AL-treated rats. Furthermore, 5α-reductase (5AR) and androgen receptor (AR), the two main factors in the pathogenesis of BPH, were decreased. In addition, the ratio of BAX and Bcl-2, an indicator of apoptosis, was increased by AL as well. Similar results were observed in AL-treated LNCaP prostate cancer cells. AL treatment suppressed the expression of the 5AR-AR axis and increased the ratio of BAX and Bcl-2. Apoptosis in the testis is considered a crucial side effect of finasteride, a 5AR inhibitor used to treat BPH. Our results showed that AL treatment did not display such effects, while finasteride treatment resulted in loss of spermatogenic cells within the prostate. Overall, these results suggest AL as a potentially safe nature-derived therapeutic agent for BPH treatment.

1. Introduction

Benign prostatic hyperplasia (BPH) is a chronic disease commonly found especially in aging men [1]. It is reported that about 90% of males over an age of 80 suffer from BPH and lower urinary tract symptoms (LUTS) [2]. The main causes of BPH are pathologically increased proliferation of the smooth muscle in the prostate, leading to an abnormal enlargement of the prostate. Patients suffering from serious BPH display symptoms such as urinary intermittency, incomplete emptying, weak stream, staining, urgency, and nocturia [3].

The detailed mechanism of BPH pathogenesis is not fully revealed, but testosterone and dihydrotestosterone (DHT) are well known as inducers of BPH [4]. After the male sex hormone testosterone is produced, it is converted into DHT by 5α-reductase (5AR). DHT is considered a main factor of BPH pathogenesis, as it is expressed five times more than testosterone in BPH patients [4]. DHT has 2- to 10-fold higher binding affinity towards androgen receptor (AR) [5], a nuclear receptor which acts as a transcription factor after activation, and in result accelerates the proliferation of prostate cells. After conversion by 5AR, DHT combines with the AR and

induces the expression of the growth factor, which leads to prostatic proliferation [6].

There are two mainly considered medical treatments for BPH. Alpha-blockers, which are inhibitors of α1-adrenergic receptors, relax the smooth muscle tone in the prostate and improve the urinal flow [7, 8]. However, the use of α-blockers is limited because of side effects such as headaches, hypotension, or ejaculation changes (absence of seminal emission, reduced ejaculation volume and force, etc.). Furthermore, the α-blocker itself cannot regulate the size of the prostate [9, 10]. Another class of medication is 5AR inhibitors, such as finasteride (Fi) and dutasteride. Suppression of 5AR by these inhibitors decreases the conversion of testosterone to DHT [11] and eventually leads to shrinking of prostate tissues. However, 5AR inhibitors can also cause side effects, such as loss of libido and erectile dysfunction [12]. Because of the side effects of existing medications, the need for alternative treatment is constantly growing [13].

Aconiti Lateralis Radix Preparata (AL), the processed daughter root of *Aconitum carmichaelii* Debx., of family Ranunculaceae, has been traditionally used as an essential herbal drug for cold sensation by stimulating heat generation in East Asia [14]. Studies have reported the anti-inflammatory, antitumor, and analgesic effects of AL [15–18], and moreover, its usage to treat colds, polyarthralgia, diarrhea, heart failure, beriberi, and edema are well known as well [19]. Nowadays, AL is clinically prescribed for diarrhea, syncope, joint pain, rheumatoid arthritis, and other inflammations [20].

The antiproliferative effect of AL on the prostate has been first reported by Dumbre et al. [21]. Dumbre's team showed that three ayurvedic plants including *Aconitum heterophyllum* suppressed prostate enlargement in testosterone-treated rats. However, this study only reports the antiproliferative effect lacking the related action mechanism. Therefore, we conducted a study to evaluate the effect of AL on BPH using testosterone propionate- (TP-) induced BPH rats and LNCaP prostate cancer cells.

2. Materials and Methods

2.1. Preparation of AL. The water extract of AL was obtained by boiling 100 g of dried roots of *Aconitum carmichaelii* Debx. in 1 L of distilled water at 100°C for 150 min based on the traditional extraction method of herbal prescriptions used in Korean medicine [22]. The solution was freeze-dried (yield 12.8%), filtered through a 0.22 μm syringe filter, evaporated, and then stored at −20°C until usage.

2.2. Chemical Reagents. TP was purchased from Wako Pure Chemical Industries (Osaka, Japan), and Fi (≥97% pure) was purchased from Sigma-Aldrich Inc. (St. Louis, MO, USA). Antibody for AR was from Pierce Biotechnology (Rockford, IL, USA), and antibody for 5AR was from Abcam Inc. (Cambridge, MA, USA). Antibody for glyceraldehyde 3-phosphate dehydrogenase (GAPDH) was from Santa Cruz Biotechnology (Santa Cruz, CA, USA), and antibodies for BAX and Bcl-2 were purchased from Cell Signaling Technology (Danvers, MA, USA).

2.3. Animals. Twelve-week-old male Sprague Dawley (SD) rats (body weight 200–220 g) were purchased from the Dae-Han Experimental Animal Center (Dae-Han Biolink, Eumsung, Korea). The animals were all maintained in conditions in accordance with the regulation issued by the Institutional Review Board of Kyung Hee University (confirmation number KHUASP(SE)-P-034). The rats were housed in a pathogen-free room maintained at 23 ± 2°C under a 12 h light/dark cycle. Water and standard laboratory diet (CJ Feed Co., Ltd., Seoul, Korea) were provided ad libitum. BPH was induced as previously described [23], that is, by a 4-week pretreatment with daily subcutaneous injections of TP (5 mg/kg/day) in the inguinal region of rats. Fifty milliliters of the injection formula were prepared by dissolving 750 mg of TP in 5 ml of 100% ethanol and then mixing with 45 mL of corn oil. Each rat was injected with 100 μL of this injection formula in the inguinal area. Normal control rats were injected with the same solvent without TP included. Then, the rats were divided into the following four groups ($n = 5$ per group) and were treated for 4 additional weeks: (a) a normal control (NC) group that received ethanol with corn oil, (b) a BPH group that received TP with corn oil, (c) a positive control group that received finasteride (Fi) (1 mg/kg/day) with TP (5 mg/kg/day), and (d) a group that received AL (20 mg/kg/day) with TP (5 mg/kg/day). AL and Fi were administrated via oral gavage. After the final treatment, animals were fasted overnight and euthanized using CO_2, and the ventral region of prostate tissues was obtained as described previously [24]. The relative prostate weight index (prostate index (PI)) was calculated as the ratio of prostate weight (mg) to body weight (100 g). The prostate tissue was divided in half; one half was fixed in 10% formalin and embedded in paraffin for histomorphological assays, and the other was stored at −80°C for further assays.

2.4. Hematoxylin and Eosin (H&E) Staining. The prostate tissue section preparation and H&E staining were performed as described previously [25]. The slides were examined using the Olympus IX71 inverted phase microscope (Olympus Co., Tokyo, Japan). Epithelial thickness and lumen area fold were measured using ImageJ 1.47v software (National Institutes of Health, Bethesda, MD, USA).

2.5. Western Blotting Assay. Protein expression analysis was performed as previously reported [26]. In brief, homogenized prostate tissues or harvested LNCaP cells were lysed with ice-cold RIPA buffer, the insoluble materials were removed, and the proteins were separated by 8% sodium dodecyl sulfate-polyacrylamide gel electrophoresis and transferred onto polyvinylidenedifluoride (PVDF) membranes (Billerica, MA, USA). The membranes were then incubated with the primary antibody at 4°C overnight and subsequently incubated with HRP-conjugated AffiniPure Goat Anti-Rabbit IgG (Jackson ImmunoResearch Labs) or

HRP-conjugated AffiniPure Goat Anti-Mouse IgG (Jackson ImmunoResearch Labs). The immunoblot intensity was quantified using ImageJ 1.47v software (National Institutes of Health).

2.6. Cell Culture. The human prostatic cancer cell line LNCaP was obtained from the Korean Cell Line Bank (Seoul, Republic of Korea). LNCaP cells were cultured in the Roswell Park Memorial Institute (RPMI) medium (Gibco, Big Cabin, OK, USA) supplemented with 100 mg/mL penicillin/streptomycin (HyClone, Logan, UT, USA) and 10% FBS (Sigma-Aldrich Inc.).

2.7. MTS Assay. LNCaP cells were seeded (2.5×10^4 cells/well) and incubated in the RPMI medium plus 10% FBS for 24 h. Then, the cells were incubated in fresh media containing various concentrations of BBR for an additional 24 h. Cell viability was monitored using the cell proliferation MTS kit by the Promega Corporation as recommended by the manufacturer as previously described [27]. The absorbance was measured at 490 nm in a VersaMax microplate reader (Molecular Devices, Sunnyvale, CA, USA).

2.8. Ultrahigh-Performance Liquid Chromatography (UHPLC) Analysis. An Agilent 1290 Infinity II LC system (Santa Clara, CA, USA) with an Agilent 6550 iFunnel Q-TOF LC/MS system was used to perform high-resolution liquid chromatography-mass spectrometry (LC-MS) of AL according to the manufacturer's instructions by the Western Seoul Center of Korea Basic Science Institute. Data acquisition was performed using 6200 series TOF/6500 series Q-TOF B.06.01 (B6172 SP1) software (Agilent, Santa Clara, CA, USA). Specific conditions for LC-MS analysis are described in Table 1.

2.9. Statistical Analysis. The data were presented as mean ± standard deviation (SD). Statistical significance ($P < 0.05$) was analyzed by the Kruskal–Wallis H test followed by Bonferroni's method as a post hoc test using GraphPad Prism 5 for Windows (GraphPad Software, San Diego, CA, USA).

Table 1: Analysis conditions for LC-MS.

LC-MS condition			
Component	Agilent 1290 Infinity II UHPLC G6650A Q-TOF MS (Agilent)		
Ion source	Dual AJS ESI		
Polarity (kV)	Positive mode (4.0) Negative mode (3.5)		
Mass range (m/z)	20–1700		
Reference masses (m/z)	Positive mode with 121.0509 and 922.0098 Negative mode with 112.9856 and 966.0007		
LC column	Agilent Eclipse Plus C18 RRHD column (50 mm × 2.1 mm, 1.8 μm)		
LC flow rate	0.300 mL/min		
Injection volume	1.00 μl		
Column temperature	30°C		
Solvent composition	A: 0.1% formic acid in water B: 0.1% formic acid in ACN		
Mobile phase	Time (min)	A (%)	B (%)
	0.0	95	5
	3.0	95	5
	13.0	10	90
	15.0	10	90
	17.0	95	5
	20.0	95	5

3. Results

3.1. AL Attenuates Prostatic Hyperplasia in TP-Induced BPH Rats. Changes in prostate tissue size, prostate weight, and prostate index are shown in Figure 1. Rats treated with TP showed an increase in prostate weight and PI by 1.74-fold and 1.88-fold compared to the normal control. AL treatment significantly decreased the prostate weight by 70% and PI by 74%. This effect was relatively higher than that in the Fi group, rats of which showed decreased prostate weight by 62% and PI by 70%. Body weight of rats did not show any difference among all groups (Figure 1(e)).

3.2. AL Restores Histological Changes of Prostate Tissues in TP-Induced BPH Rats. As shown in Figure 2(a), histology of the prostate was assessed by H&E staining. TP administration caused various histological changes in the prostate. The epithelium of the prostate gland with BPH displayed signs of proliferation such as increased epithelial thickness, overformed acinus area, and decreased lumen area. However, AL-treated rats and Fi-treated rats showed recovered histology similar to NC rats, with less pathological tissue structures (Figures 2(b) and 2(c)).

3.3. AL Regulates 5AR-AR Axis in TP-Induced BPH Rats and LNCaP Cells. The factors related to prostatic hyperplasia were examined by western blot assays using antibodies against 5AR and AR. These factors were increased in the TP-treated BPH group compared to those in the NC group. However, as shown in Figure 3(a), 5AR and AR were significantly decreased by AL treatment when compared to the TP-treated BPH group (0.73-fold and 0.63-fold, respectively). This was further confirmed in vitro, as AL treatment inhibited the expression of 5AR and AR in LNCaP prostate cells (Figure 3(b)), even though AL treatment up to 1000 μg/mL did not affect cell viability of LNCaP cells (Supplementary Figure S1).

3.4. AL Elevates BAX/Bcl-2 Ratio in TP-Induced BPH Rats and LNCaP Cells. We then evaluated the effect of AL on the ratio of BAX and Bcl-2. BAX/Bcl-2 ratio is considered an indicator of cell apoptosis, and Saker et al. have shown this ratio is important in the pathogenesis of both BPH and prostate cancer [28]. The ratio of BAX and Bcl-2 was decreased in prostate tissues of TP-induced rats, and this was restored to a level similar to that in the NC group by AL and Fi treatment (Figure 4(a)). Similar effects were observed in AL-treated LNCaP cells as well (Figure 4(b)), suggesting an apoptotic induction by AL in prostate cells.

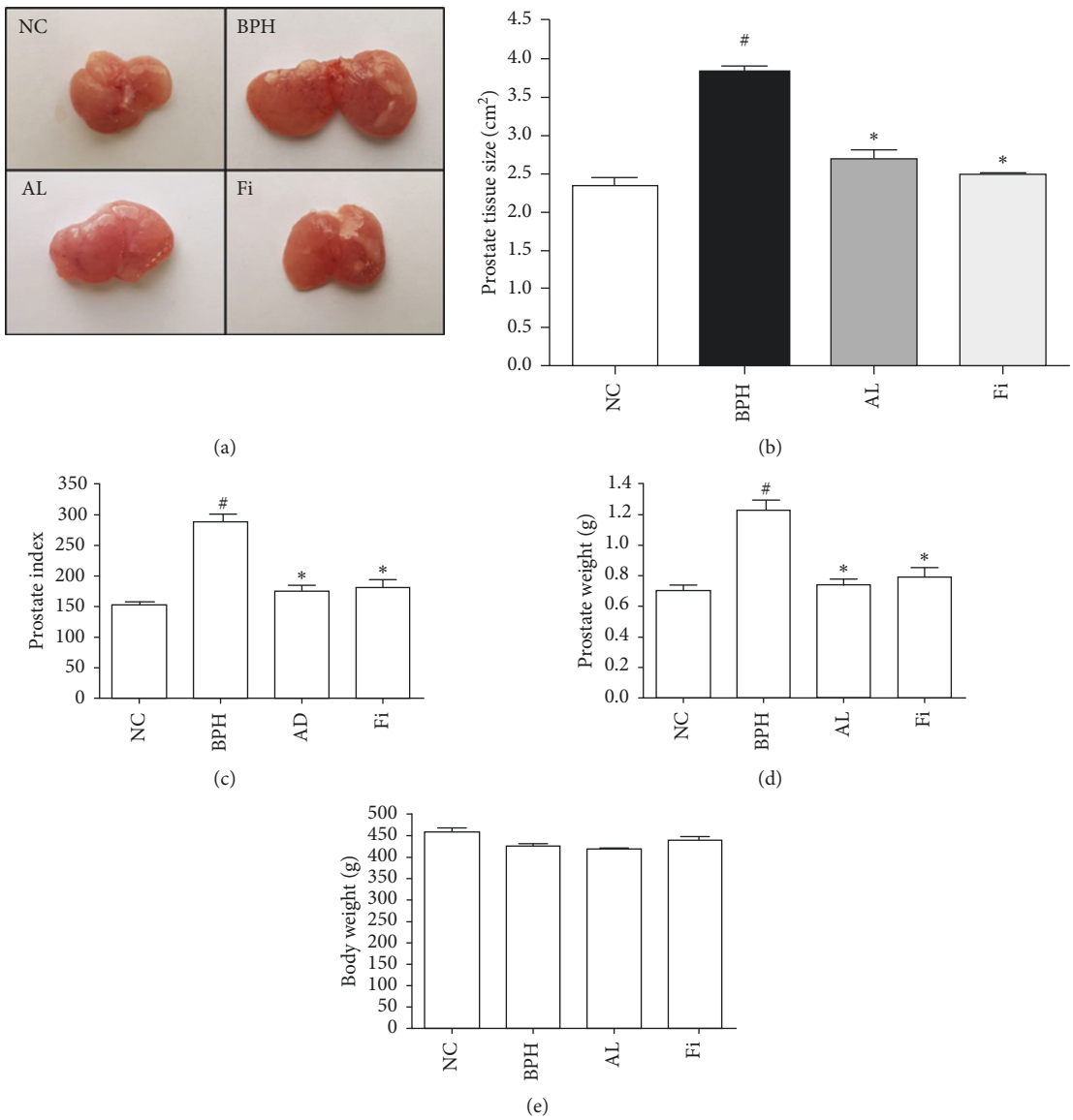

Figure 1: Effects of AL on prostate size and weight of TP-induced BPH rats. (a, b) Comparison of size of prostate tissues. (c) Prostate index value measured by dividing 100 g body weight by prostate tissue weight (mg). (d) Measurement of prostate weight of rats. (e) Measurement of body weight of rats. Values are expressed as mean ± SD. $^{\#}P < 0.05$ when compared to NC; $^{*}P < 0.05$ when compared to BPH. NC, normal control group; BPH, TP-induced BPH group; AL, AL-treated BPH group; Fi, finasteride-treated BPH group.

3.5. AL Treatment Does Not Cause Pathological Changes in Testis. One of the fatal side effects of 5AR inhibitors such as Fi is apoptotic enhancement in the testis [29, 30]. Based on these studies, we compared the histology of the testis of Fi- and AL-treated rats. As shown in Figure 5, the testicular tissue showed a proper arrangement of germinal cells in the NC and BPH groups, with no histopathologic lesions. However, in the Fi group, lower spermatogenic cell density was observed, which was improved in AL-treated rats. These results show that AL does not display toxicity in the testis and does not impact spermatogenesis.

3.6. Chromatographic Analysis of AL. We used the UHPLC method to analyze components of AL. As a result, we could identify three components with molecular weights of 239.0575, 634.2889, and 648.305 (Figure 6). Further information on the spectrum peaks is presented in Table 2.

4. Discussion

Prostate diseases can be categorized into three groups: prostatitis, BPH, and prostate cancer. Among the three diseases, BPH is the most common disease in men [31]. Prostate tissue consists of four areas: the central zone, peripheral zone, transition zone, and anterior fibromuscular stroma. BPH associates with an overproliferated transition zone and stiffness of the prostatic smooth muscle tone. These abnormal changes in the size and muscle tone cause compression on the urethra, thus leading to LUTS, a common class of symptoms in BPH [32]. The main reason which makes BPH a serious health issue is epidemiology: around

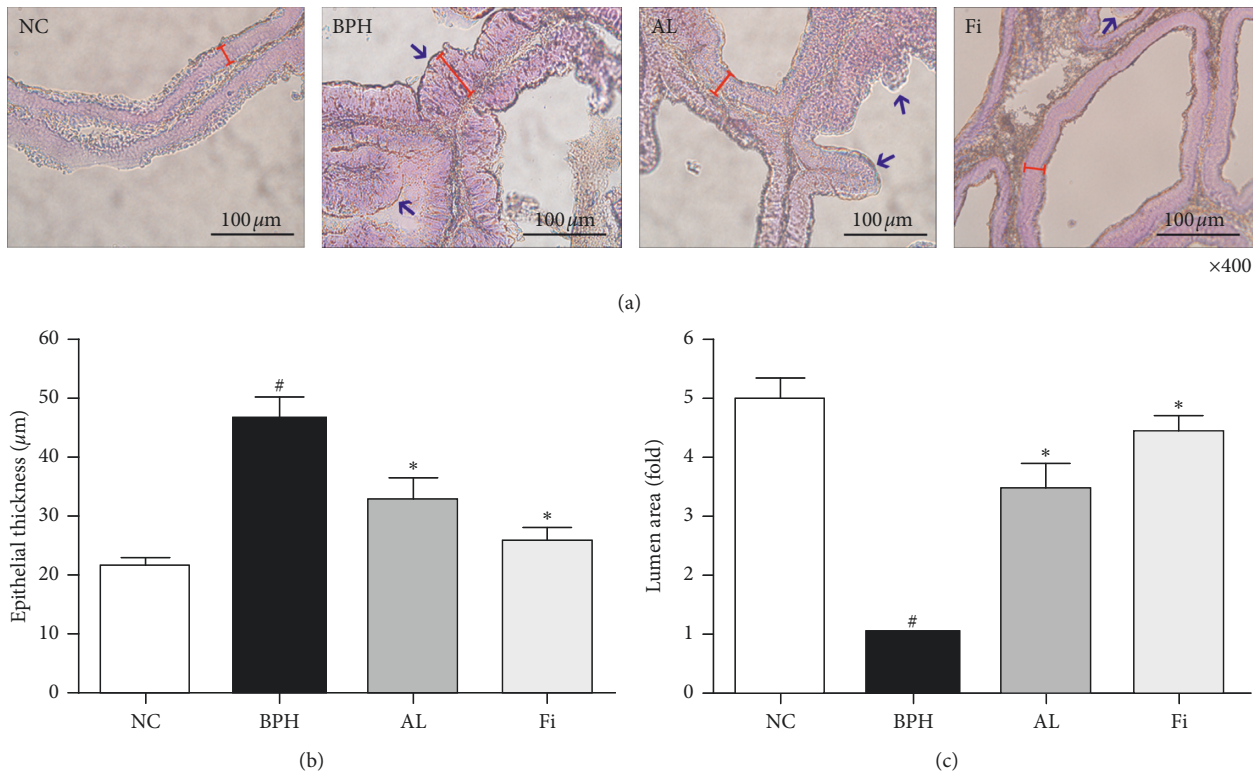

Figure 2: Effects of AL on histological changes in prostate tissues of TP-induced BPH rats. (a) Representative photomicrographs of H&E-stained prostate tissues (magnification ×400). Measurement of the (b) epithelial thickness and (c) relative lumen area of the prostate tissues using ImageJ software. Values are expressed as mean ± SD of ten or more separate measurements. $^{\#}P < 0.05$ when compared to NC; $^{*}P < 0.05$ when compared to BPH. NC, normal control group; BPH, TP-induced BPH group; AL, AL-treated BPH group; Fi, finasteride-treated BPH group.

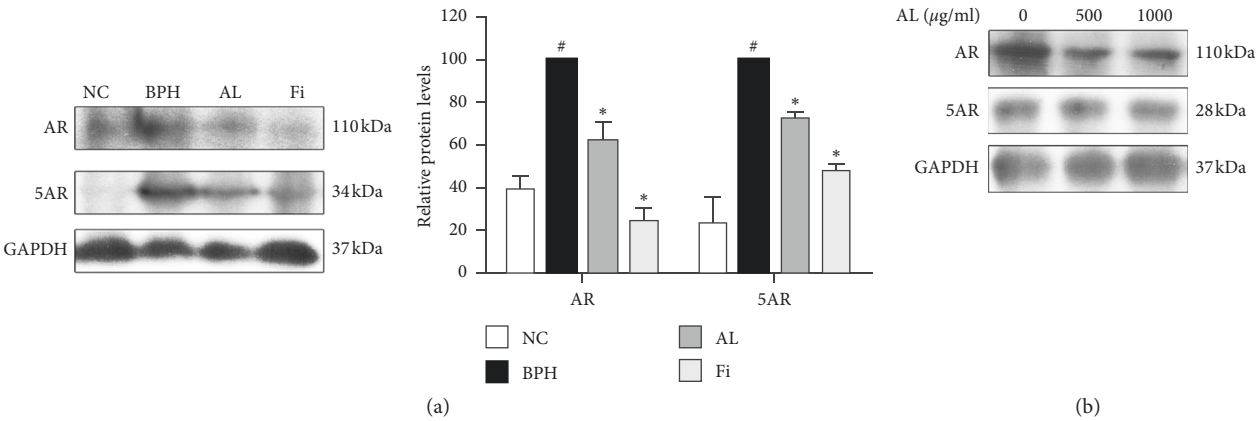

Figure 3: Effects of AL on expressions of 5AR and AR in prostate tissues of TP-induced BPH rats and LNCaP prostate cancer cells. Western blot analysis of the protein expressions of 5AR and AR from (a) prostate tissues of TP-induced BPH rats and (b) LNCaP prostate cancer cells. Protein expression values were normalized to GAPDH. Values are expressed as mean ± SD of three separate measurements. $^{\#}P < 0.05$ when compared to NC; $^{*}P < 0.05$ when compared to BPH. NC, normal control group; BPH, TP-induced BPH group; AL, AL-treated BPH group; Fi, finasteride-treated BPH group.

50% of males over 50 and 90% over 80 suffer from the symptoms of this chronic illness [2].

The pathological process of BPH associates with several molecular mechanisms. As described above, the 5AR-AR axis is considered the most crucial pathway of BPH. Besides 5AR and AR, the balance between cell proliferation and apoptosis is also closely related [33]. Apoptosis starts by two different programmed mechanisms. The extrinsic apoptosis is initiated by activation of Fas and tumor necrosis factor receptor 1, followed by cleavage of caspase-8 [34], while the intrinsic pathway begins by release of cytochrome c from the mitochondria and a subsequent activation of caspase-9 [35],

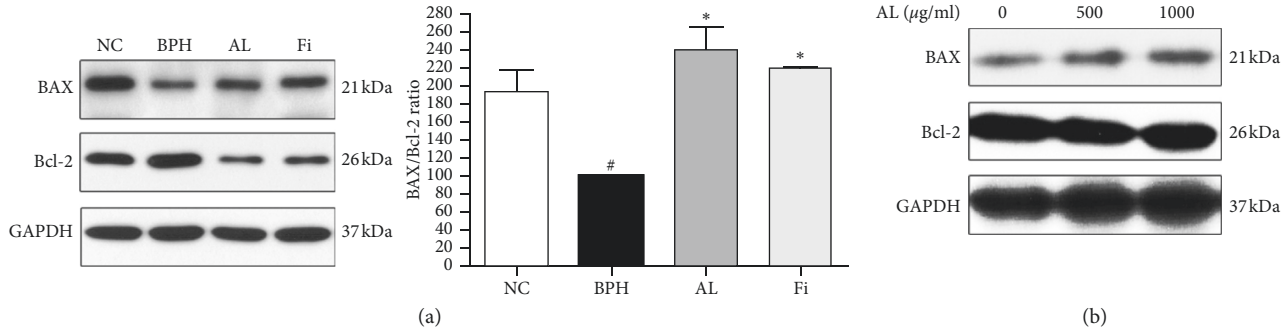

Figure 4: Effects of AL on BAX/Bcl-2 ratio in prostate tissues of TP-induced BPH rats and LNCaP prostate cancer cells. Western blotanalysis of the protein expressions of BAX and Bcl-2 from (a) prostate tissues of TP-induced BPH rats and (b) LNCaP prostate cancer cells.Values are expressed as mean ± SD of three separate measurements. $^{\#}P < 0.05$ when compared to NC; $^{*}P < 0.05$ when compared to BPH.NC, normal control group; BPH, TP-induced BPH group; AL, AL-treated BPH group; Fi, finasteride-treated BPH group.

and both pathways meet at the final few stages including cleavage of caspase-3, the effector caspase [36]. The intrinsic apoptosis is regulated by Bcl-2, a mitochondrial outer membrane-located protein which inhibits release of the proapoptotic factor cytochrome c [37]. The BAX gene was the first to be identified as a proapoptotic member among the Bcl-2 family [38]. BAX protein forms a heterodimer with Bcl-2 and then activates the apoptosis signal. Thus, the ratio of BAX and Bcl-2 determines the apoptotic sensitivity [39]. Under the normal condition, prostate tissues express relatively low levels of Bcl-2 and caspase-3, associated with a low level of apoptosis [40].

AL is the dried root of *Aconitum carmichaelii* Debx., a flowering plant of the genus *Aconitum*. As a native plant of East Asia, AL in traditional medicine has been used for centuries to treat extremely cold symptoms in China and Korea [41]. Although AL is extensively used as a potent herb in traditional Korean medicine, its toxicity requires careful preparation. Aconitine and related alkaloids are toxins which can impact the sympathetic-parasympathetic nerve systems and cardiovascular system [42]; however by heat-processing, they can be changed into rather safer alkaloids [43]. In this study, we investigated the possible use of AL as a novel herbal medication for BPH treatment.

The TP-induced BPH animal model [44] has been widely used for BPH studies because this model displays similar histologic characteristics and pathological abnormalities to humans as described by McNeal [45]. AL treatment suppressed the TP-induced enlargement of the prostate by 70% in prostate tissue weight and 74% in PI. The inhibition rate on both factors was higher than that of Fi treatment (62% in prostate tissue weight and 70% in PI). The pathohistological changes such as epithelial thickness and lumen area were recovered by AL as well. TP injection resulted in an increase of epithelial thickness and decrease of lumen area, associated with the increase of acinus numbers. AL-treated rats showed decreased thickness of the epithelium and increased lumen area while reducing the number of acini.

In addition, the two main pathways responsible for abnormal proliferation of the prostate, androgen-related pathway and apoptosis pathway, were regulated by AL treatment. As thoroughly described, the androgen-related pathway is a crucial pathogenic pathway of BPH. When testosterone is converted into the highly affinitive hormone DHT [5] by 5AR, it binds to the nuclear receptor AR and results in increased proliferation by the transcriptional activity of AR [6]. Studies including our previous ones showed improvement of BPH by suppressing these two factors [23–27]. Our current results also demonstrated that AL can reduce the expressions of 5AR and AR in both TP-induced BPH rats and LNCaP prostate cancer cells, suggesting the inhibitory effect of AL on the androgen pathway during the pathogenesis of BPH.

The balance between proliferation and apoptosis, which can be identified by BAX/Bcl-2 ratio, is also closely related to BPH [33]. While normal prostate shows a relatively low level of apoptosis, in BPH situations, imbalance between apoptosis and proliferation is displayed either by decreased apoptotic signals [40] or by increased proliferative factors such as proliferating cell nuclear antigen (PCNA) [46] and Ki67 [47]. In this study, AL treatment showed the restoration of BAX/Bcl-2 ratio which was significantly decreased by TP. In LNCaP cells, AL treatment increased the ratio of BAX and Bcl-2, indicating induced apoptosis in this prostate cancer cell line.

In addition to the suppressive effect of AL on 5AR and AR, AL treatment also significantly increased the ratio of BAX and Bcl-2, indicating upregulated apoptosis. Corresponding to previous reports [40], prostate tissues of NC rats showed relatively lower levels of Bcl-2 and higher levels of BAX, which were pathologically changed by TP injection. AL treatment restored the BAX/Bcl-2 ratio similar to that of NC rats. Similar results were observed in LNCaP prostate cancer cells, and AL treatment dose-dependently increased the ratio of BAX and Bcl-2.

5AR inhibitors such as Fi reduce the size of the prostate gland by inhibiting the activity of 5AR. However, sex-related side effects are frequently reported, including pathological apoptosis in the testis [29, 30]. Our results also demonstrated decreased cell density caused by Fi on the testis tissue, but AL-treated rats did not show any abnormal histological changes in the testis.

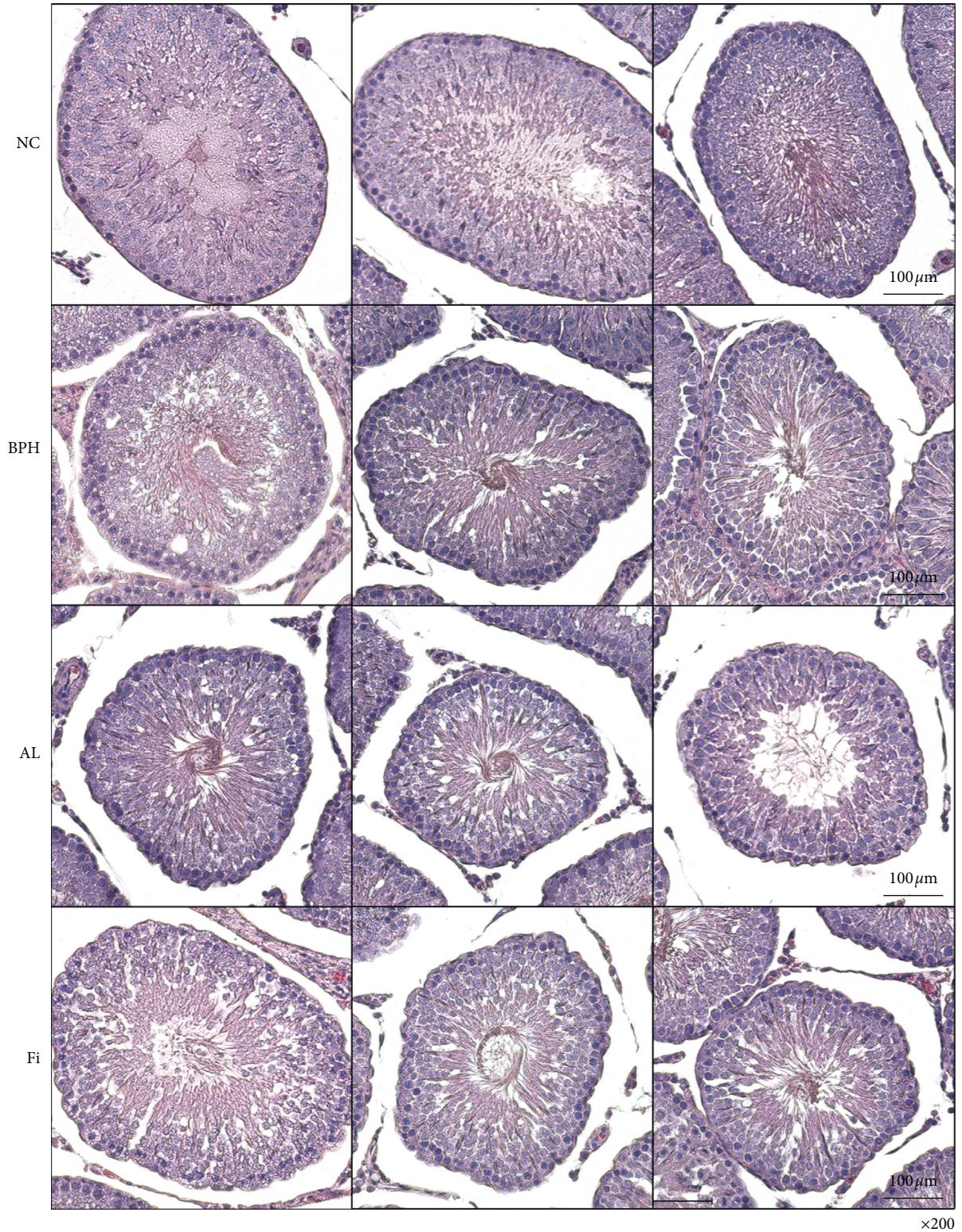

Figure 5: Effects of AL on histological changes in testis tissues of TP-induced BPH rats. Representative photomicrographs of H&E-stained testis tissues (magnification ×200) are shown. NC, normal control group; BPH, TP-induced BPH group; AL, AL-treated BPH group; Fi, finasteride-treated BPH group.

Hit identification is the basic level of small molecule discovery, and therefore, it is necessary to identify effective compounds to value the effects of natural products. Our LC-MS analysis identified three constituents which may possibly be responsible for the beneficial effect of AL on BPH. Although the molecular weight of identified compounds did not match exactly with that of previously known constituents of AL, based on previous reports [48, 49], there is a

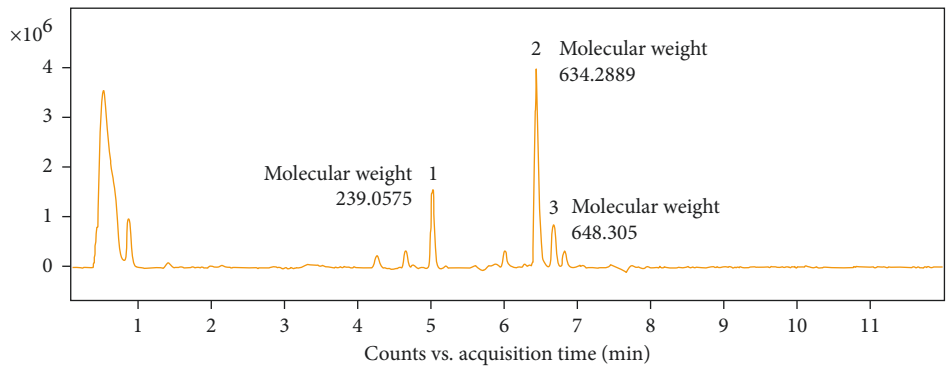

Figure 6: UHPLC analysis of AL: the representative chromatogram of AL and identification of its components.

Table 2: MS spectrum peak list.

No.	*m/z*	Abundance	Ion	Expected formula	Score
1	239.0575	764608.06	(M-H)-	$C_6H_{14}N_3O_5S$	88.81
2	634.2889	1565763	(M-H)-	$C_{20}H_{29}N_{25}O$	96.31
3	648.305	331263.47	(M-H)-	$C_{20}H_{45}N_{10}O_{14}$	97.24

possibility that component 1 (molecular weight: 239.0575) could be higenamine ($C_{16}H_{17}NO_3$; molecular weight: 271.316), component 2 (molecular weight: 634.2889) could be hypaconitine ($C_{33}H_{45}NO_{10}$; molecular weight: 615.72) or mesaconitine ($C_{33}H_{45}NO_{11}$; molecular weight: 631.719), and component 3 (molecular weight: 648.305) could be aconitine ($C_{34}H_{47}NO_{11}$; molecular weight: 645.746). However, to clarify, further studies should be carried out with different fractions and/or identified constituents to confirm which is the active compound responsible for the effects of AL.

5. Conclusions

In conclusion, we confirmed increased levels of 5AR and AR and a decreased ratio of BAX and Bcl-2 as well as the changes of the histological structure in BPH rats. These changes were reversed by AL treatment, and in addition, AL-treated LNCaP cells also showed similar results. Furthermore, AL treatment did not induce any abnormal changes in the histology of the testis as Fi treatment did. These results suggest AL as a potentially safe nature-derived therapeutic agent for BPH treatment.

Data Availability

All raw data supporting the results of this study are available from the corresponding author upon request.

Conflicts of Interest

The authors declare that they have no conflicts of interest.

Authors' Contributions

Jinbong Park and Dong-Hyun Youn contributed equally to this paper and are co-first authors.Jae-Young Um developed the experimental design and conducted the study. Jinbong Park and Dong-Hyun Youn performed the experiments. Jinbong Park wrote the manuscript. All authors read and approved the final manuscript for submission.

Acknowledgments

This study was supported by the National Research Foundation of Korea (NRF-2018R1D1A1B07049882 and NRF-2018R1A2A3075684).

Supplementary Materials

Supplementary Figure S1: effects of AL on cell viability in LNCaP cells. The MTS assay was performed in order to measure the effect of AL on cell viability in LNCaP cells. (*Supplementary Materials*)

References

[1] C. Carson 3rd and R. Rittmaster, "The role of dihydrotestosterone in benign prostatic hyperplasia," *Urology*, vol. 61, no. 4, pp. 2–7, 2003.

[2] J. Barkin, "Benign prostatic hyperplasia and lower urinary tract symptoms: evidence and approaches for best case management," *Canadian Journal of Urology*, vol. 18, pp. 14–19, 2011.

[3] S. Madersbacher, N. Sampson, and Z. Culig, "Pathophysiology of benign prostatic hyperplasia and benign prostatic enlargement: a mini-review," *Gerontology*, vol. 3, pp. 1–7, 2019.

[4] W. D. Steers, "5α-reductase activity in the prostate," *Urology*, vol. 58, no. 6, pp. 17–24, 2001.

[5] W. Gao, C. E. Bohl, and J. T. Dalton, "Chemistry and structural biology of androgen receptor," *Chemical Reviews*, vol. 105, no. 9, pp. 3352–3370, 2005.

[6] C. G. Roehrborn, "The utility of serum prostatic-specific antigen in the management of men with benign prostatic hyperplasia," *International Journal of Impotence Research*, vol. 20, no. S3, pp. S19–S26, 2008.

[7] L. Black, M. J. Naslund, T. D. Gilbert Jr., E. A. Davis, and D. A. Ollendorf, "An examination of treatment patterns and costs of care among patients with benign prostatic hyperplasia," *American Journal of Managed Care*, vol. 12, no. 4 Suppl, pp. S99–s110, 2006.

[8] C. Roehrborn and R. C. Rosen, "Medical therapy options for aging men with benign prostatic hyperplasia: focus on alfuzosin 10 mg once daily," *Clinical Interventions in Aging*, vol. 3, no. 3, pp. 511–524, 2008.

[9] T. L. Bullock and G. L. Andriole Jr., "Emerging drug therapies for benign prostatic hyperplasia," *Expert Opinion on Emerging Drugs*, vol. 11, no. 1, pp. 111–123, 2006.

[10] A. M. Traish, J. Hassani, A. T. Guay, M. Zitzmann, and M. L. Hansen, "Adverse side effects of 5α-reductase inhibitors therapy: persistent diminished libido and erectile dysfunction and depression in a subset of patients," *Journal of Sexual Medicine*, vol. 8, no. 3, pp. 872–884, 2011.

[11] S. Gravas and M. Oelke, "Current status of 5α-reductase inhibitors in the management of lower urinary tract symptoms and BPH," *World Journal of Urology*, vol. 28, no. 1, pp. 9–15, 2009.

[12] J. D. McConnell, R. Bruskewitz, P. Walsh et al., "The effect of finasteride on the risk of acute urinary retention and the need for surgical treatment among men with benign prostatic hyperplasia. Finasteride long-term efficacy and safety study group," *New England Journal of Medicine*, vol. 338, no. 9, pp. 557–563, 1998.

[13] J. B. Calixto, "Efficacy, safety, quality control, marketing and regulatory guidelines for herbal medicines (phytotherapeutic agents)," *Brazilian Journal of Medical and Biological Research*, vol. 33, no. 2, pp. 179–189, 2000.

[14] T. Suzuki, K. Miyamoto, N. Yokoyama et al., "Processed aconite root and its active ingredient neoline may alleviate oxaliplatin-induced peripheral neuropathic pain," *Journal of Ethnopharmacology*, vol. 186, pp. 44–52, 2016.

[15] Z. Wang, "Clinical application of *Radix aconiti* lateralis preparata," *Journal of Traditional Chinese Medicine*, vol. 19, no. 2, pp. 154-155, 1999.

[16] S. Schröder, K. Beckmann, G. Franconi et al., "Can medical herbs stimulate regeneration or neuroprotection and treat neuropathic pain in chemotherapy-induced peripheral neuropathy?," *Evidence-Based Complementary and Alternative Medicine*, vol. 2013, Article ID 423713, 18 pages, 2013.

[17] T. Gao, H. Bi, S. Ma, and J. Lu, "The antitumor and immunostimulating activities of water soluble polysaccharides from *Radix aconiti*, *Radix aconiti* lateralis and *Radix aconiti kusnezoffii*," *Natural Product Communications*, vol. 5, no. 3, article 1934578X1000500, 2010.

[18] W. Kim, W. Lee, J. G. Choi et al., "Inhibitory effects of Aconiti Lateralis Radix Preparata on chronic intermittent cold-induced inflammation in the mouse hypothalamus," *Journal of Ethnopharmacology*, vol. 215, pp. 27–33, 2018.

[19] M. Murayama, T. Mori, H. Bando, and T. Amiya, "Studies on the constituents of *Aconitum* species. IX. The pharmacological properties of pyro-type aconitine alkaloids, components of processed aconite powder "kako-bushi-matsu:" analgesic, antiinflammatory and acute toxic activities," *Journal of Ethnopharmacol*, vol. 35, no. 2, pp. 159–164, 1991.

[20] T. Zuo, X. S. Fan, S. Tian, C. X. Jiang, and F. Chen, "Clinical study on aconite prescriptions with incompatible herbs in different areas based on association rules and analysis on compatibility features," *Zhongguo Zhong Yao Za Zhi*, vol. 40, no. 6, pp. 1198–1202, 2015.

[21] R. K. Dumbre, M. B. Kamble, and V. R. Patil, "Inhibitory effects by ayurvedic plants on prostate enlargement induced in rats," *Pharmacognosy Research*, vol. 6, no. 2, pp. 127–132, 2014.

[22] J. Zhang, J. Han, A. Oyeleye, M. Liu, X. Liu, and L. Zhang, "Extraction methods of natural products from traditional Chinese medicines," in *Methods in Molecular Biology*, J. Hempel, C. Williams, and C. Hong, Eds., vol. 1263, pp 177-185, Humana Press, New York, NY, USA, 2015.

[23] H. M. Choi, Y. Jung, J. Park et al., "Cinnamomi cortex (*Cinnamomum verum*) suppresses testosterone-induced benign prostatic hyperplasia by regulating 5alpha-reductase," *Scientific Reports*, vol. 6, no. 1, article 31906, 2016.

[24] Y. Jung, J. Park, H. L. Kim et al., "Vanillic acid attenuates testosterone-induced benign prostatic hyperplasia in rats and inhibits proliferation of prostatic epithelial cells," *Oncotarget*, vol. 8, no. 50, pp. 87194–87208, 2017.

[25] D. H. Youn, J. Park, H. L. Kim et al., "Berberine improves benign prostatic hyperplasia via suppression of 5 alpha reductase and extracellular signal-regulated kinase in vivo and in vitro," *Frontiers in Pharmacology*, vol. 9, p. 773, 2018.

[26] D. H. Youn, J. Park, H. L. Kim et al., "Chrysophanic acid reduces testosterone-induced benign prostatic hyperplasia in rats by suppressing 5alpha-reductase and extracellular signal-regulated kinase," *Oncotarget*, vol. 8, no. 6, pp. 9500–9512, 2017.

[27] Y. Jung, J. Park, H.-L. Kim et al., "Vanillic acid attenuates obesity via activation of the AMPK pathway and thermogenic factors in vivo and in vitro," *FASEB Journal*, vol. 32, no. 3, pp. 1388–1402, 2018.

[28] Z. Saker, O. Tsintsadze, I. Jiqia, L. Managadze, and A. Chkhotua, "Importance of apoptosis markers (MDM2, Bcl-2 and Bax) in benign prostatic hyperplasia and prostate cancer," *Georgian Medical News*, vol. 249, pp. 7–14, 2015.

[29] A. Kolasa-Wolosiuk, K. Misiakiewicz-Has, I. Baranowska-Bosiacka, I. Gutowska, and B. Wiszniewska, "Androgen levels and apoptosis in the testis during postnatal development of finasteride-treated male rat offspring," *Folia Histochemica et Cytobiologica*, vol. 53, no. 3, pp. 236–248, 2015.

[30] K. K. Soni, Y. S. Shin, B. R. Choi et al., "Protective effect of DA-9401 in finasteride-induced apoptosis in rat testis: inositol requiring kinase 1 and c-Jun N-terminal kinase pathway," *Drug Design, Development and Therapy*, vol. 11, pp. 2969–2979, 2017.

[31] K. Ozer, M. O. Horsanali, S. N. Gorgel, B. O. Horsanali, and E. Ozbek, "Association between benign prostatic hyperplasia and neutrophil-lymphocyte ratio, an indicator of inflammation and metabolic syndrome," *Urologia Internationalis*, vol. 98, no. 4, pp. 466–471, 2017.

[32] U. Blankstein, B. Van Asseldonk, and D. S. Elterman, "BPH update: medical versus interventional management," *Canadian Journal of Urology*, vol. 23, no. Suppl 1, pp. 10–15, 2016.

[33] B. Pawlicki, H. Zielinski, and M. Dabrowski, "Role of apoptosis and chronic prostatitis in the pathogenesis of benign prostatic hyperplasia," *Pol Merkur Lekarski*, vol. 17, no. 100, pp. 307–310, 2004.

[34] S. Nagata, "Fas ligand-induced apoptosis," *Annual Review of Genetics*, vol. 33, no. 1, pp. 29–55, 1999.

[35] K. Wang, X. M. Yin, D. T. Chao, C. L. Milliman, and S. J. Korsmeyer, "BID: a novel BH_3 domain-only death agonist," *Genes & Development*, vol. 10, no. 22, pp. 2859–2869, 1996.

[36] W. C. Earnshaw, L. M. Martins, and S. H. Kaufmann, "Mammalian caspases: structure, activation, substrates, and functions during apoptosis," *Annual Review of Biochemistry*, vol. 68, no. 1, pp. 383–424, 1999.

[37] D. Xu, X. Wang, C. Jiang, Y. Ruan, S. Xia, and X. Wang, "The androgen receptor plays different roles in macrophage-induced proliferation in prostate stromal cells between transitional and peripheral zones of benign prostatic hypertrophy," *Excli Journal*, vol. 16, pp. 939–948, 2017.

[38] Z. N. Oltvai, C. L. Milliman, and S. J. Korsmeyer, "Bcl-2 heterodimerizes in vivo with a conserved homolog, Bax, that

accelerates programmed cell death," *Cell*, vol. 74, no. 4, pp. 609–619, 1993.

[39] S. Salakou, D. Kardamakis, A. C. Tsamandas et al., "Increased Bax/Bcl-2 ratio up-regulates caspase-3 and increases apoptosis in the thymus of patients with myasthenia gravis," *In Vivo*, vol. 21, no. 1, pp. 123–132, 2007.

[40] K. T. McVary, "BPH: Epidemiology and comorbidities," *American Journal of Managed Care*, vol. 12, no. 5 Suppl, pp. S122–S128, 2006.

[41] G. Zhou, L. Tang, X. Zhou, T. Wang, Z. Kou, and Z. Wang, "A review on phytochemistry and pharmacological activities of the processed lateral root of *Aconitum carmichaelii* Debeaux," *Journal of Ethnopharmacology*, vol. 160, pp. 173–193, 2015.

[42] T. Y. K. Chan, "Aconite poisoning," *Clinical Toxicology*, vol. 47, no. 4, pp. 279–285, 2009.

[43] A. Ameri, "The effects of *Aconitum* alkaloids on the central nervous system," *Progress in Neurobiology*, vol. 56, no. 2, pp. 211–235, 1998.

[44] T. Kato, T. Ishibe, M. Hirayama, M. Fukushige, I. Takenaka, and M. Kazuta, "Basic studies on the prostate of rat under various hormonal environment," *Endocrinologia Japonica*, vol. 12, no. 1, pp. 1–8, 1965.

[45] J. E. McNeal, "Normal and pathologic anatomy of prostate," *Urology*, vol. 17, no. Suppl 3, pp. 11–16, 1981.

[46] W. Zhong, J. Peng, H. He et al., "Ki-67 and PCNA expression in prostate cancer and benign prostatic hyperplasia," *Clinical & Investigative Medicine*, vol. 31, no. 1, pp. E8–E15, 2008.

[47] C. E. Fonseca-Alves, P. E. Kobayashi, and C. Palmieri, "Investigation of c-KIT and Ki67 expression in normal, preneoplastic and neoplastic canine prostate," *BMC Veterinary Research*, vol. 13, no. 1, p. 380, 2017.

[48] G. Bai, Y. Yang, Q. Shi, Z. Liu, Q. Zhang, and Y.-Y. Zhu, "Identification of higenamine in *Radix aconiti* lateralis preparata as a beta2-adrenergic receptor agonist," *Acta Pharmacologica Sinica*, vol. 29, no. 10, pp. 1187–1194, 2008.

[49] B. Yu, Y. Cao, and Y.-K. Xiong, "Pharmacokinetics of aconitine-type alkaloids after oral administration of Fuzi (*Aconiti lateralis Radix praeparata*) in rats with chronic heart failure by microdialysis and ultra-high performance liquid chromatography-tandem mass spectrometry," *Journal of Ethnopharmacology*, vol. 165, pp. 173–179, 2015.

Hindawi
Evidence-Based Complementary and Alternative Medicine
Volume 2019, Article ID 8619283, 9 pages
https://doi.org/10.1155/2019/8619283

Research Article

Nymphaea lotus Linn. (Nymphaeaceae) Alleviates Sexual Disability in L-NAME Hypertensive Male Rats

Poumeni Mireille Kameni,[1] **Djomeni Paul Desire Dzeufiet**,[1] **Danielle Claude Bilanda**,[1] **Marguerite Francine Mballa**,[1] **Ngadena Yolande Sandrine Mengue**,[1] **Tchinda Huguette Tchoupou**,[1] **Agnes Carolle Ouafo**,[1,2] **Madeleine Chantal Ngoungoure**,[1] **Theophile Dimo**,[1] **and Pierre Kamtchouing**[1]

[1]*Laboratory of Animal Physiology, Faculty of Science, University of Yaounde I, P.O. BOX 812, Yaounde, Cameroon*
[2]*Laboratory of Biological Sciences, Faculty of Science, University of Bamenda, P.O. BOX 39 Bambili, Bamenda, Cameroon*

Correspondence should be addressed to Poumeni Mireille Kameni; miraiye@yahoo.fr

Received 20 March 2019; Revised 20 May 2019; Accepted 28 May 2019; Published 29 July 2019

Guest Editor: Arielle Cristina Arena

Hypertension (HT) is a risk factor for erectile dysfunction (ED). This study aimed to evaluate the suppressive effect of *Nymphaea lotus* (*N. lotus*) on erectile dysfunction induced by NO deficiency in rat. 40 male rats equally divided into 4 groups received an oral treatment with 10 mg/kg/day of L-NAME, a NO blocker, during 4 weeks. Control group composed of 10 male rats received only distilled water (10 mL/kg). Thereafter oral treatments with *N. lotus* (75 and 200 mg/kg/day) and losartan (10 mg/kg/day) started and continued concomitantly with L-NAME in 3 groups for 4 additional weeks. Normal and negative controls received only distilled water. Sexual behaviour, orientation activities, anxiety, and penile histomorphology were evaluated at the end of treatment. L-NAME administration elevated significantly the blood pressure in male rats and decreased the copulatory rate by enhancing intromission latency and decreasing the numbers of intromission and ejaculation. However, the sexual motivation remains unaltered by chronic NO blockage suggesting that L-NAME induces penile dysfunction mainly by peripheral mechanisms. L-NAME chronic intake also induced anxiety, 4 weeks of *N. lotus* cotreatment prevented inhibitory effects of L-NAME on male sexual behaviour by shortening mainly ejaculation latency and postejaculatory interval while losartan does not. Losartan proved to be a more effective drug to decrease the blood pressure compared to the plant extract. Effectively, *Nymphea lotus* was able to reverse totally at 75 mg/kg the increment of hemodynamic parameters and the histological damage and exhibit anxiolytic-like effects in hypertensive male rats. *Nymphaea lotus* uses NO pathway to facilitate sexual responses at central and peripheral levels and can have a double medicinal use, against anxiety and erectile dysfunction.

1. Introduction

Erectile dysfunction (ED) is defined as the inability to achieve and/or maintain sufficient erection to allow satisfactory sexual intercourse. This symptom is quite common in people suffering from hypertension (HT). In fact, 30% of them present ED compared to normotensive people. The severity of this secondary condition is directly proportional to the severity of HT [1, 2]. Effectively, the evolution of HT is associated with several deleterious effects on the structure and function of the systemic blood vessels, so penile vascularization is not spared. The HT gradually deteriorates the integrity of the endothelial tissues, which are the support of the erection mechanism. The dysfunction of these tissues thus promotes the gradual installation of ED and is continually maintained by oxidative stress and inflammatory conditions associated with HT [3]. Indeed, free radicals and oxidative stress are toxic to the endothelium. They interfere with the signaling pathway of nitric oxide (NO), causing damage responsible for the occurrence of ED [4].

Other causes responsible for ED in people with HT are, namely, a deficiency in NO or even a psychological or nervous condition [5]. However, the involvement of the nervous system has not been clarified in the ED related to HT.

Currently, plants have received more attention regarding their use as therapeutic agents. In Cameroon, *Nymphaea lotus* Linn (*N. lotus*)—a plant belonging to the family Nymphaeaceae—is used in popular medicine for its aphrodisiac, astringent, and anti-inflammatory properties [6]. It would also produce sedative effects on the nervous system [7, 8]. Besides, pharmacological long-term blockage of NO synthesis by the chronic administration of L-NAME, an inhibitor of nitric oxide synthase (NOS), has been reported to produce systemic arterial hypertension, vascular structural change, and erectile dysfunction in animal models [9, 10]. Thus the present work has been undertaken to assess the effects of *Nymphaea lotus* Linn flowers on peripheral and central components of the mating behaviour in a rat model of NO deficiency-induced hypertension.

2. Materials and Methods

2.1. Preparation of Plant Extract. *Nymphaea lotus* Linn flowers have been collected and prepared as previously described [11]. The flowers were cleaned, dried in the shade, and then crushed. The powder obtained served for the preparation of the aqueous extract (50 g of powder per liter of tap water). The dry extract was then reconstituted in distilled water at appropriate concentrations for the experiment and administered orally in a volume of 10 mL/kg body weight.

2.2. Preliminary Qualitative Phytochemical Analysis. According to the secondary compounds highlighted, the following reagents were used for phytochemical analysis of the aqueous extract of *N. lotus* flowers: Flavonoids (Mg^{2+}), alkaloids (modified Dragendorff reagents), saponins (frothing test), Tannins (FeCl3), reducing substances (Fehling A and B Solutions), cardiac glycosides (Salkowski test), phenols ($FeCl_3$ and $K_3Fe(CN)$), anthocyanins (acid), and lipids (filter paper) [12].

2.3. Quantitative Phytochemical Analysis. The Folin-Ciocalteu'method [13] was used for the determination of total phenolic content which was calculated using a calibration curve of gallic acid serial dilutions and expressed as mg of gallic acid equivalents per g of dried extract. The total flavonoid content was determined using a calibration curve of the rutin and expressed in mg of rutin per g of dry extract [14].

2.4. Drugs and Chemicals. Nω-nitro-L-arginine methyl ester (L-NAME) and urethane were obtained from Sigma-Aldrich (St. Louis, MO, USA). Estradiol benzoate was purchased from Sigma Chemical company. Progesterone caproate was procured from Bayern Schering Pharma (Berlin, Germany) and losartan (Losar-Denk 50) was obtained from Denk Pharma (München, Germany).

2.5. Animal Treatment. The experiments were carried out in accordance with the principles of laboratory animal protection approved by the Ethics Committee of the University of Yaoundé I. Male Wistar rats used for experimentation were provided by the animal house of the Animal Physiology Laboratory (University of Yaoundé I, Cameroon). These eight weeks old rats were sexually experimented by cohabitation with females (ratio 2:1), under a natural day light cycle, and supplied *ad libitum* with water and soy free chow. After 4 weeks of cohabitation, a pretest was carried out and animals displaying hyposexual activities (< 1 ejaculation on average) were disqualified for the study. The others were randomly divided into five groups of 10 animals each and treated according to their respective body weights.

Group I: rats receiving only distilled water;

Group II: L-NAME-treated rats (10 mg/kg);

Group III: rats treated with L-NAME + losartan (10 mg/kg);

Group IV: rats treated with L-NAME + extract of *N. lotus* (75 mg/kg);

Group V: rats treated with L-NAME + extract of *N. lotus* (200 mg/kg).

The animals received L-NAME alone for 4 weeks, and then the different treatments were added concomitantly to the latter (Figure 1). All these products have been administered orally. After the last administration (Day 60), rats were fasted all night; blood pressure and heart rate were recorded in the morning (Day 61).

2.6. Behavioural Tests

2.6.1. Measurement of Anxiety and Motor-Related Behaviour. The rat Suok test (ST) is based on the measurement of animal behaviour ethological analysis of the animal's exploration in the elevated novel alley following a protocol described by Kalueff et al. [15] *(Supplementary Material)*.

2.6.2. Measurement of General Mating Behaviour. The experiment was carried out on day 60, one hour after the final treatment of the male rats. The experiment was conducted at 7:00 pm under dim light. Receptive female rats (estradiol benzoate 12 μg in olive oil injected intramuscularly 48 h prior to pairing plus progesterone 0.5 mg in olive oil injected intramuscularly 6 h prior to pairing) were introduced into the cages of male animals with 1 female to 1 male. The observation for mating behaviour was immediately commenced and continued for 30 minutes according to the method used by Kada et al. [16]. The following measurements were recorded or calculated: mount latency, the time from onset of the test to the first mount with or without penile insertion; intromission latency, the time from the introduction of the female to first penile insertion; ejaculatory latency, time from the first intromission to ejaculation; mount number, the number of the mounts without intromission prior to ejaculation; intromission number, the number of mounts with intromission before ejaculation; postejaculatory interval, time from ejaculation to the first intromission of the second copulatory series; copulatory efficiency, a measure of intromission success (calculated as percentage of mounts in which the male gained vaginal insertion).

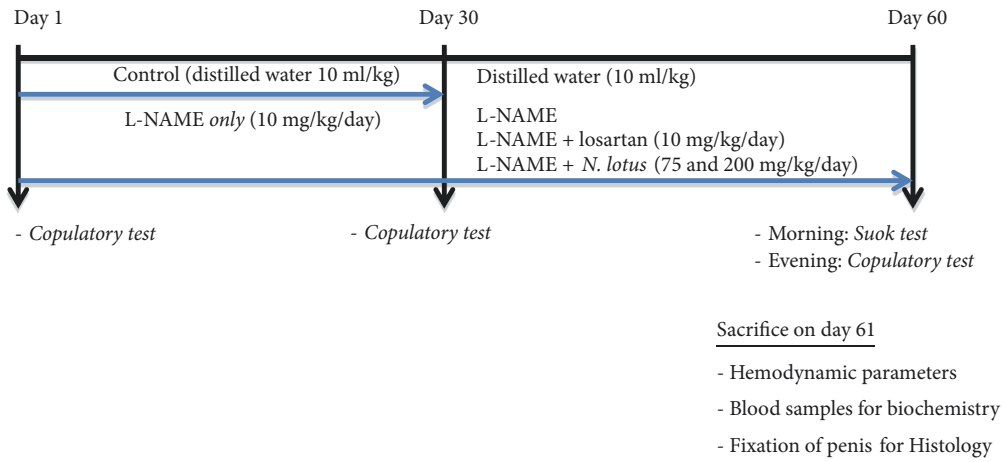

Figure 1: Experimental procedure.

Temporal patterning was expressed as non-"postejaculation" pauses number, the number of pauses following mount or intromission interrupted before ejaculation, and the cumulative duration of the non-"postejaculation" pauses, the summary of interval from the beginning of one pause to the start of the next mount.

The test was terminated if the male failed to evince sexual interest after 10 minutes from the beginning of observation. If the female did not show receptivity, another artificially warmed female replaced it.

2.7. Biochemical Parameters

2.7.1. Blood Pressure and Heart Rate Measurements. Blood pressure and heart rate were recorded by direct method [17]. Rats were anaesthetized with intraperitoneal injection of 15% ethyl carbamate (1.5 g/kg). The trachea was exposed and cannulated to facilitate spontaneous respiration. A polyethylene catheter was inserted into the rat carotid artery. This catheter was linked to the transducer connected to the recorder hemodynamic Biopac Student Lab MP type 35. Another catheter was inserted into the femoral vein and a bolus injection of 10% heparin (0.1 mL/100g body weight) was immediately administered. The animal was then equilibrated for at least 15 min before the blood parameters (systolic and diastolic blood pressure) and heart rate was recorded.

2.7.2. Relative Penile Weight and Histological Analysis. After recording of cardiovascular parameters, the animals were sacrificed by decapitation. Thereafter penis was removed and weighed using 4-digital electronic balance (Mettler PL301). For histological studies, the penile tissues were fixed in 4%PFA for 48 hours and then dehydrated in graded (50-100%) alcohol and embedded in paraffin. Thin sections (5 μm) were cut with a microtome (Reichert-Jung 2030) and stained with Mallory Trichrome staining for observations.

2.8. Data Analysis. Statistical analysis was carried out using the Statistical Package for Social Sciences version 21.0 for MAC (SPSS Inc, Chicago, IL, USA) software. Data are presented as mean ± standard error of mean (S.E.M.). One-way analysis of variance (ANOVA), followed by Tukey post hoc test, was used. A probability level less than 0.05 was accepted as significant.

3. Results

3.1. Preliminary Qualitative Phytochemical Analysis of the Aqueous Extract of N. lotus Flowers. The aqueous extract of *N. lotus* contained flavonoids, alkaloids, saponins, tannins, anthraquinones, phenolic compounds, glycosides, cardiac glycosides, but not anthocyanins and lipids (Table 1).

3.2. Total Phenolic and Flavonoids Contents of N. lotus. In *N. lotus* aqueous extract, total phenolic compound was found to be 71.29±0.11 mg/g of dried extract, calculated as gallic acid equivalent and total flavonoids compound was 7.15±0.87 mg/g of dried extract, calculated as rutin equivalent.

3.3. Effect of N. lotus Aqueous Extract on General Features of the Experimental Animal Groups. The L-NAME treatment did not alter body weight and penile weight significantly. In the same manner, losartan or *N. lotus* did not alter these parameters.

The systolic, mean, and diastolic blood pressures were significantly higher in the L-NAME group compared to the control group. Effectively, the chronic L-NAME (10 mg/kg) treatment significantly increased mean blood pressure (MBP) ($P<0.001$) versus baseline whereas additional treatment with *N. lotus* (75 mg/kg) and losartan (10 mg/kg) prevented the increment of arterial blood pressure. Contrarily, *N. lotus* at the level of 200 mg/kg significantly ($P<0.001$) enhanced the mean blood pressure compared to baseline (Table 2).

3.4. Effect of N. lotus Aqueous Extract on Behaviour

3.4.1. Effect of N. lotus Aqueous Extract on Anxiety and Motor-Related Behaviour. L-NAME administration during 60 days induced a reduction of directed exploration (34.38%), horizontal (HA) and vertical activities respectively by 19.91% and 45.45% compared to control, whereas it provokes an

Table 1: Phytochemical screening of aqueous flowers extract of *Nymphaea lotus* Linn.

Tests	Results
Tannins (Ferric chloride test)	+
Phenolic compounds (FeCl3 and K3Fe (CN))	+
Reducing substances (Fehling A and B test)	+
Alkaloids (Dragendorff's test)	+
Anthocyans (Acid)	-
Cardiac glycosides (Salkowski test)	+
Flavonoids (Mg^{2+})	+
Lipids (Filter paper)	-
Saponins (Frothing test)	+

(+): present and (-): absent.

Table 2: Effect of *Nymphaea lotus* on general features of the experimental animal groups after 60 days of treatment.

Groups	Body Weight (g)	Penile Weight (g)	PBR ($\times 10^{-2}$)	Heart rate (bpm)	Blood pressure (mmHg)		
					Systolic	Mean	Diastolic
Control	195.20±12.65	0.29±0.02	15.05±0.67	337.82±4.67	97.87±2.69	88.52±1.96	83.85±3.15
L-NAME	212.80±7.47	0.28±0.01	13.28±0.38	371.40±3.38	154.39±6.29 **a**	147.73±4.09 **a**	144.40±3.17 **a**
LNAME-LSRT	200.80±11.93	0.29±0.01	14.66±1.06	354.38±13.73	103.95±4.77 **b**	101.40±4.00 **b**	100.13±5.00 **b**
LNAME-NL75	217.00±7.64	0.32±0.02	14.61±1.13	360.13±3.42	134.27±11.08 **ac**	131.53±1.54 **abc**	130.16±4.94 **ac**
LNAME-NL200	212.00±8.67	0.29±0.01	13.47±0.18	380.55±11.34 **a**	157.70±3.79 **ac**∗	151.14±4.44 **ac**∗	149.37±4.80 **ac**

Each value represents the mean ± SEM of group. For comparisons among control and experimental groups, a = significantly different compared to Control; b = significantly different compared to L-NAME group; c = significantly different compared to LNAME-LSRT; ∗ dose-dependence between two extract doses. The exact value of P is mentioned in the text. PBR: penile weight/body weight. SBP: systolic blood pressure, DBP: diastolic blood pressure, MBP: mean blood pressure, HR: heart rate.

significant increase ($P<0.001$) of latency to leave (LL), as well as a significant increase of missteps (MS) ($P<0.01$) and motor incoordination index (MI) ($P<0.01$). Cotreatments with losartan and plant extract at the doses of 75 and 200 mg/kg induced respectively a decrease of the LL by 25.84%, 36.48%, and 43.91% compared to nontreated animals; by 26.55%, 38.98%, and 13.56% of the number of HA; and by 29.58%, 43.64%, and 56.01% of the number of MS and MI compared to L-NAME group. Contrarily to losartan, additional treatment with *N. lotus* at both doses induced a significant decrease ($P<0.05$ and $P<0.01$) of the number of defecation compared to control. All general features of the animal groups are presented at Table 3.

3.4.2. Effect of N. lotus Aqueous Extract on Orientation Activities. The aqueous extract of *Nymphaea lotus* flowers at the dose level of 200 mg/kg markedly influenced the orientation behaviour of the hypertensive animals, which showed more attraction towards female rats (Figure 2).

3.4.3. Effects of Hypertension on Male Rat Sexual Behaviour. After 60 days, L-NAME treatment drastically reduced the number of animals displaying ejaculation. Effectively all the animals achieved mounting (Table 4), but only 4/10 rats treated with L-NAME reached ejaculation within 30 min of testing (Table 5).

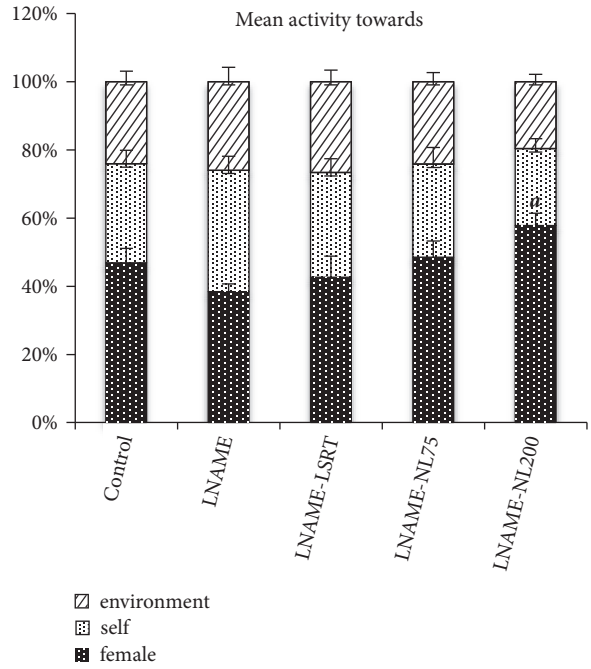

Figure 2: Effect of aqueous extract of *Nymphaea lotus* flowers on orientation activities in L-NAME treated male rats. Each bar represents the mean ± S.E.M. of group; [a] is significantly different compared to control. The exact value of P is mentioned in the text.

Table 3: Effect of *N. lotus* on anxiety and ambulatory parameters.

Measures and behavioural domains		Mean ± SEM				
		Control	LNAME	LNAME-LSRT	LNAME-NL75	LNAME-NL200
(I) Exploration						
HA	Horizontal activity	44.20±1.36	35.40±2.64	26.00±1.67 ***a***	21.60±2.01 **a**	30.60±2.29
VA	Vertical activity	4.40±0.68	2.40±0.75	2.60±0.40	4.80±0.73	4.60±0.68
SA	Stopping activity	3.00±0.32	1.40±0.24	1.60±0.40	1.80±0.58	2.80±0.58
DE	Directed exploration	32.00±2.24	21.00±1.22	23.80±4.04	28.20±1.59	34.00±1.73
LL	Latency to leave	8.87±0.73	35.64±1.52 **a**	26.43±2.86 **ab**	22.64±2.98 **ab**	19.99±1.29 **ab**
ID	Interstop distance	15.50±1.99	28.30±4.96	19.93±4.13	15.95±3.65	12.45±1.99 **b**
(II) Displacement (D)						
FD	Frequency	3.40±0.24	2.40±0.24	5.40±0.68	2.00±0.32	3.40±0.51
DD	Duration (s)	16.00±0.71	12.20±1.74	31.00±3.11	17.80±0.73	23.80±2.91
(III) Vegetative behaviours						
DB	Defecation	4.00±0.32	3.00±0.45	4.60±0.24	0.60±0.40 ***ac***	0.00±0.00 ***abc***
UR	Urination	0.4±0.4	0.00±0.00	1.00±0.63	0.20±0.20	0.00±0.00
(IV) Motor coordination						
NF	Falls	0.00±0.00	0.00±0.00	0.00±0.00	0.00±0.00	0.00±0.00
MS	Missteps	1.80±0.49	5.80±0.58 ***a***	4.60±0.81 ***a***	4.40±0.51 ***a***	5.00±0.95 ***a***
MI	Motor incoordination index	1.80±0.49	5.80±0.58 ***a***	4.60±0.81 ***a***	4.40±0.51 ***a***	5.00±0.95 ***a***

Each value represents the mean ± SEM of group. For comparisons among control and experimental groups, a = significantly different compared to Control; b = significantly different compared to L-NAME group; and c = significantly different compared to LNAME-LSRT. The exact value of P is mentioned in the text.

Table 4: Effect of *N. lotus* on consummatory patterns of hypertensive male rats.

Parameters	Days of treatment	Consummatory parameters				
		Control	LNAME	LNAME-LSRT	LNAME-NL75	LNAME-NL200
Mount frequency	Day 1	31.60±2.87	44.80±1.46 ***a***	44.80±3.25 ***a***	44.40±1.96 ***a***	42.20±1.39 ***a***
	Day 30	46.20±3.40	63.60±2.04 ***a***	66.40±2.11 ***a***	65.60±1.29 ***a***	64.20±2.06 ***a***
	Day 60	61.40±3.37	53.20±3.87	68.00±2.11	43.80±4.89 ***ac***	47.40±3.56 ***c***
Intromission frequency	Day 1	30.40±2.62	40.20±3.69	41.00±3.92	38.00±0.71	40.40±1.86
	Day 30	44.60±3.53	60.40±1.21 ***a***	62.80±1.46 ***a***	62.00±1.73 ***a***	60.40±2.25 ***a***
	Day 60	59.60±4.38	30.60±2.44 ***a***	42.80±6.63	43.40±5.18	45.00±3.39
Ejaculation frequency	Day 1	2.60±0.24	1.20±0.58	1.20±0.37	1.20±0.37	1.00±0.45
	Day 30	2.80±0.37	0.60±0.40 ***a***	0.60±0.40 ***a***	0.60±0.24 ***a***	0.60±0.40 ***a***
	Day 60	3.20±0.20	0.20±0.20 ***a***	0.00±0.00	1.60±0.51 ***ac***	2.00±0.55 ***bc***
Penile licking	Day 1	30.00±2.28	40.80±4.02	42.60±3.17	40.00±1.14	41.80±3.48
	Day 30	36.00±4.48	42.40±4.50	46.40±6.44	42.80±7.22	51.80±6.46
	Day 60	59.60±4.38	30.40±1.94 ***a***	41.40±5.90	42.00±5.21	44.60±3.20
Mean copulatory interval (sec)	Day 1	1152.27±72.14	908.16±30.44***a***	893.56±51.68***a***	902.48±43.63***a***	914.23±42.80***a***
	Day 30	1370.25±66.88	919.55±46.17 ***a***	548.78±30.12 ***ab***	565.51±39.71 ***ab***	575.28±33.85 ***ab***
	Day 60	1347.91±37.90	582.19±55.25 ***a***	Absent	1433.39±51.87 ***b***	1467.93±30.83 ***b***
Copulatory efficiency (%)	Day 1	96.58±2.62	89.24±5.91	91.99±8.20	86.31±4.29	95.65±2.32
	Day 30	96.42±1.61	95.18±1.98	94.76±2.20	94.46±1.09	94.06±1.42
	Day 60	96.61±2.23	58.59±5.87 ***a***	61.88±7.11 ***a***	98.67±1.33 ***bc***	95.02±2.68 ***bc***

Each value represents the mean ± SEM of group. For comparisons among control and experimental groups, a = significantly different compared to Control; b = significantly different compared to L-NAME group; and c = significantly different compared to LNAME-LSRT. The exact value of P is mentioned in the text.

Table 5: Effects of *N. lotus* on different parameters of sexual motivation of hypertensive male rats.

Copulatory parameters	Days of treatment	Parameters of sexual motivation				
		Control	LNAME	LNAME-LSRT	LNAME-NL75	LNAME-NL200
Mount latency (sec)	Day 1	26.60±2.09	25.60±2.01	23.80±1.16	25.20±1.62	25.60±0.87
	Day 30	20.40±1.17	25.40±1.08	24.20±1.59	26.60±1.33 ***a***	24.80±1.36
	Day 60	13.80±0.84	17.55±1.96	14.08±1.48	9.09±1.07 ***b***	8.60±1.05 ***b***
Intromission latency (sec)	Day 1	30.60±1.60	63.80±2.44 ***a***	64.80±1.46 ***a***	62.80±4.69 ***a***	60.00±2.41 ***a***
	Day 30	22.60±0.60	49.20±2.75 ***a***	48.00±1.76 ***a***	43.40±2.50 ***a***	37.80±1.56 ***abc***
	Day 60	14.20±0.71	33.90±4.10 ***a***	32.37±1.72 ***a***	23.12±2.50 ***b***	14.60±1.32 ***bc***
Ejaculation latency (sec)	Day 1	520.22±21.82	636.14±25.82	656.31±48.61	634.43±65.27	631.74±38.43
	Day 30	345.30±33.78	484.14±16.88 ***a***	482.89±22.48 ***a***	473.83±21.75 ***a***	465.74±36.81 ***a***
	Day 60	295.99±17.95	664.04±22.65 ***a***	Absent	277.59±13.35 ***b***	269.26±19.06 ***b***
Postejaculatory interval (sec)	Day 1	419.00±29.83	425.20±22.68	389.00±16.82	409.20±17.36	430.00±13.68
	Day 30	294.68±15.16	641.84±15.12 ***a***	649.00±8.53 ***a***	641.20±13.79 a	645.44±16.72 ***a***
	Day 60	252.74±14.48	714.48±18.72 ***a***	Absent	315.26±12.21 ***ab***	285.61±14.44 ***b***

Each value represents the mean ± SEM of group. For comparisons among control and experimental groups, a = significantly different compared to Control; b = significantly different compared to L-NAME group; and c = significantly different compared to LNAME-LSRT. The exact value of P is mentioned in the text.

3.4.4. Effect of N. lotus Aqueous Extract on the Inhibition of Sexual Behaviour Induced by L-NAME. The administration of L-NAME for 60 days to male rats resulted in distress in the sexual vigor of male rats, as evidenced by parameters of sexual motivation and copulatory performances studied (Tables 4 and 5). 30 days of cotreatment with losartan restored mount and intromission frequency in normal range whereas *N. lotus* reduced significantly ($P<0.05$) the frequency of mount compared to control. Both doses reduced mount frequency in a significant manner ($P<0.001$) compared to losartan (Figure 4, Table 4).

Meanwhile the intromission latency decreased significantly ($P<0.01$) following cotreatment with the plant extract at the dose of 75 mg/kg ($P<0.05$) and 200 mg/kg ($P<0.001$) compared to L-NAME. The reference drug, losartan, did not modify intromission latency compared to hypertensive untreated animals. The ejaculatory latency was absent as no ejaculation was observed in the group cotreated with losartan (Table 5).

3.4.5. Effects of Chronic Treatment with L-NAME on Temporal Patterning. The effects of L-NAME on temporal patterning sexual behaviour of male rats are presented in Figure 3. L-NAME treatment increased the *non-"postejaculation"* pauses number and their cumulative duration ($P<0.001$). 30 days cotreatment with the plant extract induced a considerable decrease in the number of pauses ($P<0.001$) and on their cumulative duration in relation to control group.

3.5. Histology. Mallory Trichrome staining revealed in L-NAME treated rat, vascular congestion (Figure 4), a decrease in smooth muscle proportion (red) and an increase in collagen level (blue) in penile tissue.

4. Discussion

The present results provide, for the first time, scientific information concerning the ability of *Nymphaea lotus* flowers aqueous extract to improve sexual performances and alleviates anxiety in L-NAME hypertensive rats. Our previous

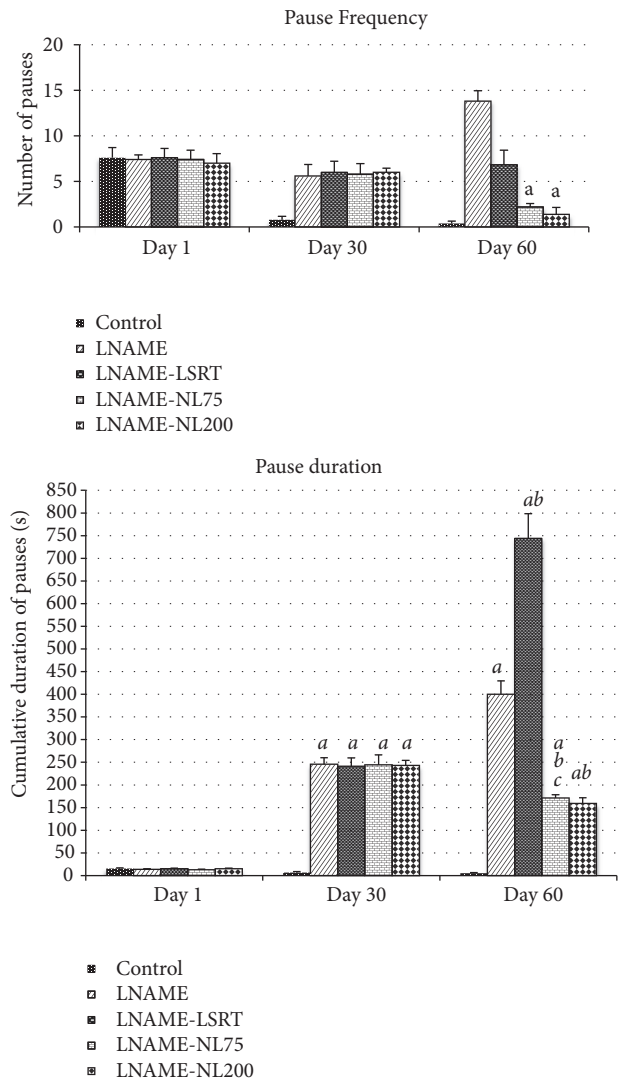

Figure 3: Effects of chronic treatment with L-NAME (10 mg/kg/day), losartan (10 mg/kg/day) or *N. lotus* (75 and 200 mg/kg/day) on temporal patterning of sexual behaviour of male rats.

Figure 4: Effects of *N. lotus* on penile histomorphology of hypertensive rats. Penile cross sections. X200; tissue sections were stained with Mallory. (1) Smooth muscle cells (orange), (2) collagen (blue), and (3) penile arteries. Arrows indicate vascular congestions.

studies have demonstrated that treating rats with L-NAME causes injury to the vascular endothelium [11], and this model is widely used to study hypertension, as well as its relative complications [18]. The results obtained in this study showed that chronic NO synthesis inhibition with L-NAME treatment at the level of 10 mg/kg for 8 weeks, caused a significant increase in blood pressure and a nonsignificant variation of heart rate compared to control. Long-term administration of the L-arginine analogue (L-NAME) to normotensive rats can induce NO-deficient hypertension. The precise mechanism is based on the fact that NO is synthesized and released from endothelial cells to mediate vasorelaxation and L-NAME reduces NO production resulting in increased total peripheral resistance and high blood pressure [19, 20]. These effects were significantly prevented by treatment with *N. lotus* at the dose of 75 mg/kg. Several explanations are possible for the constancy in heart rate of hypertensive male rats. One possibility is that the baroreceptor reflex is (indirectly) reset as a consequence of the constant chronic increase in blood pressure. Surprisingly, our results revealed an exacerbation of the blood pressure increment in rat cotreated with the extract of *N. lotus* at the dose of 200 mg/kg, suggesting dose-dependent modulatory properties of our plant extract on blood pressure.

Mount, intromission, and ejaculation frequencies are useful indices of vigor, libido, and potency [21]. An increase in ML reflects sexual motivation and increase in the number of IF and EF shows the efficiency of erection and the ease by which ejaculatory reflexes are activated [16]. After 30 days of L-NAME administration, we observed in this study a significant deficit in intromission and ejaculatory frequencies with the low efficiency of copulatory behaviour whereas mount latency and frequency remain unaltered by the L-NAME treatment compared to control. These parameters were exacerbated after additional 30 days of L-NAME treatment, suggesting progressive deficit in general consummatory mechanisms. Further, the reduced mean copulatory interval and the low percentage of copulatory efficiency exhibited in hypertensive animals indicated that it was not every mount that resulted in intromission, suggesting an erectile dysfunction in hypertensive male rats. Other authors also showed that sexual dysfunctions such as decreased libido, delayed orgasm, difficulties in maintaining an erection, and inhibition of ejaculation are common side effects of NO deficiency [9, 22].

Sexual response arousal component reflected by the mount latency appears to be not affected by the L-NAME treatment. The temporal patterning of sexual behaviour analysis probes the most complex sociosexual behaviour [10]. In a normal sexual behaviour pattern of male rat, a pause occurs only for the refractory period after an ejaculation or after satiation. Surprisingly, in this study, we observed a significant progressive increase in the number and latency of pauses not preceded by ejaculation in animals treated with L-NAME. Besides, the increased number of attempts (mounts), the prolonged refractory periods (postejaculatory interval), and finally the reduction of the copulatory efficiency suggest a difficulty to penile insertion or a general fatigue that could be explained by the pathologic increment of the blood pressure. Cotreatment with the aqueous extract of *N. lotus* flowers restores partially or totally the deficits provoked by L-NAME treatment on consummatory patterns.

Altogether, our results indicate that the aqueous extract of *N. lotus* flowers increases both sexual potency and motivation. The appetitive component of the sexual behaviour in rats is usually related to the variations of intromission latency and postejaculatory intervals, but the executive counterpart is estimated to be proportional to the changes observed in the number of mount or intromission, the ejaculation latency, and the mean copulatory interval [23]. Compounds derived from plants, such as flavonoids, have been reported to directly affect male sexual functions [24] by increasing vasorelaxation of cavernosum smooth muscle cells through activating NO-cGMP pathway [25], or interacting with central pathways that participate in libido or sexual arousal [26].

Sexual function in hypertensive rats was found to be decreased and could be due to decrease in smooth muscle level and increase in collagen level of penile tissue as evident from histopathological study. Hypertension progression is associated with progressive vascular structural damage [27] and, as our data suggest, penile vascularization does not remain unaffected. Described remodelling effects of L-NAME-induced hypertension have been effectively prevented only by the aqueous extract of *N. lotus* flowers at the dose of 75 mg/kg while losartan did not have a remarkable effect compared to model, mainly at the penile vessels level. It is mentioned that drugs that improve endothelial function, antihypertensive *like* ARA (losartan), are unable to ameliorate erectile function since they do not possess specificity of action at the level of the penile vasculature and smooth muscle cells [28]. Besides, the plant extract exhibited a localised protective potential that protects the penile vasculature from structural damage, supporting positive impact on penile blood flow, and therefore on the penile erectile function.

Chronic blockage of NO by L-NAME also produced more displacement grooming and motor coordination deficits as

assessed by increased missteps in this study, suggesting anxiety and reduced locomotor capacity in hypertensive animals [16]. Other authors previously reported that treatment with L-NAME may induce anxiety [29] and locomotor deficiency [30]. Cotreatment with the aqueous flowers extract of *Nymphaea lotus* at the both doses produced an anxiolytic-like effect as evidenced by the delayed latency to leave the center of the elevated alley (suok test), the reduced defecation and motor incoordination episodes compared to hypertensive nontreated animals. Similar to other Nymphaea genus species, our results also show that *Nymphaea lotus* possess anxiolytic properties [6, 31]. The prosexual and anxiolytic effects of *N. lotus* were consistently observed in several measures but principally in the group given the lowest dose of aqueous extract.

Considering the high comorbidity of anxiety with sexual disorders in men [32] or those with cardiovascular diseases, the anxiolytic-like effect produced by *N. lotus* at a dose with prosexual and antihypertensive effects could be considered as an additional benefit of the plant extract. Thus, *Nymphaea lotus* could be considered as a potential dual medicinal agent to treat anxiety and erectile dysfunction.

5. Conclusion

Nymphaea lotus is able to modulate blood pressure, to restore erectile function by interacting with both central and peripheral pathways. We thus suggest that the aqueous extract obtained from this plant could be considered to facilitate sexual responses regulated by both the NO pathway at central and peripheral levels.

Data Availability

The datasets analysed during the current study are available from the corresponding author upon reasonable request.

Conflicts of Interest

The authors declare that they have no conflicts of interest.

Acknowledgments

The authors wish to thank the association PCD (Pathology-Cytology-Development) for their help with histology features.

References

[1] S. Douma, M. Doumas, A. Tsakiris, and C. Zamboulis, "Male and female sexual dysfunction: Is hypertension an innocent bystander or a major contributor?" *Brazilian Journal of Hypertension*, vol. 14, pp. 139–147, 2007.

[2] M. Burchardt, T. Burchardt, L. Baer et al., "Hypertension is associated with severe erectile dysfunction," *The Journal of Urology*, vol. 164, no. 4, pp. 1188–1191, 2000.

[3] A. C. D. Gonçalves, R. Leite, and R. A. Fraga-Silva, "Evidence that the vasodilator angiotensin-(1-7)-Mas axis plays an important role in erectile function," *American Journal of Physiology-Heart and Circulatory Physiology*, vol. 293, no. 4, pp. H2588–H2596, 2007.

[4] K. K. Khanna and S. P. Jackson, "DNA double-strand breaks: signaling, repair and the cancer connection," *Nature Genetics*, vol. 27, no. 3, pp. 247–254, 2001.

[5] A. L. Burnett, "Nitric oxide in the penis: physiology and pathology," *The Journal of Urology*, vol. 157, no. 1, pp. 320–324, 1997.

[6] A. D. James, *Duke's Handbook of Medicinal Plants of the Bible*, Taylor and Francis Group, USA, 2008.

[7] A. A. Elegami, C. Bates, A. I. Gray, S. P. Mackay, G. G. Skellern, and R. D. Waigh, "Two very unusual macrocyclic flavonoids from the water lily Nymphaea lotus," *Phytochemistry*, vol. 63, no. 6, pp. 727–731, 2003.

[8] O. J. Akinjogunla, A. A. Adegoke, I. P. Udokang, and B. C. Adebayo-Tayo, "Antimicrobial potential of Nymphaea lotus (Nymphaeaceae) against wound pathogens," *Journal of Medicinal Plants Research*, vol. 3, pp. 138–141, 2009.

[9] M. Bialy, J. Beck, P. Abramczyk, A. Trzebski, and J. Przybylski, "Sexual behavior in male rats after nitric oxide synthesis inhibition," *Physiology & Behavior*, vol. 60, no. 1, pp. 139–143, 1996.

[10] M. R. Ferraz, M. M. Ferraz, R. Santos, and R. S. D. Moura, "Preventing l-NAME inhibitory effects on rat sexual behavior with hydralazine, isradipine or captopril co-treatment," *Pharmacology Biochemistry & Behavior*, vol. 75, no. 2, pp. 265–272, 2003.

[11] P. M. Kameni, D. P. D. Dzeufiet, D. C. Bilanda et al., "Protective effects of Nymphaea lotus Linn (Nymphaeaceae) on L-NAME-induced tissular oxidative damages and erectile dysfunction in hypertensive male rat," *Journal of Experimental and Integrative Medicine*, vol. 6, no. 4, pp. 1–7, 2016.

[12] G. E. Trease and W. C. Evans, *Pharmacognosy*, Ballière Tindall Press, London, UK, 1989.

[13] O. Folin and V. Ciocalteu, "192On tyrosine and tryptophane determinations in proteins," *Journal of Biological Chemistry*, vol. 73, pp. 627–650, 1927.

[14] J. V. Formica and W. Regelson, "Review of the biology of quercetin and related bioflavonoids," *Food and Chemical Toxicology*, vol. 33, no. 12, pp. 1061–1080, 1995.

[15] A. V. Kalueff, A. Minasyan, and P. Tuohimaa, "Behavioural characterization in rats using the elevated alley Suok test," *Behavioural Brain Research*, vol. 165, no. 1, pp. 52–57, 2005.

[16] S. A. Kada, P. Mieugeu, D. P. D. Dzeufiet et al., "Effect of aqueous extract of Allanblackia floribunda (Oliver) stem bark on sexual behaviour in adult male rats," *World Journal of Pharmacy and Pharmaceutical Sciences*, vol. 1, no. 2, pp. 585–600, 2012.

[17] P. Nyadjeu, E. P. Nguelefack-Mbuyo, A. D. Atsamo, T. B. Nguelefack, A. B. Dongmo, and A. Kamanyi, "Acute and chronic antihypertensive effects of *Cinnamomum zeylanicum* stem bark methanol extract in L-NAME-induced hypertensive rats," *BMC Complementary and Alternative Medicine*, vol. 13, article 27, 2013.

[18] M. O. Ribeiro, E. Antunes, G. De Nucci, S. M. Lovisolo, and R. Zatz, "Chronic inhibition of nitric oxide synthesis. A new model of arterial hypertension," *Hypertension*, vol. 20, no. 3, pp. 298–303, 1992.

[19] L. J. Ignarro, "Nitric oxide as a unique signaling molecule in the vascular system: a historical overview," *Journal of Physiology and Pharmacology*, vol. 53, pp. 503–514, 2002 (Russian).

[20] S. M. Gardiner, A. M. Compton, T. Bennett, R. M. Palmer, and S. Moncada, "Control of regional blood flow by endothelium-derived nitric oxide.," *Hypertension*, vol. 15, no. 5, pp. 486–492, 1990.

[21] M. T. Yakubu, M. A. Akani, and A. T. Oladiji, "Male sexual dysfunction and methods used in assessing medicinal plants with aphrodisiac potentials," *Pharmacognosy Reviews*, vol. 1, pp. 49–56, 2007.

[22] M. R. Ferraz, M. M. Ferraz, and R. Santos, "How REM sleep deprivation and amantadine affects male rat sexual behavior," *Pharmacology Biochemistry & Behavior*, vol. 69, no. 3-4, pp. 325–332, 2001.

[23] J. G. Pfaus, T. E. Kippin, and G. Coria-Avila, "What can animal models tell us about human sexual response?" *Annual Review of Sex Research*, vol. 14, pp. 61–63, 2003.

[24] N. Malviya, S. Jain, V. B. Gupta, and S. Vyas, "Recent studies on aphrodisiac herbs for the management of male sexual dysfunction—a review," *Acta Poloniae Pharmaceutica-Drug Research*, vol. 68, no. 1, pp. 3–8, 2011.

[25] H. Ning, Z. C. Xin, G. Lin, L. Banie, T. F. Lue, and C. S. Lin, "Effects of icariin on phosphodiesterase-5 activity in vitro and cyclic guanosine monophosphate level in cavernous smooth muscle cells," *Urology*, vol. 68, no. 6, pp. 1350–1354, 2006.

[26] K. Dhawan, S. Kumar, and A. Sharma, "Beneficial effects of chrysin and benzoflavone on virility in 2-year-old male rats," *Journal of Medicinal Food*, vol. 5, no. 1, pp. 43–48, 2002.

[27] H. D. Intengan and E. L. Schiffrin, "Vascular remodeling in hypertension: roles of apoptosis, inflammation, and fibrosis," *Hypertension*, vol. 38, no. 3, part 2, pp. 581–587, 2001.

[28] A. Aversa, R. Bruzziches, D. Francomano, and A. Lenzi, "Endothelial function and erectile dysfunction-a review: erectile dysfunction," *European Urological Review*, vol. 4, no. 2, pp. 78–82, 2009.

[29] R. Estrada-Reyes, M. Carro-Juárez, and L. Martínez-Mota, "Pro-sexual effects of *Turnera diffusa* Wild (Turneraceae) in male rats involves the nitric oxide pathway," *Journal of Ethnopharmacology*, vol. 146, no. 1, pp. 164–172, 2013.

[30] F. Therrien, P. Lemieux, S. Bélanger, M. Agharazii, M. Lebel, and R. Larivière, "Protective effects of angiotensin AT1 receptor blockade in malignant hypertension in the rat," *European Journal of Pharmacology*, vol. 607, no. 1-3, pp. 126–134, 2009.

[31] B. S. Thippeswamy, B. Mishra, V. P. Veerapur, and G. Gupta, "Anxiolytic activity of *Nymphaea alba* Linn. in mice as experimental models of anxiety," *Indian Journal of Pharmacology*, vol. 43, no. 1, pp. 50–55, 2011.

[32] I. A. Abdel-Hamid and E.-S. Saleh, "Primary lifelong delayed ejaculation: Characteristics and response to bupropion," *The Journal of Sexual Medicine*, vol. 8, no. 6, pp. 1772–1779, 2011.

Hindawi
Evidence-Based Complementary and Alternative Medicine
Volume 2019, Article ID 7249679, 8 pages
https://doi.org/10.1155/2019/7249679

Review Article

Research Progress of Male Reproductive Toxicity of Chinese Materia Medicas

Sicong Li,[1] **Chao Li**,[2] **Xiaoran Cheng**,[1] **Xin Liu**,[3] **and Mei Han**[3]

[1]*College of Management, Beijing University of Chinese Medicine, Beijing 100029, China*
[2]*Department of Emergency, China-Japan Friendship Hospital, Beijing 100029, China*
[3]*College of Chinese Medicine, Beijing University of Chinese Medicine, Beijing 100029, China*

Correspondence should be addressed to Xin Liu; xinliu1011@126.com

Received 27 February 2019; Revised 23 May 2019; Accepted 27 June 2019; Published 14 July 2019

Guest Editor: Arielle Cristina Arena

In recent years, as the infertility rate in China has been increasing year by year and semen quality decreasing, male reproductive toxicity of drugs attracts more and more attention. There are many factors that cause male reproductive toxicity, among which Chinese materia medica is an important aspect. This article will introduce the male reproductive toxicity of Chinese materia medicas grouped by different effectivenesses such as immunosuppressant, evacuant, diuretic, cardiotonic, anti-infective drug and analgesic.

1. Introduction

Over the half past century, sperm counts and sperm activity parameters of semen have shown a significant downward trend. At present, Chinese economy is developing at a rapid pace. The pace of people's life has been accelerating along with living and psychological pressure increasing. Long-time use of electronic products, such as computers and mobile phones, and intake of carbonated beverages, alcohols and tobaccos all exert bad influences on quality and quantity of sperms, which leads to the increasing number of male infertility patients. Chinese materia medicas have been favored by Chinese people and become the first choice in the clinical treatment of many diseases in China. However, male reproductive toxicities of Chinese materia medica cannot be ignored [1]. When Chinese materia medica is generally used in accord with the principle of rational prescription, it is considered by the public to be of great safety. However, by means of toxicological researches, we find that some Chinese materia medicas *in vitro and in vivo* experiments exert several negative impacts on reproductive functions. After extracted and refined by modern methods, the effective and toxic components of some Chinese materia medicas are relatively enriched. While the curative effects improve, toxicities are also enhanced and new toxicities appear [2]. The targets of male reproductive toxicity in Chinese materia medica are testes, epididymides, sperms and hormone secretion systems [3]. The consequences include failures in sexual behavior, infertility, degeneration of sexual organs and decreased sperm counts and qualities [4]. Based on the classification standard of different medicinal effectivenesses, not only the pharmacological action and mechanism of each medicine, but also the manifestation and mechanism of their reproductive toxicities are introduced in this article.

2. Immunosuppressant

Tripterygium hypoglaucum hutch and Tripterygium wilfordii can be used as immunosuppressants [5] in the treatment of rheumatoid arthritis, Behcet's disease, membranous nephropathy and other diseases.

2.1. Tripterygium Hypoglaucum Hutch. The immunosuppressive mechanism of Tripterygium hypoglaucum hutch extract [6] may be related to the increase of CD+4 CD+25 T cell level and the expression of Foxp3 mRNA. The reproductive toxicity of Tripterygium hypoglaucum hutch is mainly manifested in abnormality of sperms' morphology, quantity and activity. After 30 days of taking extraction of Tripterygium hypoglaucum hutch orally [7], the pregnancy rate of mating rats decreases from 88% to 3%. The counts and activity rates

of sperms decrease significantly. But testicular quality and tissue morphology change just a little. Only a slight decrease of number is found in spermatogenic epithelial cells in the seminiferous lumen. The spermatogenesis is trapped in the late stage, which prohibits spermatids from coming into being. After 60 days of taking extraction of Tripterygium hypoglaucum hutch, male rats lose fertility abilities, with motility and density of sperms in epididymides significantly decreasing and rates of abnormality significantly increasing. However, these changes can gradually recover after 20 days of withdrawal [8].

Damages to Sertoli cells' viability and DNA integrity are dependent on medicinal dosage and administration time. Germ cells and sperms are targets of Tripterygium hypoglaucum hutch's reproductive toxicity [9]. It can aggregate the RNA residues into large clumps in the seminiferous tubules. The DNA of sperm cells [10] which drop from the epididymides lumen are pushed to the nuclear membrane. Most sperms are deformed as broken head, nuclear pyknosis, and coiled tail. Fluorescence in situ hybridization (FISH) [11] shows that, after intraperitoneal injection of Tripterygium hypoglaucum hutch for a week, sperms in epididymides come into chromosomal nondisjunctions.

2.2. Tripterygium wilfordii. It is widely used in the treatment of rheumatoid arthritis [12], glomerulonephritis, nephrotic syndrome, lupus erythematosus and Sjogren's syndrome. It can not only inhibit T cell proliferation, spleen cell activation and antigen-induced antibody responses, but also reduce IL-2 production in spleen cell [13]. However, several components show reproductive toxicities.

2.2.1. Tripterygium wilfordii Glycoside. Apoptosis of spermatogenic cells [14] can be seen in both fertile and infertile men. However, proportion of apoptotic cells differs. Excessive apoptosis may be related to diseases or drug reproductive toxicities. The percentage of apoptotic cells [15] in semen of normal fertile males is only 0.1%, while that in infertile males significantly increases, with varicocele being 1%, sperm maturation disorder being 25%, and patients who take Tripterygium wilfordii glycoside tablets 4.5 mg/kg daily being 50%. Tripterygium glycosides [16] hinder the transformation of round spermatids into long spermatids and subsequently into spermatozoa by means of destroying actin. During the spermiogenesis, actin is present in sperm cells and sperms. Actin participates in migration of central granules, occurrence of the neck, formation of fibrous sheaths and fixation of postacrosomal sheaths under nuclear membrane [17]. As a consequence, sperms' number reduces. Tripterygium wilfordii glycosides [18] can destroy a large number of sperm cells, bend the sperms' necks as well as producing teratospermia and multitailed sperms.

Tripterygium wilfordii glycosides (GRT) [19] affect reproductive-related genes and upregulate protein expression levels of mice testicular tissues' Y chromosome Ddx3y and transcriptional activators. Tripterygium wilfordii polyglycosides [20] play a toxic role in testicular Sertoli cells and spermatogenesis process by increasing FSH levels and decreasing inhibin B as well as inhibin T levels in serum.

When the reproductive system suffers from various harmful stimulants, high activity molecules, such as reactive oxygen species (ROS) and reactive nitrogen species (RNS), are produced too much in body. The degree of oxidation exceeds the clearance ability of oxidation enzyme. Imbalance exists between the oxidative system and the antioxidant system, which leads to reproductive system damage [21]. Semen antioxidant system can slow down the lipid peroxidation process of sperms and ultimately reduce the probability of sperms' premature death. The main components of antioxidant system are superoxide dismutase, vitamin E, coenzyme Q, glutathione, NADPH-dependent glutathione peroxidase and reductase equipped in sperms.

After taking Tripterygium wilfordii polyglycoside [22] at the dosage of 30mg/kg, the activity of nitrite oxide synthase (NOS) in Leydig cells decreases significantly, which results in deterioration of reproductive functions. Nitrous oxide synthase is widely distributed in male reproductive systems, which is closely related to the regulation of testicular microcirculation, testosterone secretion, spermatids' maturation and penile erection. NOS catalyzes L-arginine to produce nitrous oxide (NO) with the presence of NADPH. NO is a cell messenger molecule which exerts extensive biological functions. It plays an important role in male reproductive systems. In addition, Tripterygium wilfordii polyglycosides [23] also exert significant effects on some other enzymes: (1) the activity of alkaline phosphatase (ALP) near basement membrane of seminiferous tubule epithelium can be weakened; (2) the activity of acid phosphatase (ACP) in Sertoli cells can be enhanced; (3) the activity of 3beta-hydroxysteroid dehydrogenase (3beta-HSD) in Leydig cells of testis can be weakened; (4) the activity of lactate dehydrogenase isoenzyme-C4 (LDH-C4) is negatively correlated with the time of administration, but it can recover partially after withdrawal.

2.2.2. Tripterygium wilfordii Lactone. The sperm deformity rate increases after 30 days of continuous administration of Tripterygium wilfordii lactone [24] at the dosage of 1.5g/kg, suggesting that it might have potential mutagenicity to spermatogenic cells. Tripterygium wilfordii lactone [25] has the ability to pass through blood-testis barrier and decrease the activities of SOD and GSH-Px in testicular tissues, thereby reducing the antilipid peroxidation effect, which not only destroys membranes of spermatogenic epithelial cells, supporting cells and stromal cells, but also leads to the decline of spermatogenic cells' functions and the downregulation of cell secretion growth factors. These results [26] suggest that lipid peroxidation of testicular tissues might be one of reasons why male reproductive dysfunctions appear after using Tripterygium wilfordii lactone.

2.2.3. Total Alkaloids of Tripterygium wilfordii. Spontaneous apoptosis of spermatogenic cells [27] (mainly spermatogonia and spermatocytes) exists in mammals during normal spermatogenesis. Testis, as a target organ of various physical and chemical toxic medicine, can be easily affected. Apoptosis of spermatogenic cells, interstitial cells and Sertoli cells are manifestations of testicular damages. After taking total

alkaloids of Tripterygium wilfordii [28] at the dosage of 10 mg/kg for six weeks, it is found that the epithelial cells of seminiferous tubules in rats' testes are damaged, the number of spermatogenic cells in seminiferous tubules decreases and the wall of seminiferous tubules becomes thinner. The damage aggravates as the dosage increases. Multinucleated giant cells come into being and are arranged in disorders [29]. When the dosage reaches to 50mg/kg, the lesion reaches the spermatocyte layer. As the number of multinucleated giant cells increases, spermatids disappear. Under electron microscopy, some sperms' mitochondrial sheaths disintegrate and the number of mitochondria decreases. The chromatin of spermatocytes is sparse. The perinuclear space becomes widened and a large number of lysosomes can be seen in the cytoplasm of spermatocytes. When the dosage reaches to 100 mg/kg, most spermatogenic cells in seminiferous tubules disappear; only sparse spermatogenic cells and supporting cells remain. When the seminiferous tubules get atrophied, necrotic and exfoliated spermatogenic cells and polynuclear giant cells can be seen. Nuclear concentration, fragmentation and dissolution necrosis changes can be observed in spermatogenic cells. Moreover, total alkaloids of Tripterygium wilfordii [30] can interfere with the synthesis of nuclear DNA in primary spermatocyte and then make mitochondria of spermatocytes swollen, cristae broken and produce visible flocculent deep-stained substances.

3. Evacuant

Rhubarb and cassia seed can be used in the treatment of habitual constipation and dynamic intestinal obstruction [31].

3.1. Rhubarb. The content of total anthraquinones in Rhubarb [32] is 1.5%~4.0%. The effective ingredients of Rhubarb in treating constipation are anthraquinone compounds. Total Anthraquinone of Rhubarb [33] can not only excite M receptors on intestinal smooth muscles, increase intestinal peristalsis, but also effectively inhibit the expression of AQP4 in rat colon and increase water content in colon. The reproductive toxicity of Rhubarb is manifested in abnormal sperm motility, quantity, and the level of reproductive hormones. Total anthraquinone [34] of Rhubarb taken at the dosage of 1g/kg for 30 days can damage the Leydig cells and Sertoli cells of Sprague Dawley (SD) rats as well as decreasing the activities of testosterone synthases and energy metabolism enzymes. As a consequence, synthesis and serum levels of testosterone reduce while serum levels of LH increase. The increase of FSH in serum is mainly due to the decrease of testosterone and the increase of compensatory regulation of hypothalamic-pituitary-testicular axis. It results in abnormal sex hormone levels in serum. Moreover, total anthraquinone of Rhubarb [35] can significantly reduce sperm counts and activity rates with testicular and epididymis index decreasing at the dosage of 1.0g/kg.

3.2. Cassia Seed. Anthraquinones [36] in Cassia seed can regulate the release of vasoactive intestinal polypeptide (VIP), increase the volume of intestinal contents, stimulate intestinal mucosa and increase intestinal peristalsis, thus treating constipation. After 90 days of taking Anthraquinones in Cassia seed orally [37] at the dosage of 1.0g/kg, the number of rats' spermatids reduces. Moreover, the testes get atrophied and become smaller in size. Microscopically, the seminiferous tubules get atrophied and the fibrous connective tissues get proliferated.

4. Diuretic

The main characteristic chemical constituent of Phytolacca is triterpenoid saponin [38], which has significant diuretic effect. However, triterpenoid saponin of Phytolacca acinosa Roxb [39] can terminate activity of all sperms in rabbit semen at the concentration of 4g/L *in vitro* test. After washing off the saponin, the sperms cannot rejuvenate. It suggests its lethal effect on rabbit sperms. At the concentration of 2.6 g/L, the total saponin of Phytolacca acinosa Roxb can terminate activity of all sperms in human semen. After washing off the saponin, human sperms cannot rejuvenate either. After reducing the concentration of saponin, spermicidal efficacy is weakened, which indicates a significant dose-effect relationship.

5. Cardiotonic

5.1. Datura Flower. Extracted from the leaves of datura flower, digitoxin [40] is mainly used for congestive heart failure. Because of its slow and lasting effect, it is suitable for long-term use in patients with chronic heart failure. However, digitoxin [41] can bring about estrogenic effects like male breast development, after long-term application at the dosage of 1mg/kg.

5.2. Ginseng. The ginseng saponin Rb3 [42] can enhance myocardial contractile function and can be used to treat myocardial contractile dysfunction. However, it can significantly decrease the activity of superoxide dismutase (SOD) [43], glutathione peroxidase (GSH-px), and total antioxidant capacity (T-AOC) in mice and elevate the concentration of malondialdehyde (MDA) to induce the apoptosis of spermatogenic cells.

6. Analgesics

6.1. Chinaberry Fruit. It is widely used in the treatment of abdominal pain caused by gastrointestinal spasm and hernia [44]. Obtained from petroleum ether extraction of Chinaberry fruit, Chinaberry fruit oil [45] is one of the most important effective components. *In vitro* tests, it is shown that 0.5 ml of Chinaberry fruit oil can kill sperms of SD rats within 20s. After 100 μl of this oil is injected into each side of SD rats' epididymides, histological examination reveals that diameters of the testicular seminiferous tubules reduce after 6 weeks. FCM (flow cytometry) examination shows that Chinaberry fruit oil can inhibit the production of testicular spermatogenic cells, stimulate non- sperm cells and increase their anabolism.

6.2. Papaya. It has similar analgesic effect with Chinaberry fruit oil, but the mechanism is different. Papaya alkaloids [46] can block calcium channels in nerve tissue, inhibit calcium influx and reduce the release of pain mediators such as prostaglandins. However, the alkaloids in Carica papaya L [47] can also inhibit the activity of steroidal enzymes in rats' testes. Both oral intake and intramuscular injection of this kind of alkaloids can lead to reversible sterility in rats.

6.3. Radix Aconiti. The water extract of Radix Aconiti has good analgesic effect. It is mainly used to treat the pain [48] caused by rheumatoid arthritis, fracture and degenerative arthritis. However, the organ index of testes and epididymides of SD rats decreases significantly after three months administration of water extract of Radix Aconiti [49] at the dosage of 8.3 g/kg.

7. Hypnotic

7.1. Albizia Flower. Lignans from Albizia flower have sedative and hypnotic effects, that are widely used in the treatment of insomnia [50]. However, after taking lignans from Albizia flower [51] intragastrically for 60 days at the dosage of 50 mg/kg, indexes of Wistar rats' testes, epididymides, seminal vesicles and prostates with productions of spermatocytes, spermatogonia, and secondary spermatocytes decreasing significantly. Not only the area of nuclei and the number of mature supporting cells in Leydig cells, but also sperms'motility decrease significantly. The contents of protein, glycogen, cholesterol, epididymal protein and sperm vesicle fructose become less and less. The diameters of deferens get thinner significantly with the infertility rate increasing. These results suggest that the lignans extracted from flower of silktree albizzia might produce reproductive toxicity by damaging testicular cells.

8. Anti-Infective Drugs

8.1. Sophora Flavescens. Water extract of Sophora flavescens [52] has a good therapeutic effect on pneumonia caused by Staphylococcus aureus, Streptococcus hemolyticus, Escherichia coli and other pathogenic bacteria *in vivo*. The main effects are imposed on sperm density (sperm count), sperm motility, abnormal sperm rate, daily sperm production, sperm cell viability, sperm mitochondrial function and sperm acrosome integrity. Matrine in Sophora flavescens [53] could stop sperms' movement instantly at the lowest effective concentration of 0.85 g/L. Morphology of sperms shows that matrine has lethal effect on sperms. In addition, Sophora alopecuroides alkaloids [54] have spermicidal or inhibitive effects on spermatogenesis.

8.2. Andrographis paniculata. Known as natural antibiotic drug [55], andrographolide has good effect on bacterial upper respiratory tract infection and bacterial dysentery. This product is diterpenoid lactone compound, which is insoluble in water and can only be given orally. After 11 weeks of administration of andrographolide [56], the walls of seminiferous tubules in mice' testes become thinner, mature sperms in lumen are absent and the sperm counts significantly reduce. During the same administration period, the higher the dosage is, the more significant reduction happens. Moreover, andrographolide [57] has certain toxic effects on spermatids and testes of mice. The mechanisms may be to block the energy source of spermatids, so that spermatocytes cannot undergo meiosis process normally. Spermatogenic epitheliums in mice testes are destroyed, so that spermatogenic cells cannot be properly differentiated, resulting in abnormality of spermatids.

8.3. Artemisia annua. Artesunate has strong killing effect on plasmodium [58] and the ability to quickly control symptoms of dysentery. However, it is found to damage DNA double strands in Sertoli cells of mice testes. After long-term use of artesunate [59], the blood-testis barrier can be hurt as a result. Short-term use of artesunate does not have a significant effect but long-term use can reduce follicle stimulating hormone, luteinizing hormone (LH), and testosterone levels in serum.

8.4. Balsam Pear. A protein named MAP30 isolated from balsam pear has been shown to inhibit HIV DNA synthesis and also eliminate herpes simplex virus. However, the water extract of Momordica charantia contains an alkaline protein with a molecular weight of 34,000, which inhibits sperm activity. After Momordica charantia L. extract [60] is directly applied to the scrotum of adult mice at the dosage of 1g/kg, some of the testicular seminiferous epitheliums come into disorder. The abnormal megakaryocytes in the proximal surface of the seminiferous tubules become more and more. Large vacuoles appear in spermatids and the mitochondria get swollen. It suggests that Momordica charantia L. extract might have strong ability to stop the development of spermatids in mice, which is related to the damage of seminiferous tubules. The Momordica charantia L. extract [61] also has a detrimental effect on spermatogenic epitheliums. Spermatids are damaged at first, with early spermatocytes getting gradually involved. The acrosome membrane of spermatids becomes thicker and shorter; the number and motility of spermatids decrease. The aberration rate increases during the metamorphosis period.

9. Anticoagulant

Many Chinese materia medicas can be used in the treatment of miocardial infarction, pulmonary embolism, stroke and other thrombotic diseases.

9.1. Earthworm. Earthworm extract can reduce blood viscosity [62] and inhibit platelet aggregation. It contains fibrinolytic substances, which can promote fibrinolysis. Earthworm extract QY-III [63] (a yellow powder containing succinic acid and hyaluronic acid) has rapid killing effects on mice and human sperms *in vitro*. Its spermicidal characteristics exist in three aspects: rapid braking, agglomeration of sperms and destruction of sperm morphology. Further researches have shown that QY-III can produce many "sperm-flocs clusters". They hinder the free movement of

sperms, destroy sperms' penetrating and power device, which makes sperms lose fertilization abilities.

10. Antidiarrheal

Papaver shell and hedgehog skin are often used to treat diarrhea caused by irritable bowel syndrome, hepatitis, inflammatory bowel diseases, chronic pancreatitis and tumors in digestive tract.

10.1. Pericarpium Papaveris. It can cause difficulty in ejaculation [64] and erection. Long-term use of morphine reduces male testosterone secretion and deteriorates secondary sexual characteristics.

10.2. Hedgehog. Saponins isolated from hedgehog skin can stabilize the acrosome membrane of sperms [65], which hinder the release of acid hydrolase and protease in sperms. Failure or obstruction of acrosome enzyme release can hinder the fertilization of eggs, thereby playing an antifertility role.

11. Antigout Drugs

11.1. Meadow Saffron. Colchicine, an alkaloid originally extracted from the liliaceous plant meadow saffron, can be used in the treatment of acute attacks of gouty arthritis to prevent joint damage caused by urate. Colchicine [66] cannot only inhibit sperms' motility, induce sperms' apoptosis, but also reduce the secretion of serum testosterone, follicle stimulating hormone (FSH) and luteinizing hormone (LH). Infertility happens when reproductive-related hormones are at abnormal level.

12. Antineoplastic Drugs

12.1. Solanine. It can significantly prolong the survival time of H22 tumor-bearing mice [67] *in vivo*. *In vitro*, solanine exerts strong inhibitory effects on the proliferation of HepG2 cells, PC-3 cells of prostate cancer, PANC-1 cells of pancreatic cancer, A2058 cells of human melanoma, HeLa cells of cervical cancer and U251 cells of human glioma. However, solanine [68] can decrease the activity of superoxide dismutase (SOD), succinate dehydrogenase (SDH) in testicular tissues and the content of glutathione (GSH) in testicular tissues. It results in the increase of free radicals in testes, abnormality in respiratory chain, blockage of tricarboxylic acid cycle, increase in osmotic pressure of the mitochondrial matrix and oxidative damage of the mitochondria [69].

12.2. Gossypol. Often used in the treatment of lymphoma and leukemia, gossypol [70] can induce cancerous cells apoptosis. After taking orally 30~60mg/kg gossypol [71] for five weeks, the testicular seminiferous tubules of rats relatively reduce, the number of spermatogenic cells significantly reduce and a small number of multinucleated giant cells can be seen. There are rare mature sperms in the seminiferous lumen. In some rats, spermatogenic epithelial loss and shedding of immature spermatogenic cells can be observed. In epididymides, gossypol can make the acrosome of sperms go into rupture and the head of sperms to break apart from their tails. The mitochondrial spiral sheaths in the middle of the sperms come into disorder and become swollen. Moreover, gossypol [72] can significantly inhibit acrosomal enzymes' activity in sperms, thus reducing fertilization opportunities. These pathological changes can recover automatically after drug withdrawal for two months.

12.3. Glycyrrhiza Uralensis Fisch. It can inhibit the proliferation of cancer cells and induce apoptosis of cancer cells [73] by inhibiting nucleotide reductase and reducing the activity of DNA synthesis rate-limiting enzyme. After 60 days of taking 450mg/kg Glycyrrhiza uralensis Fisch extract [74], the testicular tissue structures of rats undergo remarkable deterioration. Atrophy of seminiferous tubules and hyperplasia of connective tissues can be seen. The number of intermediate cells in connective tissues significantly reduces. The Glycyrrhiza uralensis Fisch [75] can lead to testicular and penile atrophy, sexual apathy and reduction in times of chasing female rats and sexual intercourse.

13. How to Look upon the Reproductive Toxicity of Chinese Materia Medicas Reasonably

Most objects of the researches mentioned above are purified single components. Traditional Chinese medical therapy does not use these single components for clinical treatment but use several medicinal materials that are combined together. One traditional Chinese medicine decoction can contain thousands of different monomers. Therefore, it is improper to abandon the use of Chinese materia medicas simply because of reproductive toxicities of some certain monomer components. In practical clinical applications, Chinese medicine treatment is often used in combination with two or more medicinal materials. In this process, the monomer components with reproductive toxicity often undergo chemical reactions, which lead to quantitative or qualitative changes. As long as Chinese materia medicas are used in scientific and reasonable ways [76], the pharmacological effects can be enhanced, the toxicity and adverse reactions can be reduced. Moreover, Chinese medicine treatment is guided by the basic theory of traditional Chinese medicine, which emphasizes on dialectical analysis of the whole condition. As long as the medical treatment is under the guidance of basic theories of traditional Chinese medicine, the reproductive toxicities can be under control. Discussions on the reproductive toxicities must pay attention to the course of treatment and dosage. The clinical application of conventional Chinese medicine is usually no more than 7 days, while the administration time of drugs in the basic researches above has far exceeded 7 days. Moreover, the dosage is neither a conventional therapeutic dosage nor a maximum safe dosage.

14. Summary

This article describes not only direct pathways in which Chinese materia medicas cause infertility by killing sperms and damaging testicular tissues, but also indirect ways of

affecting reproductive-related hormones. However, we cannot abandon the use of Chinese materia medicas because of some toxicity reports. The reproductive toxicities can also be used for clinical treatment. As long as doctors use them reasonably, toxic ingredients can be also therapeutic ingredients. For example, trichosanthin [77] has the effect of terminating mid-late pregnancy; therefore trichosanthin has been used for maternal induction of labor and shortening the labor process. It is the same for male reproductive toxicity. Chemical components [78] that kill sperms can be used for contraception at therapeutic dosage. Therefore, we must take a dialectical view of the reproductive toxicities of Chinese materia medicas, do our best to avoid adverse reactions and make unremitting efforts to improve safety of clinical applications.

Data Availability

The data used to support the findings in this study are included within the article.

Disclosure

No funder support was involved in the manuscript writing, editing, approval or decision to publish.

Conflicts of Interest

The authors declare that they have no conflicts of interest.

Authors' Contributions

Sicong Li was responsible for the initial outline, draft writing, revisions for intellectual content and final approval; Chao Li, Xiaoran Cheng and Mei Han were responsible for data interpretation, presentation, draft writing and revisions for intellectual content; Xin Liu was the corresponding author and responsible for draft writing and final approval.

Acknowledgments

The authors would like to thank all the scholars who deeply love, popularize the basic knowledge and expand the influence of Traditional Chinese Medicine.

References

[1] M. Zhang, H. Zhang, Y. Yu, H. Huang, G. Li, and C. Xu, "Synergistic effects of a novel lipid-soluble extract from Pinellia pedatisecta Schott and cisplatin on human cervical carcinoma cell lines through the regulation of DNA damage response signaling pathway," *Oncology Letters*, vol. 13, no. 4, pp. 2121–2128, 2017.

[2] J. Y. Wu, S. F. Zhang, X. Meng et al., "Research progress on reproductive toxicity of traditional Chinese medicine," *Journal of Hebei North University (Natural Science Edition)*, vol. 31, no. 6, pp. 113–116, 2015.

[3] L. L. Gao, X. T. Li, C. M. Xie et al., "The mechanism of Yishenjingjing Chinese medicine antagonizing environmental endocrine disruptors leading to gonadal dysplasia in prepubertal rats," *Chinese Journal of Biochemistry and Molecular Biology*, vol. 8, pp. 787–796, 2014.

[4] Y. L. Yuan and X. P. Zhou, "Research progress on reproductive toxicity of Tripterygium wilfordii," *Chinese Journal of Traditional Chinese Medicine*, vol. 10, pp. 2997–3000, 2013.

[5] F. Meng, J. Li, Y. Rao, W. Wang, and Y. Fu, "Gengnianchun extends the lifespan of caenorhabditis elegans via the Insulin/IGF-1 signalling pathway," *Oxidative Medicine and Cellular Longevity*, vol. 2018, Article ID 4740739, 10 pages, 2018.

[6] Y. X. Zhang, D. Huang, N. N. Li et al., "The abnormal expression of testicular reproductive related genes induced by tripterygium wilfordii and the intervention of traditional Chinese medicine for tonifying kidney," *Chinese Journal of Andrology*, vol. 5, pp. 466–471, 2012.

[7] J. Li, T. Yong, Y. H. Lv et al., "Comparative study on the effects of tripterygium glycosides on testicular tissue morphology and NOS expression in normal and adjuvant arthritis rats," *Chinese Journal of Basic Medicine*, vol. 2, pp. 153–155, 2011.

[8] S. Lewicki, W. Stankiewicz, E. Skopińska-Różewska et al., "Spleen content of selected polyphenols, splenocytes morphology and function in mice fed Rhodiola kirilowii extracts during pregnancy and lactation," *Polish Journal of Veterinary Science*, vol. 18, no. 4, pp. 847–855, 2015.

[9] J. Y. Han, Y. Yi, A. H. Huang et al., "Research ideas and methods of reproductive toxicity of traditional Chinese medicine," *Acta Pharmaceutica Sinica*, vol. 49, no. 11, pp. 1498–1503, 2014.

[10] J. X. Zhang, *Research on in vitro and in vivo Test Methods for Reproductive Toxicity of Male Animals to Chinese Animals*, Shanghai Institute of Pharmaceutical Industry, 2006.

[11] K. Alanazi, B. A. Alahmadi, A. Alhimaidi et al., "Development of spermatic granuloma in albino rats following administration of water extract of Heliotropium bacciferum Forssk," *Saudi Journal of Biological Sciences*, vol. 23, no. 1, pp. 87–91, 2015.

[12] A. de Arruda, C. A. L. Cardoso, M. D. V. Vieira, and A. C. Arena, "Safety assessment of *Hibiscus sabdariffa* after maternal exposure on male reproductive parameters in rats," *Drug and Chemical Toxicology*, vol. 39, no. 1, pp. 22–27, 2016.

[13] J. Xue, WL. Li, XZ. Wang et al., "Study on the time-effect relationship of reproductive toxicity of Andrographis paniculata," *Journal of Harbin University of Commerce (Natural Science Edition)*, vol. 5, pp. 645–648+666, 2011.

[14] M. Yimam, Y.-C. Lee, E.-J. Hyun, and Q. Jia, "Reproductive and developmental toxicity of orally administered botanical composition, UP446-Part I: effects on embryo-fetal development in New Zealand white rabbits and sprague dawley rats," *Birth Defects Research Part B: Developmental and Reproductive Toxicology*, vol. 104, no. 4, pp. 141–152, 2015.

[15] Y. B. Ji, J. C. Sun, and L. Lang, "Effects of Solanum nigrum on the expression of vimentin in mouse testis support cells," *Journal of Toxicology*, vol. 24, no. 05, pp. 352–355, 2010.

[16] N. Lu, *Rhubarb on the Relationship between Reproductive Toxicity And Dosage and Time of Female Rats*, Chengde Medical College, 2014.

[17] M. Yimam, Y.-C. Lee, E.-J. Hyun, and Q. Jia, "Reproductive and developmental toxicity of orally administered botanical composition, UP446-part II: effects on prenatal and postnatal development, including maternal function in sprague-dawley rats," *Birth Defects Research Part B: Developmental and Reproductive Toxicology*, vol. 104, no. 4, pp. 153–165, 2015.

[18] Y. Ma, S. Tian, L. Sun et al., "The effect of acori graminei Rhizoma and extract fractions on spatial memory and hippocampal

neurogenesis in Amyloid Beta 1-42 injected mice," *CNS and Neurological Disorders - Drug Targets*, vol. 14, no. 3, pp. 411–420, 2015.

[19] B. S. Low, P. K. Das, and K. Chan, "Acute, reproductive toxicity and two-generation teratology studies of a standardized quassinoid-rich extract of Eurycoma longifolia Jack in Sprague-Dawley rats," *Phytotherapy Research*, vol. 28, no. 7, pp. 1022–1029, 2014.

[20] M. Dorostghoal, S. M. Seyyednejad, and A. Jabari, "Protective effects of Fumaria parviflora L. on lead-induced testicular toxicity in male rats," *Andrologia*, vol. 46, no. 4, pp. 437–446, 2014.

[21] J. Li, D. Huang, and L. He, "Effect of roucongrong (Herba Cistanches Deserticolae) on reproductive toxicity in mice induced by glycoside of Tripterygium wilfordii," *Journal of Traditional Chinese Medicine*, vol. 34, no. 3, pp. 324–328, 2014.

[22] T. M. Sandini, M. S. Udo, T. M. Reis-Silva, M. M. Bernardi, and H. d. Spinosa, "Prenatal exposure to integerrimine N-oxide impaired the maternal care and the physical and behavioral development of offspring rats," *International Journal of Developmental Neuroscience*, vol. 36, pp. 53–63, 2014.

[23] D. Chen, N. Li, L. Lin et al., "Confocal mirco-Raman spectroscopic analysis of the antioxidant protection mechanism of the oligosaccharides extracted from Morinda officinalis on human sperm DNA," *Journal of Ethnopharmacology*, vol. 153, no. 1, pp. 119–124, 2014.

[24] X.-X. Zhang, D. Huang, N.-N. Liu et al., "GTW-induced abnormal expressions of testicular reproduction-related genes and intervention with kidney-tonifying Chinese herbs," *National Journal of Andrology*, vol. 18, no. 5, pp. 466–471, 2012.

[25] Y. Zhao, A. Liang, T. Liu et al., "Study on embryonic toxicity of Senecio scandens, Qianbai Biyanpian and total alkaloid from S. scandens in rats," *Zhongguo Zhongyao Zazhi*, vol. 35, no. 3, pp. 373–377, 2010.

[26] X. Y. Liu, A. R. Qi, D. G. Luo et al., "Research progress on reproductive toxicity and combined attenuation of Tripterygium wilfordii," *Chinese Journal of Traditional Chinese Medicine and Information*, vol. 25, no. 04, pp. 133–135, 2018.

[27] J. J. Zhang, *ExpErimental Study on Reproductive Toxicity of Aconite Chinese Male Rats in Vitro And in Vivo [Master's thesis]*, Sichuan University, 80, 2007.

[28] C. G. Sachetti, R. R. de Carvalho, F. J. R. Paumgartten, O. A. Lameira, and E. D. Caldas, "Developmental toxicity of copaiba tree (Copaifera reticulata Ducke, Fabaceae) oleoresin in rat," *Food and Chemical Toxicology*, vol. 49, no. 5, pp. 1080–1085, 2011.

[29] X. M. Zhang, Y. Xiao, J. L. Zhou et al., "Effects of licorice on testicular reproductive toxicity in male mice," *Chinese Journal of Gerontology*, vol. 13, pp. 3507–3510, 2015.

[30] C. Yu, X. Sun, and Y. Niu, "An investigation of the developmental neurotoxic potential of curcumol in PC12 cells," *Toxicology Mechanisms and Methods*, vol. 26, no. 9, pp. 635–643, 2016.

[31] Z. W. Zhang, S. C. Wang, J. Y. Xu et al., "Progress in in vitro experimental study on reproductive toxicity of traditional Chinese medicine," *Journal of Liaoning University of Traditional Chinese Medicine*, vol. 18, no. 04, pp. 89–91, 2016.

[32] Y. Tang, W. Jiang, W. Qiu et al., "Study on reproductive toxicity of kunming shanhaiqi capsule in mice," *Journal of Traditional Chinese Medicine*, vol. 10, pp. 1874–1876, 2005.

[33] J. C. Sun, *Study on the Mechanism of Cytotoxicity of Solanine on Mouse Testis [Master's thesis]*, Harbin University of Commerce, 2011.

[34] Y. Y. Chen, Y. P. Tang, E. X. Shang et al., "Incompatibility assessment of Genkwa Flos and Glycyrrhizae Radix et Rhizoma with biochemical, histopathological and metabonomic approach," *Journal of Ethnopharmacology*, vol. 229, pp. 222–232, 2019.

[35] S. Ganjalikhan Hakemi, F. Sharififar, T. Haghpanah, A. Babaee, and S. H. Eftekhar-Vaghefi, "The effects of olive leaf extract on the testis, sperm quality and testicular germ cell apoptosis in male rats exposed to busulfan," *International Journal of Fertility and Sterility*, vol. 13, no. 1, pp. 57–65, 2019.

[36] A. T. Gotardo, M. I. Mattos, I. M. Hueza, and S. L. Górniak, "The effect of Cynara scolymus (artichoke) on maternal reproductive outcomes and fetal development in rats," *Regulatory Toxicology and Pharmacology*, vol. 102, pp. 74–78, 2019.

[37] M. Mohajeri, B. Behnam, A. F. Cicero, and A. Sahebkar, "Protective effects of curcumin against aflatoxicosis: a comprehensive review," *Journal of Cellular Physiology*, vol. 233, no. 4, pp. 3552–3577, 2018.

[38] J. Y. Xu, C. Dai, J. J. Shan et al., "Determination of the effect of Pinellia ternata (Thunb.) Breit. on nervous system development by proteomics," *Journal of Ethnopharmacology*, vol. 213, pp. 221–229, 2018.

[39] C. Huang, Z. Huang, F. Ho, and W. Chan, " Berberine impairs embryonic development *in vitro* and *in vivo* through oxidative stress-mediated apoptotic processes ," *Environmental Toxicology*, vol. 33, no. 3, pp. 280–294, 2018.

[40] M. Askaripour, A. Hasanpour, F. Hosseini et al., " The effect of aqueous extract of *Rosa damascena* on formaldehyde-induced toxicity in mice testes ," *Pharmaceutical Biology*, vol. 56, no. 1, pp. 12–17, 2018.

[41] S. X. Huang, *Male Reproductive Toxicity and Mechanism of Action in Kunming Mountain Sea Bream [Master's thesis]*, Chongqing Medical University, 2014.

[42] Y. Xu, T. Chen, X. Li et al., "Veratrum nigrum inhibits the estrogenic activity of salvia miltiorrhiza bunge in vivo and in vitro," *Phytomedicine*, vol. 43, pp. 68–77, 2018.

[43] J. Zhang, L. Fang, L. Shi et al., "Protective effects and mechanisms investigation of Kuntai capsule on the ovarian function of a novel model with accelerated aging ovaries," *Journal of Ethnopharmacology*, vol. 195, pp. 173–181, 2017.

[44] Z. B. Huang, H. Q. Que, H. Y. Peng et al., "Reproductive toxicity and mechanism of triptolide in male rats," *Chinese Journal of Traditional Chinese Medicine*, vol. 23, pp. 4655–4659, 2015.

[45] X. He, X. Wang, J. Fang et al., "The genus Achyranthes : A review on traditional uses, phytochemistry, and pharmacological activities," *Journal of Ethnopharmacology*, vol. 203, pp. 260–278, 2017.

[46] Y. C. Wang, J. H. Chiang, H. C. Hsu et al., "Decreased fracture incidence with traditional Chinese medicine therapy in patients with osteoporosis: a nationwide population-based cohort study," *BMC Complementary and Alternative Medicine*, vol. 19, no. 1, article 42, 2019.

[47] Y. Chen, R. Yu, L. Jiang et al., "A comprehensive and rapid quality evaluation method of traditional Chinese medicine decoction by integrating UPLC-QTOF-MS and UFLC-QQQ-MS and its application," *Molecules*, vol. 24, no. 2, article 34, 2019.

[48] Y. Y. Cheng, Y. P. Tang, E. X. Shang et al., "Incompatibility assessment of Genkwa Flos and Glycyrrhizae Radix et Rhizoma with biochemical, histopathological and metabonomic approach," *Journal of Ethnopharmacology*, vol. 229, pp. 222–232, 2019.

[49] N. Cheng, M. Lin, N. Liu et al., "Methylmercury-induced testis damage is associated with activation of oxidative stress and

germ cell autophagy," *Journal of Inorganic Biochemistry*, vol. 190, pp. 67–74, 2019.

[50] P. Zhou, L. Sun, Q. Cheng et al., "Social support modifies an association between work stress and semen quality: results from 384 Chinese male workers," *Journal of Psychosomatic Research*, vol. 117, pp. 65–70, 2019.

[51] H. X. Zhao, N. Ma, Z. Liu et al., "Protective effect of Wuzi Yanzong recipe on testicular dysfunction through inhibition of germ cell apoptosis in ageing rats via endoplasmic reticulum stress," *Andrologia*, vol. 51, no. 2, article e13181, 2019.

[52] S. Q. Ge, P. H. Zhao, X. C. Liu, Z. Zhao, and M. Liu, "Necessity to evaluate epigenetic quality of the sperm for assisted reproductive technology," *Reproductive Sciences*, vol. 26, no. 3, pp. 315–322, 2018.

[53] T. Qin, Z. Ren, X. P. Liu et al., "Study of the selenizing Codonopsis pilosula polysaccharides protects RAW264.7 cells from hydrogen peroxide-induced injury," *International Journal of Biological Macromolecules*, vol. 125, pp. 534–543, 2019.

[54] K. K. Karna, B. R. Choi, J. H. You et al., "Cross-talk between ER stress and mitochondrial pathway mediated adriamycin-induced testicular toxicity and DA-9401 modulate adriamycin-induced apoptosis in Sprague–Dawley rats," *Cancer Cell International*, vol. 19, no. 1, p. 85, 2019.

[55] J. Zhu, Q. Q. Zhu, Y. Wang, B. Wang, Q. Lyu, and Y. Kuang, "Comparative study on risk for birth defects among infants after in vitro fertilization and intracytoplasmic sperm injection," *Systems Biology in Reproductive Medicine*, vol. 65, no. 1, pp. 54–60, 2019.

[56] J. Pan, Y. Yao, X. Guo, F. Kong, J. Zhou, and X. Meng, "Endoplasmic reticulum stress, a novel significant mechanism responsible for DEHP-induced increased distance between seminiferous tubule of mouse testis," *Journal of Cellular Physiology*, 2019.

[57] W. Liu, X. He, S. Yang et al., "Bi-allelic mutations in TTC21A induce asthenoteratospermia in humans and mice," *American Journal of Human Genetics*, vol. 104, no. 4, pp. 738–748, 2019.

[58] R. Li, Q. W. Xing, X. L. Wu et al., "Di-n-butyl phthalate epigenetically induces reproductive toxicity via the PTEN/AKT pathway," *Cell Death & Disease*, vol. 10, no. 4, p. 307, 2019.

[59] D. Zhang, Z. Zhang, Y. Wu et al., "Systematic evaluation of graphene quantum dot toxicity to male mouse sexual behaviors, reproductive and offspring health," *Biomaterials*, vol. 194, pp. 215–232, 2019.

[60] A. A. Albishtue, N. Yimer, M. Z. Zakaria et al., "Effects of EBN on embryo implantation, plasma concentrations of reproductive hormones, and uterine expressions of genes of PCNA, steroids, growth factors and their receptors in rats," *Theriogenology*, vol. 126, pp. 310–319, 2019.

[61] Y. Zhang, X. M. Yuan, Y. F. Wang et al., "Isopsoralen induces different subchronic toxicities and metabolomic outcomes between male and female Wistar rats," *Regulatory Toxicology Pharmacology*, vol. 103, pp. 1–9, 2019.

[62] C. Y. Lin, Y. J. Chen, S. H. Lee, C. Kuo, M. Lee, and M. Lee, "Uses of dietary supplements and herbal medicines during pregnancy in women undergoing assisted reproductive technologies– a study of taiwan birth cohort," *Taiwanese Journal of Obstetrics and Gynecology*, vol. 58, no. 1, pp. 77–81, 2019.

[63] I. Tarique, W. A. Vistro, X. Bai et al., "LIPOPHAGY: a novel form of steroidogenic activity within the LEYDIG cell during the reproductive cycle of turtle," *Reproductive Biology and Endocrinology*, vol. 17, no. 1, p. 19, 2019.

[64] N. An, J. Zhu, L. Ren et al., "Trends of SHBG and ABP levels in male farmers: Influences of environmental fluoride exposure and ESR alpha gene polymorphisms," *Ecotoxicology and Environmental Safety*, vol. 172, pp. 40–44, 2019.

[65] D. Zhang, Q. Chen, Q. Liu et al., "Histological and cytological characterization of anther and appendage development in asian lotus (Nelumbo nucifera Gaertn.)," *International Journal of Molecular Sciences*, vol. 20, no. 5, 2019.

[66] X. Yang, D. Zhu, H. Zhang et al., "Associations between DNAH1 gene polymorphisms and male infertility," *Medicine*, vol. 97, no. 49, article e13493, 2018.

[67] F. J. Day, A. Andersen, M. Ong et al., "Large-scale genome-wide meta-analysis of polycystic ovary syndrome suggests shared genetic architecture for different diagnosis criteria," *PLoS GenetICS*, vol. 14, no. 12, Article ID e1007813, 2018.

[68] W. Liu, W. Han, R. Wu et al., "Viral threat to male fertility," *Andrologia*, vol. 50, no. 11, article e13140, 2018.

[69] L. L. Shi, L. Yu, and J. Zhu, "Cell suspension examination versus histopathological technique in detecting sperm in the testis tissue of non-obstructive azoospermia patients undergoing testicular sperm aspiration," *Zhonghua Nan Ke Xue*, vol. 24, no. 7, pp. 622–626, 2018.

[70] C. Y. Wang, J. J. Zhang, and P. Duan, "Antagonistic effect of vitamin E on di-2-ethylhexyl phthalate-induced reproductive toxicity in male rats," *Zhonghua Nan Ke Xue*, vol. 24, no. 7, pp. 589–595, 2018.

[71] P. Li and Z. Li, "Microsurgical management of obstructive azoospermia: progress and prospects," *Zhonghua Nan Ke Xue*, vol. 24, no. 7, pp. 579-288, 2018.

[72] L. Chen, G. R. Shi, D. D. Huang et al., "Male sexual dysfunction: a review of literature on its pathological mechanisms, potential risk factors, and herbal drug intervention," *Biomedicine & Pharmacotherapy*, vol. 112, article 108585, 2019.

[73] Z. S. Huang, X. Y. Pan, J. Zhou, W. T. Leung, C. Li, and L. Wang, "Chinese herbal medicine for acute upper respiratory tract infections and reproductive safety: a systematic review," *Bioscience Trends*, vol. 13, no. 2, pp. 117–129, 2019.

[74] O. Awodele, O. Kale, A. Odewabi, M. Ekor, B. Salau, and A. Adefule-Ositelu, "Safety evaluation of Bon-santé cleanser ® polyherbal in male Wistar rats: Further investigations on androgenic and toxicological profile," *Journal of Traditional and Complementary Medicine*, vol. 8, no. 1, pp. 212–219, 2018.

[75] L. O. Bruno, R. S. Simoes, M. de Jesus Simoes, M. J. Girão, and O. Grundmann, "Pregnancy and herbal medicines: an unnecessary risk for women's health-A narrative review," *Phytotherapy Research*, vol. 32, no. 5, pp. 796–810, 2018.

[76] J. Xu, H. B. Chen, and S. L. Li, "Understanding the molecular mechanisms of the interplay between herbal medicines and gut microbiota," *Medicinal Research Reviews*, vol. 37, no. 5, pp. 1140–1185, 2017.

[77] L. BZhu, L. R. Li, S. Ying et al., "Chinese herbal medicine as an adjunctive therapy for breast cancer: a systematic review and meta-analysis," *Evidence-Based Complementary and Alternative Medicine*, vol. 2016, Article ID 9469276, 17 pages, 2016.

[78] C. T. Lam, G. W. Gong, Y. C. Lam et al., "Jujube-containing herbal decoctions induce neuronal differentiation and the expression of anti-oxidant enzymes in cultured PC12 cells," *Journal of Ethnopharmacology*, vol. 188, pp. 275–283, 2016.

Hindawi
Evidence-Based Complementary and Alternative Medicine
Volume 2019, Article ID 5346518, 9 pages
https://doi.org/10.1155/2019/5346518

Research Article

Reproductive Regulation and Oxidative Stress Alleviation of Chinese Herbal Medicine Therapy in Ovariectomised Mouse Model

Chung-Hsin Wu,[1] **Sheue-Er Wang**,[2] **Chih-Hsiang Hsu**,[1] **Yu-Tsen Hsu**,[1] **Chen-Wen Lu**,[1] **Wu-Chang Chuang**,[3] **and Ming-Chung Lee**[4]

[1]*School of Life Science, National Taiwan Normal University, Taipei City, Taiwan*
[2]*Pathological Department, Saint Paul's Hospital, Taoyuan City, Taiwan*
[3]*Sun Ten Pharmaceutical Co. Ltd., New Taipei City 23143, Taiwan*
[4]*Brion Research Institute of Taiwan, New Taipei City 23143, Taiwan*

Correspondence should be addressed to Chung-Hsin Wu; megawu@ntnu.edu.tw

Received 12 April 2019; Revised 27 May 2019; Accepted 18 June 2019; Published 7 July 2019

Guest Editor: Arielle Cristina Arena

In Taiwan, the herbal formula B401 is considered as a health supplement for middle-aged women that can alleviate sweating, anxiety, and sleep disorders. However, the relevant mechanisms are still unclear. In this study, we evaluated the beneficial effects of the herbal formula B401 therapy in the reproductive regulation of ovariectomised mice. Female ICR mice were randomised into four groups: wild-type (WT) mice with sham treatment, wild-type mice treated with the herbal formula B401, bilateral ovariectomised (OVX) mice with sham treatment, and bilateral ovariectomised mice treated with the herbal formula B401. Mice were orally given the herbal formula B401 at a dose of 30 mg/kg bw/day for 2 weeks. At the end of oral treatment with sham or the herbal formula B401, levels of reactive oxygen species (ROS), calcium, phosphorus, and estradiol-17β in the blood; uterine weight and endometrial thickness; and expressions of estrogen receptor α (ERα), estrogen receptor β (ERβ), progesterone receptor (PR), vascular endothelial growth factor (VEGF), and superoxide dismutase 2 (SOD2) in the uterine tissue were examined and then compared among the four groups of mice. We found that OVX mice decreased levels of calcium, phosphorus, and estradiol-17β in the blood, decreased uterine weight and endometrial thickness, and decreased expressions of ERα, ERβ, PR, and SOD2 in the uterine tissue but increased blood ROS levels compared with those of WT mice. In addition, OVX mice with the herbal formula B401 therapy can increase levels of calcium, phosphorus, and estradiol-17β in the blood, increase uterine weight and endometrial thickness, and increase expressions of ERα, ERβ, PR, VEGF, and SOD2 in the uterine tissue but decrease blood ROS levels. Our results may provide reasonable explanation for the reproductive regulation of the herbal formula B401 therapy.

1. Introduction

Some menopausal women experience discomfort symptoms such as hot flashes, sweating, anxiety, sleep disorders, and osteoporosis [1]. These uncomfortable symptoms are usually caused by the reduction or stoppage of ovarian estrogen production. Estrogen is the primary female sex hormone and plays multiple biological functions, including bone remodelling and neuroprotection through the modulation of the estrogen receptors: estrogen receptor α (ERα) and estrogen receptor β (Erβ) [1, 2]. Estrogen therapy is currently the most common treatment for alleviating menopausal symptoms [3]. Estrogen may affect bone remodelling by accelerating calcium and phosphorus reabsorption by the intestine and reducing calcium and phosphorus excretion from the kidney [4]. Furthermore, estrogen can reduce oxidative stress involved in the pathogenesis of the reproductive regulation. A previous study reported that ovariectomised (OVX) rats showed increased levels of reactive oxygen species (ROS) and reduced expression of antioxidant enzymes such as superoxide dismutase 2 (SOD2) [5]. Menopausal symptoms are often caused by mitochondrial oxidative stress

because of the decline of the natural antioxidant estrogen [6].

Even though estrogen therapy is considered effective for alleviating menopausal symptoms, it is associated with high risks of cardiovascular disease, endometrial hyperplasia, and breast cancer [7]. Thus, many women refuse to undergo exogenous estrogen hormone therapy and switch to alternative treatment for alleviating menopausal symptoms. In Taiwan, for menopausal symptom remission, alternative medicines such as traditional Chinese medicines are becoming popular because of their reputed safety and clinical efficacy. In traditional Chinese medicine theory, menopausal symptoms are often triggered by kidney–liver weakness [8]. Herbal formulas classified as kidney/liver-nourishing substances should be suitable for menopausal symptom remission. It is believed that complex interactions of components in herbal formulas can produce synergistic effects, and these herbal formulas show reduced side effects and toxicity. Thus, in the present study, we adopted a modified herbal formula B401 for reproductive regulation in ovariectomised mice. The herbal formula B401, consisting of *Angelica sinensis*, *Astragalus membranaceus*, *Eclipta prostrata*, *Ligustri fructus*, *Panax ginseng*, and *Rehmannia glutinosa*, is widely used in Taiwan and is considered as a health supplement that supports healthy brain and reproductive functions. Our previous studies have reported that the herbal formula B401 can suppress oxidative stress, inflammation, and apoptosis in the brain and reproductive systems of mice [9–13]. Recently, the herbal formula B401 is also used as a health supplement for middle-aged women in sweating, anxiety, and sleep disorders alleviation. However, the relevant mechanisms regarding the herbal formula B401 therapy alleviating discomfort symptoms are still unclear. Thus, in this study, we evaluated the beneficial effects of the herbal formula B401 on reproductive regulation in ovariectomised mice. We hope that our results may provide reasonable explanation for the reproductive regulation of the herbal formula B401 therapy.

2. Materials and Methods

2.1. Preparation of the Herbal Formula B401. The main components of the herbal formula B401 (US patent, No 7838048B2) are *Ang. sinensis*, *Ast. membranaceus*, *E. prostrata*, *L. fructus*, *P. ginseng*, and *R. glutinosa* in specific ratios. The chromatographic fingerprint of the herbal formula B401 was assayed on a liquid chromatography/mass spectrometry (LC/MS) analytical system equipped with a LC-20AD UFLC system (Shimadzu Corporation, Kanagawa, Japan) linked with a LCMS-8040 triple mass spectrometer (Shimadzu Corporation).

2.2. Cytotoxicity Assay. SH-SY5Y cells were treated with and without (control) the herbal formula B401 at indicated doses for 24 h to determine the IC_{50} of cytotoxicity. Subsequently, cell viability was measured through the 3-(4,5-dimethylthiazol-2-yl)-2,5-diphenyltetrazolium bromide (MTT) assay (Sigma-Aldrich Corporation, St. Louis, MO, USA). Absorbance was measured at OD 570 nm on an ELISA reader (uQuant, BioTek Inc., Vermont, USA). The percentage of cell viability was calculated as follows: [(OD 570 nm of experimental well)/(OD 570 nm of control well)] × 100%. Our cell viability assay experiment was approved by the Committee on Biological Research of National Taiwan Normal University and was implemented under the guidelines of the committee.

2.3. Animal Preparation. All ICR mice were purchased from BioLASCO Taiwan Yi-Lan Breeding Center, which has been awarded the Full Accreditation of AAALAC International. Our animal experiments were approved by the Institutional Animal Care and Use Committee of National Taiwan Normal University (Protocol number: NTNU Animal Experiments No. 104002). In accordance with the Institutional Guidelines of the Animal Care and Use Committee of NTNU, ICR mice were maintained in the animal facility at NTNU under specific pathogen-free conditions. A total of 12 female ICR mice were randomised into four groups: wild-type mice with sham treatment (WT + sham), wild-type mice with B401 treatment (WT + B401), bilateral ovariectomised mice with sham treatment (OVX + sham), and bilateral ovariectomised mice with B401 treatment (OVX + B401). All mice were housed in a constant temperature environment at 22°C ± 2°C with a 12-h light/dark cycle, and mice had *ad libitum* access to water and food. Mice received oral herbal formula B401 treatment at a dose of 30 mg/kg bw/day for 2 weeks.

2.4. Blood Biochemical Analysis. Levels of calcium and phosphorus were assayed using colorimetric assay kits (Biovision, Milpitas, CA, USA), and the concentration of estradiol-17β was assayed using an Assay Design EIA kit (Assay Design, Ann Arbor, MI, USA). Measurements of blood calcium and phosphorus levels were manipulated in line with the manufacturer's protocol. In addition, levels of ROS in the blood of the four groups of ICR mice were determined using lucigenin- and luminol-amplified chemiluminescence (CL) methods to measure $O2^{\bullet-}$ and H_2O_2 activity. Blood levels of ROS were measured using a CL analyzer (CLA-ID3 CL analyzer; Tohoku Electronic Industrial Co., Ltd., Sendai, Japan) after 1.0 mL of 0.1 mM lucigenin in phosphate-buffered saline (PBS, pH 7.4) was added to the blood samples of mice. The total CL counts of the four groups were calculated by integrating the area under the curve within 600 s.

2.5. Immunohistochemistry. After herbal formula B401 or sham treatment, the four groups of ICR mice were anaesthetised with urethane (1.5 mg/kg); subsequently, cardiac perfusion with PBS containing 4% formaldehyde (Sigma-Aldrich Corporation) was conducted. Uterine tissue specimens of mice were obtained and fixed with 4% formaldehyde (EM grade) (Sigma-Aldrich Corporation). The uterine tissue specimens were embedded in paraffin and then cut into 5-μm-thick sections. Some sections were mounted on slides and then assessed through hematoxylin and eosin (H&E) staining with a kit-based approach (Sigma-Aldrich Corporation). For immunohistochemistry (IHC) staining, following the heat-induced epitope retrieval method, uterine tissue sections were separately stained at room temperature for 1 h with antibodies for estrogen receptor α (ERα),

estrogen receptor β (ERβ), progesterone receptor (PR), and vascular endothelial growth factor (VEGF) (Cell Signaling Technology Inc., Danvers, MA, USA). Then, immunostaining was detected through incubation with biotinylated secondary antibodies (Novolink™ Polymer Detection System l, Leica Biosystems Newcastle Ltd., Newcastle, UK) for 30 min and the avidin–biotin–horseradish peroxidase (HRP) complex (Novolink™ Polymer Detection System l, Leica Biosystems Newcastle Ltd.) for additional 30 min. Immunostaining was visualised using DAB Chromogen (Novolink™ Polymer Detection System l, Leica Biosystems Newcastle Ltd.), and the slides were counterstained with hematoxylin (Novolink™ Polymer Detection System l, Leica Biosystems Newcastle Ltd.).

2.6. Western Blot Analysis. After herbal formula B401 or sham treatment, the four groups of ICR mice were anaesthetised with urethane (1.5 mg/kg); subsequently, transcardial perfusion with physiological saline was conducted. Uterine tissue specimens were homogenised in a buffer solution. Then, proteins in the separated solution were quantified using a BCA protein assay kit (Thermo Fisher Scientific Inc., Waltham, MA, USA) and separated on 12.5% or 15% SDS polyacrylamide gels (Bionovas Pharmaceuticals Inc., Washington DC, USA). The separated proteins were transferred to polyvinylidene difluoride membranes (GE Healthcare Life Sciences, Barrington, IL, USA). The antibodies used in this study were β-actin (Thermo Fisher Scientific Inc.) and superoxide dismutase 2 (SOD2) (Cell Signaling Technology Inc.), which were detected using suitable HRP-conjugated secondary antibody (Santa Cruz Biotechnology Inc.). Immunostaining was visualised using the enhanced chemiluminescence (ECL) substrate (Millipore, Billerica, MA, USA) and was quantified using ImageJ analysis software (version 1.48t, NIH, Wayne Rasband, Washington DC, USA).

2.7. Statistical Analysis. All data are presented as mean ± SEM. The data were analysed using one-way or two-way ANOVA followed by Student–Newman–Keuls multiple comparison post-test. A P value of less than 0.05 was considered significant.

3. Results

3.1. Chromatographic Fingerprint of the Herbal Formula B401. Figure 1(a) shows the chromatographic fingerprint of the herbal formula B401 obtained using LC/MS. Fifteen bioactive marker substances from the components of the herbal formula B401 were qualitatively measured using LC/MS under selected conditions. These bioactive marker substances included Z-ligustilide from *Ang. sinensis*; astragaloside, isoastragaloside, astragaloside, and astragaloside IV from *Ast. membranaceus*; calycosin-7-O-β-D-glucoside, ononin, and wedelolactone from *E. prostrata*; oleanolic acid from *L. fructus*; ginsenoside Rc and ginsenoside Rb2 from *P. ginseng*; and calycosin, formononetin, forsythiaside, and acteoside from *R. glutinosa*.

3.2. IC_{50} Values of the Herbal Formula B401. Figure 1(b)(A) shows the potential cytotoxic effect of the herbal formula B401, which was measured through the MTT assay of SH-SY5Y cells. Cells were treated with the herbal formula B401 at the concentrations of 10, 20, 40, 80, and 160 mg/mL. After 24-h B401 treatment, cell viability was examined using the MTT assay. The herbal formula B401 showed no significant cytotoxicity at any concentration. Figure 1(b)(B) shows the dose–response sigmoid curve of the herbal formula B401. The calculated IC_{50} value of the herbal formula B401 was 305.3 mg/mL for SH-SY5Y cells.

3.3. Oral B401 Treatment Effectively Increases Levels of Calcium, Phosphorus, and Estradiol-17β in the Blood of Ovariectomised Mice. Figures 2(a) and 2(b) illustrate quantified blood levels of calcium and phosphorus in WT + sham, WT + B401, OVX + sham, and OVX + B401 mice. Quantified blood levels of calcium and phosphorus in OVX + sham mice significantly decreased compared with those in WT + sham mice ($P < 0.01$), whereas quantified blood levels of calcium and phosphorus in OVX + B401 mice significantly increased compared with those in OVX + sham mice ($P < 0.01$).Figure 2(c) presents quantified serum concentrations of estradiol-17β in WT + sham, WT + B401, OVX + sham, and OVX + B401 mice. Quantified serum concentrations of estradiol-17β in OVX + sham mice significantly decreased compared with those in WT + sham mice ($P < 0.01$), whereas quantified serum concentrations of estradiol-17β in OVX + B401 mice significantly increased compared with those in OVX + sham mice ($P < 0.01$).

3.4. Oral B401 Treatment Effectively Increases Uterine Weight in Ovariectomised Mice. As shown in Figure 3(a), uterine morphology in WT + sham, WT + B401, OVX + sham, and OVX + B401 mice was observed and then compared. The thickness of the uterine wall in OVX + sham mice decreased compared with that in WT + sham mice, whereas the thickness of the uterine wall in OVX + B401 mice increased compared with that in OVX + sham mice. Figure 3(b) shows that the quantified uterine weight of OVX + B401 mice significantly decreased compared with that of WT + sham mice ($P < 0.01$), whereas the quantified uterine weight of OVX + B401 mice significantly increased compared with that of OVX + sham mice ($P < 0.01$).

3.5. Oral B401 Treatment Increases Expression of the VEGF, ERα, ERβ, and PR in the Uterine Tissue of Ovariectomised Mice. In this study, we examined the expression of VEGF in the uterine tissue in the OVX + sham and OVX + B401 mice (Figure 4). We found that OVX + B401 mice showed higher expression of VEGF in the uterine tissue than OVX + sham mice. In addition, we examined the expression of ERα, ERβ, and PR in the uterine tissue in the four groups (Figure 5). We found that OVX + sham mice showed lower expression of ERα, ERβ, and PR in the uterine tissue than WT + sham mice, whereas OVX + B401 mice showed higher expression of ERα, ERβ, and PR in the uterine tissue than OVX + sham mice.

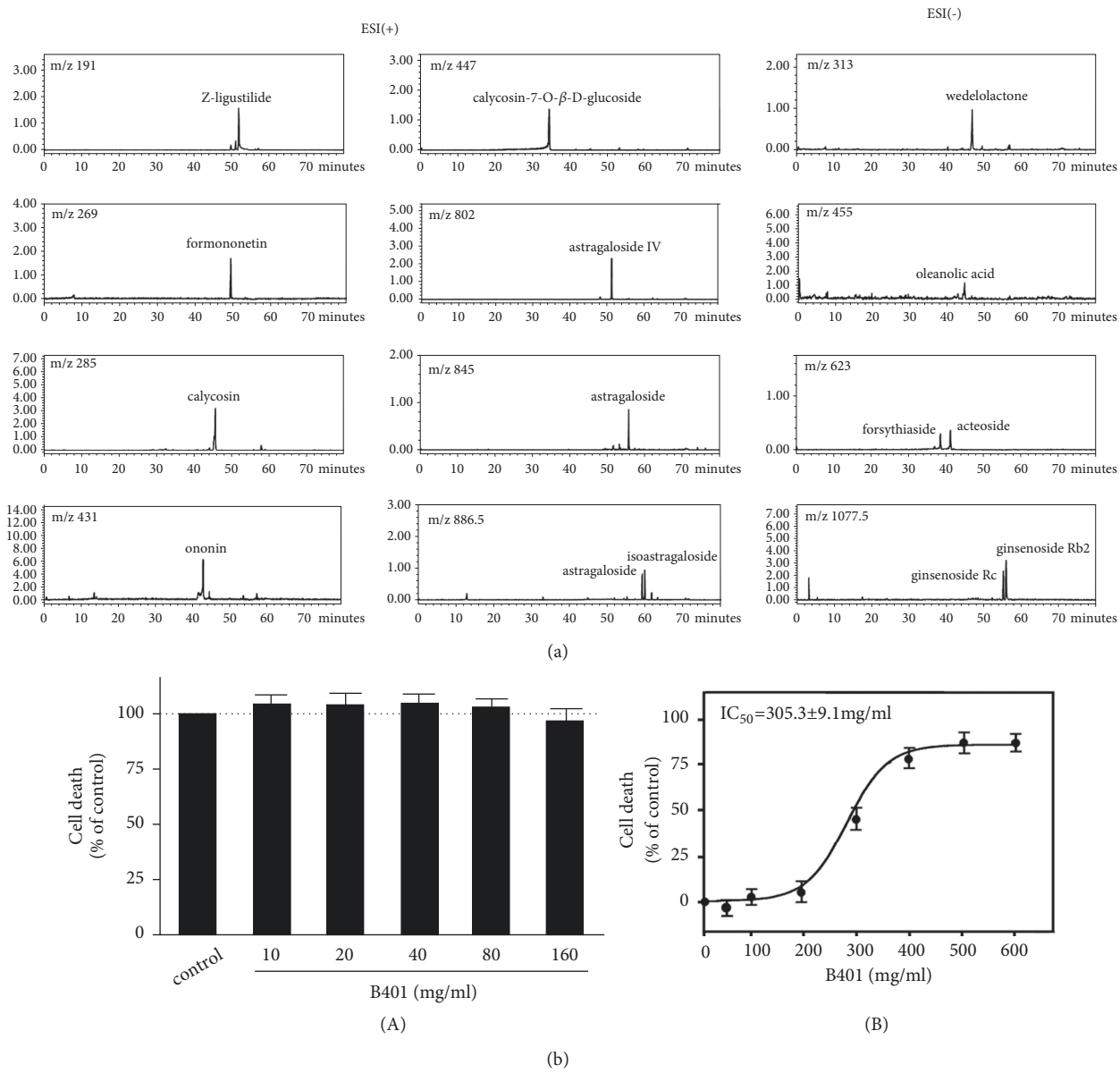

Figure 1: Chromatographic fingerprint analysis and cytotoxicity assay of the Chinese herbal formula B401. (a) Chromatographic fingerprint analysis was conducted through the LC/MS. Fifteen bioactive marker substances from the components of the herbal formula B401 were qualitatively determined within 80 min under selected LC/MS conditions. (b) (A) Cell viability of herbal formula B401 treatment measured through the MTT assay of SH-SY5Y cells. (B) The IC_{50} values of the Chinese herbal formula B401 in SH-SY5Y cells were calculated using the dose–response curve. The results are shown as mean ± SEM, and experiments were repeated three times for each treatment.

3.6. Oral B401 Treatment Effectively Reduces Blood ROS and Increases Uterine SOD2 Expression in Ovariectomised Mice. To study the effects of the herbal formula B401 on mitochondrial oxidative stress in ovariectomised mice, we examined and then compared the blood ROS count and uterine SOD2 expression among the four groups (Figures 6 and 7). Figure 6(a) shows that OVX + sham mice showed higher blood ROS counts than WT + sham mice, whereas OVX + B401 mice showed lower blood ROS counts than OVX + sham mice. Figure 6(b) presents that quantified ROS counts in the blood of OVX + sham mice significantly increased compared with the counts in the blood of WT + sham mice ($P < 0.01$), whereas quantified ROS counts in the blood of OVX + B401 mice significantly decreased compared with the counts in the blood of OVX + sham mice ($P < 0.01$). SOD2 is an antioxidant enzyme for oxidative stress. Figure 7(a) shows uterine SOD2 expression levels in WT + sham, WT + B401, OVX + sham, and OVX + B401 mice. As presented in Figure 7(b), quantified uterine SOD2 expression was significantly decreased in OVX + sham mice than in WT + sham mice ($P < 0.01$), whereas quantified uterine SOD2 expression was significantly increased in OVX + B401 mice than in OVX + sham mice ($P < 0.01$).

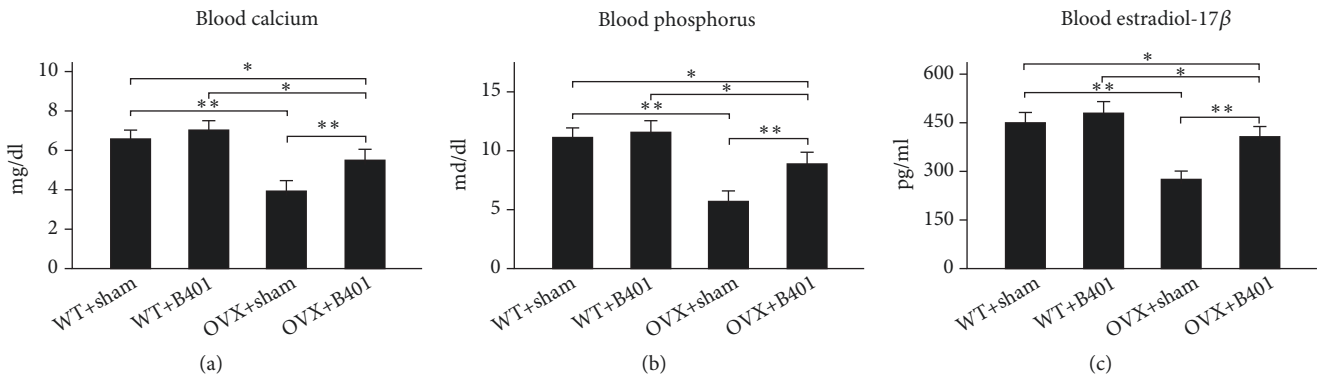

FIGURE 2: Oral B401 treatment effectively increases blood levels of calcium and phosphorus and serum levels of estradiol-17β in ovariectomized mice. Statistical comparison of quantified levels of (a) calcium, (b) phosphorus, and (c) estradiol-17β in blood/serum among WT + sham, WT + B401, OVX + sham, and OVX + B401 mice. The results are shown as mean ± SEM ($**P < 0.01$, $*P < 0.05$, two-way ANOVA followed by Student–Newman–Keuls multiple comparison post-test), and experiments were repeated three times for each treatment.

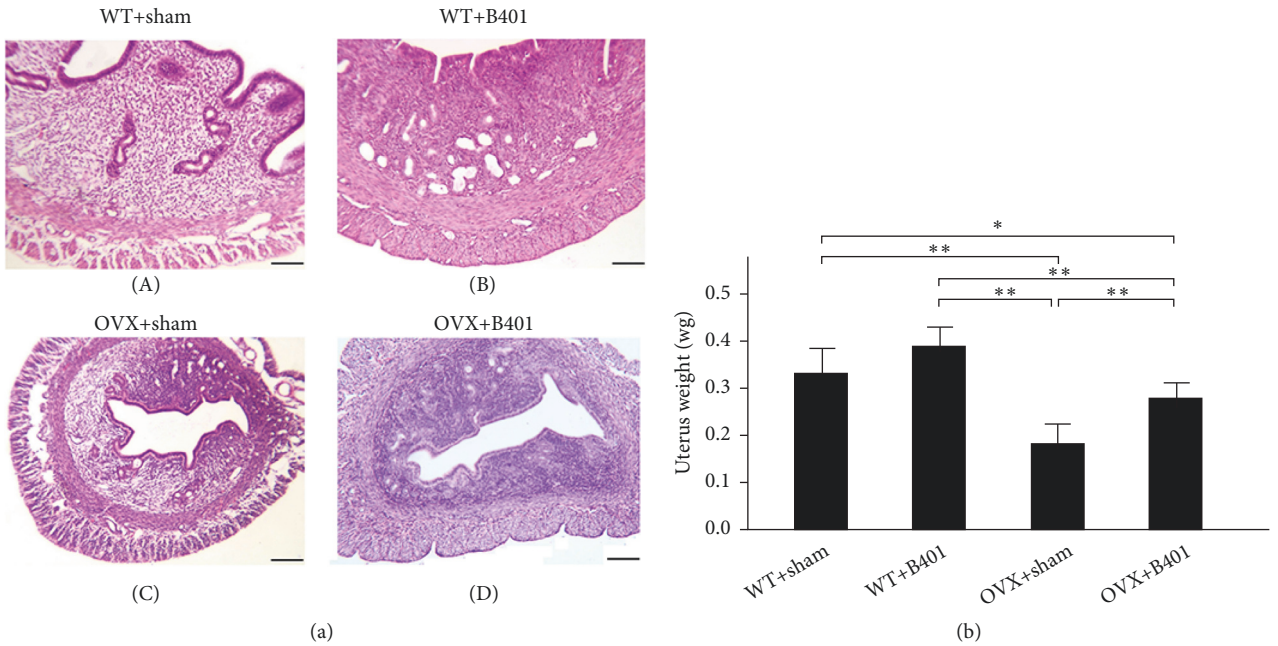

FIGURE 3: Oral B401 treatment effectively increases uterine weight in ovariectomized mice. (a) Uterine morphology in WT + sham, WT + B401, OVX + sham, and OVX + B401 mice through H&E staining. Bar scale = 100 μm. (b) Statistical comparison of quantified uterine weight among WT + sham, WT + B401, OVX + sham, and OVX + B401 mice. The results are shown as mean ± SEM ($**P < 0.01$, $*P < 0.05$, two-way ANOVA followed by Student–Newman–Keuls multiple comparison post-test), and experiments were repeated three times for each treatment.

4. Discussion

4.1. Reproductive Regulation of the Herbal Formula B401 in Ovariectomised Mice. In our previous studies, the herbal formula B401 treatment should be viable alternative treatment for the management of neurodegenerative diseases such as Alzheimer's, Huntington's, and Parkinson's diseases [9–11, 13]. In addition, we observed that most menopausal women who took the herbal formula B401 also felt that sweating, anxiety, and sleep disorders were significantly relieved. Therefore, the herbal formula B401 is currently used as a health food for middle-aged women in Taiwan. Before studying reproductive regulation of the herbal formula B401 in the ovariectomised mouse model, we should reexamine the active ingredients and cytotoxicity of the herbal formula B401. According to the MTT assay, the calculated IC_{50} value of the herbal formula B401 was 305.3 mg/mL for SH-SY5Y cells (Figure 1(b)). The IC_{50} dose of SH-SY5Y cells converted to the IC_{50} dose of ovariectomised mice should be 305 g/Kg bw/day. If safety factor calculated from 1/10 as the starting dose of human, the safety dose of the herbal formula B401 for an adult woman weighing 60 kilograms should be 1,830 g per day. In this study, those ovariectomised ICR mice received oral herbal formula B401 treatment at a dose of 30 mg/kg bw/day for 2 weeks. The converted edible dose of the herbal formula B401 for an adult woman weighing 60 kilograms is 1.8 g

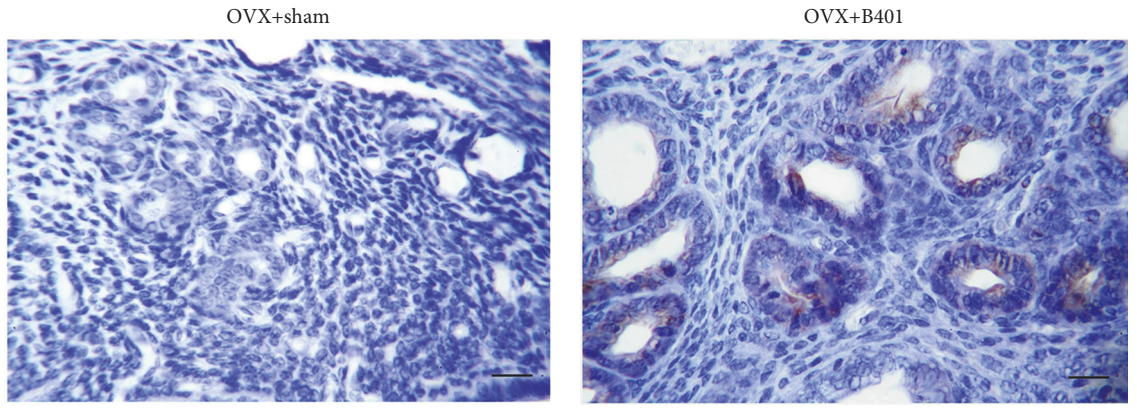

Figure 4: Oral B401 treatment enhances expression of the vascular endothelial growth factor (VEGF) in the uterine tissue of ovariectomised mice. Uterine VEGF expressions (expressed by deep brown color) in (a) OVX + sham and (b) OVX + B401 mice through IHC staining. Bar scale = 20 μm.

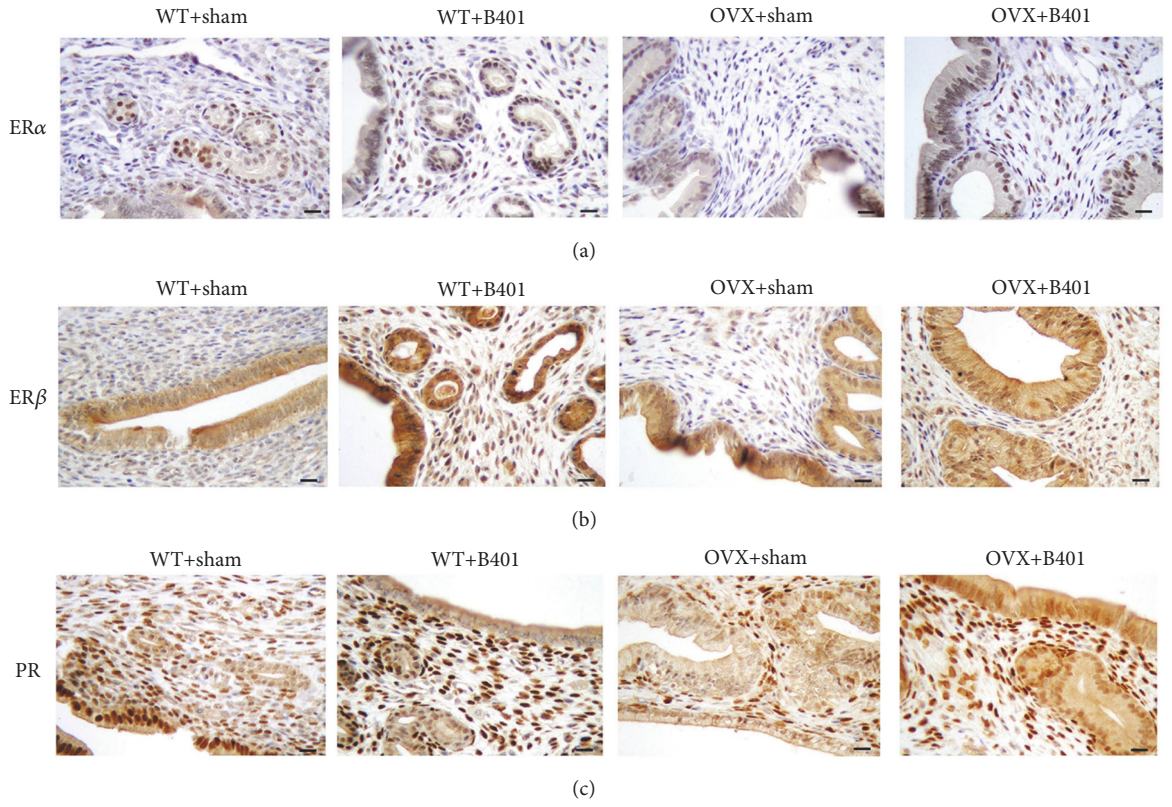

Figure 5: Oral B401 treatment enhances expressions of the estrogen receptor α (ERα), estrogen receptor β (ERβ), and progesterone receptor PR in the uterine tissue of ovariectomised mice. Uterine expression of (a) ERα, (b) ERβ, and (c) PR (expressed by deep brown color) in WT + sham, WT + B401, OVX + sham, and OVX + B401 mice through IHC staining. Bar scale = 20 μm.

per day that should be much smaller than the dose of IC_{50} value of the herbal formula B401. Thus, the herbal formula B401 should be quite safe dosage for menopausal women.

Ovariectomised female rats have a higher risk of osteoporosis [14]. In a previous study, bone mineral (calcium and phosphorus) contents were decreased in postmenopausal ovariectomised female rats, and estrogen therapy could reduce postmenopausal bone loss [15]. In addition, Estradiol-17 beta therapy could enhance endosteal bone formation in the ovariectomized mice [16]. These results clearly support our study results that ovariectomised female mice showed significant decrease in levels of calcium, phosphorus, and estradiol-17β in the blood, while showing significant

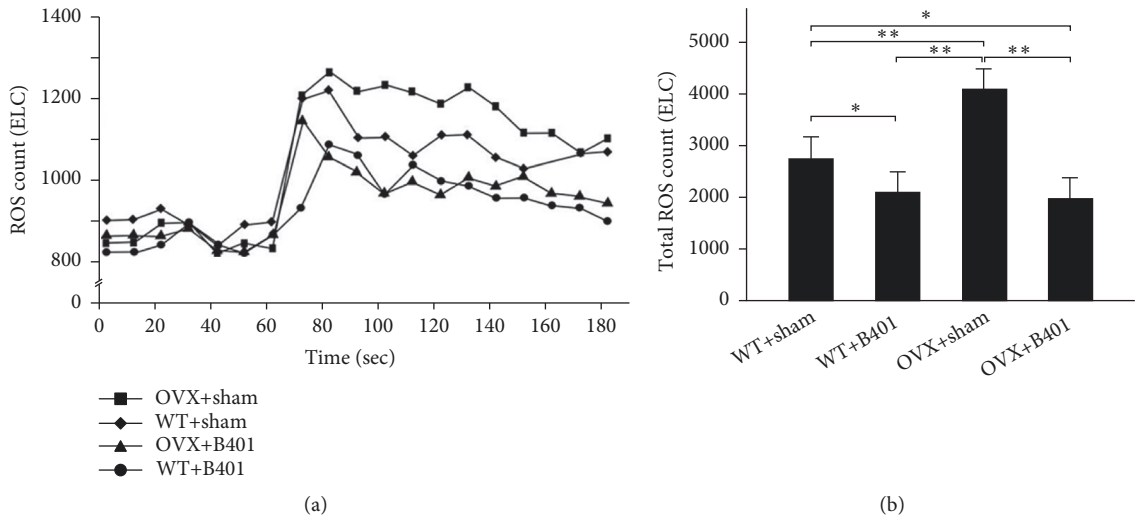

Figure 6: Oral B401 treatment effectively reduces blood ROS in ovariectomised mice. (a) Blood ROS count in WT + sham, WT + B401, OVX + sham, and OVX + B401 mice through chemiluminescence analysis. (b) Statistical comparison of quantified ROS count among WT + sham, WT + B401, OVX + sham, and OVX + B401 mice. The results are shown as mean ± SEM (∗∗P < 0.01, ∗P< 0.05, two-way ANOVA followed by Student–Newman–Keuls multiple comparison post-test), and experiments were repeated three times for each treatment.

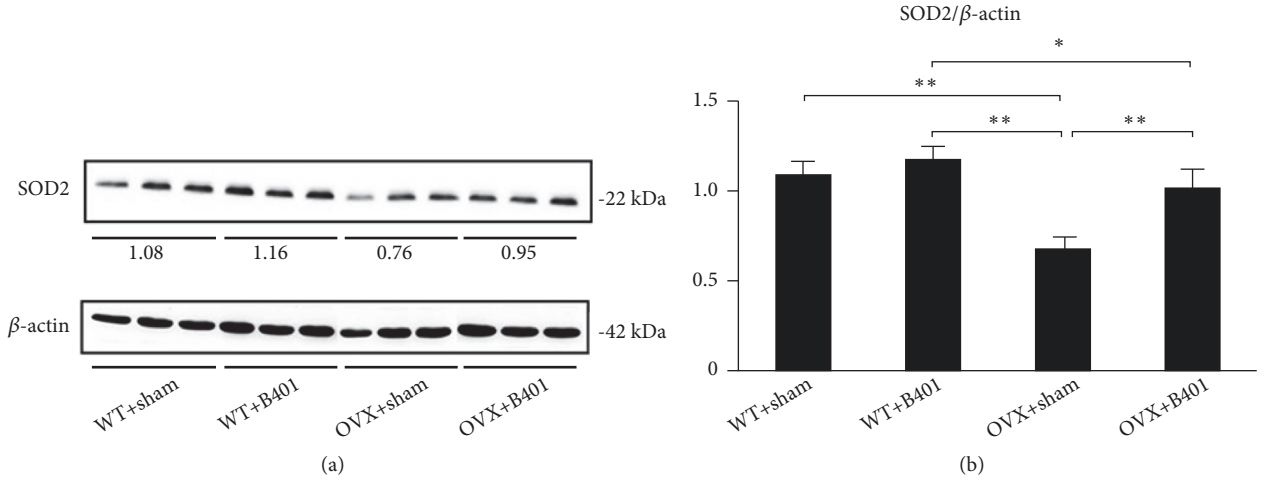

Figure 7: Oral B401 treatment effectively enhances SOD2 expression in the uterine tissue of ovariectomised mice. (a) Uterine SOD2 expression levels in WT + sham, WT + B401, OVX + sham, and OVX + B401 mice through Western blotting. (b) Statistical comparison of quantified SOD2 expression among WT + sham, WT + B401, OVX + sham, and OVX + B401 mice. The results are shown as mean ± SEM (∗∗P<0.01, ∗P< 0.05, two-way ANOVA followed by Student–Newman–Keuls multiple comparison post-test), and experiments were repeated three times for each treatment.

increased levels of calcium, phosphorus, and estradiol-17βin the blood after the herbal formula B401 therapy (Figure 2).

It has been reported that the reduction of uterine weight in ovariectomised rats might be due to reduced uterine epithelial height, expanded uterine stroma, reduced uterine myometrial thickness, and atrophic vaginal epithelium [17, 18]. In this study, we observed that ovariectomised female mice showed endometrium atrophy because of uterine weight reduction, while the herbal formula B401 therapy could increase uterine weight and endometrial thickness (Figure 3). This amelioration of uterine atrophy in ovariectomised mice might be probably due to the presence of biologically active phytoestrogen-like compounds in the herbal formula B401. Furthermore, through IHC, we found that the herbal formula B401 therapy could enhance the expression of VEGF in the uterine tissue of ovariectomised rats (Figure 4). Similar results have also been reported that ovariectomised rats with estradiol-17β therapy can increase endometrial blood flow and reduced endometrial vascular resistance [19]. The increased endometrial blood flow in ovariectomised rats with estradiol-17 beta treatment is due to increasing nitric oxide synthesis and subsequently improving endothelial function [20].

It has been reported that estrogen may play multiple biological functions by modulating ERα and ERβ [2], and PR expression can be induced by estrogen [21]. Thus, we

also examined the expression of ERα, ERβ, and PR in the uterine tissue. In this study, ovariectomised mice showed significantly decreased levels of estradiol-17β in the blood. We further found that ovariectomised mice significantly decrease expressions of uterine ERα, ERβ, and PR, whereas the herbal formula B401 therapy could enhance expressions of uterine ERα, ERβ, and PR (Figure 5). These results clearly indicate that the herbal formula B401 can increase estradiol-17β levels and increase the expression of ERα, ERβ, and PR in the uterine tissue. It is reasonable that the herbal formula B401 can be an alternative treatment for reproductive regulation.

4.2. Oxidative Stress Alleviation of the Herbal Formula B401 in Ovariectomised Mice. It has been reported that menopause is associated with metabolic disorders and oxidative stress [14]. A previous study demonstrated that ovariectomised rats showed enhanced oxidative stress in the plasma. Moreover, it has been reported that estrogen can produce antioxidant effects and reduce blood ROS [22, 23]. It has been reported that ROS can cause oxidative damage to cells, while SOD2 is an antioxidant enzyme that is responsible for O^{2-} dismutation to H_2O_2 [24]. Reduced SOD activity in ovariectomised animals may induce more accumulation of O^{2-} and inhibit other antioxidant enzymes [25]. The enhancement of the blood ROS in ovariectomised mice clearly suggests that oxidative stress is the major factor underlying menopausal symptoms. In this study, we evaluated the beneficial effects of the herbal formula B401 on mitochondrial oxidative stress in ovariectomised mice. Our study showed that ovariectomised mice significantly increase blood ROS, while the herbal formula B401 therapy could significantly decrease blood ROS (Figure 6). Furthermore, the herbal formula B401 therapy could significantly enhance uterine SOD2 expressions (Figure 7). Thus, we suggested that the herbal formula B401 might be an alternative treatment for mitochondrial oxidative stress alleviation in the reproductive regulation.

5. Conclusions

The herbal formula B401 therapy can enhance levels of calcium, phosphorus, and estradiol-17β in the blood, increase uterine weight and endometrial thickness, and improve expressions of ERα, ERβ, PR, and SOD2 in the uterine tissue but decrease blood ROS levels in ovariectomised mice. Thus we suggested that the herbal formula B401 can be a health supplement for alleviating discomfort symptoms in middle-aged women.

Abbreviations

ERα: Estrogen receptor α
ERβ: Estrogen receptor β
IC_{50}: Half maximal inhibitory concentration
IHC: Immunohistochemistry
LC/MS: Liquid chromatography/mass spectrometry
MTT: 3-(4,5-Dimethylthiazol-2-yl)-2,5-diphenyltetrazolium bromide
OVX: Ovariectomized
PR: Progesterone receptor
ROS: Reactive oxygen species
SEM: Standard error of the mean
SOD2: Superoxide dismutase 2
WT: Wild-type.

Data Availability

The subcutaneous blood flow assay, blood biochemical analysis, ROS analysis, immunohistochemistry, and Western blot analysis data used to support the findings of this study are included within the article and available from the corresponding author upon request.

Conflicts of Interest

There are no conflicts of interest in this study.

Acknowledgments

This work was supported by the funding of National Taiwan Normal University and the grants of Ministry of Science and Technology, Taiwan (MOST 107-2321-B-003-001- and MOST 107-2320-B-003-003-MY3). Also, the authors thank the Sun Ten Pharmaceutical Co. Ltd. and Brion Research Institute of Taiwan, which provided their experimental materials and conducted chromatographic fingerprint analysis of the herbal formula B401.

References

[1] H. Pan, M. Wu, C. Hsu, B. Yao, and K. Huang, "The perception of menopause among women in Taiwan," *Maturitas*, vol. 41, no. 4, pp. 269–274, 2002.

[2] T. A. Roepke, O. K. Ronnekleiv, and M. J. Kelly, "Physiological consequences of membrane-initiated estrogen signaling in the brain," *Frontiers in Bioscience*, vol. 16, no. 1, pp. 1560–1573, 2011.

[3] A. M. Kaunitz and J. E. Manson, "Management of menopausal symptoms," *Obstetrics & Gynecology*, vol. 126, no. 4, pp. 859–876, 2015.

[4] M. Ji and Q. Yu, "Primary osteoporosis in postmenopausal women," *Chronic Diseases and Translational Medicine*, vol. 1, no. 1, pp. 9–13, 2015.

[5] S. B. Doshi and A. Agarwal, "The role of oxidative stress in menopause," *Journal of Mid-Life Health*, vol. 4, no. 3, pp. 140–146, 2013.

[6] B. J. Ha, "Oxidative stress in ovariectomy menopause and role of chondroitin sulfate," *Archives of Pharmacal Research*, vol. 27, no. 8, pp. 867–872, 2004.

[7] S. Furness, H. Roberts, J. Marjoribanks et al., "Hormone therapy in postmenopausal women and risk of endometrial hyperplasia," *Cochrane Database of Systematic Reviews*, vol. 15, Article ID CD000402, 2009.

[8] L. Xu, S. Zhang, and Z. Sun, "The traditional Chinese medicine characteristics of etiology and pathogenesis of menopausal syndrome," *Journal of Traditional Chinese Medicine*, vol. 49, pp. 1031–1033, 2008.

[9] C.-H. Hsu, S.-E. Wang, C.-L. Lin et al., "Neuroprotective effects of the herbal formula b401 in both cell and mouse models

of alzheimer's disease," *Evidence-Based Complementary and Alternative Medicine*, vol. 2016, Article ID 1939052, 17 pages, 2016.

[10] C. H. Hsu, S. E. Wang, C. L. Lin, S. J. Sheu, and C. H. Wu, "Remission roles of the herbal formula B401 in mice with manganese-induced neurotoxicity," *Botanics*, vol. 2016, no. 6, pp. 1031–1033, 2016.

[11] S.-E. Wang, C.-L. Lin, C.-H. Hsu, S.-J. Sheu, C.-T. Chien, and C.-H. Wu, "Treatment with a herbal formula B401 enhances neuroprotection and angiogenesis in the R6/2 mouse model of Huntington's disease," *Drug Design, Development and Therapy*, vol. 9, pp. 887–900, 2015.

[12] C. H. Hsu, C. L. Lin, S. E. Wang, S. J. Sheu, C. T. Chien, and C. H. Wu, "Oral treatment of a herbal formula B401 alleviates penile toxicity for aging mice with manganism via enhancing synthesis of nitric oxide and angiogenesis, and suppressing oxidative stress, inflammation and apotosis," *Clinical Interventions in Aging*, vol. 10, pp. 1173–1187, 2015.

[13] S.-E. Wang, C.-L. Lin, C.-H. Hsu, S.-J. Sheu, and C.-H. Wu, "Oral treatment with the herbal formula B401 protects against aging-dependent neurodegeneration by attenuating oxidative stress and apoptosis in the brain of R6/2 mice," *Clinical Interventions in Aging*, vol. 10, pp. 1825–1837, 2015.

[14] G. A. Behr, C. E. Schnorr, and J. C. F. Moreira, "Increased blood oxidative stress in experimental menopause rat model: the effects of vitamin A low-dose supplementation upon antioxidant status in bilateral ovariectomized rats," *Fundamental & Clinical Pharmacology*, vol. 26, no. 2, pp. 235–249, 2012.

[15] M. Kim and Y. Lee, "Effects of soy isoflavone and/or estrogen treatments on bone metabolism in ovariectomized rats," *Journal of Medicinal Food*, vol. 8, no. 4, pp. 439–445, 2005.

[16] M. W. Edwards, S. D. Bain, M. C. Bailey, M. M. Lantry, and G. A. Howard, "Estradiol-17 beta stimulation of endosteal bone formation in the ovariectomized mouse: an animal model for the evaluation of bone-targeted estrogens," *Bone*, vol. 13, no. 1, pp. 29–34, 1992.

[17] L. J. Black, M. Sato, E. R. Rowley et al., "Raloxifene (LY139481 HCI) prevents bone loss and reduces serum cholesterol without causing uterine hypertrophy in ovariectomized rats," *The Journal of Clinical Investigation*, vol. 93, no. 1, pp. 63–69, 1994.

[18] S. S. M. Zaid, S. A. Sulaiman, K. N. M. Sirajudeen, and N. H. Othman, "The effects of Tualang honey on female reproductive organs, tibia bone and hormonal profile in ovariectomised rats—animal model for menopause," *BMC Complementary and Alternative Medicine*, vol. 10, article 82, 2010.

[19] R.-S. Zhang, P. H. Guth, O. U. Scremin, R. Singh, S. Pervin, and G. Chaudhuri, "Regulation of endometrial blood flow in ovariectomized rats: assessment of the role of nitric oxide," *American Journal of Physiology-Endocrinology and Metabolism*, vol. 273, no. 4, pp. H2009–H2017, 1997.

[20] I. Hernández, J. L. Delgado, J. Díaz et al., "Estradiol-17 beta prevents oxidative stress and decreases blood pressure in ovariectomized rats," *American Journal of Physiology-Regulatory, Integrative and Comparative Physiology*, vol. 279, no. 5, pp. R1599–R1605, 2000.

[21] K. Parczyk, R. Madjno, H. Michna, Y. Nishino, and M. R. Schneider, "Progesterone receptor repression by estrogens in rat uterine epithelial cells," *The Journal of Steroid Biochemistry and Molecular Biology*, vol. 63, no. 4-6, pp. 309–316, 1997.

[22] J. P. Stice, J. S. Lee, A. S. Pechenino, and A. A. Knowlton, "Estrogen, aging and the cardiovascular system," *Future Cardiology*, vol. 5, no. 1, pp. 93–103, 2009.

[23] S. Muthusami, I. Ramachandran, B. Muthusamy et al., "Ovariectomy induces oxidative stress and impairs bone antioxidant system in adult rats," *Clinica Chimica Acta*, vol. 360, no. 1-2, pp. 81–86, 2005.

[24] P.-M. Sinet and P. Garber, "Inactivation of human Cu, Zn superoxide dismutase during exposure to O_2 and H_2O_2," *Archives of Biochemistry and Biophysics*, vol. 212, no. 2, pp. 411–416, 1981.

[25] Y. Kono and I. Fridovich, "Superoxide radical inhibits catalase," *The Journal of Biological Chemistry*, vol. 257, no. 10, pp. 5751–5754, 1982.

Hindawi
Evidence-Based Complementary and Alternative Medicine
Volume 2019, Article ID 2089586, 8 pages
https://doi.org/10.1155/2019/2089586

Research Article

Polysaccharides of *Fructus corni* Improve Ovarian Function in Mice with Aging-Associated Perimenopause Symptoms

Yong Wang,[1] Jing-zhen Wu,[2] Yu Li,[2] and Xu Qi[3]

[1]*Department of Pharmacy, Jiangsu Jianhu People's Hospital, Yancheng 224700, China*
[2]*School of Medicine and Life Sciences, Nanjing University of Chinese Medicine, Nanjing 210023, China*
[3]*Department of Respiratory Medicine, The First Affiliated Hospital of Nanjing Medical University, Nanjing 210029, China*

Correspondence should be addressed to Yu Li; liyu@njucm.edu.cn and Xu Qi; qixuly@163.com

Received 5 March 2019; Revised 14 May 2019; Accepted 26 May 2019; Published 27 June 2019

Guest Editor: Glaura Fernandes

Objective. Perimenopause symptoms have an extremely high incidence in aging women. Development of new strategies to improve perimenopause symptoms is important topic in clinical context. Increasing studies have shown that the polysaccharides of *Fructus corni* (PFC) have many pharmacological activities including antiaging effects. Here, we evaluated the effects of PFC on the ovarian function in natural aging-associated perimenopause symptoms in mice. *Methods*. Natural aging mice (16-month old) were orally administrated with PFC at 1.11 g/kg daily for 24 days with none-treated young mice (3-month old) as control. Blood samples were collected for measurements of serum levels of estradiol, progesterone, luteinizing hormone (LH), and follicle stimulating hormone (FSH). Ovaries were isolated for histopathological and molecular exanimations. *Results*. We found that the aging mice had decreased number of growing follicles and corpus luteum in ovary, but treatment with PFC restored their amounts. Measurement of hormones showed that there were low serum levels of estradiol and progesterone but high levels of LH and FSH in aging mice; however PFC restored estradiol and progesterone levels but reduced LH and FSH levels. Immunohistochemical analysis with ovarian tissues also revealed that the expression of inhibin and insulin-like growth factor 1 was reduced in the ovary of aging mice but was restored by PFC. These data indicated that PFC regulated ovarian function-associated hormone levels in aging mice. Furthermore, there was reduced expression of antiapoptotic protein Bcl-2 and increased expression of proapoptotic molecules Bax and cleaved-caspase-3 in the ovary of aging mice. However, treatment with PFC upregulated Bcl-2 and downregulated Bax and cleaved-caspase-3, suggesting that PFC inhibited apoptosis of granulosa cells in the ovary of aging mice. *Conclusion*. PFC improved the ovarian function in mice, which had high potential to be developed as a safe and effective therapeutic remedy for aging-associated perimenopause symptoms.

1. Introduction

Perimenopause, also known as the menopausal transition, defines a period of time during which a series of physiological alterations mark progression toward the final menstrual period of a woman. This transition starts with the onset of menstrual irregularities and continues until menopause has occurred, which may last for a variable amount of time with a median of four years [1]. During perimenopause, a woman may suffer from a number of symptoms, including menstrual cycle changes, insomnia, dysphoric mood symptoms, and somatic symptoms [2]. It is estimated that as many as 90% of women will ask for advice on how to control or relieve these menopausal-associated symptoms, suggesting that perimenopause symptoms are important topics in the clinical practice worldwide [3].

Clear evidence has demonstrated that perimenopausal women commonly suffer from ovarian dysfunction, resulting in systemic changes of hormones mainly including estradiol and progesterone [4]. A number of basic and clinical studies have evaluated the use of hormone replacement therapy (HRT) for perimenopause symptoms [5]. Despite the therapeutic benefits of HRT, risks or problems also occur in some subpopulation in women [6]. On the other hand, understanding the pathophysiology of ovarian function decline can help guide clinical management. Granulosa cells (GCs) play an important role in the growth and development of the follicle in the process known as folliculogenesis. The major functions

of GCs include the production of sex steroids, as well as myriad growth factors thought to interact with the oocyte during its development [7]. Emerging evidence suggests that apoptosis of GCs is concomitant with aging-associated ovarian function decline leading to ovarian hormone secretion disorder [8]. Therefore, prevention of GCs apoptosis represents a novel strategy for treatment of perimenopause symptoms.

In recent years, there has been renewed interest in the potential of purified natural products to provide health and medical benefits and to prevent disease. *Fructus corni* is one of the most common traditional Chinese herbal medicines used as a common option for liver and kidney nourishing, in which polysaccharides are characterized to be the main functional components and have attracted accumulated attentions [9]. Pharmacological studies have demonstrated that the polysaccharides of *Fructus corni* (PFC) have a wide range of bioactivities, such as immunomodulatory, antioxidant, antitumor, and antiaging effects [10]. Herein, we aimed to evaluate the effects of PFC on ovarian functions in naturally aging female mice, in the hoping of revealing the therapeutic potential of PFC for women experiencing perimenopause symptoms.

2. Methods

2.1. Reagents and Antibodies. PFC (purity 95%) was purchased from Ningbo Dekang Biological Products Co., Ltd. (Ningbo, China). The primary antibodies against Bcl-2, Bax, cleaved-caspase-3, and β-actin for Western blot assays were obtained from Cell Signaling Technology (Danvers, MA, USA). The primary antibodies against inhibin, IGF-1, Bcl-2, Bax, and cleaved-caspase-3 for immunohistochemistry were provided by Proteintech Group (Chicago, IL, USA).

2.2. Animal Experiments. All animal experiments were approved by the Institutional Animal Care and Use Committee [protocol number ACU-20(20151201)], Nanjing University of Chinese Medicine, and conformed to the Guide for the Care and Use of Experimental Animals. Ten young female ICR mice (3-month old, body weight 20±2 g) and 20 aging female ICR mice (16-month old, body weight 50±5 g) were provided by the Experimental Animal Center of Nanjing University of Chinese Medicine. All mice were housed in plastic cages (5 mice per cage) and maintained in standardized conditions at 20 ± 2°C room temperature, 40 ± 5% relative humidity, and a 12 h light/dark cycle. Water and pelleted food were available ad libitum. Animals were acclimated to the animal facility for 1 week. The 20 aging mice were randomly divided into two groups: aging model group (n=10) and PFC intervention group (n=10). The 10 young mice were set as control group. The mice in PFC intervention group were administrated with PFC at a dose of 1.11 g/kg daily by gavage for continuous 24 days. This dose used in mice was calculated from human clinical doses based on the body weight and body surface area in accordance with the published methods [11]. The young control mice and aging model mice were given normal saline daily by gavage (0.5 ml/mouse) for continuous 24 days. Of note, the estrous phase of each mouse was checked by vaginal smears before grouping and during the experiments according to reported methods [12]. The mice with regular estrous phase were used for experiments, and we made sure that the mice in each group at similar estrus stages when they were euthanized. At the end of experiments, all mice were anaesthetized by inhalation of ether followed by blood collection via retro orbital sinus. Then, mice were killed by decapitation followed by isolation of bilateral ovaries for histopathological and molecular exanimations.

2.3. Hematoxylin-Eosin (HE) Staining. Mouse left ovaries were fixed in 10% neutral buffered formalin. After washing with phosphate-buffered saline, the fixed tissues were dehydrated in graded ethanol and embedded in paraffin. Five serial paraffin sections (5 μm thickness of each) were sliced from each sample using a sliding microtome, and paraffin was removed using xylene. Tissue sections were stained with HE reagents according to standard procedures [13]. Images were blindly taken at random fields under a microscope (Nikon, Tokyo, Japan). The number of growing follicles and corpus luteum per field was counted. Representative views are shown.

2.4. Measurements of Serum Hormone Levels. Blood samples from mice were incubated at room temperature for 1 h to allow clotting. Serum was extracted after centrifugation and aliquoted. Serum levels of estradiol, progesterone, luteinizing hormone (LH), and follicle stimulating hormone (FSH) were measured using their corresponding radioimmunoassay kits (Tianjin Jiuding Medical Bioengineering Co., Ltd., Tianjin, China) according to the manufacturer's instructions.

2.5. Real-Time PCR. Total RNA was isolated from mouse right ovarian tissues using TRIzol reagent (Invitrogen, Carlsbad, CA, USA). First-strand cDNA was synthesized with 1 μg of total RNA using a PrimeScript RT reagent kit (TakaraBio, Tokyo, Japan). The quantitative real-time PCR was performed using IQTM SYBR Green supermix and the iQ5 real-time detection system (Bio-Rad Laboratories, Hercules, CA, USA). Reaction mixtures contained 7.5 μl of SYBR Green I dye master mix (Quanta), 2 pM each of forward and reverse primers. Thermocycler conditions included initial denaturation at 50°C and 95°C (10 min each), followed by 40 cycles at 95°C (15 s) and 60°C (1 min). Glyceraldehyde phosphate dehydrogenase (GAPDH) was used as the invariant control mRNA abundance was determined by $2^{-\Delta\Delta CT}$ method [14]. The primers of genes (GenScript, Nanjing, China) were as follows: Bcl-2: (forward) 5′-CCCACCTGTGGTCCATCT-GAC-3′, (reverse) 5′-CGGTAGCGACGAGAGAAGTC-3′; Bax: (forward) 5′-CTGGATCCAAGACCAGGGTG-3′, (reverse) 5′-GGGGTCCCGAAGTAGGAGAG-3′; GAPDH: (forward) 5′-TGACAACAGCCTCAAGAT-3′, (reverse) 5′-GAGTCCTTCCACGATACC-3′. Results were from triplicate experiments.

2.6. Western Blot Analyses. Protein abundance was detected using Western blot analyses according to the reported

procedures [15]. Briefly, total lysates from mouse right ovarian tissues were prepared with RIPA buffer (50 mM Tris, pH 7.2; 150 mM NaCl; 0.5% sodium deoxycholate; 0.1% sodium dodecyl sulfate; 1% Nonidet P-40; 10 mM NaF; 1 mM Na_3VO_4; protease inhibitor cocktail). Lysates were sonicated for 10 s and centrifuged at 14, 000 rpm for 10 min at 4°C. Protein concentrations were determined by bicinchoninic acid assay with BSA as a standard (Pierce, Rockford, IL, USA). Equivalent amounts of protein (50 μg/lane) were separated on 7.5%-12% SDS-polyacrylamide gel and transferred to polyvinylidene difluoride membranes (Millipore, Bedford, MA, USA). Membranes were incubated with phosphate buffer solution containing 0.05%Tween 20 and 5% nonfat dry milk to block nonspecific binding and were incubated with primary antibodies (dilution 1:1000), then with appropriate secondary antibodies conjugated to horseradish peroxidase (dilution 1:10000). Immunoreactive bands were visualized by using Renaissance chemiluminescence reagent (Perkin-Elmer Life Science, Boston, MA, USA). β-actin was used as an invariant control for equal loading of total proteins. The levels of target protein bands were densitometrically determined using Image Lab Software 3.0. The variation in the density of bands was expressed as fold changes compared to the control in the blot after normalization to β-actin. Presented blots are representative of three independent experiments.

2.7. Immunohistochemistry. Five serial sections (5 μm thickness of each) of mouse left ovarian tissues were incubated with the primary antibodies against inhibin (dilution 1: 100), IGF-1 (dilution 1: 100), Bcl-2 (dilution 1: 100), Bax (dilution 1:100), or cleaved-caspase-3 (dilution 1:100) for immunohistochemical analysis using standard methods [16]. Images were blindly taken at random fields under a microscope (Nikon, Tokyo, Japan). For each slice, five fields were randomly selected for quantitative analysis. Image Pro Plus 6.0 software (Media Cybernetics, Rockville, MD, USA) was used to calculate the positive staining area (%). Representative views are shown.

2.8. Statistical Analysis. Data were presented as mean ± SD, and results were analyzed using SPSS16.0 software. The significant differences of normally distributed data was determined by one-way ANOVA with post hoc Tukey's test for comparison between multiple groups under the condition that F achieved $P < 0.05$, and there was no significant variance inhomogeneity. For the nonnormally distributed data, Kruskal-Wallis H test was used to determine significant differences between multiple groups. Values of $P < 0.05$ were considered to be statistically significant.

3. Results

3.1. PFC Improves Ovarian Histology and Increases Follicles and Corpus Luteum in Aging Mice. We initially examined the histology of mouse ovary. Compared with the young control mice, there were less ovarian follicles and corpus luteum in ovarian cortex, but more atresia follicles in aging mice; however, treatment with PFC recovered these histological features to a certain extent compared with the aging model mice (Figure 1(a)). Consistently, quantification of growing follicles showed that the number of growing follicles was significantly decreased in the ovary of aging model mice, which was remarkably recused by treatment with PFC (Figure 1(b)). Moreover, the number of corpus luteum was significantly decreased in the ovary of aging model mice, but administration of PFC significantly restored the amount of corpus luteum (Figure 1(c)). Altogether, these data indicated that PFC improved ovarian histology and restored follicles and corpus luteum in aging mice.

3.2. PFC Regulates Ovarian Function-Associated Hormone Levels in Aging Mice. We next determined the alterations in the hormone levels associated with ovarian function. We observed that the serum levels of estradiol and progesterone were significantly declined in aging model mice compared to the young control mice, but their serum concentrations were significantly rescued by PFC (Figures 2(a) and 2(b)). In addition, the serum levels of LH and FSH were significantly increased in aging model mice compared to the young control mice, but PFC intervention effectively reduced their serum concentrations in aging mice (Figures 2(c) and 2(d)). Immunohistochemical analysis with ovarian tissues additionally showed that the ovarian expression of inhibin and insulin-like growth factor 1 (IGF-1) were considerably downregulated in aging model mice but were restored by treatment PFC (Figure 2(e)). Taken together, PFC regulated ovarian function-associated hormone levels in aging mice.

3.3. PFC Prevents Apoptosis of Ovarian GCs in Aging Mice. Real-time PCR analysis showed that the mRNA expression of antiapoptotic protein Bcl-2 was decreased, but the mRNA expression of proapoptotic protein Bax was increased in the ovary of aging mice; however, PFC significantly restored Bcl-2 mRNA expression but diminished Bax mRNA expression (Figure 3(a)). Western blot analyses confirmed the changes of Bcl-2 and Bax expression at the protein levels in the ovary of the three groups of mice (Figure 3(b)). Additionally, the protein abundance of cleaved-caspase-3 was significantly increased in the ovary of aging mice, but was abrogated by PFC (Figure 3(c)). Immunohistochemical analyses with ovarian tissues gave consistent results on the changes of the above apoptosis regulatory molecules (Figure 4). Altogether, these findings suggested that PFC prevented apoptosis of ovarian GCs in aging mice.

4. Discussion

Understanding menopause-associated pathologies and developing novel approaches to manage perimenopause symptoms are important topics in current clinical context. The decrease in estrogen secretion is closely related to the occurrence of perimenopause symptoms. Thus, a commonly used model of perimenopause symptoms can be established via ovariectomy, but this model makes estrogen undetectable [17]. Actually, there is a gradual change of hormones in natural menopause that begins to appear

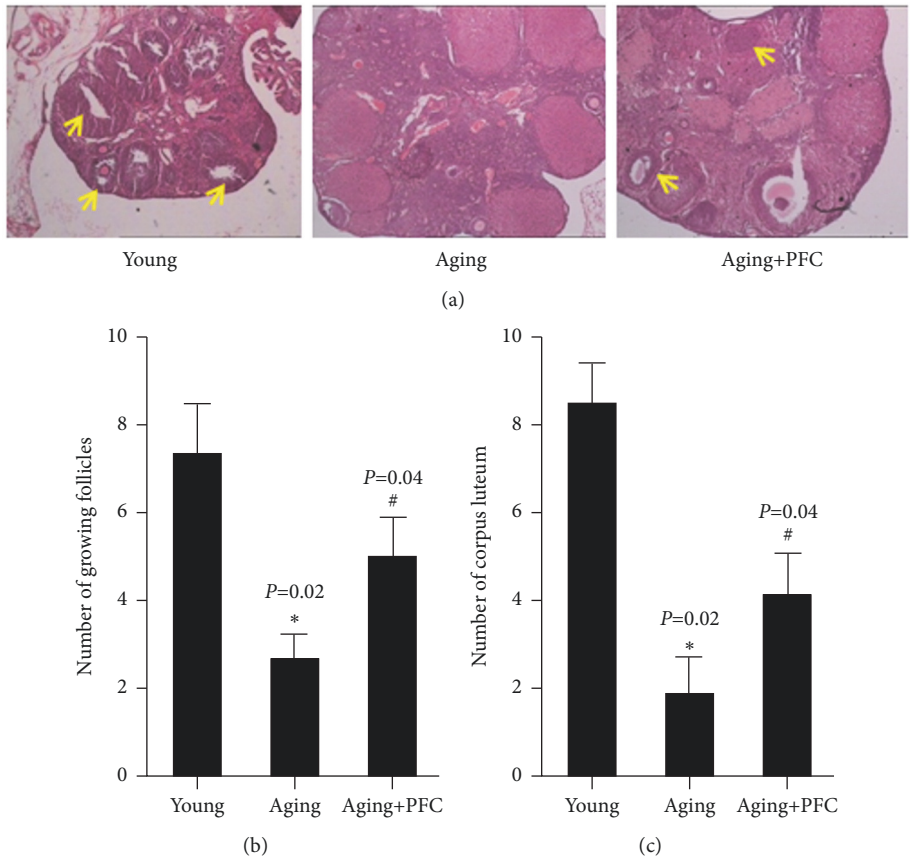

FIGURE 1: PFC improves ovarian histology and increases follicles and corpus luteum in aging mice. (a) HE staining with ovarian tissues. The yellow arrows indicate the growing follicles. (b) Quantification of growing follicles in ovarian tissues. (c) Quantification of corpus luteum in ovarian tissues. For statistical significance in this figure, $*P < 0.05$ compared with the young control group; $^{\#}P < 0.05$ compared with the aging model group; Kruskal-Wallis H test.

at perimenopause and alters over this transition prior to reaching postmenopause. Ovariectomy also eliminates some other hormones that are likely to play critical roles in menopause; especially, the central modulators of LH, FSH, and gonadotropin-releasing hormone are depleted [18]. Given that the rodents, similar to human, undergo natural hormonal fluctuations in the middle age [19], we used a naturally aging mouse model for experiments in current study, because this model allows for the retention of ovary with an apparent transitional period and thus can more accurately replicate the physical process of aging-associated decline of female reproductive system in human. To eliminate the possible bias introduced in the results, we carefully checked the estrus cycle of each mouse before and during the experiments, because the stages of estrus cycle analogous to menstrual cycle in humans determine the type and sizes of follicles and hormonal levels. We used the mice with regular estrus cycle for experiments and made sure that the mice in each group were at similar stages of the cycle when they were euthanized for examinations.

Over the past decades, investigations of menopause and HRT have produced a great deal of confusion about their effects on women's health. For instance, the evidence for HRT's neuroprotective effects for cognitive disorders in menopausal women was mixed [20]. However, HRT initiated during perimenopause reduced the risk of dementia and had cognitive benefits [21]. Natural products have increasingly been valued as therapeutic opportunities for human diseases. Many studies have reported that PFC had antiaging effects. For example, some studies examined the effects of PFC on D-galactose-induced aging in rats and found that PFC at 0.28 g/kg by gavage for 30 days increased the activity of superoxide dismutase, inhibited lipid peroxidation, and upregulated the mRNA expression of nerve growth factor mRNA [9]. It was also reported that treatment with PFC-containing rabbit serum at a low concentration of 1.5% for 48 h exerted antiaging effects on human dermal fibroblasts cells *in vitro* [9]. All these findings promoted us to ask whether PFC could improve ovarian function in aging-associated perimenopause symptoms. Indeed, we observed that PFC improved ovarian histology and hormone secretion in aging mice. Notably, PFC downregulated the serum concentrations of LH and FSH, two important hormones secreted by gonadotropic cells of the anterior pituitary gland [22], which were consistent with the common phenomenon of high serum levels of LH and FSH in women after menopause because of the decreased

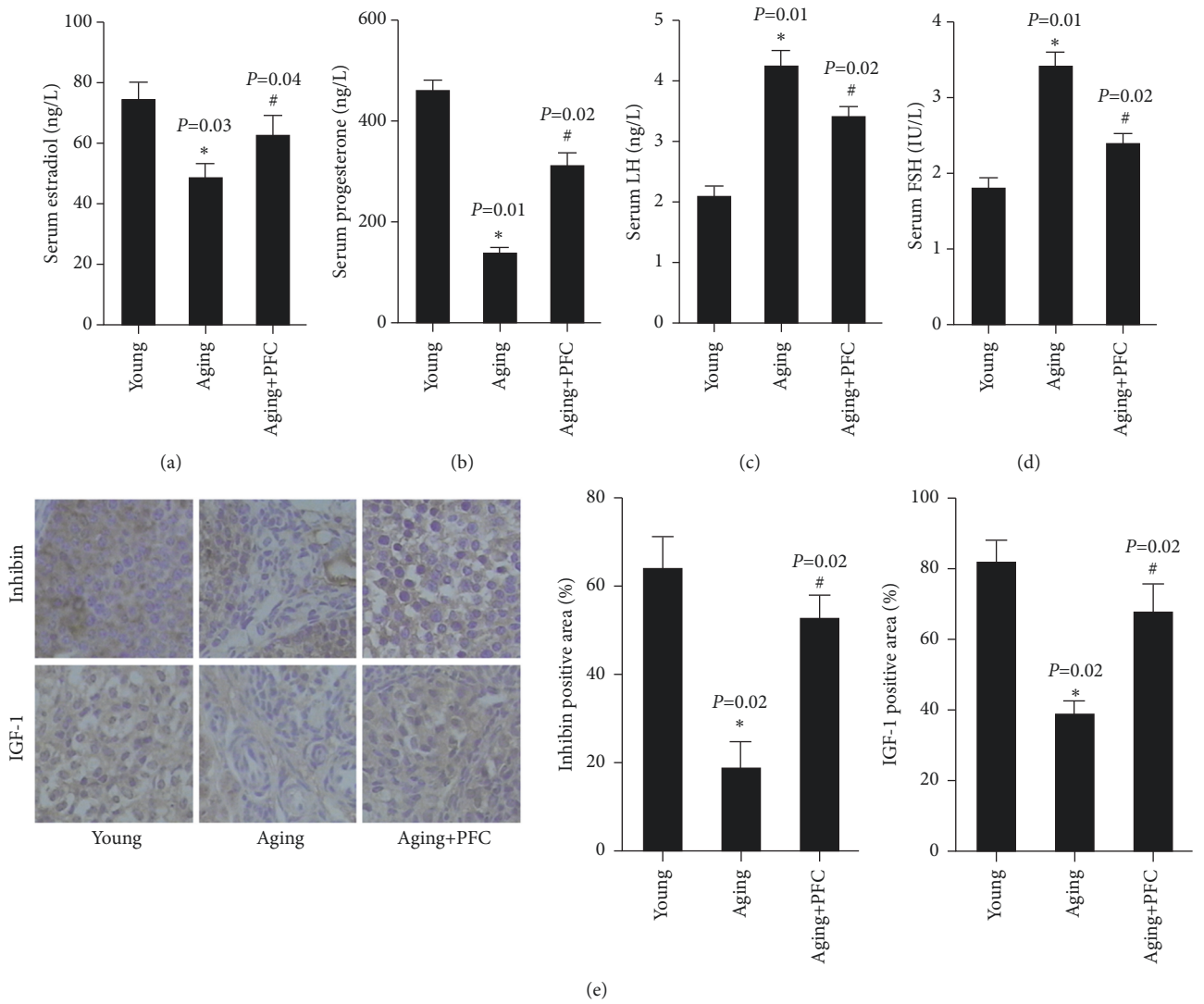

Figure 2: PFC regulates ovarian function-associated hormone levels in aging mice. (a) Serum estradiol levels. (b) Serum progesterone levels. (c) Serum LH levels. (d) Serum FSH levels. (e) Immunohistochemical analyses of inhibin and IGF-1 in mouse ovarian tissues with quantification of positive staining area. For statistical significance in this figure, $*P < 0.05$ compared with young control group; $^{\#}P < 0.05$ compared with aging model group; one-way ANOVA with post hoc Tukey's test for (a-d); Kruskal-Wallis H test for (e).

feedback control of pituitary secretion due to the low levels of estradiol and progesterone. Additionally, we observed that the expression of IGF-1 was reduced in the ovary of aging mice but upregulated by PFC treatment. IGF-1 has been implicated in follicle development and is considered to mediate the actions of gonadotrophins and growth hormone at the ovarian level [23]. IGF-1 can be secreted by GCs irrespective of their progestogenic status. In aggregate, our data revealed that PFC might exert systemic regulatory effects probably including the effects on central hormone secretion in aging mice and that regulation of growth factor system was also involved in PFC improvement of ovarian function.

We further performed molecular examinations to elucidate the mechanisms underlying PFC's effects. Our data suggested that apoptosis of GCs was possibly involved in the decreased ovarian function in aging mice. Specifically, Bcl-2 expression was decreased and Bax expression was increased, suggesting the activation of mitochondrial apoptosis pathway. Indeed, mitochondrial dysfunction has been implicated in cellular senescence in general and, in particular, ovarian aging [24]. Recent studies have validated this association by studying mitochondrial DNA copy number as a potential biomarker of embryo viability and the use of mitochondrial nutrients and autologous mitochondrial transfer as a potential treatment for poor ovarian function and response [24]. Although apoptosis occurs as a physiological process in the ovary, being highly important throughout the phases of follicular development, apoptosis in dominant follicles may interfere in ovulation and oocyte quality [25]. Therefore, excessive apoptosis of GCs definitely has negative effects on ovarian function during perimenopause symptoms [8]. Our current findings indicated that PFC considerably reduced

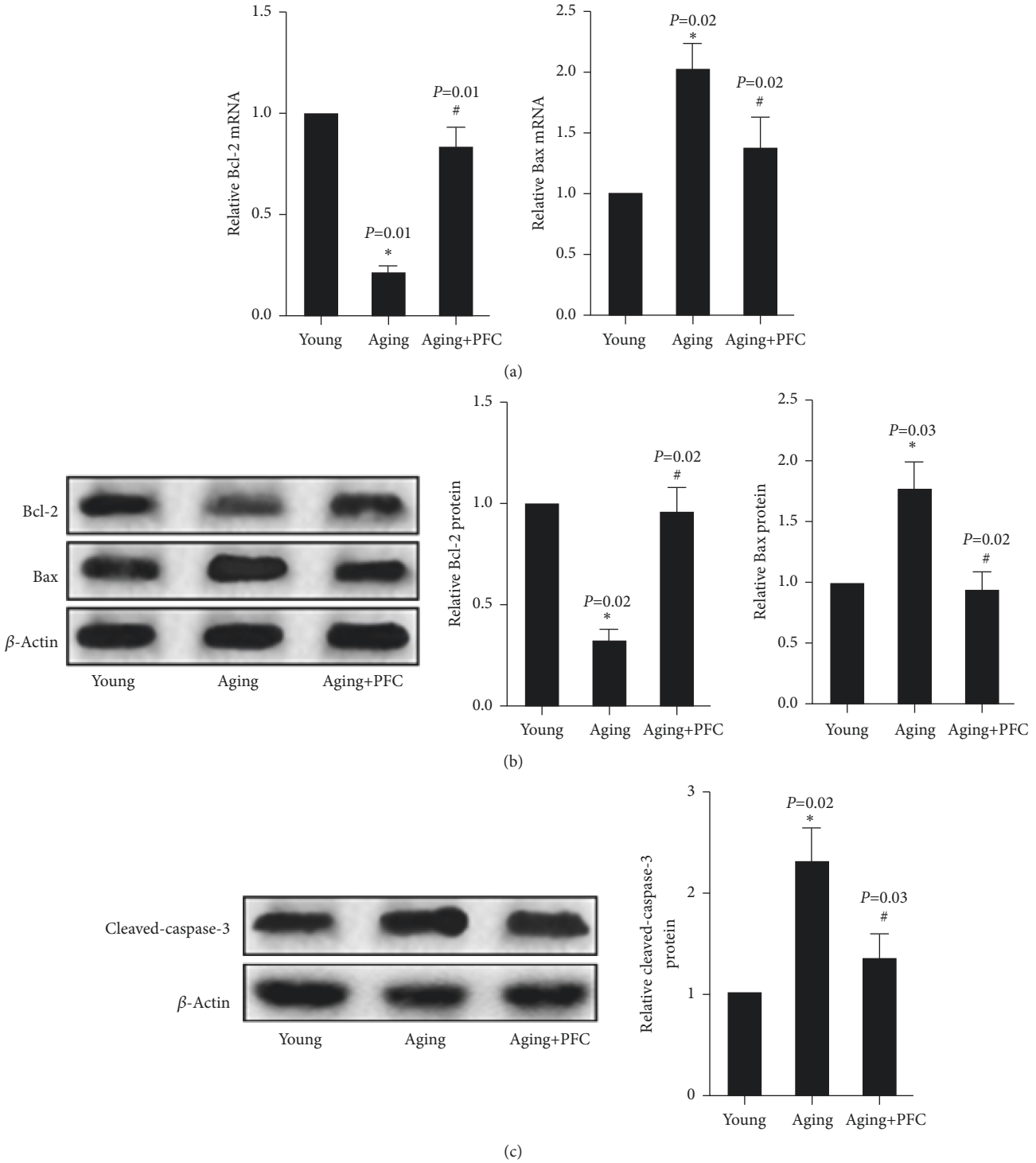

Figure 3: PFC prevents apoptosis of ovarian GCs in aging mice. (a) Real-time PCR analyses of mRNA expression of Bcl-2 and Bax in ovarian tissues. (b) Western blot analyses of protein abundance of Bcl-2 and Bax in ovarian tissues with quantification. (c) Western blot analyses of protein abundance of cleaved-caspase-3 in ovarian tissues with quantification. For statistical significance in this figure, $*P < 0.05$ compared with young control group; $^{\#}P < 0.05$ compared with aging model group; Kruskal-Wallis H test.

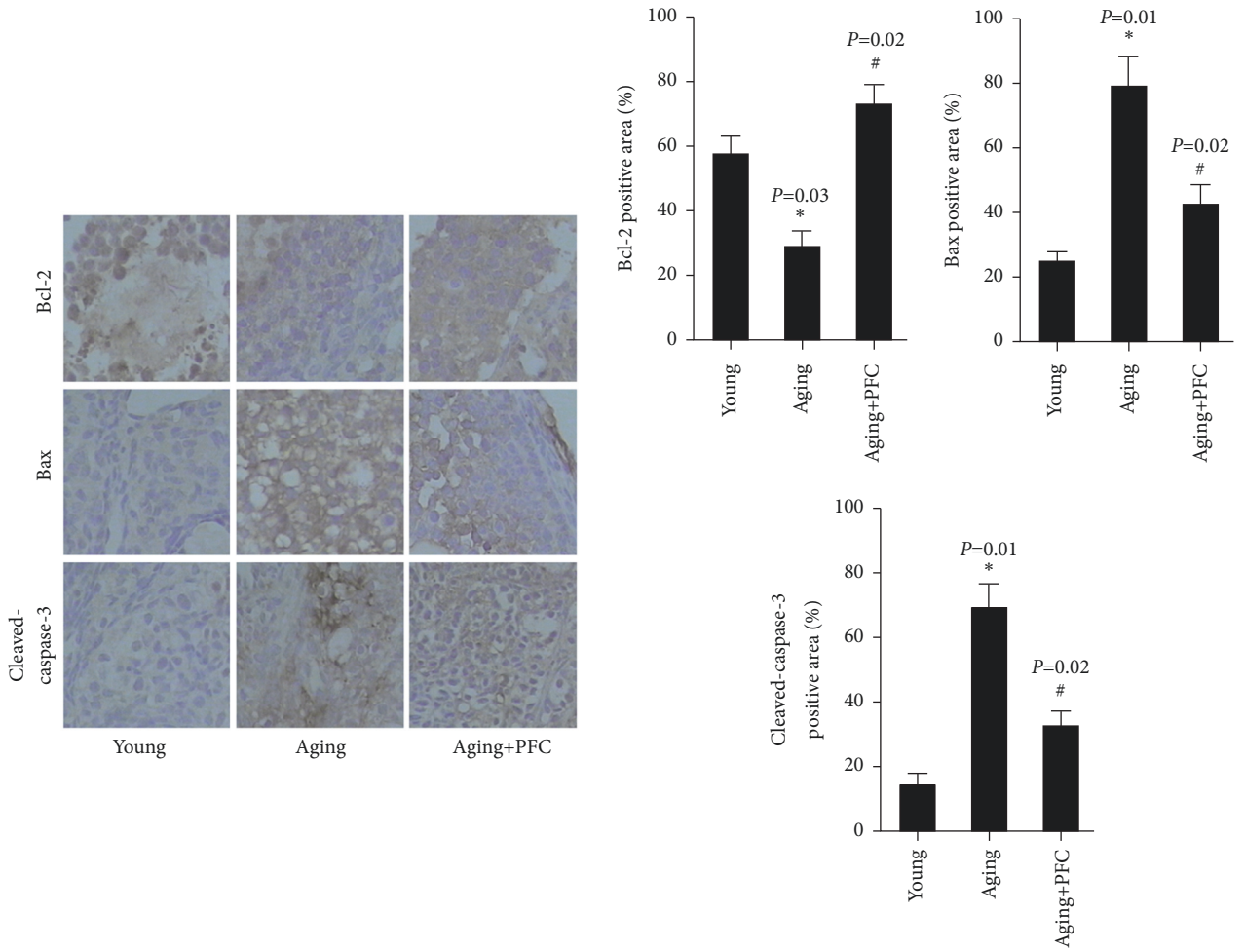

Figure 4: Immunohistochemical analyses of apoptosis-associated molecules Bcl-2, Bax, and cleaved-caspase-3 in mouse ovarian tissues with quantification. For statistical significance in this figure, $*P < 0.05$ compared with young control group; $^{\#}P < 0.05$ compared with aging model group; Kruskal-Wallis H test.

apoptosis of GCs in the ovary of aging mice, which could be the molecular basis for PFC improvement of ovarian histology and function. Further experiments are required to determine whether other apoptotic mechanisms were involved in PFC's effects.

5. Conclusions

Our data demonstrated that PFC effectively improved the ovarian function in aging-associated perimenopause symptoms through improving histology and hormone endocrine, which could be associated with inhibition of apoptosis of GCs. We suggested PFC as a promising therapeutic option for perimenopause symptoms.

Abbreviations

FSH: Follicle stimulating hormone
GAPDH: Glyceraldehyde phosphate dehydrogenase
GC: Granulosa cells
HE: Hematoxylin-eosin
HRT: Hormone replacement therapy
IGF-1: Insulin-like growth factor 1
LH: Luteinizing hormone
PFC: Polysaccharides of *Fructus corni*.

Data Availability

The data used to support the findings of this study are available from the corresponding author upon request.

Ethical Approval

The present study was approved by the Animal Ethics Committee of Nanjing University of Chinese medicine (Nanjing, China).

Conflicts of Interest

The authors report no conflicts of interest.

Authors' Contributions

Yong Wang, Yu Li, and Xu Qi contributed to the study design. Yong Wang and Jing-zhen Wu performed experiments. Yong Wang, Jing-zhen Wu, and Yu Li performed data analysis and interpretation. Yu Li and Xu Qi were responsible for manuscript preparation. All authors read and approved the final manuscript.

Acknowledgments

This work was supported by the National Natural Science Foundation of China (no. 30772851) and the Project Founded by School of Basic Medicine of Nanjing University of Chinese Medicine (08JCQN10).

References

[1] N. Santoro, "Perimenopause: From research to practice," *Journal of Women's Health*, vol. 25, no. 4, pp. 332–339, 2016.

[2] E. Toffol, N. Kalleinen, A. S. Urrila et al., "The relationship between mood and sleep in different female reproductive states," *BMC Psychiatry*, vol. 14, p. 177, 2014.

[3] L. Delamater and N. Santoro, "Management of the perimenopause," *Clinical Obstetrics and Gynecology*, vol. 61, no. 3s, pp. 419–432, 2018.

[4] N. Pestana-Oliveira, B. Kalil, C. M. Leite et al., "Effects of estrogen therapy on the serotonergic system in an animal model of perimenopause induced by 4-vinylcyclohexen diepoxide (VCD)," *eNeuro*, vol. 5, no. 1s, 2018.

[5] E. A. MacGregor, "Migraine, menopause and hormone replacement therapy," *Post Reproductive Health*, vol. 24, no. 1, pp. 11–18, 2018.

[6] J. L. Gordon and S. S. Girdler, "Hormone replacement therapy in the treatment of perimenopausal depression," *Current Psychiatry Reports*, vol. 16, no. 12, p. 517, 2014.

[7] C. Tatone and F. Amicarelli, "The aging ovary—the poor granulosa cells," *Fertility and Sterility*, vol. 99, no. 1, pp. 12–17, 2013.

[8] C. P. Almeida, M. C. F. Ferreira, C. O. Silveira et al., "Clinical correlation of apoptosis in human granulosa cells—A review," *Cell Biology International*, vol. 42, no. 10, pp. 1276–1281, 2018.

[9] Y. Wu, X. Wang, B. Shen, L. Kang, and E. Fan, "Extraction, structure and bioactivities of the polysaccharides from fructus corni," *Recent Patents on Food, Nutrition & Agriculture*, vol. 5, no. 1, pp. 57–61, 2013.

[10] X. Sun, L. Kong, and L. Zhou, "Protective effect of fructus corni polysaccharide on hippocampal tissues and its relevant mechanism in epileptic rats induced by lithium chloride-pilocarpine," *Experimental and Therapeutic Medicine*, vol. 16, no. 1, pp. 445–451, 2018.

[11] A. Nair and S. Jacob, "A simple practice guide for dose conversion between animals and human," *Journal of Basic and Clinical Pharmacy*, vol. 7, no. 2, pp. 27–31, 2016.

[12] N. Bagheripour, S. Zavareh, M. T. Ghorbanian, S. H. Paylakhi, and S. R. Mohebbi, "Changes in the expression of OCT4 in mouse ovary during estrous cycle," *Veterinary Research Forum: An International Quarterly Journal*, vol. 8, no. 1, pp. 43–48, 2017.

[13] V. Gupta, L. Holets-Bondar, K. F. Roby, G. Enders, and J. S. Tash, "A tissue retrieval and postharvest processing regimen for rodent reproductive tissues compatible with long-term storage on the international space station and postflight biospecimen sharing program," *BioMed Research International*, vol. 2015, Article ID 475935, 12 pages, 2015.

[14] K. J. Livak and T. D. Schmittgen, "Analysis of relative gene expression data using real-time quantitative PCR and the 2(-Delta Delta C(T)) Method," *Methods*, vol. 25, no. 4, pp. 402–408, 2001.

[15] D. Sun, W. Shen, F. Zhang et al., "Alpha-Hederin inhibits interleukin 6-induced epithelial-to-mesenchymal transition associated with disruption of JAK2/STAT3 signaling in colon cancer cells," *Biomedicine & Pharmacotherapy*, vol. 101, pp. 107–114, 2018.

[16] J. S. Kang, C. J. Lee, J. M. Lee, J. Y. Rha, K. W. Song, and M. H. Park, "Follicular expression of c-Kit/SCF and inhibin-alpha in mouse ovary during development," *The Journal of Histochemistry and Cytochemistry*, vol. 51, no. 11, pp. 1447–1458, 2003.

[17] O. N. Lekontseva, C. F. Rueda-Clausen, J. S. Morton, and S. T. Davidge, "Ovariectomy in aged versus young rats augments matrix metalloproteinase- mediated vasoconstriction in mesenteric arteries," *Menopause*, vol. 17, no. 3, pp. 516–523, 2010.

[18] W. A. Rocca, B. R. Grossardt, and L. T. Shuster, "Oophorectomy, menopause, estrogen treatment, and cognitive aging: clinical evidence for a window of opportunity," *Brain Research*, vol. 1379, pp. 188–198, 2011.

[19] T. A. Van Kempen, T. A. Milner, and E. M. Waters, "Accelerated ovarian failure: a novel, chemically induced animal model of menopause," *Brain Research*, vol. 1379, pp. 176–187, 2011.

[20] J. H. Morrison, R. D. Brinton, P. J. Schmidt, and A. C. Gore, "Estrogen, menopause, and the aging brain: how basic neuroscience can inform hormone therapy in women," *The Journal of Neuroscience*, vol. 26, no. 41, pp. 10332–10348, 2006.

[21] P. M. Maki, "Hormone therapy and cognitive function: Is there a critical period for benefit?" *Neuroscience*, vol. 138, no. 3, pp. 1027–1030, 2006.

[22] M. Filatov, Y. Khramova, E. Parshina, T. Bagaeva, and M. Semenova, "Influence of gonadotropins on ovarian follicle growth and development in vivo and in vitro," *Zygote*, vol. 25, no. 3, pp. 235–243, 2017.

[23] N. Shit, K. V. H. Sastry, R. P. Singh, N. K. Pandey, and J. Mohan, "Sexual maturation, serum steroid concentrations, and mRNA expression of IGF-1, luteinizing and progesterone hormone receptors and survivin gene in Japanese quail hens," *Theriogenology*, vol. 81, no. 5, pp. 662–668, 2014.

[24] T. Wang, M. Zhang, Z. Jiang, and E. Seli, "Mitochondrial dysfunction and ovarian aging," *American Journal of Reproductive Immunology*, vol. 77, no. 5, 2017.

[25] A. Rolaki, P. Drakakis, S. Millingos, D. Loutradis, and A. Makrigiannakis, "Novel trends in follicular development, atresia and corpus luteum regression: A role for apoptosis," *Reproductive BioMedicine Online*, vol. 11, no. 1, pp. 93–103, 2005.

Hindawi
Evidence-Based Complementary and Alternative Medicine
Volume 2019, Article ID 7543460, 13 pages
https://doi.org/10.1155/2019/7543460

Research Article

Brain Cortical and Hippocampal Dopamine: A New Mechanistic Approach for *Eurycoma longifolia* Well-Known Aphrodisiac Activity and Its Chemical Characterization

Shahira M. Ezzat[1,2] **Marwa I. Ezzat**[1] **Mona M. Okba**[1] **Salah M. Hassan**[3] **Amgad I. Alkorashy**[4] **Mennatallah M. Karar**[5] **Sherif H. Ahmed**[6] **and Shanaz O. Mohamed**[7]

[1]*Pharmacognosy Department, Faculty of Pharmacy, Cairo University, Kasr El-Ainy Street, Cairo 11562, Egypt*
[2]*Pharmacognosy Department, Faculty of Pharmacy, October University for Modern Science and Arts (MSA), 6th of October 12566, Egypt*
[3]*Department of Biochemistry, Faculty of Science, Ain Shams University, Cairo, Egypt*
[4]*Department of Biochemistry, Faculty of Pharmacy, Al-Azhar University, Cairo, Egypt*
[5]*Zewail City of Science and Technology, Cairo, Egypt*
[6]*Department of Biochemistry, Faculty of Agriculture, Cairo University, Cairo, Egypt*
[7]*School of Pharmaceutical Sciences, Universiti Sains Malaysia, Malaysia*

Correspondence should be addressed to Mona M. Okba; mona.morad@pharma.cu.edu.eg

Received 7 February 2019; Revised 6 April 2019; Accepted 5 May 2019; Published 2 June 2019

Guest Editor: Glaura Fernandes

Eurycoma longifolia Jack (Fam.: Simaroubaceae), known as Tongkat Ali (TA), has been known as a symbol of virility and sexual power for men. Metabolic profiling of the aqueous extract of *E. longifolia* (AEEL) using UPLC-MS/MS in both positive and negative modes allowed the identification of seventeen metabolites. The identified compounds were classified into four groups: quassinoids, alkaloids, triterpenes, and biphenylneolignans. AEEL is considered safe with oral LD_{50} cut-off >5000 mg/kg. Oral administration of 50, 100, 200, 400, or 800 mg/kg of AEEL for 10 consecutive days to Sprague-Dawley male rats caused significant reductions in mounting, intromission, and ejaculation latencies and increased penile erection index. AEEL increased total body weight and relative weights of seminal vesicles and prostate. Total and free serum testosterone and brain cortical and hippocampal dopamine content was significantly elevated in treated groups with no significant effects on serotonin or noradrenaline content.

1. Introduction

The World Health Organization defines infertility as the inability of a couple to bring a pregnancy to term after one year or more of regular, unprotected sexual intercourse or achieve conception [1]. Infertility is a major clinical concern, affecting 15% of all reproductive-aged couples, and male factors are responsible for 25% of these cases [2]. The decline of male fertility has been highlighted as a serious public health issue in this century and associated with advancing age, incorrect lifestyles, and several environmental toxicants [3]; investigating alternative therapies to manage male infertility may prove cost-effective and may provide the patient with a holistic approach to medicine.

Eurycoma longifolia Jack or "Tongkat Ali" is a herb which has been claimed to possess various medicinal properties. Traditionally, people believe that this herb can be used as remedies for sexual dysfunction, constipation, cancer, leukemia, exercise recovery, loss of libido, aging, stress, high blood pressure, malaria, osteoporosis, diabetes, fever, and glandular swelling [4]. *E. longifolia* has been taken for its aphrodisiac properties for males [5]. In Malaysia, it was taken to improve strength and power during sexual activities [6]. *E. longifolia* extracts lead to an increase in sexual arousal and motivation and frequency of sexual activity in both rats and mice [7]. *E. longifolia* is famously known for its aphrodisiac effect, which is due to its ability to stimulate the production or action of androgen hormones, especially testosterone.

Clinical and experimental studies indicate additional pharmacological activities of *E. longifolia*. The plant was shown to enhance immunity [8], improve quality of life and mood [9], protect against osteoporosis [10], and prevent obesity [11].

Phytochemical studies on this herb revealed that this herb possesses quassinoids which give the bitter taste [4]. These quassinoids include eurycomanone, eurycomalactone, laurycolactone, eurycolactone D, eurycolactone F, and eurycolactone E [6]. Pharmacological activity of this plant is attributed to these various quassinoids and also tirucallane-type triterpenes, squalene derivatives, biphenylneolignans, canthine-6-1, and beta carboline alkaloids [5].

However, studies investigating the *in vivo* effects of *E. longifolia* extract on male reproductive functions, especially its effects on spermatozoa, are limited to sperm concentration and motility or to the serum testosterone concentration. Therefore, this study aimed at investigating the effect of aqueous extract of *E. longifolia* (AEEL) in a broader manner on general well-being, the brain cortical and hippocampal content of dopamine, serotonin, and noradrenaline. In addition, the parameters of sexual behavior (mount latency (ML), ejaculation latency (EL), intromission latency (IL), postejaculatory interval (PEI), and penile erection index), FSH, LH, free and total testosterone, and relative sex organ (testes, prostate, and seminal vesicles) to body weights were investigated. Furthermore a metabolic profiling of the aqueous extract was performed using UPLC-MS/MS.

2. Materials and Methods

2.1. Chemicals and Kits. AccuBind™ total testosterone and free testosterone ELISA kits were purchased from Monobind Inc., Lake Forest, CA, USA (CAT. #: 3725-300 and 5325-300, respectively). FSH, LH, and ELISA kits were acquired from BioCheck, Inc., CA, USA (CAT. #: BC-1029 and BC-1031, respectively). Dopamine, serotonin, and noradrenaline ELISA kits were obtained from Glory Science Co., Ltd, TX, USA (CAT. #: 90356, A1082, and 30587, respectively). All chemicals were of the highest commercial grade. The aqueous extract of *E. longifolia* was supplied by Technology Park Malaysia (TPM) Corporation Sdn. Bhd., Kuala Lumpur, Malaysia. Acetonitrile and Methanol were both of HPLC grade, purchased from Sigma Aldrich Chemie GmbH, Steinheim, Germany.

2.2. Plant Material. Eurycoma longifolia Jack roots were obtained from HCA products Sdn Bhd. Spring 2015. The plant was kindly identified in the Forest Research Institute, Malaysia. A voucher specimen (5-09-2015) was kept in the herbarium of Pharmacognosy Department, Faculty of Pharmacy, Cairo University, Cairo, Egypt.

2.3. Extraction. The dried powdered roots (1.5 kg) of *E. longifolia* were boiled with 10-liter distilled water for 15 min. and then kept for 1 h.; after that, the aqueous extract was filtered and lyophilized to obtain 800 g of pale brown powder of the aqueous extract of *E. longifolia* (AEEL).

2.4. UPLC-MS/MS Analysis of AEEL. Chromatographic separations were performed on an Agilent 6420 triple quad UPLC system (Agilent, California, USA) equipped with Acquity BEH shield reversed phase 18 column (1500 × 2.1 mm, particle size 1.7 μm; Waters Milford, USA). The mobile phase was a binary solvent system consisting of solvent A (acetonitrile) and solvent B (water with 0.1% formic acid). The following were considered: the UPLC gradient at a flow rate of 0.3 ml/min: 0–5 min, isocratic 10 % B; 5–15 min, linear from 10 to 70 % B; 15–32 min, linear from 70 to 90 % B; 32–40 min, isocratic 90% B, 40–50 min, linear from 90 to 95 % B, 50–56 min, linear from 95 to 50 % B, 56–60 min, linear from 50 to 10 % B, isocratic 10% B, 61–70 min. The injection volume was 3.1 μl. Eluted compounds were detected from m/z 100 to 1000 using a MS QQQ mass spectrometer equipped with an electrospray ion source in negative ion mode. Metabolites were characterized by their mass spectra, relative retention times, and comparison to literature.

2.5. Animals. Sprague–Dawley rats of both sexes, weighing from 200g to 250g, were purchased from the Animal Facility of Misr University for Science and Technology (MUST), 6th of October City, Giza, Egypt. They were housed, females and males, separately in the animal facility at 50 ± 10% RH (Relative Humidity), 22 ± 3°C, and 12 h dark/light cycle. They were provided with pellet diet and water *ad libitum*. The animals were acclimatized to the housing environment for 7 days before dosing. The study was conducted in accordance with internationally accepted principles for laboratory animal use and care and was approved by Ethics Committee, Faculty of Pharmacy, Cairo University, Cairo, Egypt (MP 2161).

2.6. Determination of LD_{50}. Determination of LD_{50} of AEEL was done according to OECD Guideline #423 (OECD; [12]) on Sprague-Dawley rats. Based on a previous pilot study in our laboratories, AEEL was administered orally to 3 animals using gastric feeding gavage at a dose of 2000 mg/kg (10 mL/kg dosing volume). The tested animals were observed for mortality after 24 h of administration. The test was repeated at the same dose using 3 extra animals. Thereafter, the animals were monitored daily for behavioral changes and weekly for changes in body weight. Necropsy was done on day 14 after administration of the single dose of the extract.

2.7. Evaluation of Aphrodisiac Activity. Male rats (48) were divided into 6 groups of 8 rats each. The control group received 3 mL/kg of water, whilst the other 5 groups received 50, 100, 200, 400, and 800 mg/kg of AEEL suspended in water as a single oral daily dose for 10 days. On day 11, male and female rats were mated and sexual behavior parameters along with total body weights were evaluated.

After 24 hours, blood samples were obtained from all male rats by retroorbital plexus puncture method for hormonal assessment under light anesthesia. Then, animals were killed by deep anesthesia with sodium pentobarbital and assessed for relative sex organ (testes, prostate, and seminal vesicles) to body weights and brain neurotransmitters content.

2.8. Sexual Behavior Test. The sexual behavior of males was observed by well-trained technicians, without knowing

the study protocol, in an air conditioned, sound-attenuated room lit with a faint red light, amid the first period of the dark cycle of day 10. Single male rats were transferred into rectangular glass monitoring cages (40×50×40 cm) and allowed to get accommodated to the testing chamber for 15 min. Then, sexually receptive female rats were presented in the cages (1 female per cage) and the mating test began. The undermentioned parameters of sexual behavior were assessed as beforehand explained [13, 14]. Mount latency (ML) is defined as time (in seconds) from the introduction of the female to the first mount; ejaculation latency (EL) is defined as time (in seconds) from the first intromission to ejaculation; intromission latency (IL) is defined as time (in seconds) from introduction of the female to the first intromission (vaginal penetration); postejaculatory interval (PEI) is defined as time (in seconds) from ejaculation to the first intromission of the second copulatory series, and penile erection index = % rats exhibiting erection × mean number of erections.

2.9. Determination of FSH, LH, and Free and Total Testosterone. Investigating serum hormonal levels was performed by measuring FSH, LH, and total and free testosterone. Hormonal levels were quantified in the collected rat sera using the provided rat ELISA kits, according to the product instructions.

The assays of FSH and LH are based on sandwich ELISA technique using specific monoclonal antibody coated on a 96-well plate. A dose-response curve could be generated by using several different serum references of known antigen concentration. The antigen concentration of an unknown could be ascertained from this curve [15, 16].

2.10. Assessment of Dopamine, Serotonin, and Noradrenaline. Brains were rapidly removed and placed in ice-cold buffer, and brain regions were dissected and frozen on dry ice using procedures previously described [17, 18]. Brain neurotransmitters (dopamine, serotonin, and noradrenaline) content was quantified in the collected rat brain cortical and hippocampal tissues using the provided ELISA kits, according to the manufacturer instructions, based on the sandwich technique.

2.11. Statistical Analysis. Data are presented as mean ± SD. Statistical analysis was done using one-way ANOVA followed by Dunnett's post-hoc test for comparison of each treatment group and control. The 0.05 level of probability was used as the criterion for significance. All statistical analyses were done using GraphPad InStat software version 3 (La Jolla, CA, USA). Graphs were sketched using GraphPad Prism software version 5 (ISI® software, CA, USA).

3. Results

3.1. UPLC-MS/MS. The chemical composition of AEEL was examined using UPLC-MS/MS. All the metabolites were characterized by the interpretation of their mass spectra and the data provided by databases and literature.

Seventeen compounds were identified using UPLC-MS/MS in both positive modes in which protonated and/or alkali adduct analyte molecules were generally observed in the mass spectra and negative modes where operation peaks corresponding to deprotonated analyte molecules are observed (Figures 1(a)-1(b); Table 1). Eight quassinoids were identified in the positive mode, and peak **1** (Rt 15.01 min) showed a molecular ion peak $[M+H]^+$ at *m/z* 351.100 which is corresponding to the molecular formula $C_{18}H_{19}ClO_5$. The presence of a chlorine atom was confirmed by the appearance of an isotope peak $[M+2]^+$ at *m/z* 352.000 in addition to a peak at 315.010 corresponding to $[(M+H)\text{-}HCl]^+$. This compound was identified as Eurycolactone B [19]. Peak **2** (Rt 20.05 min) showed a molecular ion $[M+H]^+$ at *m/z* 365.0000 which could be correspondent to the molecular formula $C_{19}H_{24}O_7$ that produced MS^2 fragment at *m/z* 347.000 and 318.900 equivalent to $[(M+H)\text{-}H_2O]^+$ and $[(M+H)\text{-}CH_2O_2]^+$, respectively. This fragmentation pattern is characteristic to the quassinoid 6α-hydroxyeurycomalactone [20].

Mass data of peak **3** (Rt 21.92 min) had a molecular ion peak $[M+H]^+$ at *m/z* 409.000 ($C_{20}H_{24}O_9$) and showed a daughter ion at *m/z* 391.000 corresponding to the loss of a water molecule $[(M+H)\text{-}H_2O]^+$ and another ion at 345.100 corresponding to $[(M+H)\text{-}CO]^+$. This compound was identified as Eurycomanone [21]. Peak **4** (Rt 23.63 min) showed a molecular ion at *m/z* 413.200 and a MS^2 *m/z* 395.100 and 376.800 with the loss of 18 and 36 amu corresponding to $[(M+H)\text{-}H_2O]$ and $[(M+H)\text{-}2H_2O]$, respectively. This compound was regarded as 13β,18-dihydroeurycomanol ($C_{20}H_{28}O_9$) [20]. This compound was also detected in the negative mode as $[M\text{-}H]^-$ at *m/z* 411.100.

Eurycomanol-2-*O*-β-D-glucopyranoside was assigned to peak **6** (Rt 24.21 min) based on the MS; molecular ion at *m/z* 573.100 for molecular formula $C_{26}H_{36}O_4$ and MS^2 *m/z* 375.200 due to the cleavage of sugar moiety and the loss of 2 water molecules. The daughter ion at *m/z* 375 lost another water molecule to give ion at *m/z* 357.000. The consecutive cleavage of a $-CH_2O-$ residue followed by the neutral loss of CO from product ion at *m/z* 357.000 led to the appearance of the fragment at *m/z* 299.100 [21], and this compound was also detected in the negative mode with $[M\text{-}H]^-$ at *m/z* 571.100. Another quassinoid appeared at peak **7** (Rt 29.54 min) that showed a molecular ion peak $[M+3H]^+$ at *m/z* 383.200 with a daughter ion peak at *m/z* 365.100 $[(M+3H)\text{-}H_2O]$ due to the loss of a water molecule. This peak was identified as 15β-Hydroxyklaineanone [20]. Peak **9** (Rt 38.36 min) also showed a molecular ion peak $[M+H]^+$ at *m/z* 413.100 corresponding to the molecular formula $C_{20}H_{28}O_9$; it showed MS^2 at *m/z* 395.200 $[(M+H)\text{-}H_2O]$ that resulted from a loss of a water molecule; this quassinoid was identified as 5α, 14β, 15β-Trihydroxyklaineanone [20]. Peak **11** (Rt 45.76 min) showed a molecular ion peak at *m/z* 455.102 ($C_{22}H_{30}O_{10}$) and gave daughter ions at *m/z* at 454.100 and 436.000 corresponding to M^+ and $[M\text{-}H_2O]^+$. This compound was identified as 6α-Acetoxy-14,15β-dihydroxyklaineanone [22].

Moreover, five quassinoids were detected in the negative mode as peaks **5**, **8**, **10**, **12**, and **13**. Peak **5** (Rt 23.90 min) showed a molecular ion peak $[M\text{-}H]^-$ at *m/z* 443.300 consistent with the molecular formula $C_{20}H_{28}O_{11}$. This peak gave daughter ions at m/z 427.100 and 413.000 due to the loss

Table 1: Peak assignments of *E. longifolia* aqueous extract metabolites using UPLC-MS/MS in positive and negative ionization modes.

Peak	t_R (min)	$[M-H]^-$	$[M+H]^-$	Molecular formula	Identification	MS^2
1	15.01		351.100	$C_{18}H_{19}ClO_5$	Eurycolactone B	352.000, 315.010, 290.800
2	20.05		365.000	$C_{19}H_{24}O_7$	6α-Hydroxyeurycomalactone	347.000, 318.900, 202.100
3	21.92		409.000	$C_{20}H_{24}O_9$	Eurycomanone	391.000, 373.200, 345.100, 225.000
4	23.63	411.100	413.200	$C_{20}H_{28}O_9$	13β,18-dihydroeurycomanol	395.100, 376.800, 319.000, 291.200
5	23.90	443.300		$C_{20}H_{28}O_{11}$	13β,21-dihydroxyeurycomanol	427.100, 413.000, 379.300
6	24.21	571.100	573.100	$C_{26}H_{36}O_4$	Eurycomanol-2-O-β-D-glucopyranoside	375.200, 357.000, 299.100
7	29.54		383.200	$C_{20}H_{28}O_7$	15β-Hydroxyklaineanone	365.100, 326.800, 266.000, 202.100
8	29.98	395.100		$C_{20}H_{28}O_8$	14,15β-Dihydroxyklaineanone	377.000, 359.100, 349.300
9	38.36		413.100	$C_{20}H_{28}O_9$	5α, 14β, 15β-Trihydroxyklaineanone	395.200
10	38.43	315.100		$C_{18}H_{20}O_5$	Laurycolactone B	271.200, 256.001
11	45.76		455.102	$C_{22}H_{30}O_{10}$	6α-Acetoxy-14,15β-dihydroxyklaineanone	454.100, 436.000
12	45.91	391.100		$C_{20}H_{24}O_8$	(α/β-epoxide) Ailanthone	373.100, 363.200
13	46.18	573.122		$C_{26}H_{38}O_{14}$	Iandonoside B	555.000, 513.900
14	46.52		251.200	$C_{15}H_{10}O_2N_2$	9-Methoxycanthin-6-one	236.100, 233.000, 216.200
15	46. 69	279.000		$C_{16}H_{12}O_3N_2$	5,9-Dimethoxycanthin-6-one	264.000, 251.100, 237.000
16	47.45	265.100		$C_{15}H_{10}O_3N_2$	11-Hydroxy-10-methoxycanthin-6-one	250.200, 247.300, 222.200
17	47.91		389.000	$C_{21}H_{24}O_7$	2-Hydroxy-3,2′,6′-trimethoxy-4′-(2,3-epoxy-1-hydroxypropyl)-5-(3-hydroxy-1-propenyl)-biphenyl	371.110, 357.001, 343.100, 295.000

of -CH and -CH_2O, respectively. It was identified as 13β,21-dihydroxyeurycomanol. Peak **8** (Rt 29.98 min) was identified as 14,15β-Dihydroxyklaineanone as it showed a molecular ion peak $[M-H]^-$ at *m/z* 395.100 and MS^2 at *m/z* 377.000 due to the loss of H_2O (18 amu), 359.100 with the loss of $2H_2O$ (36 amu), and 349.300 due to the loss of $-CH_2O_2$ [20]. Peak **10** (Rt 38.43 min) was with a molecular ion at *m/z* 315.100 corresponding to the molecular formula $C_{18}H_{20}O_5$ and had fragmentation ions at *m/z* 271.200 and 256.001 due to the loss of CO_2 [(M-H)-CO_2] and [(M-H)-CO_2-CH_3]. This fragmentation pattern was in consistence with that of Laurycolactone B [23]. Peak **12** (Rt 45.91 min) was identified as (α/β-epoxide) Ailanthone ($C_{20}H_{24}O_8$) with a base peak *m/z* 391.100 corresponding to $[M-H]^-$ and MS^2 at *m/z* 373.100 [(M-H)-H2O] and 363.200 [(M-H)-CO]. Peak **13** (Rt 46.18 min) was with molecular ion at *m/z* 573.122 corresponding to the molecular formula $C_{26}H_{38}O_{14}$ and was identified as Iandonoside B; it showed MS^2 at *m/z* 555.000 [(M-H)-H2O], 513.900 [(M-H)-$C_2H_3O_2$] [20].

Three alkaloids of cathin-6-one type were also detected: one was detected in the positive ionization mode as peak **14** and two were detected in the negative ionization mode as peaks **15** and **16**. Peak **14** (Rt 46.52 min) showed a molecular ion peak $[M+H]^+$ at *m/z* 251.200 corresponding to the molecular formula $C_{15}H_{10}O_2N_2$. It showed also daughter ions at *m/z* 236.100 and 233.000 due to the peaks [(M+H)-CH_3] and [(M+H)-H_2O], respectively. This compound was identified as 9-methoxycanthin-6-one [20]. Peak **15** (Rt 46.69 min) was with a molecular ion peak $[M-H]^-$ at *m/z* 279.000 corresponding to the molecular formula $C_{16}H_{12}O_3N_2$. MS^2 appeared at m/z 264.000 [(M-H)-CH_3], 251.100 [(M-H)-CO], and 237.000 [(M-H)-C_2H_2O]. This compound could be identified as 5,9-dimethoxycanthin-6-one [24]. Peak **16** (Rt 47.45 min) had a molecular ion peak $[M-H]^-$ at 265.100 corresponding to $C_{15}H_{10}O_3N_2$. Its daughter ions MS^2 were detected at *m/z* 250.200 [(M-H)-CH_3], 247.300 [(M-H)-H_2O], and 222.200 [(M-H)-CHNO]; thus this was identified as 11-hydroxy-10-methoxycanthin-6-one [24].

Furthermore, a biphenylneolignan was observed in the positive ionization mode detected as Peak **17** (Rt 47.91 min) that had a molecular ion peak $[M+H]^+$ at 389.000 ($C_{21}H_{24}O_7$) with MS^2 at 371.110 [(M+H)-H_2O], 357.001 [(M-H)-CH_4O],

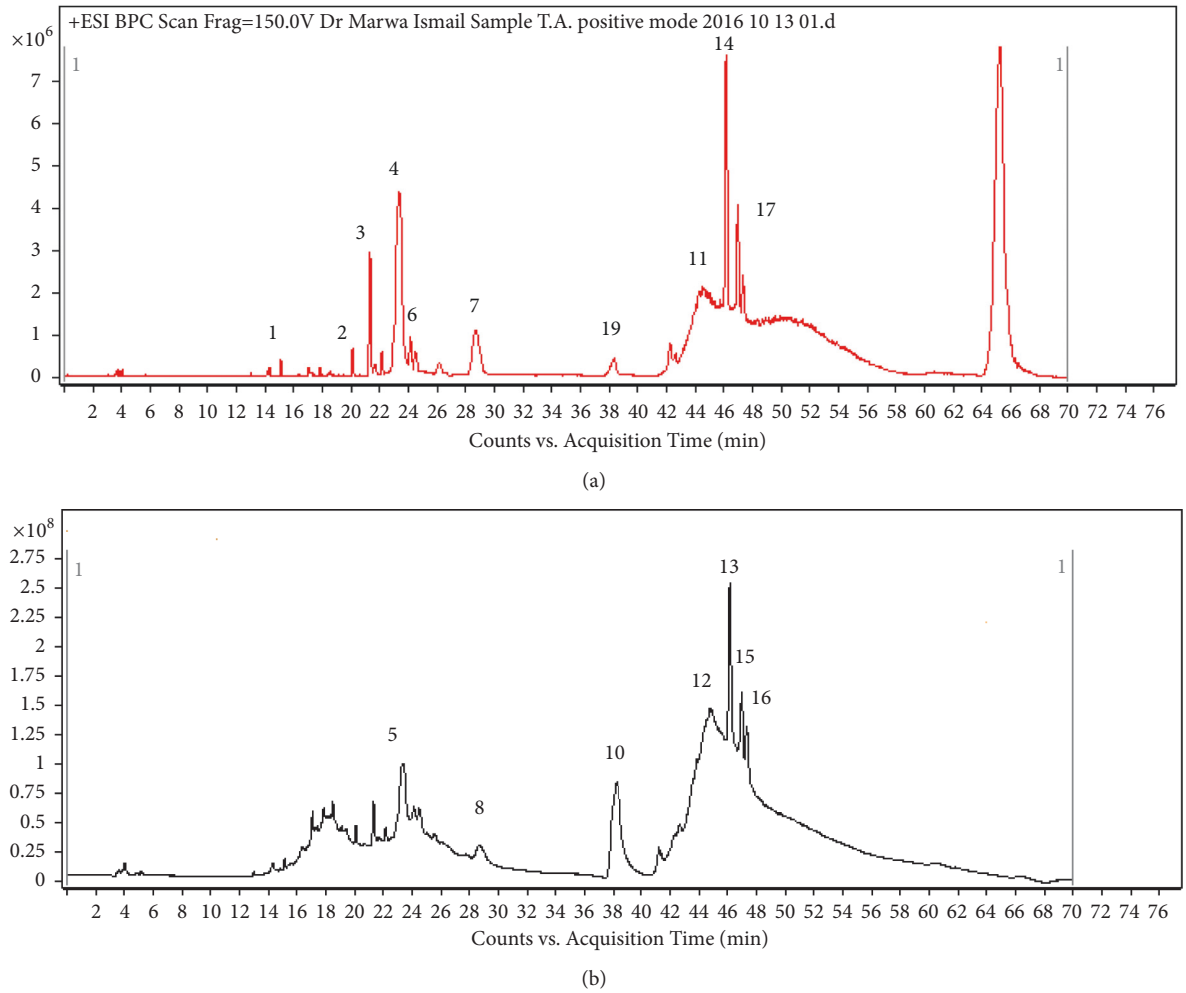

Figure 1: A representative UPLC-positive ionization MS trace (a) and negative ionization MS trace (b) of the aqueous extract of *E. longifolia* roots. Peak numbers follow those listed in Table 1 for metabolite identification using UPLC-MS/MS.

and 343.100 [(M-H)-C_2H_6O] which was consistent with the biphenylneolignan;2-hydroxy-3,2′,6′-trimethoxy-4′-(2,3-epoxy-1-hydroxypropyl)-5-(3-hydroxy-1-propenyl)-biphenyl [22]. The identified compounds structures are presented in Figures 2 and 3.

3.2. Determination of LD_{50}. A repeated single oral dose of AEEL (2000 mg/kg) did not show any mortality at 24 h after administration. Therefore, *E. longifolia* extract is considered unclassified according to the OECD with oral LD_{50} cut-off >5000 mg/kg.

3.3. Evaluation of Sexual Behavior. Oral administration of AEEL (100, 200, 400, and 800 mg/kg) caused dose-related enhancement of male rat sexual behavior (Table 2). This was evidenced by significant reductions in ML, IL, and EL with doses 100, 200, 400, and 800 mg/kg as compared to the control group. Furthermore, the smallest dose (50 mg/kg) did not show significant changes in male rat behavior as compared to the control. However, no significant difference in PEI was recorded between control and treated animals. In addition, there was an improvement in male rats penile erection which was evidenced by a significant increase in penile erection index at the highest three doses (200, 400, and 800 mg/kg) compared to the respective control (Figure 4(a)).

3.4. Assessment of Body and Relative Organ-To-Body Weights. The oral administration of AEEL resulted in significant (2.1, 2.6, and 2.9-fold) increases in total body weight (TBW) of male rats at 200, 400, and 800 mg/kg, respectively (Figure 4(b)). Also, relative weights of prostate and seminal vesicles were increased significantly at doses of 400 and 800 mg/kg (Table 3). However, relative testicular weights were not significantly changed with AEEL administration.

3.5. Assessment of Serum FSH, LH, and Free and Total Testosterone. Our data indicated that AEEL oral administration to male rats leads to significant elevation of total testosterone serum level by 67.1%, 127.8%, and 288.9% of control level at 200, 400, and 800 mg/kg, respectively (Figure 5(a)). Interestingly, serum level of free testosterone was significantly elevated compared to the corresponding control, starting

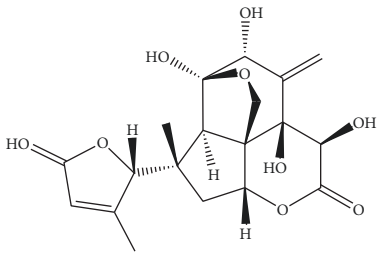

Eurylactone B

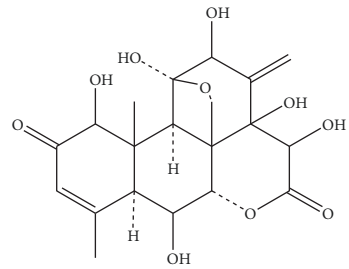

6α-hydroxyeurycomalactone

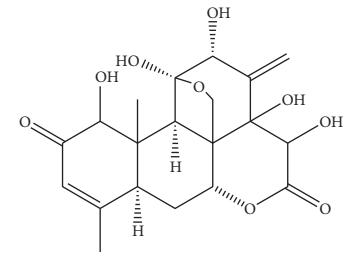

Eurycomanone

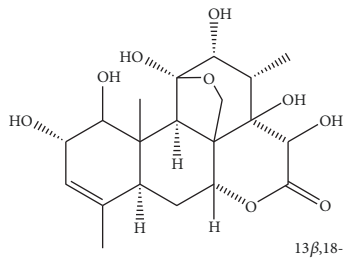

13β,18-dihydroeurycomanol

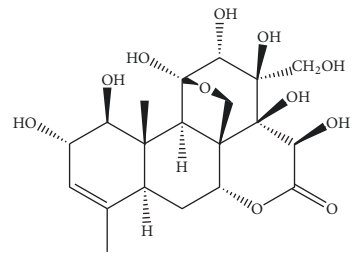

13B,21-dihydroxyeurycomano

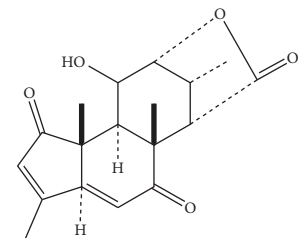

Laurycolactone B

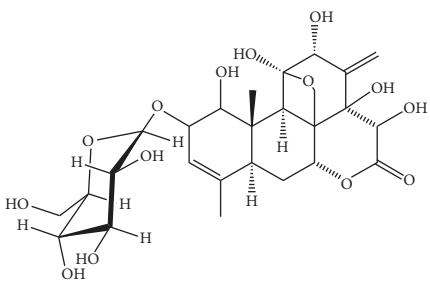

Eurycomanol-2-O-β-D-glucopyranoside

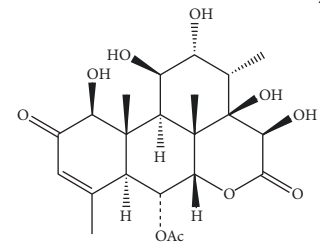

6α-Acetoxy-14,15β-dihydroxyklaineanone

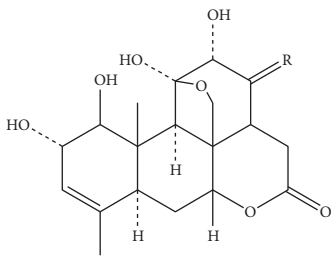

(α/β-epoxide) Ailanthone

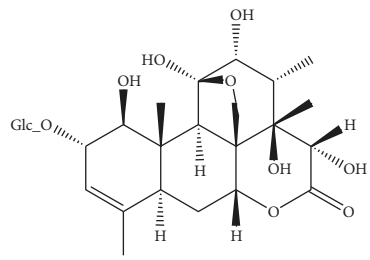

Iandonoside B

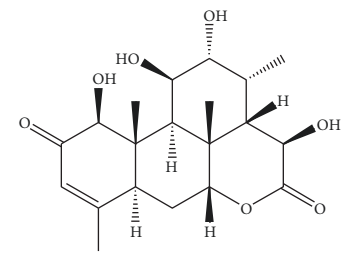

15β-Hydroxyklaineanone

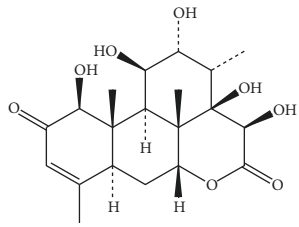

14β, 15β-Trihydroxyklaineanone

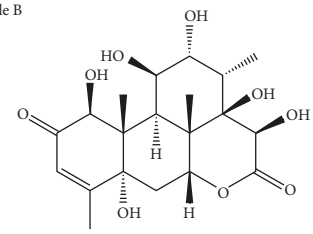

5α, 14β, 15β-Trihydroxyklaineanone

Figure 2: Structures of the identified quassinoids.

Table 2: Effect of *E. longifolia* root extract on male rats sexual behavior.

Group	Dose (mg/kg)	ML (sec.)	IL (sec.)	EL (sec.)	PEI (sec.)
Control		373.6 ± 6.56	525.6 ± 6.65	1045.8 ± 15.3	304 ± 4.34
AEEL	50	355.8 ± 21.77	482.5* ± 21.15	975.8* ± 25.18	298.5 ± 14.77
	100	280.3* ± 4.98	410.5* ± 12.37	836.6* ± 17.21	301.3 ± 9.42
	200	192.3* ± 17.79	242.16* ± 16.49	542.5* ± 35.6	299.8 ± 8.84
	400	160.5* ± 7.68	169.5* ± 7.39	341.6* ± 7.96	301.5 ± 10.01
	800	143.39* ± 7.13	153.3* ± 5.35	296.6* ± 7.76	305.8 ± 7.11

E. longifolia was given as a single oral daily dose for 10 consecutive days. Values are mean ± SD. n=8.
∗ Significantly different from the corresponding control at $p < 0.05$.
AEEL: aqueous extract of *E. longifolia;* EL = Ejaculation Latency, IL = Intromission Latency, ML = Mount Latency, and PEI = Post-Ejaculatory Interval.

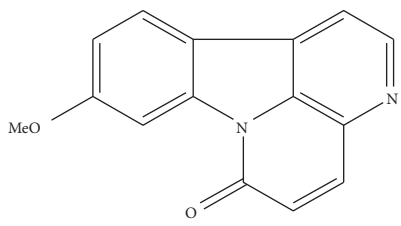

9-Methoxycanthin-6-one

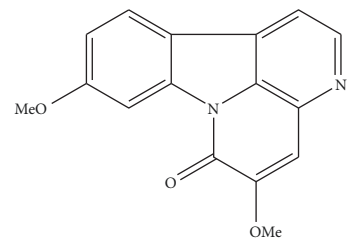

5,9-Dimethoxycanthin-6-one

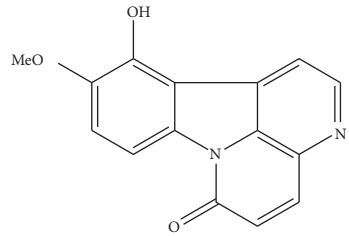

11-hydroxy-10-methoxycanthin-6-one

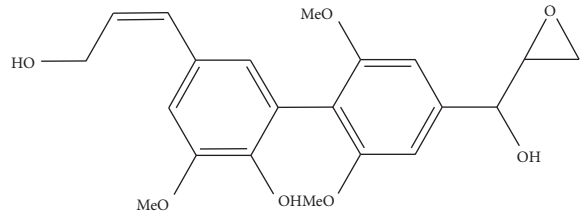

2-hydroxy-3,2`,6`-trimethoxy-4`-(2,3-epoxy-1-hydroxypropyl)-5-(3-hydroxy-1-propenyl)-biphenyl

Figure 3: Structures of the identified alkaloids, triterpene, and biphenylneolignan.

from the lowest dose (2.2-fold at 50 mg/kg) and reaching 5-fold at the highest dose (800 mg/kg) (Figure 5(b)).

A reverse pattern was observed with FSH and LH levels. There were significant decreases in both FSH and LH levels at higher doses (200, 400, and 800 mg/kg), as compared to the corresponding control values. Serum levels of FSH were decreased by 21.4%, 18.9%, and 29.5% of the control level at 200, 400, and 800 mg/kg, respectively (Figure 5(c)). The decline in serum level of LH was more prominent than that of FSH. It was decreased by 24.3%, 53.2%, and 75.6% of its corresponding control values at the same doses, respectively (Figure 5(d)).

3.6. Evaluation of Brain Cortical and Hippocampal Dopamine, Serotonin, and Noradrenaline. Our evaluation indicated that AEEL oral administration to male rats resulted in significant elevation of cortical dopamine level at 200, 400, and 800 mg/kg (Figure 6(a)). However, no apparent effect was detected on cortical serotonin or noradrenaline levels (Figures 6(b) and 6(c)), respectively. The same pattern was recorded with hippocampal content of dopamine, serotonin, and noradrenaline. Hippocampal dopamine was significantly elevated at the higher doses (200, 400, and 800 mg/kg) (Figure 7(a)), while no significant change was observed with

Table 3: Effect of *E. longifolia* root extract on relative weights of testes, seminal vesicles, and prostate in male rats.

Group	Dose (mg/kg)	Testes/TBW	Seminal Vesicles/TBW	Prostate/TBW
Control		0.0067 ± 0.0004	0.0024 ± 0.0006	0.0015 ± 0.0004
AEEL	50	0.0074 ± 0.0009	0.0035 ± 0.0008	0.0016 ± 0.0004
	100	0.0079 ± 0.0014	0.0032 ± 0.0006	0.0016 ± 0.0002
	200	0.0079 ± 0.0011	0.0035 ± 0.0011	0.0020 ± 0.0003
	400	0.0075 ± 0.0012	0.0043* ± 0.0006	0.0024* ± 0.0004
	800	0.0079 ± 0.0005	0.0049* ± 0.0006	0.0026* ± 0.0003

E. longifolia was given as a single oral daily dose for 10 consecutive days. Values are mean ± SD. n=8.
∗Significantly different from the corresponding control at $p < 0.05$.
AEEL: aqueous extract of *E. longifolia;* TBW = Total Body Weight.

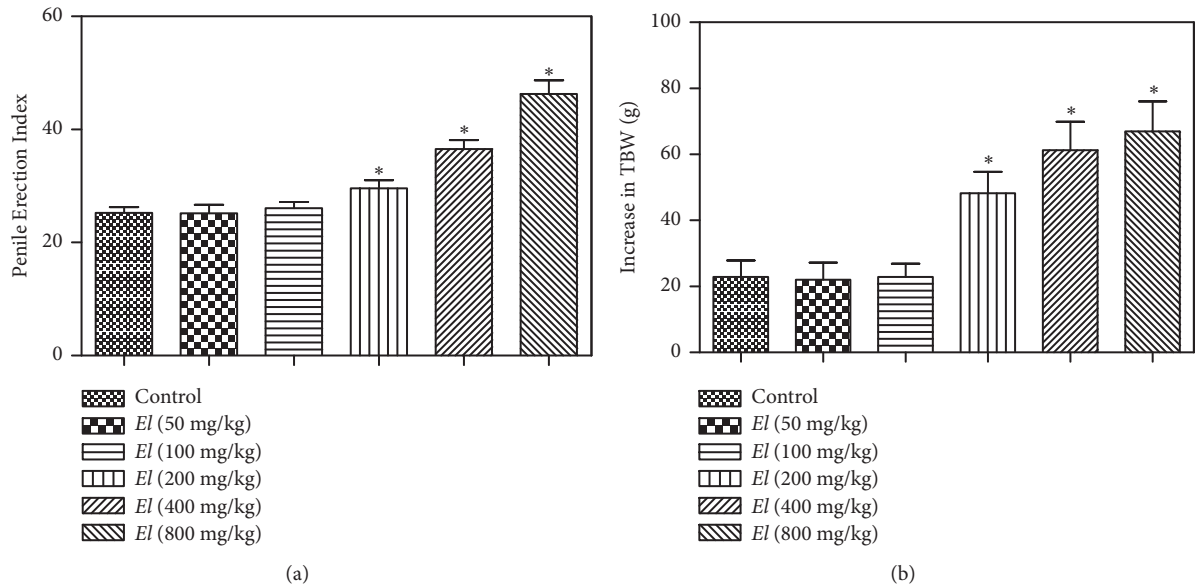

Figure 4: *Effect of E. longifolia root extract (a) on penile erection index of male rats and (b) on the increase of total body weight (TBW) of male rats. E. longifolia* was given as a single oral daily dose for 10 consecutive days. Values are mean ± SD. Statistical analysis was carried out by one-way *ANOVA* followed by *Dunnett post hoc* test. n=8. ∗Significantly different from the control at $p < 0.05$. TBW = Total Body Weight; *EL* = *E. longifolia*.

serotonin or noradrenaline content (Figures 7(b) and 7(c)), respectively.

4. Discussion

In Malaysia, *E. longifolia* has been reputed by Malays as a traditional remedy used as an adaptogen for energy and vitality and is well known for its aphrodisiac activities [25]. Although traditional use of *E. longifolia* as an aphrodisiac herb is well-recognized, there is a paucity of information on the possible underlying mechanisms. Therefore, the present study was conducted to substantiate the aphrodisiac activity of *E. longifolia.*

Initially, metabolic profiling of AEEL was performed using UPLC-MS/MS. A previous study was conducted which involved the LC-MS/MS analysis of the aqueous extracts of *E. longifolia* to discriminate between two samples cultivated in two different locations in Malaysia using the positive ionization mode [20]. Here we reported the identification of eighteen compounds using UPLC-MS/MS in both modes. The identified compounds could be classified into four groups: thirteen quassinoids, three alkaloids, a triterpene, and a biphenylneolignan.

LD_{50} of AEEL was determined in Sprague-Dawley rats according to OECD Guideline #423(OECD) (Supplementary File (available here)). *E. longifolia* was found to be safe and unclassified with oral LD_{50} cut-off >5000 mg/kg. This is consistent with the previous studies which indicated the same oral LD_{50} [4]. Administration of *E. longifolia* (50-800 mg/kg) to male rats resulted in obvious improvement of sexual behavior. This is evidenced by significant reductions in mounting, intromission, and ejaculation latencies and significant increase in penile erection index, at high dose levels. These findings gain support by several studies highlighting the aphrodisiac activities of *E. longifolia* which indicated an improvement in all parameters of sexual behavior towards receptive females [26–28]. In addition, the present study indicated that AEEL exhibits a significant anabolic effect, manifested by increased total body weight as well as relative seminal vesicles and prostate weights. This is in line with

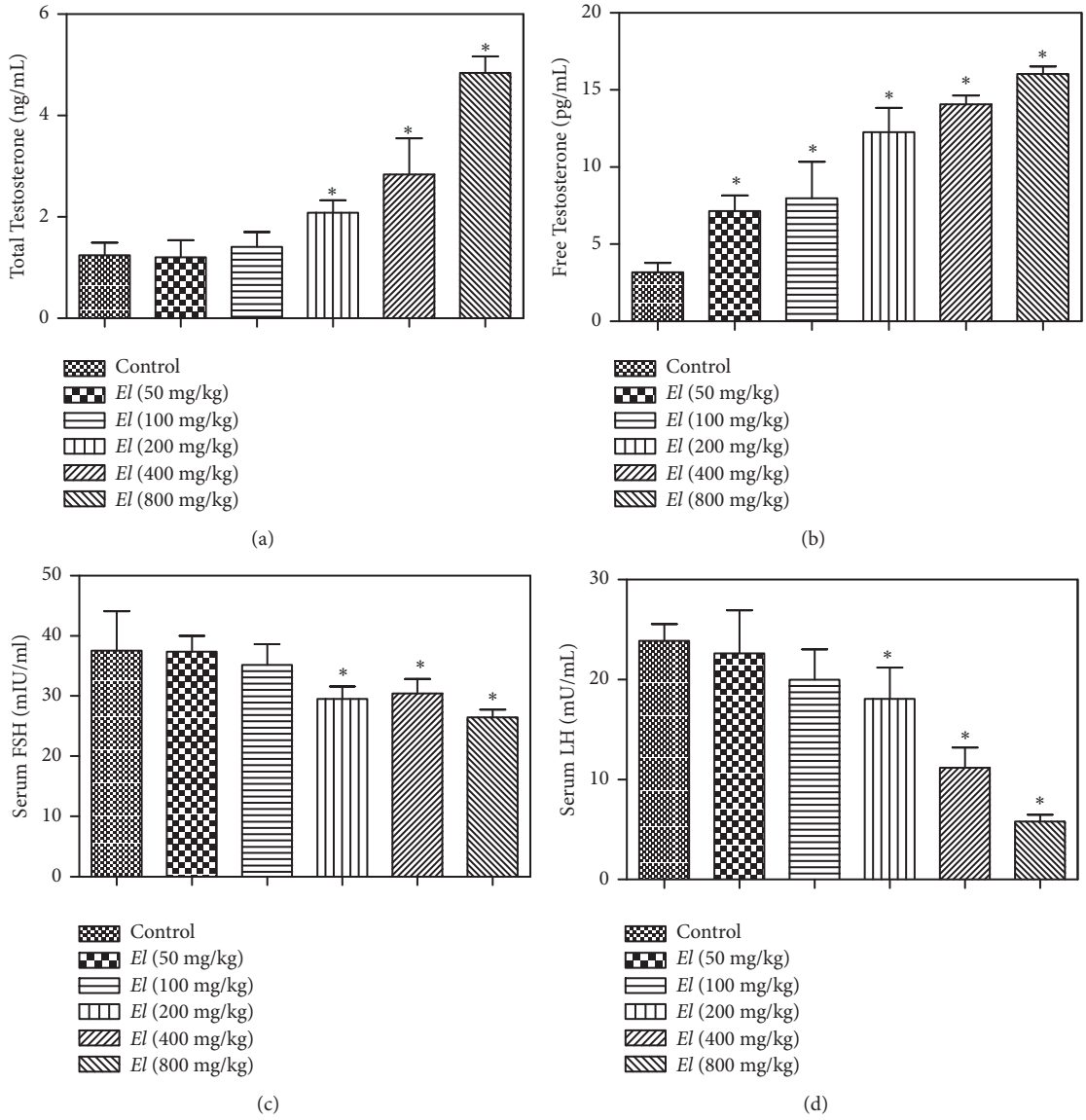

Figure 5: *Effect of E. longifolia root extract on serum levels of total testosterone (a), free testosterone (b), FSH (c), and LH (d) of male rats. E. longifolia* was given as a single oral daily dose for 10 consecutive days. Values are mean ± SD. Statistical analysis was carried out by one-way *ANOVA* followed by *Dunnett post hoc* test. n=8. ∗Significantly different from the corresponding control at $p < 0.05$. *EL* = *E. longifolia*, FSH = Follicle Stimulating Hormone, and LH = Luteinizing Hormone.

a previous study that reported that *E. longifolia* promoted the growth of both rat ventral prostate and seminal vesicles [5].

Assessment of the impact of AEEL on the pituitary-gonadal axis indicated significant elevation of the serum levels of total and free testosterone. This was confirmed by other studies which showed an increase in testosterone concentration after treatment of male rats with AEEL [29]. Rationally, a compensatory decline in FSH and LH levels was observed at the same dose range. This could be explained by the negative feedback inhibition mechanism controlling the internal endocrine environment. The elevated testosterone level explains the observed increase in sexual desire. This also provides an additional justification for the observed AEEL anabolic effect and the increase of sex organs weight.

Due to their key roles in behavioral functions including sexual behavior, the brain cortical and hippocampal contents of dopamine, serotonin, and noradrenaline were evaluated. Brain cortex and hippocampus are important structures in the sexual reward system [30, 31]. Dopamine plays a major role in most types of reward-motivated behavior including sexual reward [31], and serotonin is thought to be a contributor to feelings of happiness and well-being [32], while noradrenaline increases arousal and attentiveness and endorses vigilance [33]. Interestingly, AEEL administration was able to elevate dopamine but not serotonin or noradrenaline

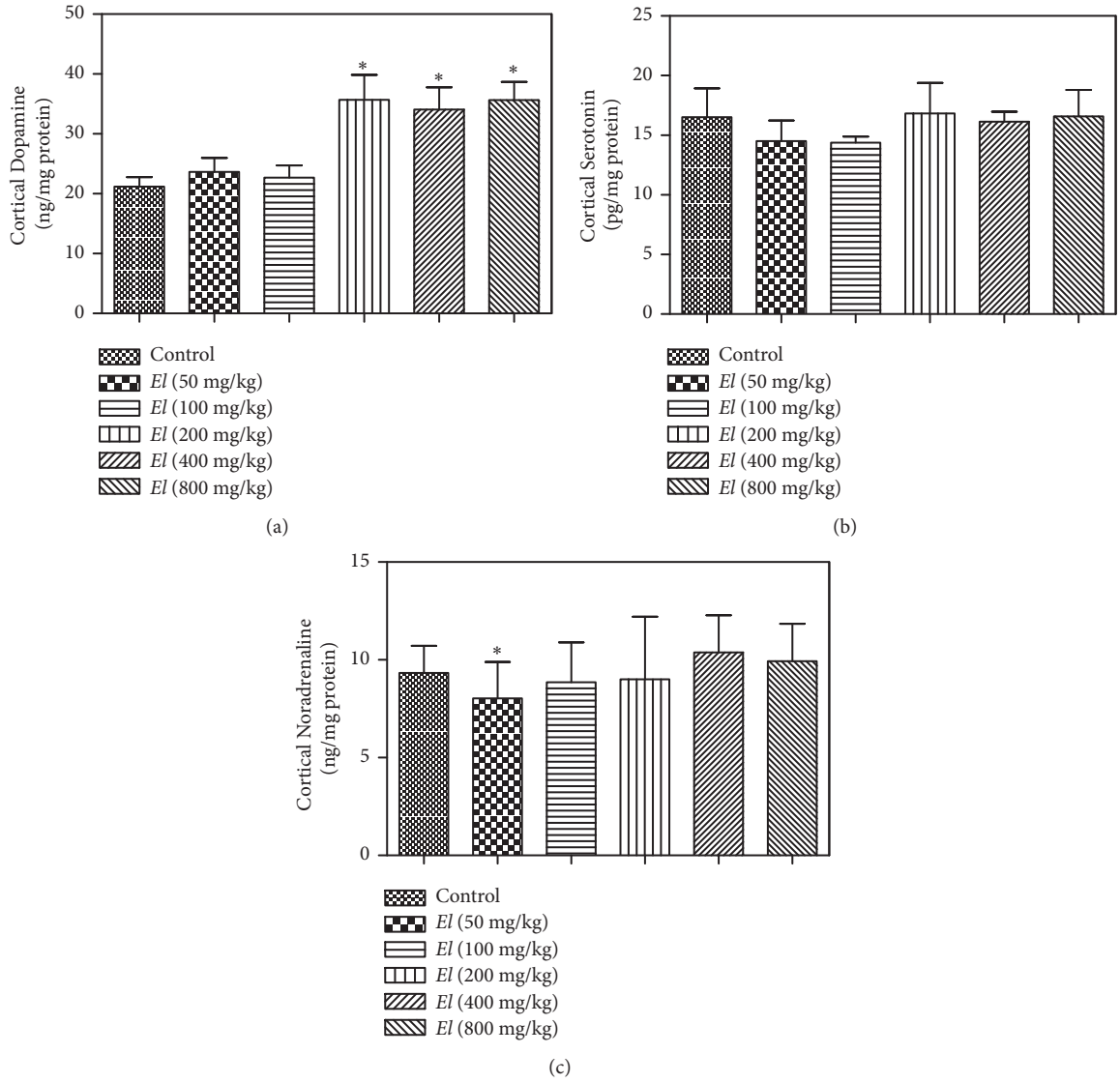

Figure 6: *Effect of E. longifolia root extract on cortical content of dopamine (a), serotonin (b), and noradrenaline (c) in male rats. E. longifolia* was given as a single oral daily dose for 10 consecutive days. Values are mean ± SD. Statistical analysis was carried out by one-way *ANOVA* followed by *Dunnett post hoc* test. n=8. ∗Significantly different from the corresponding control at $p < 0.05$. *EL = E. longifolia.*

contents. Most types of reward, including sexual reward, involve an increase in brain dopamine. This is supported by the observed hypersexuality associated with dopamine-enhancing antiparkinsonian therapy [34]. Further, adverse effects of dopaminergic antagonist antipsychotics include decreased libido [35].

Collectively, the observed enhancement of free testosterone levels by *E. longifolia* was reflected on the possible negative feedback actions on LH and FSH levels as well as modulation of related brain neurotransmitters. Androgens modulate male sexual behavior and act at both the central and peripheral nervous system levels [36]. The testosterone-induced enhancement of dopamine release and its impact on the control of sexual behavior has been previously described. The stimuli from a receptive female lead to the release of dopamine in different brain areas. These include the nigrostriatal system, the mesolimbic system, and the medial preoptic area. The previous presence of testosterone is permissive for dopamine release and increases copulatory rate and efficiency and coordinates genital reflexes [37].

The positive effect of *E. longifolia* in the improvement of sexual behavior may be attributed to its active constituents such as quassinoids and in particular the major one, eurycomanone which was detected as peak **3** in UPLC-MS/MS analysis of AEEL. Eurycomanone was reported to induce testosterone production [4] and was also reported to enhance testosterone steroidogenesis at the Leydig cells through its inhibitory effect on the final step of transformation of testosterone to estrogen through aromatase enzyme inhibition [38]. Moreover, high concentration of eurycomanone has inhibitory effect on phosphodiesterase [38].

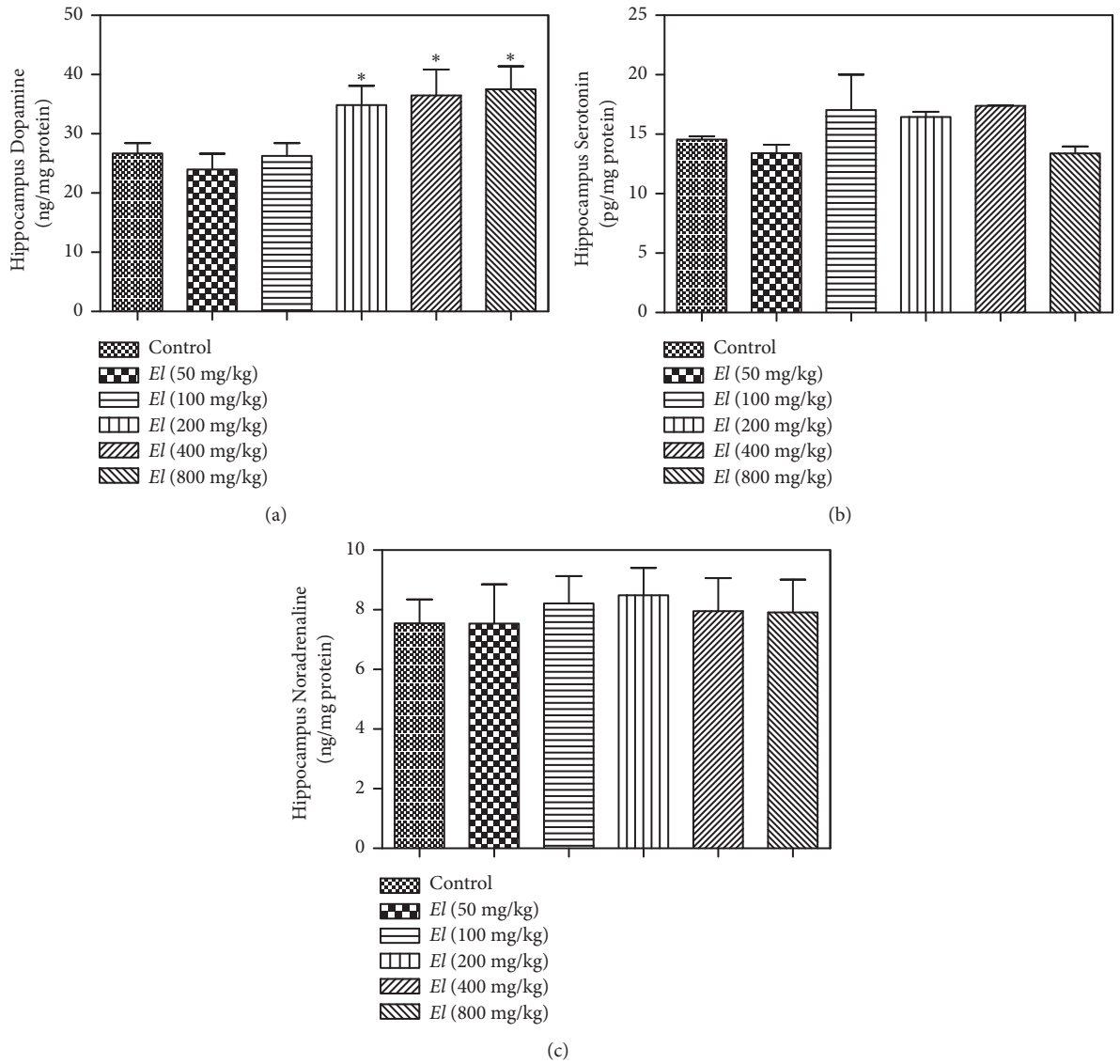

Figure 7: *Effect of E. longifolia roots on hippocampal content of dopamine (a), serotonin (b), and noradrenaline (c) in male rats. E. longifolia* was given as a single oral daily dose for 10 consecutive days. Values are mean ± SD. Statistical analysis was carried out by one-way *ANOVA* followed by *Dunnett post hoc* test. n=8. ∗Significantly different from the corresponding control at $p < 0.05$. *EL = E. longifolia*.

5. Conclusion

The current data confirm the aphrodisiac and anabolic activities of *E. longifolia* roots aqueous extract in male Sprague-Dawley rats. This can be attributed, at least partly, to elevation of blood testosterone level as well as enhancement of brain cortical and hippocampal dopamine content.

Data Availability

The data used to support the findings of this study are included within the article.

Disclosure

The study was not funded by a third party.

Conflicts of Interest

The authors declare no competing financial interests.

Authors' Contributions

Shahira M. Ezzat, Mona M. Okba, and Marwa I. Ezzat identified the metabolites and wrote the paper. Salah M. Hassan, Amgad I. Alkorashy, MMA, and Sherif H. Ahmed performed the pharmacological work. Shanaz O. Mohamed coordinated the whole work.

Acknowledgments

This research was made possible as part of Ministry of Agriculture Malaysia initiative under the New Key Economic

Areas Entry Point Project on High Value Herbals awarded to Natural Wellness Biotech (M) Sdn Bhd. The authors express their gratitude and appreciation for the trust and opportunity given. Authors extend their gratitude to Cairo University for their collaboration and excellent teamwork.

Supplementary Materials

OECD guidelines. *(Supplementary Materials)*

References

[1] P. J. Rowe, F. H. Comhaire, T. B. Hargreave, A. M. A. Mahmoud, and World Health Organization, *WHO Manual for the Standardized Investigation, Diagnosis and Management of the Infertile Male*, Cambridge University Press, Cambridge, UK, 2000.

[2] J. P. Jarow, I. D. Sharlip, A. M. Belker et al., "Best practice policies for male infertility," *The Journal of Urology*, vol. 167, no. 5, pp. 2138–2144, 2002.

[3] A. Ilacqua, G. Izzo, G. P. Emerenziani, C. Baldari, and A. Aversa, "Lifestyle and fertility: the influence of stress and quality of life on male fertility," *Reproductive Biology and Endocrinology*, vol. 16, no. 1, 2018.

[4] S. Rehman, K. Choe, and H. Yoo, "Review on a traditional herbal medicine, eurycoma longifolia Jack (Tongkat Ali): its traditional uses, chemistry, evidence-based pharmacology and toxicology," *Molecules*, vol. 21, no. 3, Article ID 331, 2016.

[5] H. H. Ang, H. S. Cheang, and A. P. M. Yusof, "Effects of Eurycoma longifolia Jack (Tongkat Ali) on the initiation of sexual performance of inexperienced castrated male rats," *Journal of Experimental Animal Science*, vol. 49, no. 1, pp. 35–38, 2000.

[6] H. H. Ang, Y. Hitotsuyanagi, H. Fukaya, and K. Takeya, "Quassinoids from Eurycoma longifolia," *Phytochemistry*, vol. 59, no. 8, pp. 833–837, 2002.

[7] H. H. Ang, K. L. Lee, and M. Kiyoshi, "Eurycoma longifolia jack enhances sexual motivation in middle-aged male mice," *Journal of Basic and Clinical Physiology and Pharmacology*, vol. 14, no. 3, pp. 301–308, 2003.

[8] P. He, Z. Dong, Q. Wang, Q. Zhan, M. Zhang, and H. Wu, "Structural characterization and immunomodulatory activity of a polysaccharide from *Eurycoma longifolia*," *Journal of Natural Products*, vol. 82, no. 2, pp. 169–176, 2019.

[9] A. George, J. Udani, N. Z. Abidin, and A. Yusof, "Efficacy and safety of Eurycoma longifolia (Physta®) water extract plus multivitamins on quality of life, mood and stress: a randomized placebo-controlled and parallel study," *Food & Nutrition Research*, vol. 62, 2018.

[10] P. Jayusman, I. Mohamed, E. Alias, N. Mohamed, and A. Shuid, "The effects of quassinoid-rich eurycoma longifolia extract on bone turnover and histomorphometry indices in the androgen-deficient osteoporosis rat model," *Nutrients*, vol. 10, no. 7, p. 799, 2018.

[11] D. Balan, K. Chan, D. Murugan, S. AbuBakar, and P. Wong, " Antiadipogenic effects of a standardized quassinoids-enriched fraction and eurycomanone from *Eurycoma longifolia*," *Phytotherapy Research*, vol. 32, no. 7, pp. 1332–1345, 2018.

[12] M. I. Tambi, M. K. Imran, and R. R. Henkel, "Standardised water-soluble extract of Eurycoma longifolia, Tongkat ali, as testosterone booster for managing men with late-onset hypogonadism?" *Andrologia*, vol. 44, supplement 1, pp. 226–230, 2012.

[13] C.-O. Malmnäs and B. J. Meyerson, "P-chlorophenylalanine and copulatory behaviour in the male rat," *Nature*, vol. 232, no. 5310, pp. 398–400, 1971.

[14] C. Bell, "Clinical guide to laboratory tests. 3rd edition. Norbert W. Tietz, ed," *Transfusion*, vol. 35, no. 11, pp. 972-972, 1995.

[15] S. W. Smith, "Free testosterone," *AACC Endo*, vol. 11, no. 3, pp. 59–62, 1993.

[16] K. Chan and C. Choo, "The toxicity of some quassinoids from eurycoma longifolia," *Planta Medica*, vol. 68, no. 7, pp. 662–664, 2002.

[17] J. F. Bowyer, A. J. Harris, R. R. Delongchamp et al., "Selective changes in gene expression in cortical regions sensitive to amphetamine during the neurodegenerative process," *NeuroToxicology*, vol. 25, no. 4, pp. 555–572, 2004.

[18] S. Spijker, "Dissection of rodent brain regions," *Neuromethods*, vol. 57, pp. 13–26, 2011.

[19] H. H. Ang, Y. Hitotsuyanagi, and K. Takeya, "Eurycolactones A-C, novel quassinoids from Eurycoma longifolia," *Tetrahedron Letters*, vol. 41, no. 35, pp. 6849–6853, 2000.

[20] L. S. Chua, N. A. Amin, J. C. Neo et al., "LC-MS/MS-based metabolites of Eurycoma longifolia (Tongkat Ali) in Malaysia (Perak and Pahang)," *Journal of Chromatography B*, vol. 879, no. 32, pp. 3909–3919, 2011.

[21] C.-H. Teh, V. Murugaiyah, and K.-L. Chan, "Developing a validated liquid chromatography-mass spectrometric method for the simultaneous analysis of five bioactive quassinoid markers for the standardization of manufactured batches of *Eurycoma longifolia* Jack extract as antimalarial medicaments," *Journal of Chromatography A*, vol. 1218, no. 14, pp. 1861–1877, 2011.

[22] H. Morita, E. Kishi, K. Takeya, H. Itokawa, and Y. Iitaka, "Highly oxygenated quassinoids from Eurycoma longifolia," *Phytochemistry*, vol. 33, no. 3, pp. 691–696, 1993.

[23] B. Mutschlechner, S. Schwaiger, T. V. A. Tran, and H. Stuppner, "Development of a selective HPLC-DAD/ELSD method for the qualitative and quantitative assessment of commercially available Eurycoma longifolia products and plant extracts," *Fitoterapia*, vol. 124, pp. 188–192, 2018.

[24] K. Mitsunaga, K. Koike, T. Tanaka et al., "Canthin-6-one alkaloids from *Eurycoma longifolia*," *Phytochemistry*, vol. 35, no. 3, pp. 799–802, 1994.

[25] R. Bhat and A. A. Karim, "Tongkat Ali (*Eurycoma longifolia* Jack): a review on its ethnobotany and pharmacological importance," *Fitoterapia*, vol. 81, no. 7, pp. 669–679, 2010.

[26] H. H. Ang and K. L. Lee, "Effect of *Eurycoma longifolia* Jack on orientation activities in middle-aged male rats," *Fundamental & Clinical Pharmacology*, vol. 16, no. 6, pp. 479–483, 2002.

[27] H. H. Ang, T. H. Ngai, and T. H. Tan, "Effects of Eurycoma longifolia Jack on sexual qualities in middle aged male rats," *Phytomedicine*, vol. 10, no. 6-7, pp. 590–593, 2003.

[28] H. H. Ang, K. L. Lee, and M. Kiyoshi, "Sexual arousal in sexually sluggish old male rats after oral administration of eurycoma longifolia jack," *Journal of Basic and Clinical Physiology and Pharmacology*, vol. 15, no. 3-4, pp. 303–309, 2004.

[29] M. C. Solomon, N. Erasmus, and R. R. Henkel, "*In vivo* effects of *Eurycoma longifolia* Jack (Tongkat Ali) extract on reproductive functions in the rat ," *Andrologia*, vol. 46, no. 4, pp. 339–348, 2014.

[30] J. G. Pfaus and L. A. Scepkowski, "The biologic basis for libido," *Current Sexual Health Reports*, vol. 2, no. 2, pp. 95–100, 2005.

[31] W. Schultz, "Neuronal reward and decision signals: from theories to data," *Physiological Reviews*, vol. 95, no. 3, pp. 853–951, 2015.

[32] S. N. Young, "How to increase serotonin in the human brain without drugs," *Journal of Psychiatry & Neuroscience*, vol. 32, no. 6, pp. 394–399, 2007.

[33] C. W. Berridge, B. E. Schmeichel, and R. A. España, "Noradrenergic modulation of wakefulness/arousal," *Sleep Medicine Reviews*, vol. 16, no. 2, pp. 187–197, 2012.

[34] G. Bronner, J. Aharon-Peretz, and S. Hassin-Baer, "Sexuality in patients with Parkinson's disease, Alzheimer's disease, and other dementias," *Handbook of Clinical Neurology*, vol. 130, pp. 297–323, 2015.

[35] M. J. Just, "The influence of atypical antipsychotic drugs on sexual function," *Neuropsychiatric Disease and Treatment*, vol. 11, pp. 1655-1656, 2015.

[36] A. M. Isidori, J. Buvat, G. Corona et al., "A critical analysis of the role of testosterone in erectile function: from pathophysiology to treatment—a systematic review," *European Urology*, vol. 65, no. 1, pp. 99–112, 2014.

[37] E. M. Hull, D. S. Lorrain, J. Du et al., "Hormone-neurotransmitter interactions in the control of sexual behavior," *Behavioural Brain Research*, vol. 105, no. 1, pp. 105–116, 1999.

[38] B.-S. Low, S.-B. Choi, H. Abdul Wahab, P. Kumar Das, and K.-L. Chan, "Eurycomanone, the major quassinoid in Eurycoma longifolia root extract increases spermatogenesis by inhibiting the activity of phosphodiesterase and aromatase in steroidogenesis," *Journal of Ethnopharmacology*, vol. 149, no. 1, pp. 201–207, 2013.

Hindawi
Evidence-Based Complementary and Alternative Medicine
Volume 2019, Article ID 4341592, 8 pages
https://doi.org/10.1155/2019/4341592

Research Article

Rho-Kinase II Inhibitory Potential of *Eurycoma longifolia* New Isolate for the Management of Erectile Dysfunction

Shahira M. Ezzat,[1,2] **Mona M. Okba**,[1] **Marwa I. Ezzat**,[1] **Nora M. Aborehab**,[3] **and Shanaz O. Mohamed**[4]

[1]*Pharmacognosy Department, Faculty of Pharmacy, Cairo University, Kasr El-Ainy Street, Cairo 11562, Egypt*
[2]*Pharmacognosy Department, Faculty of Pharmacy, October University for Modern Sciences and Arts (MSA), 6th October 12566, Egypt*
[3]*Biochemistry Department, Faculty of Pharmacy, October University for Modern Sciences and Arts (MSA), 6th October 12566, Egypt*
[4]*School of Pharmaceutical Sciences, Universiti Sains Malaysia, Malaysia*

Correspondence should be addressed to Mona M. Okba; mona.morad@pharma.cu.edu.eg

Received 31 January 2019; Revised 18 March 2019; Accepted 21 April 2019; Published 15 May 2019

Guest Editor: Arielle Cristina Arena

Background. Eurycoma longifolia Jack (Fam.: Simaroubaceae), known as Tongkat Ali (TA), has been known as a symbol of virility and sexual power. The aim of the study was to screen *E. longifolia* aqueous extract (AE) and isolates for ROCK-II inhibition. *Results.* The AE (1-10 μg/ml) showed a significant inhibition for ROCK-II activity (62.8-81%) at $P < 0.001$ with an IC_{50} (651.1 ± 32.9 ng/ml) compared to Y-27632 ([(+)-(*R*)-*trans*-4-(1-aminoethyl)-*N*-(4-pyridyl)cyclohexanecarboxamide dihydrochloride]) (68.15-89.9 %) at same concentrations with an IC_{50} (192 ± 8.37 ng/ml). Chromatographic purification of the aqueous extract (AE) allowed the isolation of eight compounds; stigmasterol **T1**, *trans*-coniferyl aldehyde **T2,** scopoletin **T3**, eurycomalactone **T4**, 6α-hydroxyeurycomalactone **T5**, eurycomanone **T6**, eurycomanol **T7**, and eurycomanol-2-*O*-β-D-glucopyranoside **T8**. This is the first report for the isolation of **T1** and **T3** from *E. longifolia* and for the isolation of **T2** from genus *Eurycoma*. The isolates (at 10 μg/ml) exhibited maximum inhibition % of ROCK-II 82.1 ± 0.63 (T2), 78.3 ± 0.38 (T6), 77.1 ± 0.11 (T3), 76.2 ± 3.53 (T4), 74.5 ± 1.27 (T5), 74.1 ± 2.97 (T7), 71.4 ± 2.54 (T8), and 60.3 ± 0.14 (T1), where the newly isolated compound *trans*-coniferyl aldehyde **T2** showed the highest inhibitory activity among the tested isolated compounds and even higher than the total extract AE. The standard Y-27632 (10 μg/ml) showed 89.9 ± 0.42 % inhibition for ROCK-II activity when compared to control at $P < 0.0001$. *Conclusion.* The traditional use of *E. longifolia* as aphrodisiac and for male sexual disorders might be in part due to the ROCK-II inhibitory potential.

1. Introduction

Libido refers to a fluctuating state of sexual desire [1]. The 21st century has seen the evolution of a lot of firms and clinics that claim to treat reduced libido in males [2]. Studies have reported a prevalence of the Hypoactive Sexual Desire Disorder (HSDD) in men between 1 and 20% [3]. It is estimated that 30-40% of people around the world experience lack of sexual interest for at least several months in any given year [2]. Nowadays, sexual desire is controlled by some external factors including psychiatric disorders as depression, some types of medications including antidepressants, some diseases as diabetes and hypothyroidism, social and interpersonal problems, and other conditions causing inhibited or decreased dopamine release, leading to sexual dysfunction, general lack of sexual desire, and decreased libido [1]. Alteration in libido also may be due to some biochemical messengers, such as levels of serum steroid hormone (mainly testosterone), feedback after sexual stimulation, and disturbances in the brain neurotransmitters [4]. Till this moment, the only available medicines indicated to increase male libido are some herbal drugs and hormonal therapy in cases of testosterone deficiency [5].

E. longifolia (Tongkat Ali, Genus: Eurycoma; Family: Simaroubaceae) is one of the most well-known tropical plants, indigenous to Southeast Asian countries like Vietnam, Malaysia, and Indonesia. It is known as 'Tongkat Ali' where in Malaysia 'Ali' refers to "walking stick" because this plant roots

are twisted and long. The plant (particularly roots) has been traditionally used for reducing fever and fatigue and for its unique antimalarial, antipyretic, antiulcer, and its aphrodisiac properties. Body builders have been recently focusing on regular intake of its root extracts to improve muscular mass and strength [6–8].

A large number of phytochemicals have been detected and identified from E. longifolia roots including eurycomanone, eurycomaoside, eurycolactone, eurycomalactone, canthin-6-one alkaloids, quassinoid diterpenoids, β-carboline alkaloids, tirucallane-type triterpenes, biphenylneolignans, laurycolactone, and squalene derivatives [9, 10]. *E. longifolia* has gained wide appreciation for its uniqueness in enhancing sexual power which was supported by some literature in experimental animals [11–15]. It has been utilized by Malaysian men for hundreds of years to enhance the quality and performance of sexual exercise [6, 7].

Around the world, there has been a gigantic increment in the utilization of this plant. There are about two hundred Tongkat Ali products, mostly focusing on the sexual enhancing properties. It is available either as crude root powder, in capsules blended with different aphrodisiac drugs, as an added substance blended with ginseng or coffee, or in other healthcare products as a substitute for ginseng [8].

Corpus cavernosum smooth muscle (CCSM) and penile arteries relaxation results in blood trapping in the penis leading to raised intracavernous pressure (ICP) which plays a pivotal role as penile erection [16].

RhoA and ROCK are found in different tissues in the body and responsible for regulating many functions. In spite of their presence in the neural and endothelial tissues of the human corpora, but their prominent effects are obvious in penile erection through modulation of cavernous sinusoidal and arteriolar smooth-muscle cells contractile state [17].

Although Tongkat Ali traditional use as an aphrodisiac herb is well-recognized, there is no sufficient information on the possible underlying mechanisms. Therefore, this study was designed to evaluate *E. longifolia* AE and isolated biophytochemicals potential in management of erectile dysfunction (ED).

2. Materials and Methods

2.1. Plant Material. The roots of *Eurycoma longifolia* Jack were obtained from HCA products Sdn Bhd. Spring 2015. The plant was kindly identified in the Forest Research Institute, Malaysia. A voucher specimen (5-09-2015) was kept in the herbarium of Pharmacognosy Department, Faculty of Pharmacy, Cairo University, Cairo, Egypt.

2.2. Preparation of the Aqueous Extract (AE). The collected roots were washed with running water and then dried on an open surface and dried by exposure to sunlight for 1 or 2 days to ensure freedom of humidity. The dried roots were then chipped to 5 mm particles. The dried chipped roots (40 kg) were boiled with 200 liters of RO water (water purified with reverse osmosis) for 3 hours; the extract was concentrated in a rotary evaporator for 3 hours at 60°C to 20 liters. The extract was then dried in a spray dryer by heating for 6h and 30 min at a temperature of 120°C and yielded 1.6 kg powdered extract where the extract yield is 4%.

2.3. Rock-II Inhibition Assay. The assay was done as mentioned in ADP-Glo™ Kinase Assay (SER-THR KINASE SERIES: ROCK2 Kinase assay) (Promega, USA) and Y-27632 [(+)-(*R*)-*trans*-4-(1-aminoethyl)-*N*-(4-pyridyl)cyclohexanecarboxamide dihydrochloride] was used as standard drug; luminescence was recorded using Topotecan, USA, Spark 10 M, multimode microplate reader. A vehicle control for 5% DMSO was used in the assay to check the interference. Standard curve for ROCK-II enzyme was done (Figure 2). Serial dilution and IC_{50} of the AE was performed in triplicate.

2.4. Fractionation of the AE and Isolation of Its Major Phytochemicals

2.4.1. General. Silica gel 60 (70 - 230 mesh ASTM; Fluka, Steinheim, Germany), Diaion HP-20 AG, Sephadex LH-20 (Pharmacia Fine Chemicals AB, Uppsala, Sweden), and reversed phase silica gel (RP-18) (70-230 mesh) for column chromatography (75-150 μm, Mitsubishi Chemical Industries Co. Ltd). Thin-layer chromatography (TLC) (silica gel GF_{254} precoated plates- Fluka) was done using this solvent systems: S_a: *n*-Hexane: ethyl acetate (7:3 v/v); S_b; ethyl acetate-methanol-water-formic acid (10:1.6:1.2:1 v/v). Chromatograms detections were performed under UV light (at 254 and 366 nm) and sprayed by *p*-anisaldehyde sulphuric acid spray reagent. Bruker NMR was used for ^{13}C-NMR (125 MHz) and ^{1}H-NMR (400 MHz). The NMR spectra were observed in DMSO and CD_3OD. Chemical shifts are given in δ (ppm) relative to internal standard TMS.

2.4.2. Isolation of the Major Phytochemicals. For isolation of the major compounds, 500 grams of AE were suspended in 800 ml distilled water then defatted with methylene chloride (300 mLx 3). The organic and aqueous layers were separated. The organic layer was evaporated using rotary evaporator under reduced pressure at 40°C to yield 8 gm of methylene chloride residue (MeCl). The aqueous layer was kept for further fractionation.

MeCl (8 g) was fractionated over a silica gel column (80 g). Gradient elution was done using *n*-hexane-methylene chloride then methylene chloride-methanol mixtures. The polarity was increased by 10 % incriminations of methylene chloride in *n*-hexane every 50 ml till 100% methylene chloride then further 1% incriminations of methanol in methylene chloride till 7% methanol. Fractions (20 ml) were collected to obtain 60 fractions which were then monitored by TLC using solvent system (S_1). Subfraction (60% methylene chloride in *n*-hexane) was washed with methanol to yield pure compound **T1** (white crystals, 25 mg). Subfraction (80% methylene chloride in *n*-hexane) was chromatographed over a silica gel column. The elution carried out using *n*-hexane-ethyl acetate (85:15 v/v). Similar fractions were pooled together to yield compound **T2** (white crystals, 20 mg). Fraction (1% methanol in methylene chloride) was chromatographed over a sephadex LH20 using methanol-water (7:3 v/v) as eluent to yield one compound **T3** (yellowish

white crystals, 34 mg). Fraction (6% methanol in methylene chloride) was chromatographed over a sephadex LH20 using *n*-butanol-isopropanol-water (4:1:5 v/v) as eluent to yield a fraction containing two major spots with minor impurities. This fraction was further purified by rechromatography over silica gel column. It was gradient eluted using *n*-hexane-ethyl acetate (10-30%) mixtures to yield two pure compounds **T4** (white crystals, 68 mg) and **T5** (white crystals, 52 mg).

The defatted aqueous solution was chromatographed on diaion HP-20 AG (500 g) column. Elution was carried out with water, followed by methanol-water (50%), methanol-water (75%), and methanol (100%) to give four fractions (D1-D4), respectively. The solvent in each case was evaporated using rotary evaporator to yield solid residues weighing 154, 35, and 10 g, respectively. Methanol-water (50%) (D2) fraction (35g) was further fractionated over a silica gel (100 g) column where elution was carried out by *n*-hexane: ethyl acetate. Gradient elution was carried out by *n*-hexane-ethyl acetate and ethyl acetate-methanol-water mixtures. The polarity was increased by 10 % incriminations of ethyl acetate every 100 ml till 100% ethyl acetate then further incrimination of methanol (till 1.6%) and water (till 1.3%). Fractions (20 ml, each) were combined to give 60 fractions which were monitored by TLC using solvent systems (Sb). Subfraction (80% ethyl acetate in *n*-hexane) was fractionated over a silica (RP) column. The elution carried out using water-methanol as eluent. The fractions eluted with 10% and 20% methanol give compounds **T6** (white powder, 83 mg) and **T7** (white powder, 90 mg), respectively. Subfraction (0.9% methanol, 0.3% water in ethyl acetate) was chromatographed over a sephadex column eluted with 50% methanol then silica gel column eluted with ethyl acetate-methanol (9:1 v/v) to give compound **T8** (white crystals, 80 mg).

2.5. Rock-II Inhibition Assay. The assay was repeated as mentioned in Section 2.3 on the AE fractions and the isolates T1-T8.

The assay performance measure was used to validate the screening assay quality through calculation of Z-factor according to methodology of Zhang et al., 1999 [18].

2.6. Statistical Analysis. Enzyme inhibition by tested samples is expressed as mean ± SD and analyzed using Prism program version 6 (GraphPad Software, Inc., San Diego CA); comparisons among tested samples were carried out using one-way analysis of variance (ANOVA) followed by Bonferroni's multiple comparisons test. $P < 0.05$ was considered significant.

3. Results

3.1. Evaluation of AE Rock-II Inhibition Potential. Concentrations at (1-10 μg/ml) of the AE and Y-27632 as a standard showed a significant inhibition for ROCK-II activity (62.8-81%). The inhibition of ROCK-II activity at $P < 0.001$ was recorded in Table 1. IC_{50} in ROCK-II inhibition assay of AE (651.1 ± 32.9 ng/ml) and Y-27632 were recorded in Table 2.

3.2. Fractionation of AE and Isolation of the Major Phytochemicals. Chromatographic fractionation of *E. longifolia* roots AE allowed the isolation of one sterol: stigmasterol, **T1**; a phenolic compound: *trans*-coniferyl aldehyde **T2**; one coumarin: scopoletin **T3**; and 5 known quassinoids namely eurycomalactone **T4**, 6α- hydroxyeurycomalactone **T5**, eurycomanone **T6**, eurycomanol **T7,** and eurycomanol-2-*O*-β-D-glycopyranoside **T8**. The isolated compounds were identified via their co-TLC comparison to authentic reference samples, physicochemical characters, and spectroscopic analysis and through comparing their 1D and 2D NMR data with the previously published data. ^{1}H NMR and ^{13}CNMR data of the isolated phytochemicals are presented in Tables S1 and S2 in the supplementary file. The structures of the isolated phytochemicals are shown in Figure 1.

3.3. Evaluation of Rock-II Inhibition Potential of AE Fractions and Isolates. All tested samples and Y-27632 standard at concentration range (0.01-10 μg/ml) showed a significant inhibition for ROCK-II activity.

At dose 10 μg/ml, MeCl, D1, D2, D3, D4 showed a maximum inhibition % of (86.3 ± 0.71), (90.1 ± 0.84), (86.1 ± 0.42), (90.25 ± 0.07), (87.05 ± 0.21), respectively.

The isolates (at 10 μg/ml) exhibited maximum inhibition % of 82.1 ± 0.63 (T2), 78.3 ± 0.38 (T6), 77.1 ± 0.11 (T3), 76.2 ± 3.53 (T4), 74.5 ± 1.27 (T5), 74.1 ± 2.97 (T7), 71.4 ± 2.54 (T8), and 60.3 ± 0.14 (T1). The standard Y-27632 (10 μg/ml) showed (89.9 ± 0.42) inhibition % for ROCK-II activity when compared to vehicle control at $P < 0.0001$. Nonsignificant difference was found between MeCl, D1, D2, D3, D4 at concentration 10 μg/ml compared to Y-27632 at the same concentration against the inhibition of ROCK-II activity at $P < 0.001$ as presented in Table 1.

IC_{50} of ROCK-II inhibition assay of all tested AE fractions, isolates, and Y-27632 were recorded in Table 2.

Nonsignificant difference was found between MeCl, D1, D2, D3 and D4 with IC50 (162.8 ± 3.35, 105 ± 3.56, 153 ± 14.1, 91.1 ± 6.63, and 189.3 ± 21.9, respectively) compared to Y-27632 IC_{50} (192 ± 8.37); these fractions showed a prominent effect as the same effect as Y-27632 in ROCK-II inhibition.

The assay performance measure was evaluated by calculation of Z-factor which was equal to 0.802 which indicated that it is an excellent assay [18].

4. Discussion

E. longifolia roots AE has gained wide recognition for enhancing the virility and sexual prowess. It has been utilized by Malaysian men for hundreds of years to enhance the quality and performance of sexual exercises [6, 7]. Although traditional use of *E. longifolia* as an aphrodisiac herb is well-recognized, there is a paucity of information on the possible underlying mechanisms. Therefore, the present study aimed at substantiating the aphrodisiac activity of *E. longifolia*.

ROCK-II inhibition assay was performed using ADP-Glo™ Kinase Assay and Y-27632 was used as standard; this method was preferred more than ELISA technique due to the absence of several washing steps and false results that may happen due to the interference with horseradish peroxidase as the extracts have ant-oxidant activity.

Table 1: Effect of aqueous extract (AE), fractions and isolates on percentage inhibition of ROCK-II activity.

Treatment (s)	Concentrations (μg/ml)	% of inhibition of ROCK-II ± SD
Control	-	*0*
Vehicle control	5%	2.06 ± 0.075
AE	10	81 ± 0.21∗
AE	1	62.8 ± 0.84∗
AE	0.1	16.3 ± 1.26∗
AE	0.01	3.18 ± 2.4
MeCl	10	*86.3*± 0.71∗
MeCl	1	76.8 ± 0.84∗
MeCl	0.1	46.9 ± 0.56∗
MeCl	0.01	17.2 ± 1.27∗
D1	10	*90.1*± 0.84∗
D1	1	76.3 ± 1.69∗
D1	0.1	55.8 ± 0.14∗
D1	0.01	21.1 ± 1.83∗
D2	10	*86.1*± 0.42∗
D2	1	74.04 ± 0.01∗
D2	0.1	49.65 ± 0.21∗
D2	0.01	18.9 ± 3.39∗
D3	10	*90.25*± 0.07∗
D3	1	80.15 ± 0.48∗
D3	0.1	61.8 ± 0.42∗
D3	0.01	17.9 ± 1.83∗
D4	10	*87.05*± 0.21∗
D4	1	74.05 ± 0.35∗
D4	0.1	46.1 ± 4.37∗
D4	0.01	14.5 ± 1.98∗
T1	10	60.3 ± 0.14∗
T1	1	27.35 ± 2.47∗
T1	0.1	13.3 ± 2.26∗
T1	0.01	2.78 ± 1.84
T2	10	82.1 ± 0.63∗
T2	1	68.5 ± 0.35∗
T2	0.1	33.2 ± 1.55∗
T2	0.01	10.62 ± 2.94∗
T3	10	77.1 ± 0.11∗
T3	1	66.15 ± 0.07∗
T3	0.1	25 ± 2.47∗
T3	0.01	10.1 ± 3.34∗
T4	10	76.2 ± 3.53∗
T4	1	54 ± 0.42∗
T4	0.1	25.7 ± 2.47∗
T4	0.01	6.13 ± 0.44∗
T5	10	74.5 ± 1.27∗
T5	1	55.3 ± 0.45∗
T5	0.1	23.6 ± 2.4∗
T5	0.01	8.1 ± 2.27∗
T6	10	78.3 ± 0.38∗
T6	1	57.1 ± 0.56∗
T6	0.1	26.4 ± 2.61∗
T6	0.01	5.4 ± 3.74
T7	10	74.1 ± 2.97∗
T7	1	49.6 ± 7.89∗

Table 1: Continued.

Treatment (s)	Concentrations (μg/ml)	% of inhibition of ROCK-II ± SD
T7	0.1	19.4 ± 0.14∗
T7	0.01	5.85 ± 2.93
T8	10	71.4 ± 2.54∗
T8	1	46.5 ± 1.62∗
T8	0.1	17 ± 0.77∗
T8	0.01	4.06 ± 3.8
Y-27632	10	*89.9*± 0.42∗
Y-27632	1	68.15 ± 2.75∗
Y-27632	0.10	42.15 ± 2.19∗
Y-27632	0.01	22.5 ± 1.27∗

AE: aqueous extract; **D1**: water (100%); **D2:** methanol-water (50%); **D3**: methanol-water (75%); **D4**: methanol (100%) diaion fractions; **MeCl:** methylene chloride fraction; **T1:** stigmasterol; **T2:** *trans*-coniferyl aldehyde; **T3:** scopoletin; **T4:** eurycomalactone; **T6**: 6α- hydroxyeurycomalactone; **T6**: eurycomanone; **T7**: eurycomanol; **T8**: and eurycomanol-2-*O*-β-D-glucopyranoside.
∗ Significant from Vehicle control at $P < 0.0001$

Table 2: IC_{50} of aqueous extract (AE) of *E. longifolia* root, its fractions, and its isolates expressed as mean ± SD. Assay was performed in triplicates

Sample	IC_{50} (ng/ml)
AE	651.1 ± 32.9∗
MeCl	162.8 ± 3.35∗
D1	105 ± 3.56∗
D2	153 ± 14.1#
D3	91.1 ± 6.63∗
D4	189.3 ± 21.9
T1	6141 ± 540∗
T2	358 ± 31.1∗
T3	525 ± 42.8∗
T4	794 ± 95.5∗
T5	829 ± 41∗
T6	677 ± 51.1∗
T7	1112 ± 73.7∗
T8	1441 ± 175∗
Y-27632	192 ± 8.37

IC50 values are mean ± SD. Statistical analysis was carried out by one-way ANOVA followed by Bonferroni post-hoc test. n=3
∗Significantly different from Y-27632 at $P < 0.001$
Significant different from Y-27632 at $P < 0.01$
AE: aqueous extract; **D1**: water (100%); **D2:** methanol-water (50%); **D3**: methanol-water (75%); **D4**: methanol (100%) diaion fractions; **MeCl:** methylene chloride fraction; **T1:** stigmasterol; **T2:** *trans*-coniferyl aldehyde; **T3:** scopoletin; **T4:** eurycomalactone; **T6**: 6α- hydroxyeurycomalactone; **T6**: eurycomanone; **T7**: eurycomanol; **T8**: and eurycomanol-2-*O*-β-D-glucopyranoside.

Smooth-muscle contraction is regulated by the cytosolic Ca^{2+} concentration and by the calcium sensitivity of myofilaments. The major mechanism of Ca^{2+} sensitization of smooth-muscle contraction is achieved by the inhibition of the myosin light chain phosphatase (MLCP) that dephosphorylates the Myosin light chain in smooth muscle through RhoA/Rho-kinase pathway. The active, GTP bound form of the small GTPase RhoA activates a serine/threonine kinase, Rho-kinase (ROCK-II), which phosphorylates the regulatory subunit of MLCP and inhibits phosphatase activity leading to contraction of smooth muscle through Ca^{2+} sensitivity. MLCP converts the active phosphorylated myosin light chain (MLC) to inactive one so relaxation of the muscle occurs [19].

AE purification led to the isolation of eight compounds. Compound **T2** was isolated as needle crystals. Its ^{1}HNMR spectrum showed three aromatic protons arranged in ABX system which was characterized by three doublets at δ_H 6.99 (1H, d, J=1.76 Hz), 6.88 (1H,d, J=8.16 Hz), and 7.04 (1H, dd, J=1.8,8.16 Hz) assigned to H-2, H-5, and H-6. In addition two *trans*-olefinic protons appeared at δ_H 7.31 (1H, d, J=15.8 Hz, H-7) and 6.49 (1H, dd, J=7.70,15.8 Hz, H-8) and an aldehydic group which appeared as a doublet at δ_H 9.56 (1H, d, J=7.70 Hz, H-9) and finally a methoxy group at δ_H 3.82 as a singlet. The coupling constants $J_{7,8}$ and $J_{8,9}$ indicated that $\Delta^{7,8}$ is trans and that CHO is linked to H-8; this was confirmed from HMBC correlations between 7.31 (1H, d, J=15.8 Hz, H-7) and C-8 at δ_C 126.4 and CHO at δ_C 193.6 and also the correlations of δ_H 9.56 (1H, d, J=7.70 Hz, H-9) with C-7 at δ_C 153.1 and C-8 at δ_C 126.4. The position of OCH_3 at C-3 was deduced from long-range coupling between δ_H 3.82 and C-3 at δ_C 146.9. The assignments of carbons were deduced from ^{1}H-^{13}C correlations in HSQC. This compound was identified as *trans*-coniferyl aldehyde [20], which is isolated here for the first time from genus *Eurycoma*.

Compounds T1, T3-T8 spectral data were in agreement with the reported data of stigmasterol [21], scopoletin [22], eurycomalactone, 6α- hydroxyeurycomalactone [23], eurycomanone [23], eurycomanol [23], and eurycomanol-2-*O*-β-D-glycopyranoside [24]. This is the first report for the isolation of T1 and T3 from E. longifolia and for the isolation of T2 from genus *Eurycoma*.

Among the different doses used for the AE, MeCl, fractions and isolates, all of them exhibited more than 50% of ROCK-II inhibition at higher dose which indicate the use of this potent herbal drug in the management of erectile dysfunction. It is worth noting that maximum inhibition of ROCK-II was recorded for trans-coniferyl aldehyde (T2)

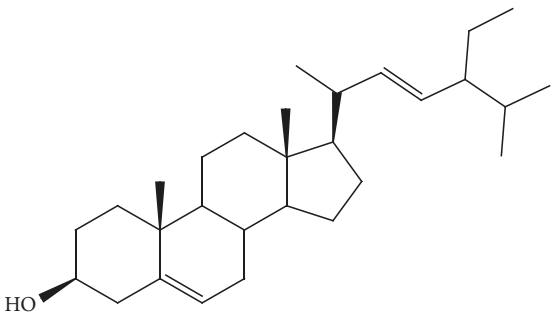

T1: Stigmasterol

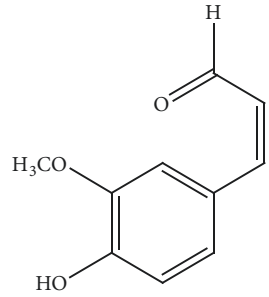

T2: Coniferyl aldehyde

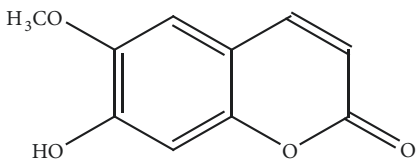

T3: Scopoletin

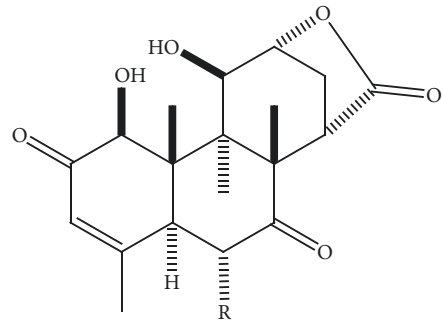

T4: Eurycomalactone R=H

T5: 6α- hydroxyeurycomalactone R=OH

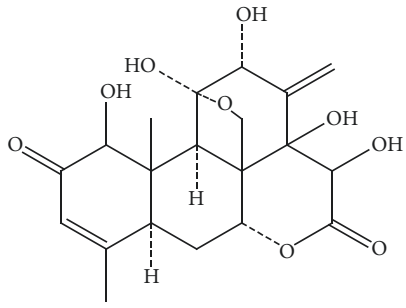

T6: Eurycomanone

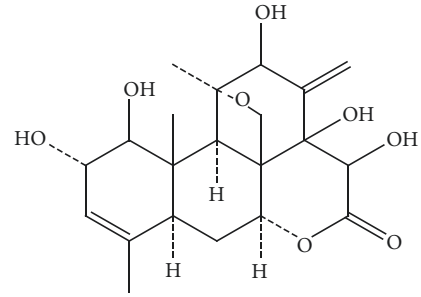

T7: Eurycomanol

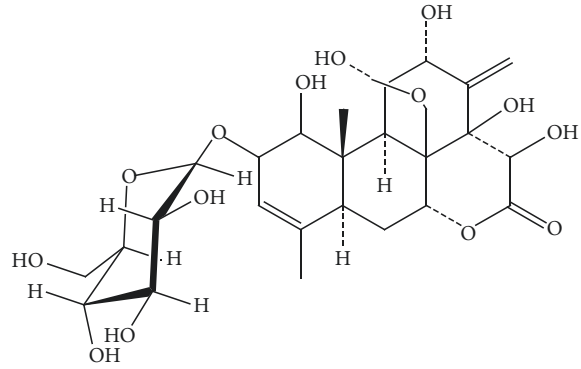

T8: Eurycomanol-2-O-β-D-glucopyranoside

Figure 1: Structure of the isolated compounds (T1-8).

82.1% which is isolated from *Eurycoma* for the first time. Previous studies reported the potential antimutagenic, antioxidant [25], and anti-inflammatory properties of coniferyl aldehyde [26], but its effect on erectile dysfunction was not studied before.

Although the ROCK-II inhibitory potential of *E. longifolia* crude extract was studied once before [16], this is the first report to evaluate the inhibition activity of *E. longifolia* isolates (T1-T8) on ROCK-II that manage erectile dysfunction.

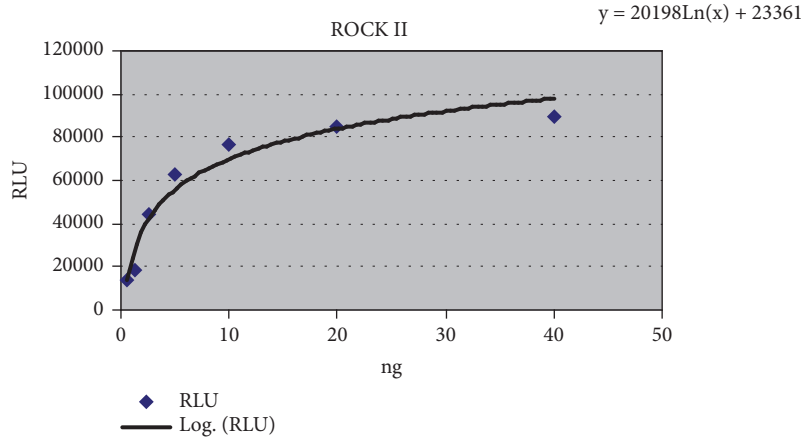

Figure 2: *ROCK-II enzyme standard curve.* x-axis represents the concentration from (40 ng/ml, 20 ng/ml, 10 ng/ml, 5 ng/ml, 2.5 ng/ml, 1.25 ng/ml and 0.625 ng/ml) and Y-axis represents ΔRLU.

In a recent review about *E. longifolia* chemistry and evidence-based pharmacology, many *E. longifolia* isolated compounds pharmacological activities were reported [6]. All *E. longifolia* previously isolated compounds activities on ROCK-II that manage erectile dysfunction were not reported. Compounds isolated in our study exhibited other activities rather than improvement of sexual behavior; eurycomalactone and eurycomanol-2-*O*-β-D-glycopyranoside antimalarial activity [27], 6α- hydroxyeurycomalactone cytotoxic activity [28], and eurycomanol are the regulators of signaling pathways involved in proliferation, cell death, and inflammation [29], except for eurycomanone which was reported to improve sexual behavior by other mechanisms more than affecting erectile dysfunction.

Beside the herein reported potent effect in managing the erectile dysfunction, the positive effect of *E. longifolia* in the improvement of sexual behavior may be attributed to its active constituents such as quassinoids and in particular the major one, eurycomanone, which was isolated and identified in the present work. Eurycomanone was reported to induce testosterone production [6] and was also reported to enhance testosterone steroidogenesis at the Leydig cells through its inhibitory effect on the final step of transformation of testosterone to estrogen through aromatase enzyme inhibition [30]. Moreover, high concentration of eurycomanone has inhibitory effect on phosphodiesterase [30].

It is worth mentioning that the IC_{50} of the MeCl and the diaion fractions (D1–D4) is less than that of the isolated pure compounds (Table 2). Hence, these fractions have better ROCK inhibitory potential than the isolated compounds (T1-8). Further studies are highly recommended to verify if this is due to the synergistic effects of the compounds in the mentioned fractions or there are much more potent compounds to be isolated from these fractions.

5. Conclusion

Our research revealed that the traditional use of *E. longifolia* as aphrodisiac and for male sexual disorders might be partially due to the ROCK-II inhibitory activity. To confirm our hypothesis, our future work is to study the in vivo aphrodisiac effect of the plant in animal model.

Data Availability

The data used to support the findings of this study are included within the article.

Disclosure

The study was not funded by a third party.

Conflicts of Interest

The authors declare no conflicts of interest.

Acknowledgments

This research was made possible as part of the Ministry of Agriculture Malaysia initiative under the New Key Economic Areas Entry Point Project on High Value Herbals awarded to Natural Wellness Biotech (M) Sdn Bhd. The authors express their gratitude and appreciation for the trust and opportunity given. Authors extend their gratitude to Cairo University for their collaboration and excellent teamwork.

Supplementary Materials

^{1}H NMR data of the isolated phytochemicals are presented in Tables S1. ^{13}CNMR data of the isolated phytochemicals are presented in Tables S2. *(Supplementary Materials)*

References

[1] K. A. Montgomery, "Sexual desire disorders," *Psychiatry (Edgmont)*, vol. 5, no. 6, pp. 50–55, 2008.

[2] E. O. Laumann, A. Paik, D. B. Glasser et al., "A cross-national study of subjective sexual well-being among older women and men: findings from the global study of sexual attitudes and

behaviors," *Archives of Sexual Behavior*, vol. 35, no. 2, pp. 143–159, 2006.

[3] L. A. Brotto, "The DSM diagnostic criteria for hypoactive sexual desire disorder in men," *The Journal of Sexual Medicine*, vol. 7, no. 6, pp. 2015–2030, 2010.

[4] J. G. Pfaus and L. A. Scepkowski, "The biologic basis for libido," *Current Sexual Health Reports*, vol. 2, no. 2, pp. 95–100, 2005.

[5] S. Kotta, S. Ansari, and J. Ali, "Exploring scientifically proven herbal aphrodisiacs," *Pharmacognosy Reviews*, vol. 7, no. 13, pp. 1–10, 2013.

[6] S. U. Rehman, K. Choe, and H. H. Yoo, "Review on a traditional herbal medicine, eurycoma longifolia Jack (Tongkat Ali): Its traditional uses, chemistry, evidence-based pharmacology and toxicology," *Molecules*, vol. 21, no. 3, article 331, 2016.

[7] R. Bhat and A. A. Karim, "Tongkat Ali (*Eurycoma longifolia* Jack): a review on its ethnobotany and pharmacological importance," *Fitoterapia*, vol. 81, no. 7, pp. 669–679, 2010.

[8] B. J. Indu and L. T. Ng, *Herbs: The Green Pharmacy of Malaysia*, Malaysian Agricultural Research and Development Institute, Malaysia, 2000.

[9] K. Miyake, Y. Tezuka, S. Awale, F. Li, and S. Kadota, "Quassinoids from Eurycoma longifolia," *Journal of Natural Products*, vol. 72, no. 12, pp. 2135–2140, 2009.

[10] E. Bedir, H. Abou-Gazar, J. N. Ngwendson, and I. A. Khan, "Eurycomaoside: a new quassinoid-type glycoside from the roots of eurycoma longifolia," *Chemical & Pharmaceutical Bulletin*, vol. 51, no. 11, pp. 1301–1303, 2003.

[11] H. H. Ang, T. H. Ngai, and T. H. Tan, "Effects of Eurycoma longifolia Jack on sexual qualities in middle aged male rats," *Phytomedicine*, vol. 10, no. 6-7, pp. 590–593, 2003.

[12] H. H. Ang, K. L. Lee, and M. Kiyoshi, "Eurycoma longifolia jack enhances sexual motivation in middle-aged male mice," *Journal of Basic and Clinical Physiology and Pharmacology*, vol. 14, no. 3, pp. 301–308, 2003.

[13] H. H. Ang and T. H. Ngai, "Aphrodisiac evaluation in non-copulator male rats afterchronic administration of Eurycoma longifolia Jack," *Fundamental & Clinical Pharmacology*, vol. 15, no. 4, pp. 265–268, 2001.

[14] H. H. Ang and K. L. Lee, "Effect of *Eurycoma longifolia* Jack on orientation activities in middle-aged male rats," *Fundamental & Clinical Pharmacology*, vol. 16, no. 6, pp. 479–483, 2002.

[15] H. H. Ang, K. L. Lee, and M. Kiyoshi, "Sexual arousal in sexually sluggish old male rats after oral administration of eurycoma longifolia jack," *Journal of Basic and Clinical Physiology and Pharmacology*, vol. 15, no. 3-4, pp. 303–309, 2004.

[16] S. K. Goswami, P. Manoj Kumar, R. Jamwal, S. Dethe, A. Agarwal, and I. Mohammed Naseeruddin, "Screening for Rho-kinase 2 inhibitory potential of Indian medicinal plants used in management of erectile dysfunction," *Journal of Ethnopharmacology*, vol. 144, no. 3, pp. 483–489, 2012.

[17] F. B. M. Priviero, L.-M. Jin, Z. Ying, C. E. Teixeira, and R. C. Webb, "Up-regulation of the RhoA/Rho-kinase signaling pathway in corpus cavernosum from endothelial nitric-oxide synthase (NOS), but not neuronal NOS, null mice," *The Journal of Pharmacology and Experimental Therapeutics*, vol. 333, no. 1, pp. 184–192, 2010.

[18] J.-H. Zhang, T. D. Y. Chung, and K. R. Oldenburg, "A simple statistical parameter for use in evaluation and validation of high throughput screening assays," *Journal of Biomolecular Screening*, vol. 4, no. 2, pp. 67–73, 1999.

[19] A. P. Somlyo and A. V. Somlyo, "Signal transduction by G-proteins, Rho-kinase and protein phosphatase to smooth muscle and non-muscle myosin II," *The Journal of Physiology*, vol. 522, no. 2, pp. 177–185, 2000.

[20] E.-K. Lim, R. G. Jackson, and D. J. Bowles, "Identification and characterisation of Arabidopsis glycosyltransferases capable of glucosylating coniferyl aldehyde and sinapyl aldehyde," *FEBS Letters*, vol. 579, no. 13, pp. 2802–2806, 2005.

[21] A. Edilu, L. Adane, and D. Woyessa, "In vitro antibacterial activities of compounds isolated from roots of Caylusea abyssinica," *Annals of Clinical Microbiology and Antimicrobials*, vol. 14, no. 1, artilce 15, 2015.

[22] M.-J. Ahn, S.-J. Hur, E.-H. Kim et al., "Scopoletin from Cirsium setidens increases melanin synthesis via CREB phosphorylation in B16F10 cells," *Korean Journal of Physiology & Pharmacology*, vol. 18, no. 4, pp. 307–311, 2014.

[23] K.-L. Chan, C.-Y. Choo, N. R. Abdullah, and Z. Ismail, "Antiplasmodial studies of Eurycoma longifolia Jack using the lactate dehydrogenase assay of Plasmodium falciparum," *Journal of Ethnopharmacology*, vol. 92, no. 2-3, pp. 223–227, 2004.

[24] F. Ebrahimi, B. Ibrahim, C. H. Teh, V. Murugaiyah, and C. K. Lam, "1HNMR-based discriminatory analysis of eurycoma longifolia from different locations and establishing a profile for primary metabolites identification and quassinoids quantification," *Planta Medica*, vol. 83, no. 1-2, pp. 172–182, 2017.

[25] H. H. Chen, T. C. Wang, Y. Lee et al., "Novel Nrf2/ARE activator, trans-Coniferylaldehyde, induces a HO-1-mediated defense mechanism through a dual p38α/MAPKAPK-2 and PK-N3 signaling pathway," *Chemical Research in Toxicology*, vol. 28, no. 9, pp. 1681–1692, 2015.

[26] M. Akram, K.-A. Kim, E.-S. Kim et al., "Selective inhibition of JAK2/STAT1 signaling and iNOS expression mediates the anti-inflammatory effects of coniferyl aldehyde," *Chemico-Biological Interactions*, vol. 256, pp. 102–110, 2016.

[27] K. Chan, M. O'Neill, J. Phillipson, and D. Warhurst, "Plants as sources of antimalarial drugs. part 3. Eurycoma longifolia," *Planta Medica*, vol. 52, no. 02, pp. 105–107, 1986.

[28] S. Park, N. X. Nhiem, P. V. Kiem et al., "Five new quassinoids and cytotoxic constituents from the roots of Eurycoma longifolia," *Bioorganic & Medicinal Chemistry Letters*, vol. 24, no. 16, pp. 3835–3840, 2014.

[29] S. Hajjouli, S. Chateauvieux, M.-H. Teiten et al., "Eurycomanone and eurycomanol from Eurycoma longifolia jack as regulators of signaling pathways involved in proliferation, cell death and inflammation," *Molecules*, vol. 19, no. 9, pp. 14649–14666, 2014.

[30] B.-S. Low, S.-B. Choi, H. Abdul Wahab, P. Kumar Das, and K.-L. Chan, "Eurycomanone, the major quassinoid in Eurycoma longifolia root extract increases spermatogenesis by inhibiting the activity of phosphodiesterase and aromatase in steroidogenesis," *Journal of Ethnopharmacology*, vol. 149, no. 1, pp. 201–207, 2013.

Hindawi
Evidence-Based Complementary and Alternative Medicine
Volume 2019, Article ID 8453635, 13 pages
https://doi.org/10.1155/2019/8453635

Research Article

Morinda Officinalis Polysaccharides Attenuate Varicocele-Induced Spermatogenic Impairment through the Modulation of Angiogenesis and Relative Factors

Zhu Zhu[1,2] **Xiaozhen Zhao**[1,3] **Feng Huang**[1] **Feng Wang**[1] **and Wei Wang**[1,4]

[1]*Department of Human Anatomy and Histo-Embryology, School of Basic Medical Sciences, Fujian Medical University, Fuzhou 350122, China*
[2]*Department of Pathology, Mengchao Hepatobiliary Hospital of Fujian Medical University, Fuzhou, Fujian, China*
[3]*Key Laboratory of Brain Aging and Neurodegenerative Diseases of Fujian Provincial Universities and Colleges, Fuzhou 350122, China*
[4]*Research Center for Neurobiology, School of Basic Medical Sciences, Fujian Medical University, Fuzhou 350122, China*

Correspondence should be addressed to Feng Wang; fjwf95168@163.com and Wei Wang; wwfjmu@163.com

Received 30 January 2019; Accepted 28 March 2019; Published 11 April 2019

Guest Editor: Wellerson Scarano

Evidence supporting best treatment practices for varicocele is lacking. The effects of a water-soluble polysaccharide extracted from *Morinda officinalis* (MOP) on the progression of varicocele were evaluated in the present study. The extracted MOP was confirmed as having a high purity of 98% with scant protein contamination, and it mainly consisted of glucose, lactose, and xylose at a molar ratio of 7.63:1.23:0.95 glucose:lactose:xylose. MOPs were administered to experimental left varicocele rats immediately after surgery at doses ranging from 25 to 200 mg/kg. As detected by sperm analysis and histopathological staining, the intragastric administration of 100 mg/kg MOPs significantly improved the sperm parameters of bilateral cauda epididymis, attenuated seminiferous epithelial structures, and inhibited germ cell apoptosis. The results of immunofluorescence and immunoblot showed that administration of 100 mg/kg MOPs effectively inhibited angiogenesis in the bilateral testes but modulated the expression of vascular endothelial growth factor (VEGF), matrix metalloproteinase 2 (MMP2), and MMP9 mildly. These results indicate that inhibition of angiogenesis may be one of the mechanisms by which MOP exerts its inhibitive activities on the progression of varicocele, whereas a relative upregulation of VEGF and MMP-9 may be crucial for the spermatogenetic protective effects of 100 mg/kg MOP administration.

1. Introduction

Male infertility has been a global social concern because male pathogeny of infertility accounts for approximately 50% of infertility in couples. Varicocele, defined as the dilation and tortuosity of the pampiniform venous plexus in the spermatic cord, is the predominant cause of male infertility due to its prevalence of 45-81% in secondary male infertility and 19-41% in primary male infertility [1]. Varicocele is widely regarded as being responsible for gonadotropin attenuation and spermatogenesis impairment [2]. Dilated and thickened walls of internal spermatic veins, the typical characteristics of varicocele, lead to increased blood stasis and venous volume pressure. Varicocele repair (varicocelectomy) is the common clinical therapy offered to symptomatic or infertile varicocele patients [3–5], and it effectively improves sperm quality while reducing testicle hypoxia and angiogenesis, which are important and adaptive pathophysiological events reported in varicocele patients and in an experimental rat model of varicocele in venous diseases [6, 7]. However, certain defects of varicocelectomy, such as high recurrence rates (7-35%) and controversial effects on pregnancy, make the applications of surgical repair questionable in the era of assisted reproduction [4, 8, 9]. Additionally, the American Society for Reproductive Medicine (ASRM) guidelines recommend against the surgical correcting of subclinical varicocele, which has a prevalence of 55-70% in infertile men [10, 11]. Evidence supporting best treatment practices for varicocele is lacking, and there is an especially low level of evidence to support radiological or surgical intervention

for varicoceles in children and adolescents [12]. Thus, the development of effective medicine to prevent the progression of varicocele is urgently needed.

Morinda officinalis (*M. officinalis*), of the family Rubiaceae, is a vine that has been widely cultivated in southeastern China for more than 2,000 years and whose roots are frequently added to local soups as a nutrient supplement. The dried roots of *M. officinalis* have long been considered as aphrodisiac tonics for young males, and they have been used in 103 Chinese traditional medicine preparations for the treatment of many diseases, such as impotence, menstrual disorders, depression, osteoporosis, and inflammation [13–16]. *M. officinalis* contains carbohydrate constituents, iridoid lactone, anthraquinone, iridoid glucoside, and other compounds [17]. Previous studies have reported that the aqueous extract from *M. officinalis* could significantly increase the sperm count and number of seminiferous cells in rats with impaired reproduction [18, 19]. Water-soluble polysaccharides of MO (MOPs), one of the main bioactive components in this aqueous extract, account for 7-21% of the dry weight of *M. officinalis*, and they have been previously reported to increase the number of seminiferous cells and promote hypothalamic GnRH secretion in varicocele-induced reproductive disorder [20, 21]. However, MOPs are effective in attenuating the sperm count and testicle morphology at a wide range of doses according to the previous studies (50-300 mg/kg body weight), but the optimal effective dose and the definite mechanisms involved in spermatogenic epithelium repair are still unclear.

In the present study, crude MOPs extracted via water extraction and alcohol precipitation were administered to experimental left varicocele (ELV) rats to investigate the effects on varicocele-induced testicular angiogenesis. The results are conducive to assess the optimal dosages and identify the mechanisms of MOPs in varicocele progression.

2. Materials and Methods

2.1. Extraction, Purification, and Analysis of MOPs. *M. officinalis* dried roots purchased from Fuzhou herb market (Fujian, China) were used to extract water-soluble MOPs by the water extraction and alcohol precipitation method. The crude MOPs were deproteinized by using Sevag reagent [20].

The phenol-sulfuric acid colorimetric method, using glucose as a standard, was used to determine the total carbohydrate content of MOPs [22]. The Bradford method, using bovine serum as a standard, was used to quantify the protein content [23]. The ultraviolet-visible (UV) spectra of the samples were recorded using a UV-2102PC spectrophotometer (UNICO, Shanghai), and the IR spectrum was recorded with a Spectrum 65 FT-IR spectrometer (PerkinElmer, Waltham) in the range of 400-4000 cm^{-1}. The homogeneity and molecular weight of the MOPs were evaluated by high-performance gel permeation chromatography (HPGPC) using a dextran standard to calibrate the column and establish a standard curve. After the MOPs were hydrolyzed with trifluoroacetic acid (TFA), the product was analyzed using an Agilent 1260 liquid chromatograph (Agilent Technologies, Santa Clara) with an Alltech 2000 evaporative light scattering detector.

2.2. Animals, ELV Model Establishment, and Groups. Seventy mature male Sprague-Dawley rats (6 weeks old, 200 ± 20 g) purchased from the Laboratory Animal Center of Fujian Medical University (No. SCXK(Min)2012-0001) were maintained five to a cage at 22°C on a 12-h light/dark cycle. All animal experiments and procedures were approved and supervised by the local ethics committee (No. 2015-29) and conducted in compliance with the National Research Council's guidelines.

Rats were randomly divided into the following seven groups (n=10 per group): sham-operated group (SO group), ELV group, double-distilled water group (ddH_2O group), and four MOP-treated groups that were treated with MOP at doses of 25 mg/kg, 50 mg/kg, 100 mg/kg, and 200 mg/kg (M25, M50, M100, and M200 groups, respectively). An ELV rat model was established by partially ligating the left renal vein as previously described [24]. MOPs were dissolved in ddH2O to formulate into solutions with concentrations of 12.5 mg/ml, 25 mg/ml, 50 mg/ml, and 100 mg/ml, which were intragastrically administered to rats in group M25, M50, M100, and M200. The animals were subjected to 6-week medication after reviving from analepsia. The experimental animals were intragastrically administered at 8 am every day, with the dose calculated on the rats' weight of the day. Rats in ddH2O group were intragastrically administrated 2 ml/kg ddH2O instead. After gavage administrated each morning, the rats were sent to metabolic cages (3M12B440, Tecniplast, Varese, Italy) one per cage to collect 24-hour urine samples and stool samples. An animal was excluded if 24-hour urine or stool abnormally reduced during medication. An animal was included in the study only if renal atrophy did not occur.

2.3. Sperm Analysis. Sperm suspensions from the bilateral cauda epididymis were stained and analyzed following a method previously described [21]. The sperm count and percentage of rats with sperm morphologic abnormalities were individually observed and recorded by two researchers [25].

2.4. Histopathological Staining and Apoptosis Tests. Bilateral testicular tissue samples were harvested, fixed, dehydrated, and made into frozen sections (20 μm) using a cryostat (CM 1950, Leica). Sections were stained with hematoxylin and eosin (H&E) and imaged with an inverted light microscope (Ti-s, Nikon). The Johnsen score (JS) was used to grade testicular injury and spermatogenesis [26]. Seminiferous tubules and interstitial tissue in 10 sections of each specimen were observed, and 5 areas in each section were observed by ×100 magnification to count the number of vessels. The mean number of vessels was recorded as the microvessel density (MVD) of each specimen to evaluate the degree of angiogenesis. Only vessels with a clearly defined lumen or well-defined linear vessel shape were counted as microvessels. Newly formed vessels with only one layer of endothelial cells were excluded.

The *in situ* terminal deoxynucleotidyl transferase-mediated dUTP nick-end labeling (TUNEL) assay was used to detect the apoptosis cells in the seminiferous tubule (*in situ* apoptosis detection kit, ab206386, Abcam). The negative

control sections were incubated with dH_2O instead of TdT labeling reaction mix. Apoptotic germ cells were quantified by counting the number of TUNEL-stained nuclei per seminiferous tubular cross section. Cross sections of 100 tubules per specimen were assessed, and the mean number of apoptotic nuclei per cross section (apoptotic index, AI) was calculated.

2.5. Determination of the Expression of Angiogenesis-Related Factors. Frozen sections (20 μm) of bilateral testicular samples were rewarmed, rehydrated, blocked with 10% donkey serum, and incubated with primary antibodies, including antibodies against CD34 (dilution 1:1000, ab81289, Abcam), caspase-3 (dilution 1:100, sc-1225, Santa Cruz), vascular endothelial growth factor (VEGF, dilution 1:500, AB1316, Abcam), p-AKT (dilution 1:1500, #13038, Cell Signaling Technology, Inc.), matrix metalloproteinase 2 (MMP2, dilution 1:250, ab92536, Abcam), and MMP9 (dilution 1:500, ab58803, Abcam), at 4°C for 24 h. The controls were incubated with 10% donkey serum but not primary antibodies. The sections were then incubated with secondary antibodies, including Alexa 488-conjugated donkey anti-goat IgG (A-11055, Invitrogen), and Alexa 555-conjugated donkey anti-rabbit IgG (A-31572, Invitrogen). After the nuclei were dyed by DAPI (62247, Thermo Fisher Scientific Inc.), the sections were imaged and analyzed with a laser scanning confocal microscope (SP8, Leica Microsystems, Inc.).

Bilateral testicle samples were homogenized in RIPA buffer (R0278, Sigma-Aldrich). A total of 30 μg of protein was loaded onto gels and subjected to 12% SDS-PAGE. After the proteins were transferred to membranes, primary antibodies targeting VEGF (dilution 1:1000), p-AKT (dilution 1:2000), AKT (dilution 1:2000, #2920, Cell Signaling Technology, Inc.), MMP2 (dilution 1:1000), MMP9 (dilution 1:1000), and GAPDH (ab 8245, Abcam) were used to detect the protein expressions. After the samples were incubated with horseradish peroxidase-conjugated secondary antibodies (ab6721, ab6789, ab6885, Abcam), the bands were visualized with ECL Western blotting substrate (ab65623, Abcam), and the relative integrated intensities of the bands were expressed as the integrated intensity divided by the intensity of GAPDH.

2.6. Statistical Analysis. Image-Pro Plus 6.0 (Media Cybernetics, Inc.) was used to analyze the immunofluorescence and immunoblot pictures, and SPSS 20.0 (IBM) was used to conduct statistical analysis. After tested by the one-sample Kolmogorov-Smirnov test, normally distributed continuous data were expressed as the mean ± standard deviation (SD). Statistical differences were analyzed using one-way analysis of variance (ANOVA), then the least significant difference test was performed to identify differences between two groups. $P<0.05$ was considered statistically significant.

3. Results

3.1. Physicochemical and Structural Characterization of MOP. No characteristic absorption peaks for either proteins or nucleic acids were detected at 280 and 260 nm on the UV spectra (Figure 1(a)). The total carbohydrate content of MOP was 97%, as determined by the phenol-sulfuric acid method. The IR spectrum of MOP showed several absorption peaks related to polysaccharide moieties at 3410, 2890, 1670, 1409, 1258, 1080, 890, 837, and 785 cm^{-1} (Figure 1(b)). There was one single and symmetrical peak on the HPGPC profile of MOP, indicating that the MOP was a homogeneous polysaccharide with a weighted average molecular weight of 1141, a raw average molecular weight of 1648, and a polydispersity of 1.444 (Figure 1(c)). Additionally, MOP comprised six types of monosaccharides: glucose, lactose, xylose, maltose, fructose, and sucrose, and the molar ratio for these was 7.63, 1.23, 0.95, 0.87, 0.72, and 0.64, respectively, which indicated that glucose was the predominant monosaccharide in MOP.

3.2. The Effects of MOP on Sexual Performance and Sperm Morphology. Compared to the SO group, the sperm count of bilateral cauda epididymis were significantly decreased in the ELV and ddH_2O groups ($P<0.05$); furthermore, these groups also had higher bilateral percentages of abnormal sperm ($P<0.05$) (Table 1). Compared to the ELV group, the sperm counts of the M50 and M100 groups were increased, and the percentages of abnormal sperm were decreased ($P<0.05$). Additionally, sperm in bilateral cauda epididymis of the M200 group showed an elevated percentage of abnormality, as well as numerous cell debris and fragments, although the bilateral sperm count of the M200 group was significant increased compared to that of the ELV group ($P<0.05$).

3.3. The Effects of MOP on Testicular Morphology, Apoptosis, and Angiogenesis. Compared to normal testicular histology and spermatogenesis, the ipsilateral seminiferous tubules of the ELV and ddH_2O groups showed severe damage, such as the absence of spermatogenic cells and impaired interstitial tissue, and the contralateral seminiferous tubules also showed disordered germinal cell arrangement and increased cellular debris in the lumen. The bilateral spermatocyte count increased after MOP treatment and was accompanied with reduced cell loss, increased degree of ordered cell arrangement and more sperm in the lumen. However, despite the presence of spermatocyte edema and disordered germinal cell arrangement in several seminiferous tubules, the bilateral testicular tissues from rats in the M100 group showed a well-preserved testicular histology (Figure 2(a)).

As shown in Figure 2(c), the JS of bilateral testis in the ELV and ddH_2O groups was significantly decreased compared to the SO group ($P<0.05$). The JS of bilateral testis in the MOP-treated groups was significantly increased compared to that of the ELV group ($P<0.05$). The JS of bilateral testis in the M50 group was significantly increased compared to that in the M25 group ($P<0.05$), and the JS of bilateral testis in the M100 group was significantly increased compared to that in the M50 group ($P<0.05$). Compared to that in the SO group, the JS of ipsilateral testis in the M200 group showed no significant difference, while the JS of contralateral testis was significantly decreased ($P<0.05$).

The MVD of bilateral testis in the ELV and ddH_2O groups was significantly increased compared to that of the SO group (Figure 2(d), $P<0.05$), while the MVD of bilateral testis in the

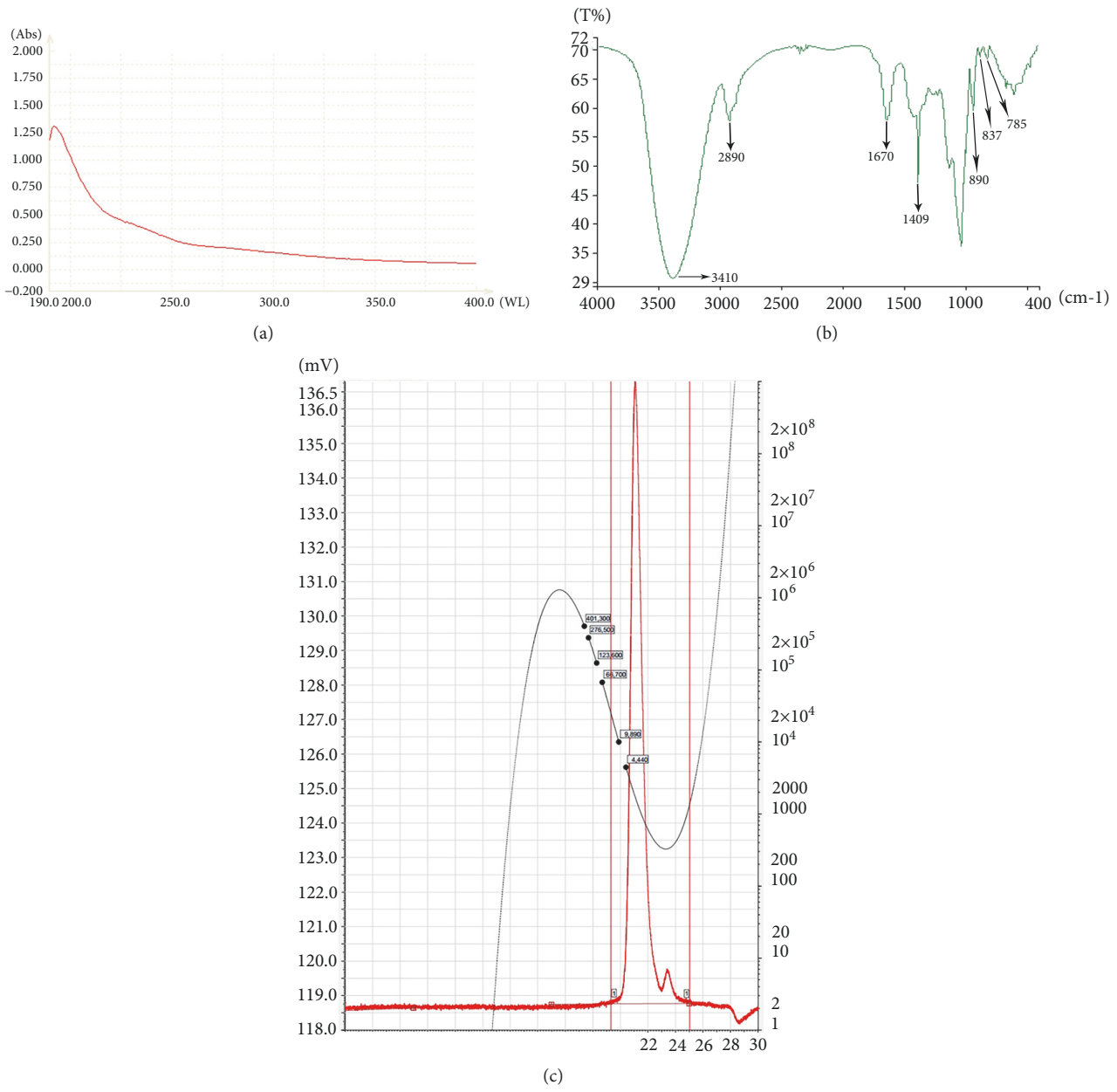

FIGURE 1: *UV and FT-IR spectra and HPGPC profile of MOP.* (a) UV spectra. (b) FT-IR spectra. (c) A dextran standard with different molecular weights was used to establish a standard curve (black curve). There was one single and symmetrical peak on the HPGPC profile of MOP (red curve).

MOP-treated groups was significantly decreased compared to that in the ELV group ($P<0.05$). The MVD of bilateral testis was lowest in the MOP100 group among all the MOP-treated groups ($P<0.05$).

As detected by TUNEL staining, several apoptotic cells, including spermatogonial cells and Sertoli cells, were observed in the bilateral seminiferous tubules of the SO group (Figure 2(b)). For the severe damage of lumen cells, it was difficult to calculate apoptotic spermatogenic cells in the ipsilateral testis of the ELV group and ddH_2O group, and the AI of these groups were marked as ∞. The AI of contralateral testis in ELV group and ddH_2O group was significantly increased compared to that in the SO group (Table 1, $P<0.05$). The AI of contralateral testis in the MOP-treated groups was significantly decreased compared to that in the ELV group ($P<0.05$). Among all the MOP-treated groups, the bilateral AI in M100 group was lowest, and the bilateral AI in the M200 group was the highest ($P<0.05$, Table 1).

The caspase-3-immunofluorescence-stained sections of the ELV group and ddH_2O group showed that positive caspase-3 reactions were found in the nuclei and cytoplasm of spermatogenic cells and basement membrane of seminiferous tubules in both the endothelium and adventitial of vessels and cells in the interstitial spaces, as shown in Figure 3(a).

Table 1: Sperm parameters and testes apoptosis value of the experimental groups.

	sperm count		abnormal sperm (%)		Testes apoptosis (AI)	
	ipsilateral	contralateral	ipsilateral	contralateral	ipsilateral	contralateral
SO group	196.38±13.64	199.25±9.12	9.83±0.67	9.66±0.84	1.19±0.22	1.18±0.31
ELV group	96.21±9.11[a]	128.63±12.15[a]	53.37±7.89[a]	46.62±6.21[a]	∞[a]	12.87±2.92[a]
ddH_2O group	98.73±8.99[a]	126.31±9.34 [a]	51.21±6.36[a]	47.73±7.47[a]	∞[a]	13.36±4.18[a]
M25 group	121.37±14.41[a]	141.63±8.14 [a]	42.24±3.83[a]	36.63±4.12[a]	7.27±2.18[ab]	7.66±2.38[ab]
M50 group	168.71±11.24[b]	187.71±13.36[b]	21.23±2.47[ab]	16.62±1.34[ab]	5.15±1.18 [ab]	5.28±1.23[ab]
M100 group	183.43±18.21[b]	194.47±9.22[b]	10.29±0.87[b]	10.08±0.77[b]	3.31±1.12	2.54±1.01[b]
M200 group	162.38±16.88[ab]	183.88±12.37[ab]	48.61±4.29[a]	52.27±5.53[a]	8.36±2.24[ab]	7.87±1.67[ab]

[a] $P<0.05$ compared to the SO group.
[b] $P<0.05$ compared to the ELV group.

Compared to those in the ELV group, the fluorescence intensities of caspase-3 in the bilateral testis of the M25, M50, and M100 groups were significantly decreased ($P<0.05$), while the fluorescence intensities of caspase-3 in the bilateral testis of the M200 group were significantly increased ($P<0.05$). Positive caspase-3 reactions were observed in the nuclei and cytoplasm of spermatogenic cells but not in the vessels and cells in the interstitial spaces in the M100 group, and the M100 group showed the lowest expression of caspase-3 in the bilateral testes among all experimental groups ($P<0.05$).

3.4. The Effects of MOP on Angiogenesis-Related Factors. In the ipsilateral testis from the ELV group, immunofluorescence imaging indicated that CD34 immunoreactivity was mainly shown in the basement membrane of seminiferous tubules and adventitial of vessels in the interstitial spaces, and weak immunoreactivity of CD34 was also found in several spermatogenic cells (Figure 3(a)). The contralateral testes of the ELV group showed a similar result. No obvious CD34 immunoreactivity was observed in bilateral testes sections of the SO group. The fluorescence intensities of CD34 in the MOP-treated groups significantly decreased compared to those in the ELV group ($P<0.05$), and the fluorescence intensities of CD34 in the M100 group were the lowest among those of the four MOP-treated groups ($P<0.05$).

VEGF immunoreactivity was mainly shown in the seminiferous tubules of several Sertoli cells and in the interstitial spaces of Leydig cells for the bilateral testes from the SO group, whereas VEGF immunoreactivity was also shown in the nuclei of spermatogenic cells and vessels of bilateral testis of the ELV group (Figure 4(a)). Compared to those of the ELV group, the fluorescence intensities of VEGF in the M25, M50, and M200 groups were significantly decreased ($P<0.05$), while no significant difference was shown in the M100 group. For the colocalization of p-AKT and VEGF in testes shown by immunofluorescence, p-AKT immunoreactivity in the bilateral testes of the experimental groups showed similar expression characteristics and trends as those of VEGF.

MMP-2 and MMP-9 immunoreactivity was mainly shown in the nuclei and cytoplasm of spermatogenic cells, Sertoli cells, and Leydig cells, as well as in the vessels of interstitial spaces. Compared to that of the SO group, the fluorescence intensities of MMP-2 and MMP-9 in the ELV group and M100 group showed no significant differences, while the fluorescence intensities of MMP-2 and MMP-9 in the M25, M50, and M200 groups were significantly decreased (Figure 5, $P<0.05$).

The Western blot results showed that, compared to the those in the SO group, the relative intensities of VEGF and the relative ratio of phospho-AKT to the total counterpart were significantly increased in the ELV and ddH_2O groups compared to the other groups (Figure 6, $P<0.05$). However, the levels of these proteins were significantly decreased in the M50 and M100 groups ($P<0.05$) compared to in the ELV group. The expression of contralateral MMP2 in the ELV group was significantly increased compared to that in the SO group ($P<0.05$), and 100 mg/kg MOP treatment significantly increased both ipsilateral and contralateral MMP2 more than those in the ELV group ($P<0.05$). Both the ipsilateral and contralateral MMP9 of the ELV group were increased compared to those of the SO group ($P<0.05$). MOP treatment significantly decreased contralateral MMP9 compared to ELV ($P<0.05$), while both the ipsilateral and contralateral expression of MMP9 in M100 group were highest among the MOP-treated groups ($P<0.05$).

4. Discussion

In this study, a classic experimental varicocele rat model was established, and MOP treatment immediately after surgery was performed, which aimed to illustrate the effects of MOP on the progression of varicocele. The results showed that 100 mg/kg MOP treatment significantly attenuated injury to the seminiferous epithelium and decreased germ cell apoptosis. It is notable that 100 mg/kg MOP showed excellent inhibitive effects on angiogenesis but mild inhibition on some crucial angiogenesis-related factors, such as VEGF, MMP2, and MMP9. Effective angiogenesis inhibition without excessive inhibition of VEGF and MMPs may be one of the major mechanisms and advantages of MOP administered at an early stage of varicocele.

Apoptosis, which occurs during normal spermatogenesis, has a critical regulatory role in spermatogenesis. Increased apoptosis of germ cells has been reported in specimens of male patients with varicocele and in samples from rats with varicocele in the rat model [27, 28]. As detected by TUNEL staining and as evaluated by AI in this study, bilateral testicular apoptosis levels in the ELV group were

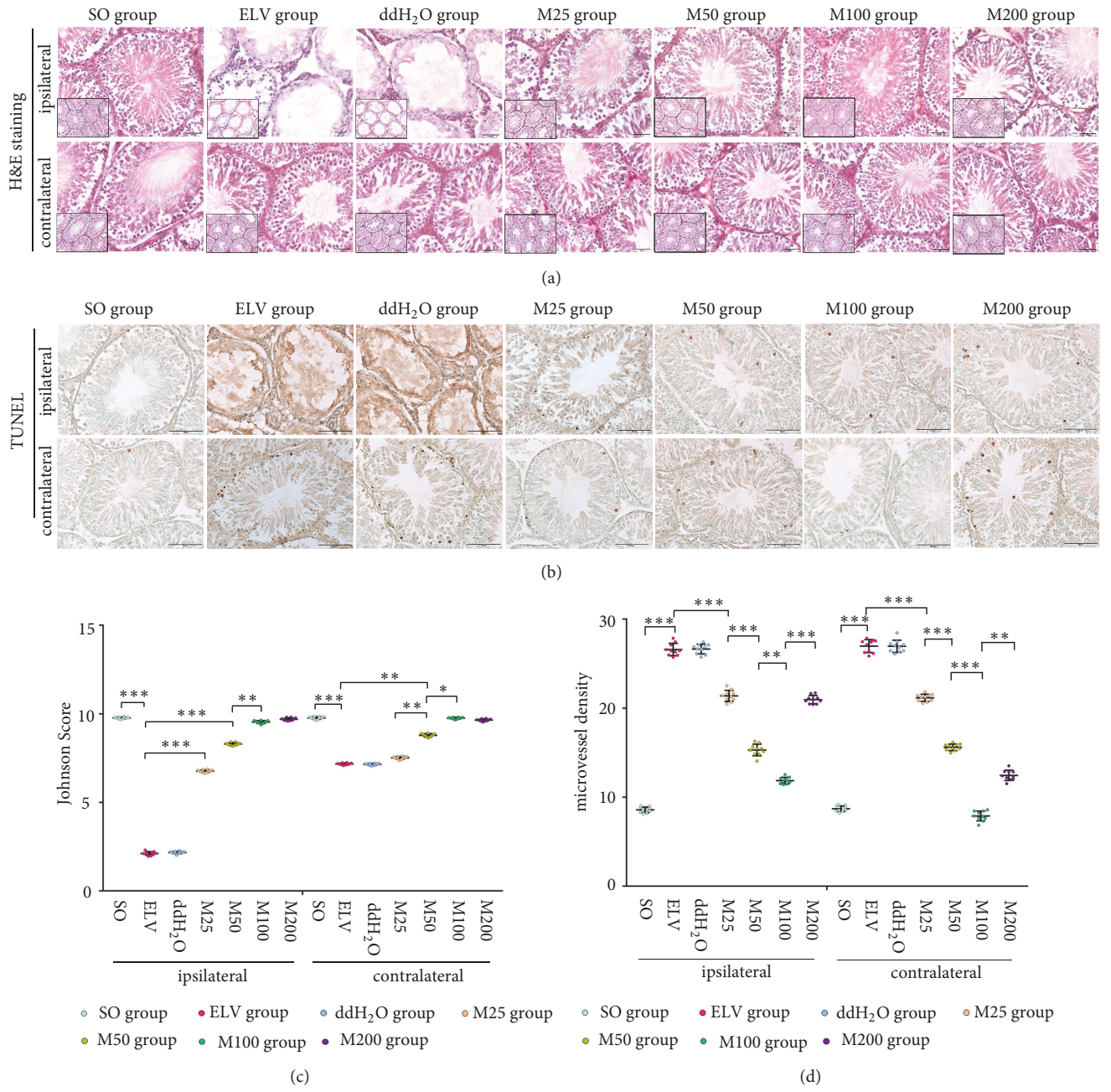

Figure 2: Histopathological staining and apoptosis test results of the experimental groups. (a) H&E staining. (b) TUNEL staining. (c) Johnson scores of bilateral testes. (d) Microvessel density of bilateral testes. ∗: $P<0.05$; ∗∗: $P<0.01$; ∗ ∗ ∗: $P<0.001$.

increased by more than 5 times compared to those in the SO group, which indicated the varicocele rat model was successfully established in this study. MOP, at the dose of 25-100 mg/kg, attenuated bilateral germ cell apoptosis in a dose-dependent manner. Immunofluorescence and immunoblotting of caspase-3, which is the major executioner protease within the apoptotic cascade, showed similar differences among experimental groups on TUNEL staining, which indicated 100 mg/kg was the optimal dose of intragastric-administered MOP to attenuate bilateral testicular apoptosis.

Angiogenesis that refers the growth of new vessels has been reported as a visible response to hypoxia caused by varicocele, which decreases the apoptosis of vascular cells and attributes to dilated and thickened walls of vessels [6]. Angiogenesis, for the progression of varicocele, is a double-edged sword in the progression of varicocele: angiogenesis attenuates increased blood stasis and venous pressure in varicocele, whereas angiogenesis may aggravate the venous volume in ipsilateral testes and slow blood reflux. Although angiogenesis has been generally reported in varicocele, current studies about the effects of angiogenesis on the progression of varicocele are still inconsistent. Polydeoxyribonucleotide has been reported to inhibit the histologic changes in rat experimental varicocele through improving

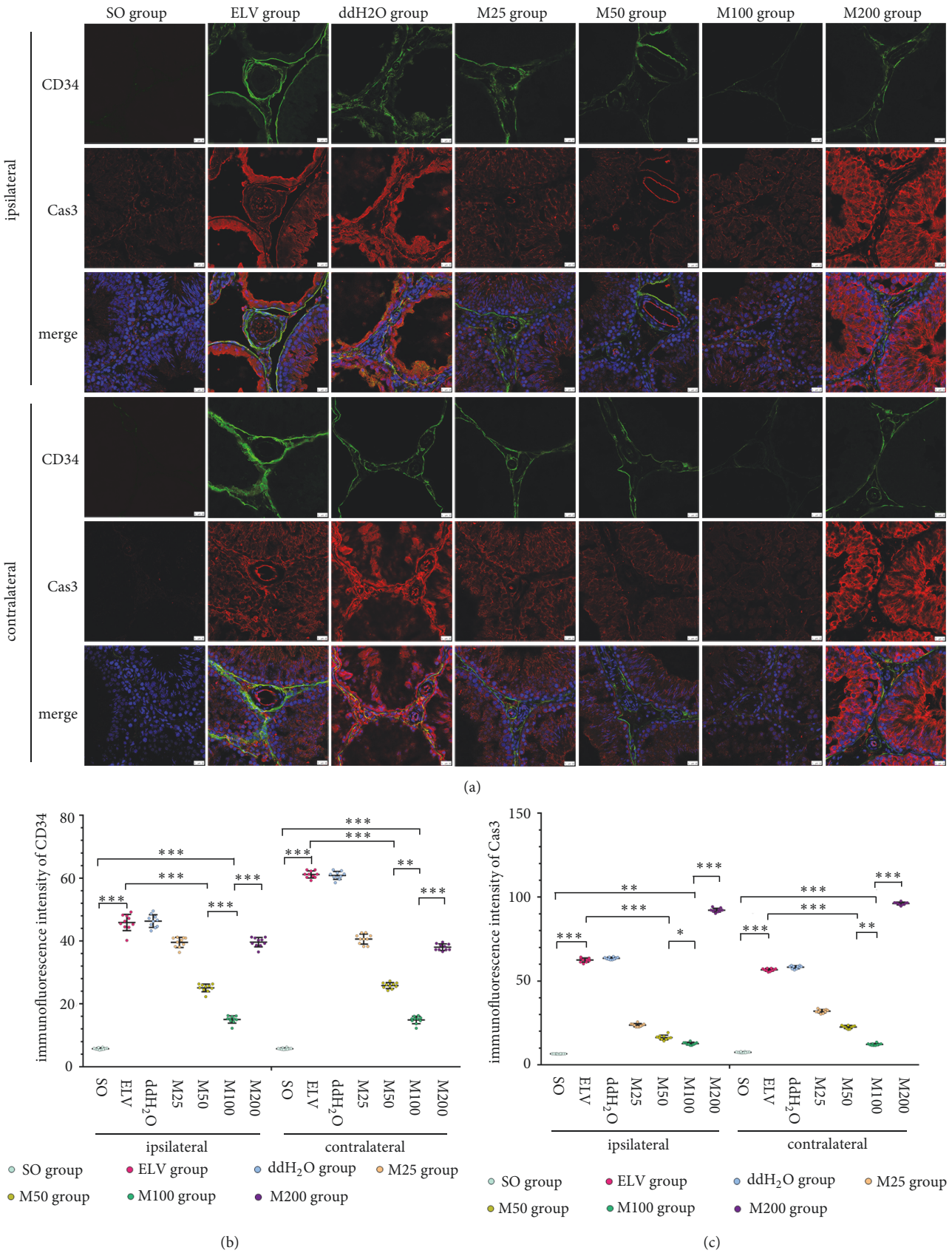

Figure 3: Effects of MOPs on expression of CD34 and Cas3 in bilateral testes. (a) Immunofluorescence of CD34 and Cas3 in bilateral testes. Green: CD34. Red: Cas3. Blue: nucleus. (b) Immunofluorescence intensities of bilateral CD34. (c) Immunofluorescence intensities of bilateral Cas3. ∗: $P<0.05$; ∗∗: $P<0.01$; ∗ ∗ ∗: $P<0.001$.

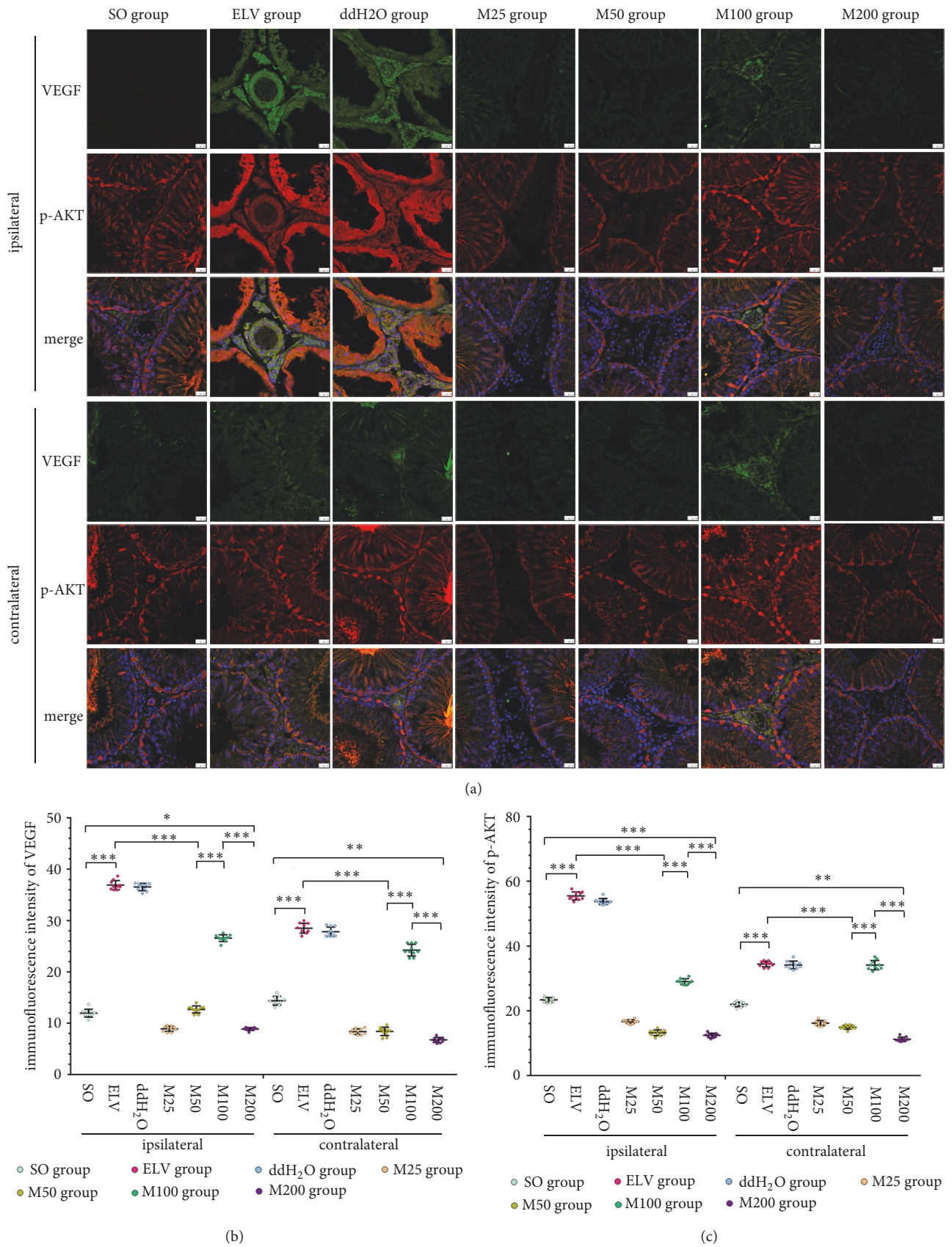

Figure 4: Effects of MOPs on expression of VEGF and p-AKT in bilateral testes. (a) Immunofluorescence of VEGF and p-AKT in bilateral testes. Green: VEGF. Red: p-AKT. Blue: nucleus. (b) Immunofluorescence intensities of bilateral VEGF. (c) Immunofluorescence intensities of bilateral p-AKT. ∗: $P<0.05$; ∗∗: $P<0.01$; ∗ ∗ ∗: $P<0.001$.

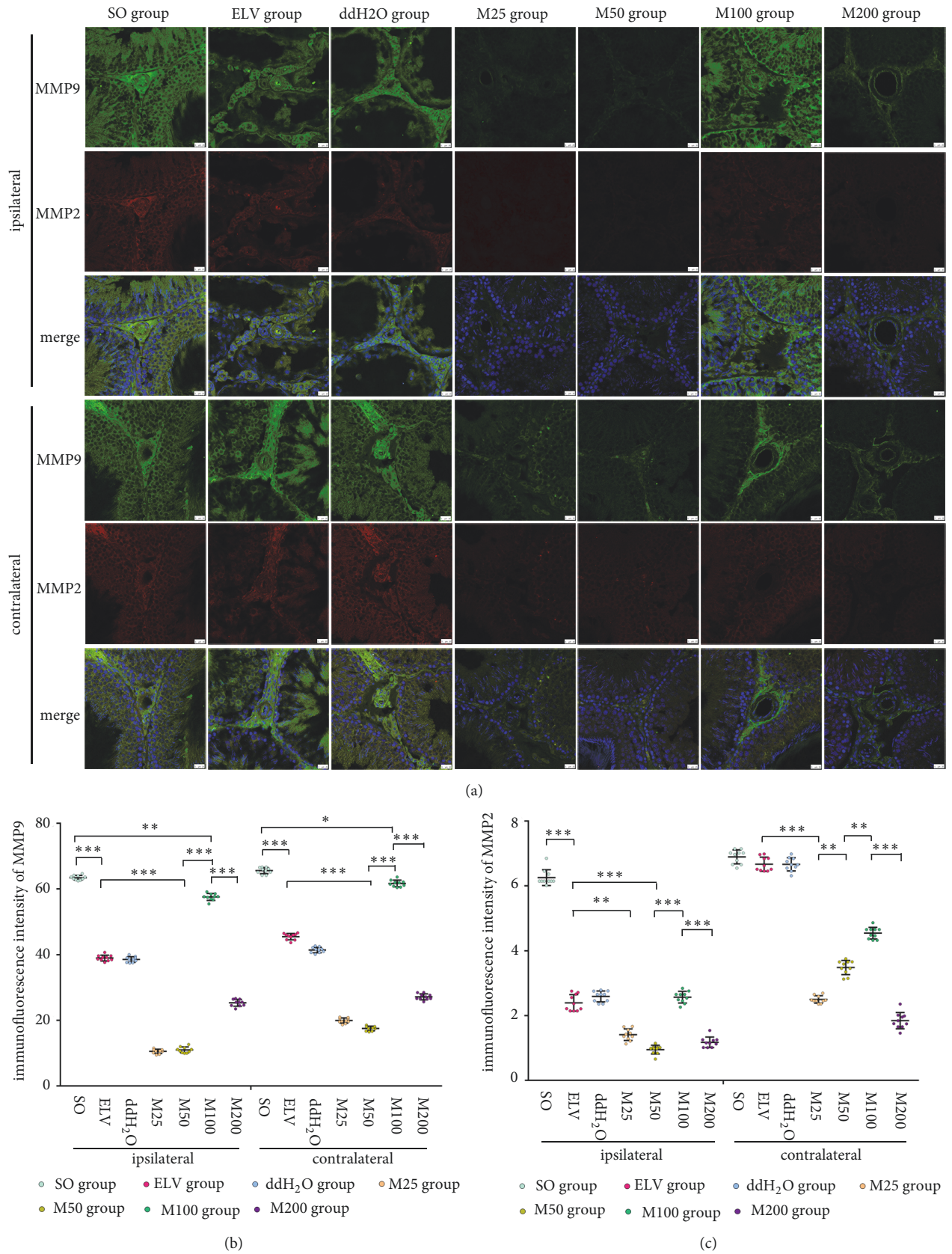

Figure 5: Effects of MOPs on expression of MMP2 and MMP9 in bilateral testes. (a) Immunofluorescence of MMP2 and MMP9 in bilateral testes. Green: MMP9. Red: MMP2. Blue: nucleus. (b) Immunofluorescence intensities of bilateral MMP9. (c) Immunofluorescence intensities of bilateral MMP2. ∗: $P<0.05$; ∗∗: $P<0.01$; ∗ ∗ ∗: $P<0.001$.

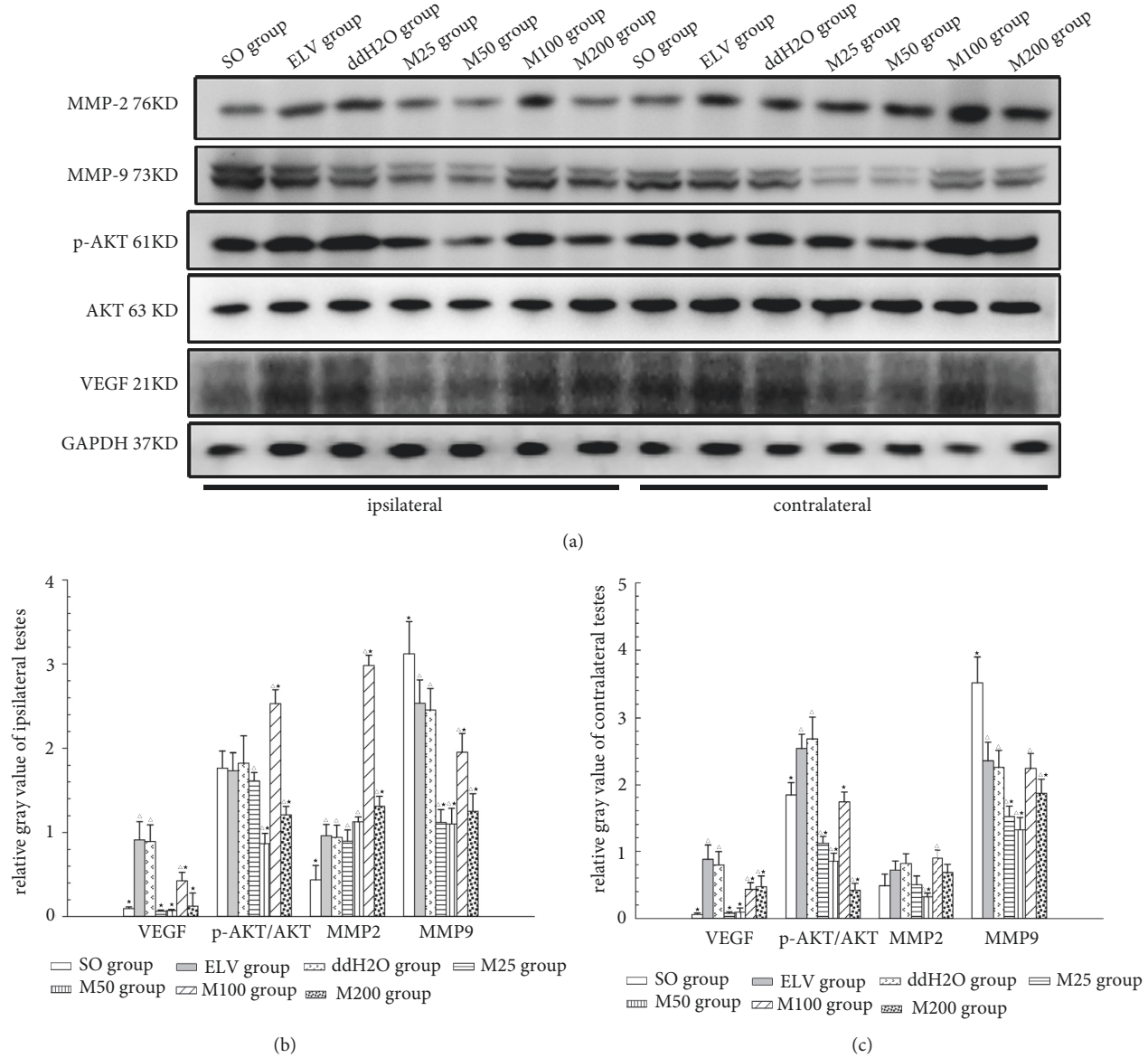

Figure 6: Effects of MOPs on the expression of MMP2 and MMP9 in bilateral testes. (a) Immunofluorescence of MMP2 and MMP9 in bilateral testes. Green: MMP9. Red: MMP2. Blue: nucleus. (b) Immunofluorescence intensities of bilateral MMP9. (c) Immunofluorescence intensities of bilateral MMP2. ∗: $P<0.05$; ∗∗: $P<0.01$; ∗ ∗ ∗: $P<0.001$.

intratesticular VEGF production and vascularization [29]. However, some studies have found that both varicocelectomy and spironolactone administration attenuated spermatogenesis by protecting the tissue from angiogenesis [5, 30]. This study used the microvessel intensity and the expression of CD34 to evaluate angiogenesis, and the results showed 100 mg/kg MOP, which was the most effective dosage in attenuating the bilateral histology of seminiferous epithelium, showed the most significant inhibition of bilateral angiogenesis. Additionally, 25–100 mg/kg MOP showed significant antiangiogenic effects with a dosage-effect relationship, which seems to indicate that MOP attenuates bilateral testicular injury through antiangiogenic effects, while the changes of angiogenesis relative factors were not such consistent with the results of angiogenesis.

VEGF, a specific mitogen of vascular endothelial cells and an angiogenic peptide, has been found to be increased in testicular endothelial cells in varicocele patients and in the germ cell cytoplasm in experimental varicocele rats [31]. In this study, increases of VEGF expression were also detected in germ cells and vessel endothelium. VEGF plays different roles in different cells in the testes: VEGF inhibits the spermatogonial proliferation and spermatogenesis but promotes proliferation and testosterone release of Leydig cells [32, 33]. Administration of 100 mg/kg MOP did not inhibit the contralateral expression of VEGF in the seminiferous tubules, and VEGF expressed in Leydig cells of interstitial tissues increased by more than 10 times. Different from other antiangiogenic drugs or other dosages of MOP, 100 mg/kg MOP showed excellent inhibition of angiogenesis

but a specific upregulation on VEGF in the Leydig cells. Phospho-AKT is a crucial downstream protein kinase of VEGF, and its activation has been reported stimulating the expression of both VEGF and MMP-9 [34]. 100 mg/kg MOP administration did not change the expression of phospho-AKT, no matter whether it was in germ cells or in interstitial tissues.

MMPs, the main mediators of extracellular matrix degradation, are involved in pathological processes of connective tissue disease, such as inguinal hernia and chronic venous disorders. MMP-2 and MMP-9 have been found in the interstitium and seminiferous tubules [35], while the changes in MMPs in varicocele are controversial: decreased MMP-2 and MMP-9 levels have been reported in experimental varicocele, while a higher expression of MMP-9 has been reported in varicocele patients. The MMP-9 positive cell ratio did not significantly change in bilateral testes, for both the germ cells and the cells in the interstitium. MOP administration, except the dose of 100 mg/kg, significantly decreased the expression of MMP-9, whereas 100 mg/kg MOP administration significantly increased the MMP-9 level in ipsilateral seminiferous tubule but decreased the ipsilateral interstitium MMP-9 level. The contralateral MMP-9 expression in germ cells and interstitium also has been inhibited. MMP-9 has been reported to serve as the common thread in various diseases in which excessive MMP-9 induces a progressive disorder of collagen metabolism [36]. We speculate that MMP-9 is necessary for the stability of the interstitium, lower expression causes accumulation and widening of the interstitium, and higher expression leads to injury to and loosening of the interstitium. The inconsistencies of the effects of 100 mg/kg MOP on bilateral seminiferous tubules suggest that MMP-9 exerts different effects under different blood stasis conditions. In addition, the effects of MOP on the expression of MMP-2 seem inconsistent with that of MMP-9, which may suggest the different role of these two MMPs in spermatogenesis and interstitium stability.

It is notable that, after one-week intragastric administration of 100 mg/kg MOPs, the faecal output of rats with experimental varicocele increased by 60% compared with that of the ELV group, and the weight gain was 50% lower than that of the ELV group. However, after 2-6 weeks of intragastric administration of 100 mg/kg MOPs, the faecal output and weight gain of rats showed no significant difference with that of the experimental varicocele rats. The above results suggested that MOPs may produce side effects of enhancing gastrointestinal motility and increasing faecal excretion at preliminary stage of administration, lasting for about one week. For MOP with a no observed adverse effect levels value of 100 mg/kg in rats, the human equivalent dose can be estimated by a conversion based on body weight and body surface, which will be 16.2 mg/kg. Thus, the daily dose of MOP for a 60-kg human is about 972 mg. As previous reports, the polysaccharides account for 10-20% of the total weight in *M. Officinalis*, which means the dose of 100 mg/kg MOP is similar to treatment dosage of 4.86–9.72 g *M. Officinalis* which is closed to the treatment dosage 5-10 g in Chinese traditional medicine.

It is worth mentioning that 200 mg/kg MOP significantly increased the apoptosis level of germ cells in contralateral testes detected by TUNEL and caspase-3, and excessive apoptosis may be the reason of high percentage of abnormal sperm in epididymis. The effects of 200 mg/kg MOP administration on inhibition of angiogenesis and upregulation of VEGF and MMP-9 seem equal to 50 mg/kg MOP administration, which reversely validates the effects on angiogenesis and relative factors may be one of the mechanisms of reproductive repair effects of 100 mg/kg MOP.

In this study, the administration period was restricted to 6 weeks to evaluate the apoptosis and angiogenesis in bilateral testes. The observation period was shorter to obtain the long-term prognosis after MOP treatment. Moreover, the timing of medical treatment is important, especially for the adolescent. Although this study indicates the postoperative administration of MOP attenuated varicocele-induced bilateral testicular injuries, the point at which the testicular damage has reached a critical point or the amount of waiting before administrating MOP has not been determined. In addition, the results of this study indicate that the inhibition of angiogenesis without downregulating VEGF and MMP-9 is one of the mechanisms of 100 mg/kg MOP inhibiting varicocele progression, but the underlying reason of this apparent controversy is still unclear. Thus, further studies are required to investigate the changes of some upstream or relative biological events, hypoxia especially.

In conclusion, the MOP extracted and administered in this study had a high purity of 98% and was of high quality. The GPC showed that the polydispersity of the MOP was 1.444 and that the MOP primarily consisted of glucose (retention time, 7.286), lactose (retention time, 13.409), and xylose (retention time, 5.578) at a molar ratio of 7.63:1.23:0.95, respectively. Administration of 100 mg/kg of MOP attenuated the disordered structure of seminiferous epithelium and assist in spermatogenesis. Inhibition of angiogenesis may be one of the mechanisms by which MOP exerts its activities, while relative upregulation of VEGF and MMP-9 may be crucial for the spermatogenetic protective effects of 100 mg/kg MOP administration.

Data Availability

The TIF and JPG data used to support the findings of this study are available from the corresponding author upon request. Relevant previously reported data are cited at relevant places within the text as [18–21].

Conflicts of Interest

The authors have no conflicts of interest to declare.

Authors' Contributions

Zhu Zhu carried out the genetic studies and drafted the manuscript. Xiaozhen Zhao prepared and took photos of the immunofluorescence assay. Feng Huang helped perform the operations. Feng Wang conducted the extraction and analysis of MOPs. Wei Wang designed this study and helped

draft the manuscript. All authors read and approved the final manuscript.

Acknowledgments

This work is supported by grants from the Natural Science Foundation of Fujian Province (nos. 2016J01705 and 2016J01766), the Joint Funds for Science and Technology Innovation of Fujian Province (nos. 2016Y9034 and 2017Y9111), the Education Department of Fujian Province (no. 2018B013), Fuzhou Health and Family Planning Commission (no. 2018-S-wt8), the Fuzhou Science and Technology Bureau (no. 2018-S-103-6), and Fujian Medical University (no. 2017XQ1164).

References

[1] M. Zavattaro, C. Ceruti, G. Motta et al., "Treating varicocele in 2018: current knowledge and treatment options," *Journal of Endocrinological Investigation*, vol. 41, no. 12, pp. 1365–1375, 2018.

[2] C. K. Naughton, A. K. Nangia, and A. Agarwal, "Pathophysiology of varicoceles in male infertility," *Human Reproduction Update*, vol. 7, no. 5, pp. 473–481, 2001.

[3] D. Johnson and J. Sandlow, "Treatment of varicoceles: techniques and outcomes," *Fertility and Sterility*, vol. 108, no. 3, pp. 378–384, 2017.

[4] M. A. Will, J. Swain, M. Fode, J. Sonksen, G. M. Christman, and D. Ohl, "The great debate: Varicocele treatment and impact on fertility," *Fertility and Sterility*, vol. 95, no. 3, pp. 841–852, 2011.

[5] M. R. Goren, F. Kilinc, F. Kayaselcuk, C. Ozer, I. Oguzulgen, and E. Hasirci, "Effects of experimental left varicocele repair on hypoxia-inducible factor-1α and vascular endothelial growth factor expressions and angiogenesis in rat testis," *Andrologia*, vol. 49, no. 2, 2017.

[6] J. Lee, C. Lai, W. Yang, and T. Lee, "Increased expression of hypoxia-inducible factor-1α and metallothionein in varicocele and varicose veins," *Phlebology: The Journal of Venous Disease*, vol. 27, no. 8, pp. 409–415, 2012.

[7] S.-H. Wang, W.-K. Yang, and J.-D. Lee, "Increased expression of the sonic hedgehog and vascular endothelial growth factor with co-localization in varicocele veins," *Phlebology*, vol. 32, no. 2, pp. 115–119, 2017.

[8] K. Rotker and M. Sigman, "Recurrent varicocele," *Asian Journal of Andrology*, vol. 18, no. 2, pp. 229–233, 2016.

[9] M. G. Sönmez and A. H. Haliloğlu, "Role of varicocele treatment in assisted reproductive technologies," *Arab Journal of Urology*, vol. 16, no. 1, pp. 188–196, 2018.

[10] Practice Committee of the American Society for Reproductive Medicine and Society for Male Reproduction and Urology, "Report on varicocele and infertility: A committee opinion," *Fertility and Sterility*, vol. 102, no. 6, pp. 1556–1560, 2014.

[11] T. P. Kohn, S. J. Ohlander, J. S. Jacob, T. M. Griffin, L. I. Lipshultz, and A. W. Pastuszak, "The effect of subclinical varicocele on pregnancy rates and semen parameters: a systematic review and meta-analysis," *Current Urology Reports*, vol. 19, no. 7, p. 53, 2018.

[12] J. A. Locke, M. Noparast, and K. Afshar, "Treatment of varicocele in children and adolescents: A systematic review and meta-analysis of randomized controlled trials," *Journal of Pediatric Urology*, vol. 13, no. 5, pp. 437–445, 2017.

[13] J.-H. Zhang, H.-L. Xin, Y.-M. Xu et al., "Morinda officinalis How. – A comprehensive review of traditional uses, phytochemistry and pharmacology," *Journal of Ethnopharmacology*, vol. 213, pp. 230–255, 2018.

[14] M.-S. Chang, W.-N. Kim, W.-M. Yang, H.-Y. Kim, J.-H. Oh, and S.-K. Park, "Cytoprotective effects of Morinda officinalis against hydrogen peroxide-induced oxidative stress in Leydig TM3 cells," *Asian Journal of Andrology*, vol. 10, no. 4, pp. 667–674, 2008.

[15] Y. K. Lee, H. J. Bang, J. B. Oh, and W. K. Whang, "Bioassay-Guided isolated compounds from morinda officinalis inhibit Alzheimer's disease pathologies," *Molecules*, vol. 22, no. 10, 2017.

[16] K. Jiang, D. Huang, D. Zhang et al., "Investigation of inulins from the roots of Morinda officinalis for potential therapeutic application as anti-osteoporosis agent," *International Journal of Biological Macromolecules*, vol. 120, pp. 170–179, 2018.

[17] M. Yoshikawa, S. Yamaguchi, H. Nishisaka, J. Yamahara, and N. Murakami, "Chemical constituents of chinese natural medicine, morindae radix, the dried roots of Morinda officinalis how.: structures of morindolide and morofficinaloside," *Chemical & Pharmaceutical Bulletin*, vol. 43, no. 9, pp. 1462–1465, 1995.

[18] B. Song, F. Wang, and W. Wang, "Effect of aqueous extract from morinda officinalis f. c. how on microwave-induced hypothalamic-pituitary-testis axis impairment in male sprague-dawley rats," *Evidence-Based Complementary and Alternative Medicine*, vol. 2015, Article ID 360730, 10 pages, 2015.

[19] F.-J. Wang, W. Wang, R. Li, B. Song, Y.-H. Zhang, and Y.-X. Zhou, "Morinda officialis how extract improves microwave-induced reproductive impairment in male rats," *Zhonghua Nan Ke Xue*, vol. 19, no. 4, pp. 340–345, 2013.

[20] L. Zhang, X. Zhao, F. Wang, Q. Lin, and W. Wang, "Effects of morinda officinalis polysaccharide on experimental varicocele rats," *Evidence-Based Complementary and Alternative Medicine*, vol. 2016, Article ID 5365291, 11 pages, 2016.

[21] Z. Zhu, F. Huang, F. Wang, Y. Zhang, X. Zhao, and W. Wang, "Morinda Officinalis polysaccharides stimulate hypothalamic gnrh secretion in varicocele progression," *Evidence-Based Complementary and Alternative Medicine*, vol. 2017, Article ID 9057959, 12 pages, 2017.

[22] T. Masuko, A. Minami, N. Iwasaki, T. Majima, S.-I. Nishimura, and Y. C. Lee, "Carbohydrate analysis by a phenol-sulfuric acid method in microplate format," *Analytical Biochemistry*, vol. 339, no. 1, pp. 69–72, 2005.

[23] N. J. Kruger, "The Bradford method for protein quantitation," *Methods in Molecular Biology*, vol. 32, pp. 9–15, 1994.

[24] D. C. Saypol, S. S. Howards, T. T. Turner, and E. D. Miller Jr., "Influence of surgically induced varicocele on testicular blood flow, temperature, and histology in adult rats and dogs," *The Journal of Clinical Investigation*, vol. 68, no. 1, pp. 39–45, 1981.

[25] A. J. Wyrobek and W. R. Bruce, "Chemical induction of sperm abnormalities in mice," *Proceedings of the National Acadamy of Sciences of the United States of America*, vol. 72, no. 11, pp. 4425–4429, 1975.

[26] S. E. Johnsen, "Testicular biopsy score count-a method for registration of spermatogenesis in human testes: normal values and results in 335 hypogonadal males," *Hormones*, vol. 1, no. 1, pp. 2–25, 1970.

[27] M. Tek, S. Çayan, N. Yilmaz, I. Oğuz, E. Erdem, and E. Akbay, "The effect of vascular endothelial growth factor on spermatogenesis and apoptosis in experimentally varicocele-induced adolescent rats," *Fertility and Sterility*, vol. 91, no. 5, supplement, pp. 2247–2252, 2009.

[28] K. Zhang, Z. Wang, H. Wang, Q. Fu, H. Zhang, and Q. Cao, "Hypoxia-induced apoptosis and mechanism of epididymal dysfunction in rats with left-side varicocele," *Andrologia*, vol. 48, no. 3, pp. 318–324, 2016.

[29] S. Arena, L. Minutoli, F. Arena et al., "Polydeoxyribonucleotide administration improves the intra-testicular vascularization in rat experimental varicocele," *Fertility and Sterility*, vol. 97, no. 1, pp. 165–168, 2012.

[30] M. Gökhan-Köse, Ş. Erdem, Ç. Peşkircioğlu, and B. Çaylak, "Angiogenesis inhibition impairs testicular morphology in experimental left varicocele rat model," *Actas Urológicas Españolas (English Edition)*, vol. 38, no. 7, pp. 459–464, 2014.

[31] J. G. Reyes, J. G. Farias, S. Henríquez-Olavarrieta et al., "The hypoxic testicle: physiology and pathophysiology," *Oxidative Medicine and Cellular Longevity*, vol. 2012, Article ID 929285, 15 pages, 2012.

[32] G. Hwang, S. Wang, W. Tseng, C. Yu, and P. S. Wang, "Effect of hypoxia on the release of vascular endothelial growth factor and testosterone in mouse TM3 Leydig cells," *American Journal of Physiology-Endocrinology and Metabolism*, vol. 292, no. 6, pp. E1763–E1769, 2007.

[33] K. Shiraishi and K. Naito, "Involvement of vascular endothelial growth factor on spermatogenesis in testis with varicocele," *Fertility and Sterility*, vol. 90, no. 4, pp. 1313–1316, 2008.

[34] T. Liu, W. Zhou, B. Cai et al., "IRX2-mediated upregulation of MMP-9 and VEGF in a PI3K/AKT-dependent manner," *Molecular Medicine Reports*, vol. 12, no. 3, pp. 4346–4351, 2015.

[35] L. L. Robinson, N. A. Sznajder, S. C. Riley, and R. A. Anderson, "Matrix metalloproteinases and tissue inhibitors of metalloproteinases in human fetal testis and ovary," *MHR: Basic science of reproductive medicine*, vol. 7, no. 7, pp. 641–648, 2001.

[36] R. Serra, G. Buffone, G. Costanzo et al., "Altered metalloproteinase-9 expression as least common denominator between varicocele, inguinal hernia, and chronic venous disorders," *Annals of Vascular Surgery*, vol. 28, no. 3, pp. 705–709, 2014.

Hindawi
Evidence-Based Complementary and Alternative Medicine
Volume 2019, Article ID 9610629, 8 pages
https://doi.org/10.1155/2019/9610629

Research Article

Formononetin Enhances the Tumoricidal Effect of Everolimus in Breast Cancer MDA-MB-468 Cells by Suppressing the mTOR Pathway

Qianmei Zhou,[1] **Weihong Zhang**,[2] **Tian Li**,[2] **Runwei Tang**,[2] **Chaoran Li**,[2] **Shuai Yuan**,[2] **and Desheng Fan**[3]

[1]*Institute of Interdisciplinary Integrative Medicine Research, Shanghai University of Traditional Chinese Medicine, Shanghai 201203, China*
[2]*Breast Surgery Department, Baoshan Branch, Shuguang Hospital Affiliated to Shanghai University of Traditional Chinese Medicine, Shanghai 201900, China*
[3]*Pathology Department, Baoshan Branch, Shuguang Hospital Affiliated to Shanghai University of Traditional Chinese Medicine, Shanghai 201900, China*

Correspondence should be addressed to Weihong Zhang; hongwz1022@sina.com

Received 18 December 2018; Accepted 27 February 2019; Published 17 March 2019

Guest Editor: Arielle Cristina Arena

Background. Formononetin, an active ingredient isolated from the traditional Chinese medicinal herb *Astragalus membranaceus*, has anticancer and chemoresistance-reducing biological activities. We evaluated the efficacy of formononetin in improving the tumoricidal effect of everolimus by suppressing the mTOR pathway in breast cancer cells. *Methods.* Cell survival was assessed using an MTT assay. Apoptosis was detected using flow cytometry. Proteins related to the mTOR pathway were detected and assessed using real-time PCR and Western blot analysis. *Results.* The results showed that formononetin enhances the efficacy of everolimus in suppressing breast cancer cell growth both in vitro and in vivo. The combination of formononetin and everolimus resulted in a 2-fold decrease in tumor volume and a 21.6% decrease in cell survival. The apoptosis ratio in cells treated with formononetin and everolimus increased by 27.9%. Formononetin and everolimus also inhibited the expression of p-mTOR and p-P70S6K and increased the expression of PTEN and p-4EBP-1. Notably, formononetin alone inhibited p-Akt expression but not everolimus. *Conclusions.* Formononetin enhances the tumoricidal effect of everolimus by inhibiting the activity of Akt.

1. Introduction

Breast cancer is the most common malignant tumor in women [1]. The incidence of breast cancer among women in China is rising [2, 3]. Triple-negative breast cancer (TNBC) is a special type of breast cancer, where expressions of estrogen receptor, progesterone receptor, and human epidermal growth factor receptor-2 (Her-2) are all negative. It accounts for approximately 10%–20% of all breast cancers. It has the worst prognosis among all breast cancer types, with characteristics such as rapid metastasis, drug resistance, and high mortality [4].

mTOR is a type of serine/threonine protein kinase belonging to the PI3k family. It plays an important role in protein synthesis and autophagy. Abnormal expression of mTOR leads to conditions such as diabetes and tumor development [5]. mTOR has 2 key complexes, the mTORC1 and mTORC2. mTORC1 promotes protein synthesis by phosphorylating 2 key effectors, namely, p70S6 kinase 1 (S6K1) and eIF4E binding protein (4EBP) [6]. mTORC1 regulates cell growth and metabolism, whereas mTORC2 regulates cell proliferation and survival by phosphorylating the AGC family of kinases (PKA/PKG/PKC). mTORC2 is critical to the phosphorylation and activation of Akt. The activated Akt promotes cell survival, proliferation, and growth [7, 8].

Everolimus is an inhibitor of serine-threonine kinase mammalian target of rapamycin (mTOR) [9]. It has been

reported that everolimus has broad antitumor activities in preclinical models and used in combination with trastuzumab in several clinical trials [10]. However, the effect of everolimus against TNBC does not have satisfactory efficacy for clinical use.

Formononetin is an active ingredient isolated from the traditional Chinese medicinal herb *Astragalus membranaceus* and has various pharmacologic effects, such as tumor growth inhibition, wound healing, estrogen-like effects, antioxidant activity, and anti-inflammatory effects [11, 12]. Formononetin can exert antitumor effects by inducing cell apoptosis, arresting the cell cycle, inhibiting angiogenesis, and reversing multidrug resistance [13, 14].

Recent studies have shown that formononetin can inhibit tumor growth and induce apoptosis by regulating the PI3k pathway [15]. However, whether the combination of formononetin and everolimus can synergistically provoke cancer cell death remains unclear. In this study, we showed that formononetin significantly enhances the tumoricidal effect of everolimus both in vitro and in vivo. Most importantly, we determined the underlying mechanisms for this effect in MDA-MB-468 cells.

2. Materials and Methods

2.1. Reagents and Cell Culture. Everolimus was purchased from Sigma-Aldrich (MO, USA). Formononetin was obtained from the National Institute for the Control of Pharmaceutical and Biological Products (Beijing, China). Annexin V-FITC and propidium iodide (PI) were obtained from Sigma-Aldrich (MO, USA). The antibodies against mTOR, p-mTOR, Akt, p-Akt, PTEN, p-4EBP-1, and p-p70s6k were obtained from Cell Signaling Technology (MA, USA). Human breast cancer MDA-MB-468 cells were cultured in an RPMI 1640 medium supplemented with 10% fetal calf serum and 0.01 mg/mL insulin at 37°C with 5% CO_2 in a humidified atmosphere.

2.2. Tumor Xenograft and Treatment. Seven-week-old female nu/nu athymic mice, 18-20 g, were obtained from Academia Sinica (Shanghai, China). All procedures conformed to animal welfare considerations and were approved by the Ethical Committee of Shanghai Traditional Chinese Medicine (09001, March 5, 2014). MDA-MB-468 cells (1×10^7/mL) were injected into the mammary fat pad (m.f.p.) of the mice [16]. When tumors developed (approximately 10 days), the mice (n = 10) were treated with formononetin 50 mg/kg [17] and everolimus 2 mg/kg (Animal dosage of everolimus was converted according to clinical dosage) and combined treatment of formononetin (50 mg/kg) and everolimus (2 mg/kg). Untreated animals were given physiological saline as control. All mice were treated once a day via gavage for 4 weeks. After 4 weeks of treatment, blood was collected from the eyes and animals were sacrificed by cervical dislocation. The tumors were immediately removed, freed from connective and adipose tissue, and weighed.

2.3. Cell Growth Inhibition Test. The cell survival was determined by 3-(4,5-dimethylthiazol-2-yl)-2,5-diphenyltetrazolium bromide (MTT) assay [18]. Various concentrations of formononetin with or without everolimus were then added to the MDA-MB-468 cells for varying lengths of time followed by the addition of MTT for another 4 h. Cytotoxicity was expressed as a percentage of (number of cells surviving/total number of untreated cells).

2.4. Flow Cytometric Analysis. MDA-MB-468 cells (10^6/mL) were cultured in 6-well plates. When the culture reached 70%–80% confluence, cells were treated with formononetin (150 μmol/L), everolimus (100 nmol/L), or formononetin (150 μmol/L) plus everolimus (100 nmol/L) for 48 h. Cells were subjected to annexin V-PI dual staining assay or PI staining according to the manufacturer's protocol. Stained cells were identified using a fluorescence-activated cell sorter (Becton Dickinson, CA, USA), and the percentage of apoptotic cell population was determined using ModFit LT3.0 software (Becton Dickinson, CA, USA).

2.5. RNA Isolation, Reverse Transcription, and Real-Time PCR. Equal amounts (2 μg) of total mRNA from formononetin and everolimus-treated cells were subsequently transcribed into cDNA using M-MuLV reverse transcriptase (Thermo Fisher Scientific) (Waltham, MA, USA). All reactions were performed in a final volume of 20 μL. The qRT-PCR reaction conditions were as follows: activation at 95°C for 10 min with 40 cycles of denaturation at 95°C for 15 s, primer annealing and extension at 60°C for 1 min, and ramping back to 95°C. Human-specific primers for 5′-GCAATATGTTCATAACGATGGCTGTGG-3′ (PTEN forward) and 5′-GAACTGGCAGGTAGAAGGCAACTC-3′ (PTEN reverse), 5′-TTGGAGAACCAGCCCATAAGA-3′ (mTOR forward) and 5′-ATGAGATGTCGCTTGCTTGATAA-3′ (mTOR reverse), 5′-CGCCTGCCCTTCTACAACC-3′ (Akt forward) and 5′-TCATACACATCTTGCCACACGA-3′ (Akt reverse), 5′-GGGCTAGCGATGTCCGGGGGCAGCAGCTG-3′ (4EBP1 forward) and 5′-GGAAGCTTAATGTCCATCTCAAACTGTGACTC-3′ (4EBP1 reverse), 5′-GGGCTAGCGATGAGGCGACGAAGGAGGCGG-3′ (p70s6k forward) and 5′-GGGGTACCTAGATTCATACGCAGGTGCTCTG-3′ (p70s6k reverse) were designed. Expression was assessed using the ΔCt method.

2.6. Western Blot Analysis. When human breast cancer MDA-MB-468 cells in 6-well plates reached 90% confluence, the cells were washed with PBS and cell total proteins were extracted. Then proteins were subjected to SDS-PAGE and Western blot analysis. Protein expressions were detected using primary antibodies (1:1000) and secondary antibodies (1:800) conjugated with horseradish peroxidase and ECL reagents (Pharmacia, Buckinghamshire, UK). Quantitative analyses of Western blots were performed using Alpha Ease FC (FluorChem FC2) software. The density ratio of proteins to GAPDH as spot density was calculated using analysis tools.

2.7. siRNA Transfection. Transfection was performed with Lipofectamine 2000 (Invitrogen, California, USA) following

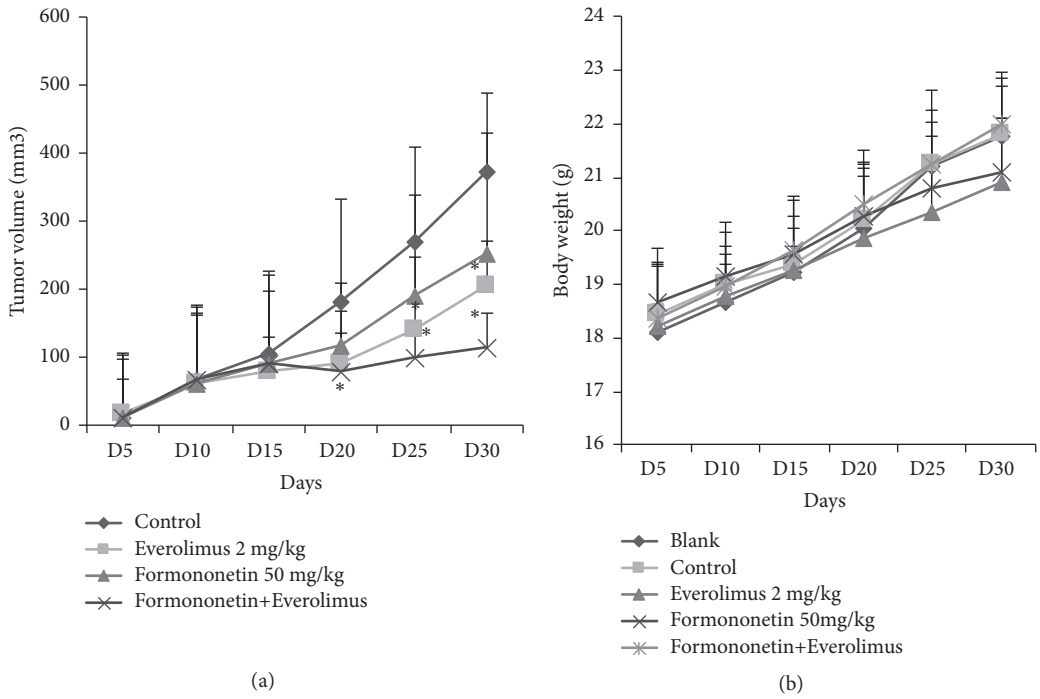

Figure 1: Effect of formononetin or formononetin plus everolimus on tumor outgrowth. (a) Mice were first injected with MDA-MB-468 cells for 2 weeks to establish the xenograft model. Mice were then administered formononetin (50 mg/kg), everolimus (2 mg/kg), or formononetin plus everolimus. After 4 weeks, mice were sacrificed and tumors were excised and weighed. $*p < 0.05$ versus control. (b) Body weights of animals treated with formononetin or formononetin plus everolimus for 4 weeks.

the manufacturer's instructions. siRNA transfection was performed 24 h before formononetin and everolimus treatment. siRNA duplexes, including Akt siRNA (sc-43609) and control-scrambled siRNA (sc-37007), were obtained from Santa Cruz Biotechnology (Dallas, TX, USA).

2.8. Statistical Analysis. Statistical differences were identified using 2-tailed Student t tests. Data are presented as mean ± standard deviation. A p value of < 0.05 was considered statistically significant.

3. Results

3.1. Combined Formononetin and Everolimus Treatment Suppresses Tumor Masses Significantly. To determine the effect of formononetin on in vivo tumor outgrowth, we used MDA-MB-468 breast cancer xenografts. Tumor growth was significantly inhibited in the formononetin 50 mg/kg alone group compared with the control group ($p < 0.05$). Tumor volume shrank from 472.7 to 253.6 mm^3 on the 30th day of tumor growth. Moreover, in the presence of formononetin, everolimus resulted in a 2-fold reduction in tumor volume. These results suggest that formononetin can synergistically enhance the tumoricidal effect of everolimus in human breast cancer cells (Figure 1(a)).

Furthermore, formononetin was observed to be safe in the MDA-MB-468 xenograft model. None of the mice died with everolimus alone or combined formononetin-everolimus treatment. Mice receiving formononetin and everolimus had no apparent weight loss and had a healthy appetite (Figure 1(b)). These results suggest that formononetin inhibited tumor growth safely.

3.2. Formononetin Significantly Enhances the Tumoricidal Effect of Everolimus. To determine the underlying mechanism, we analyzed the cytotoxicity of formononetin with or without everolimus on MDA-MB-468 cells. Cells were then exposed to various concentrations of formononetin and everolimus for 12, 24, and 48 h. Cell viability was determined using an MTT assay. The results showed that formononetin or everolimus alone inhibited cell survival in a dose- and time-dependent manner. Moreover, the half-maximal inhibitory concentrations of formononetin and everolimus alone were 150 μmol/L and 100 nmol/L for 48 h, respectively (Figures 2(a) and 2(b)). When formononetin was used with everolimus, cell survival decreased by 21.6%. These results suggest that formononetin alone can inhibit breast cancer cell growth. Formononetin can synergistically enhance the tumoricidal effect of everolimus in MDA-MB-468 breast cancer cells (Figure 2(c)).

3.3. Formononetin and Everolimus Synergistically Induce Apoptosis in MDA-MB-468 Cells. To determine the effect of formononetin and everolimus treatment on cell apoptosis, we performed flow cytometry on MDA-MB-468 cells that were exposed to either one of the drugs or both for 48 h. The apoptosis ratio among cells treated with formononetin (150 μmol/L), everolimus (100 nmol/L), or formononetin

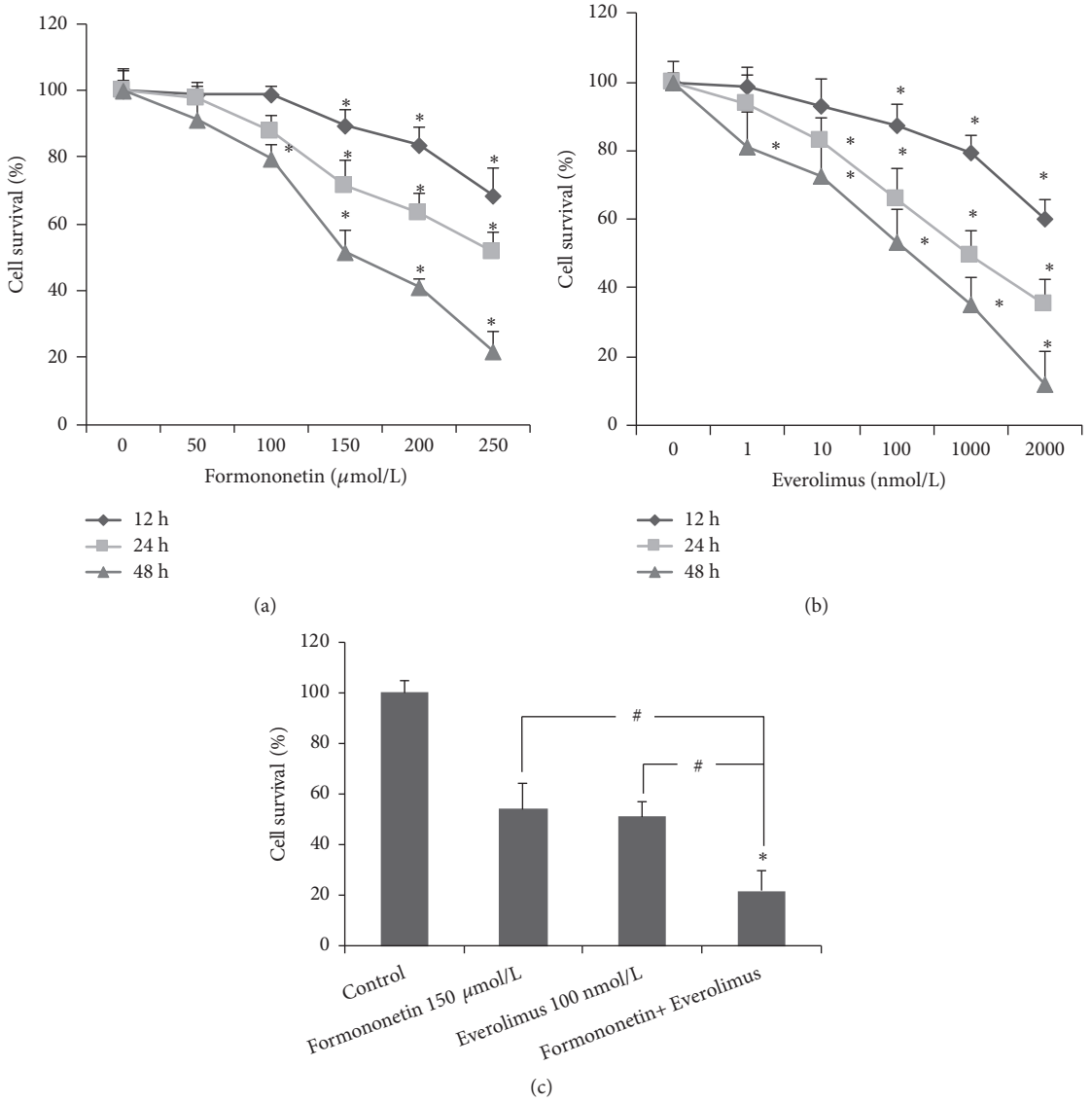

Figure 2: Sensitivities of MDA-MB-468 cells to formononetin and everolimus. An MTT assay was performed to determine the cell number, as described in Section 2. MDA-MB-468 cells were incubated in formononetin at 50, 100, 150, 200, and 250 μmol/L (a) and everolimus at 1, 10, 100, 1000, and 2000 nmol/L (b) for 12, 24, and 48 h. (c) Both everolimus alone or formononetin and everolimus combined inhibited cell growth for 48 h. Values are means ± SE from 3 independent experiments. $*p < 0.05$ versus control. $^{\#}p<0.05$ versus both everolimus and formononetin alone.

+ everolimus was 21.5%, 25.7%, and 53.8%, respectively (Figure 3(a)). Cell cycle analysis showed that hypodiploid peaks also appeared with different treatments (Figure 3(b)). These results indicate that formononetin and everolimus result in apoptosis.

3.4. Effect of Formononetin and Everolimus on the mTOR Pathway. Tumor growth has been shown to be regulated through the mTOR pathway. Everolimus is an inhibitor of mTORC1. In this study, we investigated the mechanisms by which formononetin exerted its effect on tumor growth using qRT-PCR. PTEN mRNA and 4EBP-1 mRNA had higher expression in the formononetin group than in the control group. P70s6k mRNA levels decreased ($p<0.05$) (Figure 4(a)). We further confirmed the efficacy of formononetin through Western blotting. Formononetin and everolimus also inhibited the expression of p-mTOR and p-P70S6K and increased that of PTEN and p-4EBP-1. However, formononetin alone inhibited the level of p-Akt but everolimus did not (Figure 4(b)).

To evaluate the effect of formononetin on the Akt pathway, silencing of Akt was validated using Western blotting. We found that the level of mTOR was restored to that in the control group after application of formononetin. However, in the presence of Akt siRNA, everolimus had no significant effect on the expression of mTOR. The expressions of p-4EBP-1 and p-P70S6K were all reversed by formononetin with Akt siRNA (Figure 4(c)). These results demonstrate that

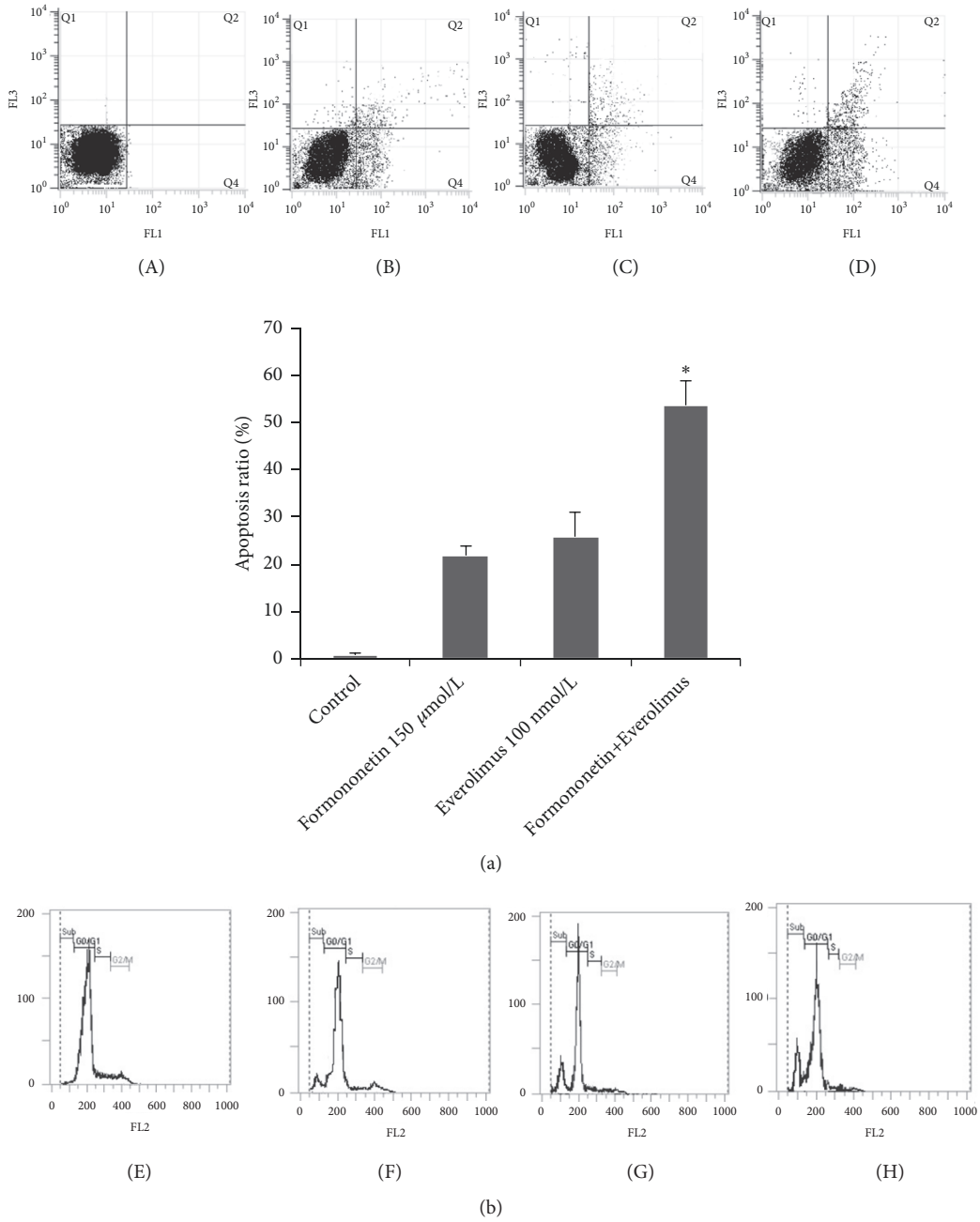

Figure 3: Effect of everolimus alone or both formononetin and everolimus on apoptosis in MDA-MB-468 cells. MDA-MB-468 cells were treated with formononetin (150 μmol/L), everolimus (100 nmol/L), or both for 48 h. Cells were subsequently stained for annexin V-PI (a) and PI only (b) followed by flow cytometric analysis. (A) and (E) control, (B) and (F) formononetin (150 μmol/L), (C) and (G) everolimus (100 nmol/L), and (D) and (H) formononetin + everolimus. $*p<0.05$ versus formononetin or everolimus alone.

the inhibition of the mTOR pathway by formononetin is associated with Akt.

4. Discussion

mTOR is often considered a downstream effector of numerous mutant oncogene pathways, such as the PI3K/Akt pathway and the Ras/Raf/Mek/Erk (MAPK) pathway, causing overactivation of mTOR and hence cancer [19]. Patients with overexpression of p-mTOR had worse prognosis in early tri-negative breast cancer [20]. Everolimus was found to have inhibitory activity only on the mTORC1 complex and had no apparent effect on the mTORC2 complex [21]. This indicates its limitations as an antitumor agent. In this study, we evaluated whether formononetin can inhibit tumor growth by suppressing the mTOR pathway and whether it can enhance the efficacy of everolimus.

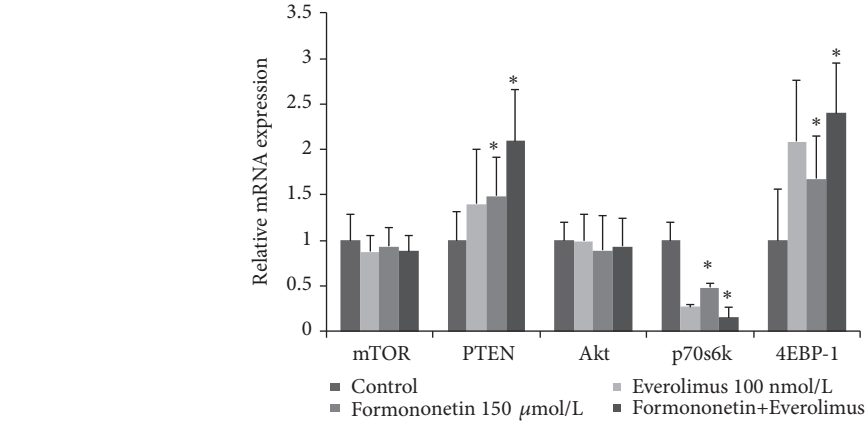

(a)

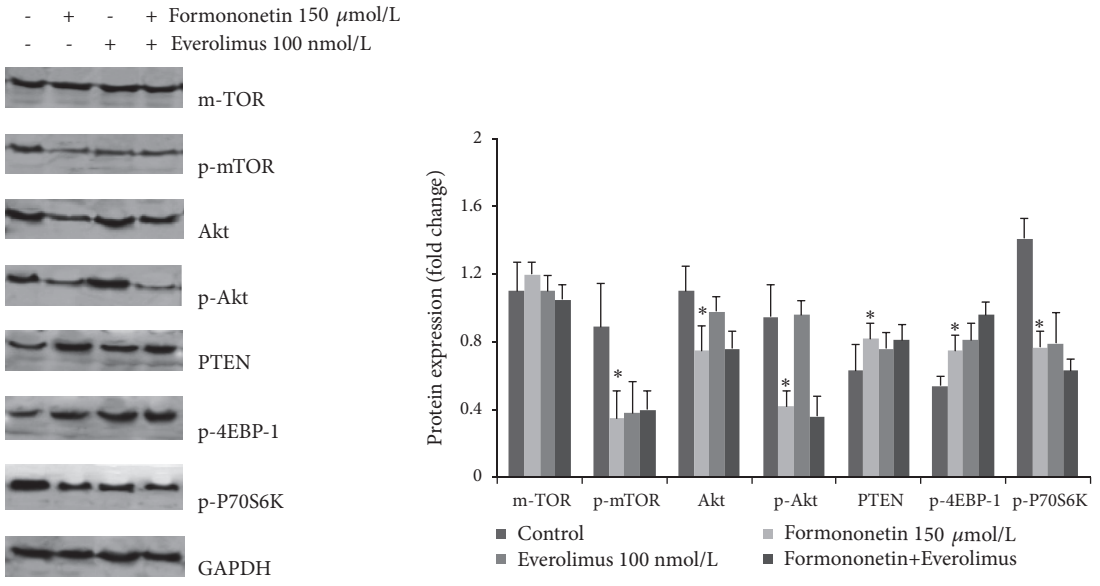

(b)

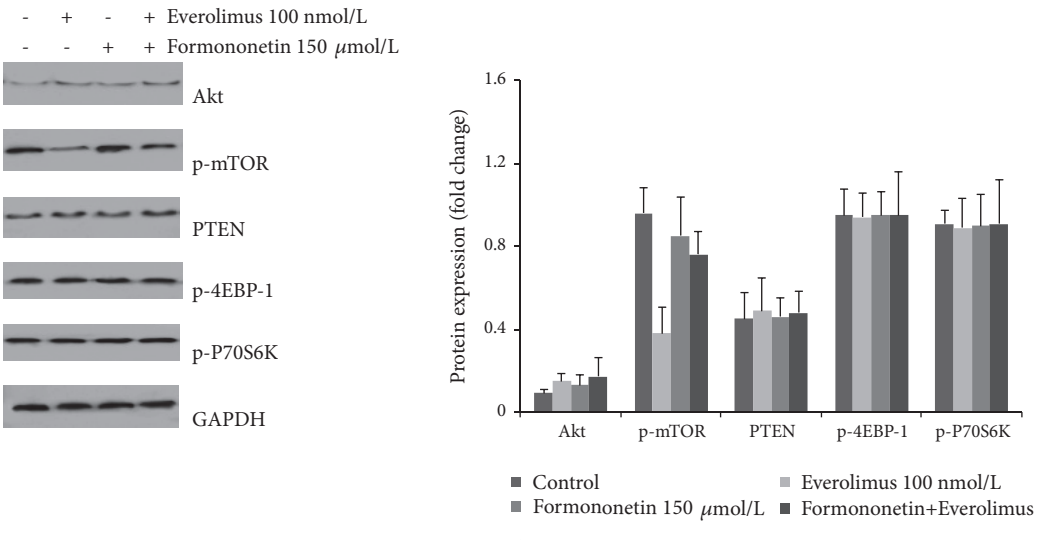

(c)

Figure 4: Effect of everolimus alone or both formononetin and everolimus on the mTOR pathway. MDA-MB-468 cells were treated with formononetin (150 μmol/L), everolimus (100 nmol/L), or both for 48 h. (a) PTEN, mTOR, Akt, P70S6K, and 4EBP-1 mRNA were identified using qRT-PCR analysis. $*p<0.05$ versus control. (b) The expressions of mTOR, p-mTOR, Akt, p-Akt, PTEN, p-4EBP-1, and p-P70S6K were determined using Western blotting. (c) In the presence of Akt siRNA, the levels of p-mTOR, Akt, PTEN, p-4EBP-1, and p-P70S6K were observed on treatment with either everolimus alone or both formononetin and everolimus.

We found that formononetin alone could inhibit the growth of breast cancer cells; our results are in line with those of a previous study [14]. We further showed that formononetin improved the efficacy of everolimus in suppressing breast cancer cell growth both in vitro and in vivo (Figures 1 and 2). In this study, we showed that a clinical dosage of 2 mg/kg everolimus significantly decreased tumor masses in the MDA-MB-468 xenograft model. Notably, the inclusion of formononetin in everolimus treatment resulted in a 2-fold decrease in tumor volume compared with that with everolimus alone (Figure 1(a)). Moreover, the combination treatment is safe (Figure 1(b)). Our results strongly indicate that formononetin may be used to enhance antitumoricidal effect of everolimus.

Proliferation and apoptosis of tumor cells are the key steps in the onset and development of cancer [22]. We found that both formononetin and everolimus or everolimus alone inhibited cell growth in MDA-MB-468 cells (Figure 2). To determine whether cell death induced by formononetin and everolimus was related to apoptosis, the apoptosis rate and cell cycle were evaluated. The results showed that the combination of formononetin and everolimus results in a 2-fold increase in apoptosis (Figure 3). Our results support the hypothesis that the synergistic tumor-killing effect of formononetin and everolimus treatment at least partially contributes to a greater efficacy in inducing apoptosis than with formononetin or everolimus alone.

Moreover, we found that formononetin and everolimus alone inhibited the expression of p-mTOR and p-P70S6K and increased that of p-4EBP-1. However, formononetin alone inhibited the level of p-Akt and everolimus did not (Figures 4(a) and 4(b)). In the presence of Akt siRNA, the expressions of p-4EBP-1 and p-P70S6K were all reversed by formononetin. These results suggest that the inhibition of the mTOR pathway by formononetin is associated with Akt. Phosphorylation and activation of Akt are the most critical roles of mTORC2 [23, 24]. Therefore, we conclude that formononetin may enhance the antitumor effect of everolimus by additionally inhibiting mTORC2.

In summary, our study demonstrated that formononetin can improve the tumoricidal effect of everolimus. Formononetin can augment everolimus in inhibiting the mTOR pathway by effectively inhibiting mTORC2. The combination treatment of formononetin and everolimus may be an effective approach for breast cancer chemotherapy.

Data Availability

The data used to support the findings of this study are available from the corresponding author upon request.

Disclosure

Qianmei Zhou and Weihong Zhang are co-first authors.

Conflicts of Interest

The authors declare that they have no conflicts of interests.

Acknowledgments

This research was supported by National Nature Science Foundation of China (Grants nos. 81503578 and 81803934), Shanghai Health and Family Planning Commission Research Fund Project (201540036), and National Nature Science Nurturing Project of Baoshan Branch, Shuguang Hospital Affiliated to Shanghai University of Traditional Chinese Medicine (GZRPYJJ-201702).

References

[1] L. A. Torre, R. L. Siegel, E. M. Ward, and A. Jemal, "Global cancer incidence and mortality rates and trends—an update," *Cancer Epidemiology, Biomarkers & Prevention*, vol. 25, no. 1, pp. 16–27, 2016.

[2] W. Chen, R. Zheng, P. D. Baade et al., "Cancer statistics in China, 2015," *CA: A Cancer Journal for Clinicians*, vol. 66, no. 2, pp. 115–132, 2016.

[3] M. Ghoncheh, Z. Pournamdar, and H. Salehiniya, "Incidence and mortality and epidemiology of breast cancer in the world," *Asian Pacific Journal of Cancer Prevention*, vol. 17, no. S3, pp. 43–46, 2016.

[4] P. Kumar and R. Aggarwal, "An overview of triple-negative breast cancer," *Archives of Gynecology and Obstetrics*, vol. 293, no. 2, pp. 247–269, 2016.

[5] R. A. Saxton and D. M. Sabatini, "mTOR signaling in growth, metabolism, and disease," *Cell*, vol. 168, no. 6, pp. 960–976, 2017.

[6] A. Kezic, L. Popovic, and K. Lalic, "mTOR inhibitor therapy and metabolic consequences: where do we stand?" *Oxidative Medicine and Cellular Longevity*, vol. 2018, Article ID 2640342, 2018.

[7] D. Bridges and A. R. Saltiel, "Phosphoinositides: key modulators of energy metabolism," *Biochimica et Biophysica Acta (BBA) - Molecular and Cell Biology of Lipids*, vol. 1851, no. 6, pp. 857–866, 2015.

[8] S. Mukaida, B. A. Evans, T. Bengtsson, D. S. Hutchinson, and M. Sato, "Adrenoceptors promote glucose uptake into adipocytes and muscle by an insulin-independent signaling pathway involving mechanistic target of rapamycin complex 2," *Pharmacological Research*, vol. 116, pp. 87–92, 2017.

[9] M. Marinov, A. Ziogas, O. E. Pardo et al., "AKT/mTOR pathway activation and BCL-2 family proteins modulate the sensitivity of human small cell lung cancer cells to RAD001," *Clinical Cancer Research*, vol. 15, no. 4, pp. 1277–1287, 2009.

[10] G. Jerusalem, A. Fasolo, V. Dieras et al., "Phase i trial of oral mTOR inhibitor everolimus in combination with trastuzumab and vinorelbine in pre-treated patients with HER2-overexpressing metastatic breast cancer," *Breast Cancer Research and Treatment*, vol. 125, no. 2, pp. 447–455, 2011.

[11] P. K.-K. Lai, J. Y.-W. Chan, L. Cheng et al., "Isolation of anti-inflammatory fractions and compounds from the root of astragalus membranaceus," *Phytotherapy Research*, vol. 27, no. 4, pp. 581–587, 2013.

[12] S. Li, Y. Dang, X. Zhou et al., "Formononetin promotes angiogenesis through the estrogen receptor alpha-enhanced ROCK pathway," *Scientific Reports*, vol. 5, no. 1, 2015.

[13] J. Chen, X. Zhao, Y. Ye, Y. Wang, and J. Tian, "Estrogen receptor beta-mediated proliferative inhibition and apoptosis in human breast cancer by calycosin and formononetin," *Cellular Physiology and Biochemistry*, vol. 32, no. 6, pp. 1790–1797, 2013.

[14] J. Chen, X. Zhang, Y. Wang, Y. Ye, and Z. Huang, "Differential ability of formononetin to stimulate proliferation of endothelial cells and breast cancer cells via a feedback loop involving MicroRNA-375, RASD1, and ERα," *Molecular Carcinogenesis*, vol. 57, no. 7, pp. 817–830, 2018.

[15] R. Zhou, L. Xu, M. Ye, M. Liao, H. Du, and H. Chen, "Formononetin inhibits migration and invasion of MDA-MB-231 and 4T1 breast cancer cells by suppressing MMP-2 and MMP-9 through PI3K/AKT signaling pathways," *Hormone and Metabolic Research*, vol. 46, no. 11, pp. 753–760, 2014.

[16] Q.-M. Zhou, X.-F. Wang, X.-J. Liu et al., "Curcumin improves MMC-based chemotherapy by simultaneously sensitising cancer cells to MMC and reducing MMC-associated side-effects," *European Journal of Cancer*, vol. 47, no. 14, pp. 2240–2247, 2011.

[17] W. Hu and Z. Xiao, "Formononetin induces apoptosis of human osteosarcoma cell line U2OS by regulating the expression of Bcl-2, Bax and MiR-375 in vitro and in vivo," *Cellular Physiology and Biochemistry*, vol. 37, no. 3, pp. 933–939, 2015.

[18] L. Yang, D. D. Wei, Z. Chen, J. S. Wang, and L. Y. Kong, "Reversal of multidrug resistance in human breast cancer cells by Curcuma wenyujin and Chrysanthemum indicum," *Phytomedicine*, vol. 18, no. 8-9, pp. 710–718, 2011.

[19] B. C. Grabiner, V. Nardi, K. Birsoy et al., "A diverse array of cancer-associated MTOR mutations are hyperactivating and can predict rapamycin sensitivity," *Cancer Discovery*, vol. 4, no. 5, pp. 554–563, 2014.

[20] G. Lazaridis, S. Lambaki, G. Karayannopoulou et al., "Prognostic and predictive value of p-Akt, EGFR, and p-mTOR in early breast cancer," *Strahlentherapie und Onkologie*, vol. 190, no. 7, pp. 636–645, 2014.

[21] S. H. Hare and A. J. Harvey, "mTOR function and therapeutic targeting in breast cancer," *American Journal of Cancer Research*, vol. 7, no. 3, pp. 383–404, 2017.

[22] S. Shrestha, A. Sorolla, J. Fromont, P. Blancafort, and G. R. Flematti, "Aurantoside c targets and induces apoptosis in triple negative breast cancer cells," *Marine Drugs*, vol. 16, no. 10, p. E361, 2018.

[23] R. R. Katreddy, L. R. Bollu, F. Su et al., "Targeted reduction of the EGFR protein, but not inhibition of its kinase activity, induces mitophagy and death of cancer cells through activation of mTORC2 and Akt," *Oncogenesis*, vol. 7, no. 1, 2018.

[24] K. Xu, G. Chen, X. Li et al., "MFN2 suppresses cancer progression through inhibition of mTORC2/Akt signaling," *Scientific Reports*, vol. 7, no. 1, Article ID 41718, 2017.

Hindawi
Evidence-Based Complementary and Alternative Medicine
Volume 2019, Article ID 3807207, 10 pages
https://doi.org/10.1155/2019/3807207

Research Article

Phytochemical Evaluation, Embryotoxicity, and Teratogenic Effects of *Curcuma longa* Extract on Zebrafish (*Danio rerio*)

Akinola Adekoya Alafiatayo,[1,2] **Kok-Song Lai**,[3] **Ahmad Syahida**,[1] **Maziah Mahmood**,[1] **and Noor Azmi Shaharuddin**[1,4]

[1]*Department of Biochemistry, Faculty of Biotechnology and Biomolecular Sciences, Universiti Putra Malaysia, 43400 Serdang, Selangor, Malaysia*
[2]*Department of Sciences, College of Science & Technology, Waziri Umaru Federal Polytechnic, Birnin Kebbi, Nigeria*
[3]*Department of Cell and Molecular Biology, Faculty of Biotechnology and Biomolecular Sciences, Universiti Putra Malaysia, 43400 Serdang, Selangor, Malaysia*
[4]*Institute of Plantation Studies, Universiti Putra Malaysia, 43400 Serdang, Selangor, Malaysia*

Correspondence should be addressed to Noor Azmi Shaharuddin; noorazmi@upm.edu.my

Received 7 November 2018; Revised 7 February 2019; Accepted 13 February 2019; Published 5 March 2019

Guest Editor: Wellerson Scarano

Curcuma longa L. is a rhizome plant often used as traditional medicinal preparations in Southeast Asia. The dried powder is commonly known as cure-all herbal medicine with a wider spectrum of pharmaceutical activities. In spite of the widely reported therapeutic applications of *C. longa*, research on its safety and teratogenic effects on zebrafish embryos and larvae is still limited. Hence, this research aimed to assess the toxicity of *C. longa* extract on zebrafish. Using a reflux flask, methanol extract of *C. longa* was extracted and the identification and quantification of total flavonoids were carried out with HPLC. Twelve fertilized embryos were selected to test the embryotoxicity and teratogenicity at different concentration points. The embryos were exposed to the extract in the E3M medium while the control was only exposed to E3M and different developmental endpoints were recorded with the therapeutic index calculated using the ratio of LC50/EC50. *C. longa* extract was detected to be highly rich in flavonoids with catechin, epicatechin, and naringenin as the 3 most abundant with concentrations of 3,531.34, 688.70, and 523.83μg/mL, respectively. The toxicity effects were discovered to be dose-dependent at dosage above 62.50μg/mL, while, at 125.0μg/mL, mortality of embryos was observed and physical body deformities of larvae were recorded among the hatched embryos at higher concentrations. Teratogenic effect of the extract was severe at higher concentrations producing physical body deformities such as kink tail, bend trunk, and enlarged yolk sac edema. Finally, the therapeutic index (TI) values calculated were approximately the same for different concentration points tested. Overall, the result revealed that plants having therapeutic potential could also pose threats when consumed at higher doses especially on the embryos. Therefore, detailed toxicity analysis should be carried out on medicinal plants to ascertain their safety on the embryos and its development.

1. Introduction

Plants are source of natural chemical compounds with pharmacological and therapeutic properties. They are widely used for the production of pharmaceutical drugs and play major role in the management of both significant and minor illnesses [1–3]. Although these natural compounds are valuable, some contain toxic compounds with detrimental effect on human's health [4–6]. Numerous findings have been reported on the toxicity effect of medicinal plants on human organs such as kidneys, liver, and heart [7–9] but there are limited reports describing the embryo toxicity and teratogenic effect of *C. longa* extract.

In developing countries, traditional medical practices are the main source of primary healthcare provider. World Health Organization (WHO) reported that 80% of the global population depends on traditional medicine for their healthcare [10]. In recent times the use of natural remedy from plant

is becoming more popular among the developed countries as they see medicinal herbs as safe alternatives to orthodox medicines [11].

Curcuma longa L. is a rhizome plant that belongs to the family Zingiberaceae; it is often used as traditional medicinal preparations and in everyday culinary. It is a perennial herb widely cultivated in Southeast Asia and distributed throughout world tropical and subtropical regions. The powder form is known as turmeric, popularly used for medicinal purpose and regarded as cure-all herbal medicine with wide spectrum of pharmaceutical activities. Ayurvedic medicine uses turmeric against anorexia, diabetic wounds, biliary disorder, hepatic disorder, and cough while the Chinese traditional medicine claimed its usage for abdominal pains and icterus management [12].

Several therapeutic and pharmacologic properties of *C. longa* have recently been reported; antioxidant activity [13–15], cardiovascular and antidiabetic effects [16–18], inflammatory and edematic disorders [19–21], anticancer [22–25], antimicrobial [26, 27], hepatoprotection [24, 25], protection against Alzheimer's [28–30], and photo protector [12, 31]. Although majority of spices and medicinal herbs are commonly presumed to be safe, adverse effects occasionally arise after the consumption of herbal products. The statistical assessment carried out in 2013 by the Malaysian Adverse Drug Reaction Advisory Committee (MADRAC) in conjunction with the National Pharmaceutical Control Bureau and the Health Ministry revealed that 11,473 adverse drug reaction cases were recorded and 0.2% were attributed to herbal medicine [32]. In most nations, toxicity and safety evaluations are not compulsory as a basis for registering herbal product and absence of policies to regulate the production of herbal product contributed to ineffective, substandard, and possible hazardous consumption.

Despite the widely reported safe pharmaceutical and therapeutical applications of *C. longa,* there is no research finding reporting the embryotoxic and teratogenic effects. Therefore, in this study, the methanol extract of *Curcuma longa* was examined for its flavonoids content, concentration, and the *in vivo* embryotoxic and developmental effects using zebrafish embryos and larvae assay as a model.

2. Material and Methods

2.1. Plant Material. The rhizome of *C. longa* was planted at Taman Pertanian Universiti (University Agricultural Park), Universiti Putra Malaysia, and the plant harvested after 4 weeks of planting. It identity was confirmed by the residence botanist at the Biodiversity Unit, Institute of Bioscience (IBS), Universiti Putra Malaysia, and the plant was deposited in the IBS herbarium with voucher number SK 2849/15 assigned.

2.2. Animals and Treatment. The maintenance of zebrafish was done in accordance with OECD Fish Embryo Acute Toxicity Test (FET) Draft Guideline of 2006 and approval was given by Universiti Putra Malaysia Institutional Animal Care and Use Committee (UPM/IACUC/AUP No. R024/2014). Adult, wild type, zebrafish (> 6 months old) were bought from a local supplier (Aquatics International Sdn. Bhd. Subang, Shah Alam, Malaysia) and kept and maintained at least for 4 weeks for acclimatization to dechlorinated tap water prior to the initial spawning. The adult fish were maintained in 200 L aquarium tank equipped with a continuous flow water system with a maximum density of 1g fish/L tap water at 26±1°C with a constant light cycle of 14:10-hour light-dark at pH 6.8-7.2. They were fed in the morning with brine shrimps (Artemia) supplied by Great Salt Lake Artemia Cysts, Sanders Brine Shrimp Company, Ogden, USA, and at noon with dried flakes (TetraMin™ Blacksburg, VA). Nitrate, Nitrite, and Ammonia content were checked and maintained below the recommended levels using ammonia test kit. The condition of the fish health was daily monitored.

2.3. Production of Fertilized Eggs. The wild-type zebrafish (> 6 months old) with high potential to produce fertilized eggs were selected for spawning. The male and female zebrafish were maintained in aquarium tanks separately with a recommended water volume of 1 litre per fish and fixed 10 hours of dark periods and 14hrs of light. During the spawning period, excess water filtering and feeding were avoided and cleanness of aquaria and water quality were frequently monitored. Prior to the toxicity testing on embryos, standard method of breeding described in [33] was adopted. Eggs production was from the spawning groups (males and females) at ratio 2:3, respectively. The spawning tank contains 5 L of aquarium water fitted with spawning enhancers which consist of artificial plants and spawn trap (egg collector). Five spawning tanks of zebrafish were set up to have enough eggs needed for the experiment. Mating occurred within 30 mins in the morning at the time the light was turned on and eggs were collected; the brood zebrafish were subsequently returned back to their resting aquarium tanks. Thereafter, the selection of the fertilized embryos was done and was rinsed trice in embryo medium (E3M) and the fertilized embryos were kept at 28°C and allowed to develop for 6 hours.

2.4. Curcuma longa Extract Preparation. Curcuma longa rhizomes were harvested after 4 weeks of growth. The collected samples were washed and diced into smaller sizes and then dried to a constant weight at 60°C using Memmert Incubators-53L, Model INB 400. The dried sample was ground into a powder form and stored in a clean air tight container.

2.5. Extraction. About 0.5 g of each sample was accurately weighed into a reflux flask using GR 200 model of "AND" analytical balance, and 25 mL of 80% methanol was added to each sample. These mixtures were refluxed for 2 hours at 60°C using MTOPS extraction mantle. The resulting mixtures were filtered with Whatman No.1 filter paper, and filtrate was stored in an amber bottle (15 mL) and kept in -20°C refrigerator [34].

2.6. HPLC Separation and Quantification of Flavonoid Content in Curcuma longa Extract. Total flavonoid content extraction for HPLC analysis was carried out by hydrolysis method explained in [35]. About 0.25 g of dried sample was

extracted using 10 mL of 60% methanol in aqueous containing 20 mM sodium diethyldithiocarbamate (NaEDTC) as an antioxidant. Subsequently, 2.5 mL of 6 M HCl was then added to the mixture, and this was transferred to a round bottom flask and refluxed for 2hrs at 90°C for the hydrolysis process. The resulting extracts were cooled to room temperature and then filtered with 0.45 μm filter (Minisart RC15, Sartorius, Germany). Finally, 20 μL was transferred into HPLC vial for the identification and quantification of individual flavonoid using reverse-phase HPLC with 150 × 3.9 mm C_{18} symmetry column.

2.6.1. Preparation of Flavonoid Standards. The flavonoid standards were prepared for HPLC analysis by weighing 1.0 mg each and dissolving in 1.0 mL of methanol. The standard compounds dissolved were filtered through with 0.45 μm filter (Minisart RC15, Sartorius, Germany). Various concentrations of standard compounds were made to produce standard curve and these were transferred into HPLC vial to quantify the level of individual flavonoid using reverse-phase HPLC with 150 × 3.9 mm C_{18} symmetry column. Similarly, the same procedure was done for Apigenin with little modification which is 0.2 mL of dimethyl sulfoxide (DMSO) was used to dissolve 1.0 mg of Apigenin to make a total volume of 1.0 mL. All prepared flavonoid standards were stored in -20°C freezer.

2.6.2. HPLC Protocol for Flavonoid Separation. Using reverse-phase high performance liquid chromatography (HPLC), the rhizome extracts and flavonoid standards were analysed from the Thermo Scientific Ultimate 3000 RSLC System. It comprises Dionex Rapid Separation Autosampler with NCS-3500RS module with dual-gradient pump and DAD spectral scan. Diode Array detector was used for both UV variants and fluorescence. Separation of compounds was done using reverse-phase separations at ambient temperature using 150×3.9 mm I.D., 4 μm C_{18} Nova-Pak column from Waters (Milford, MA, USA). The mobile phase comprises 2% acetic acid (aqueous) for solvent A and 0.5% acetic acid (aqueous) plus acetonitrile (50:50 v/v) for solvent B and gradient elution was carried out as follows: 0-4 min 2% B, 4 – 40 min 100% B, 40–45 min 100% B, and 46–50 min 50% B. The mobile phase was filtered using 0.45 μm membrane filter under vacuum and column elution was at flow rate of 1 mL/min and detection at a wavelength of 254nm. Flavonoids were identified by comparing retention time and UV spectrum with commercial standards as shown in Figure 1, while the concentration of identified flavonoids was determined using standard curve prepared from commercial flavonoids [35].

2.7. Preparation and Dilutions of Tests Extracts. The extracts (*C. longa*) treatment concentration on zebrafish embryos and larvae were prepared in 24 wells plate separately by diluting 50 μL stock with 49,950 μL of embryo medium (E3M) to produce 125 μg in 0.1% DMSO for *C. longa* and each extract was further diluted 2× dilution factor (1:1) across the well to have 125, 62.5, 31.25, 15.63, and 7.8 μg in 5 mL of E3M having 0.1%. DMSO is the most frequently used solvent for delivery of extracts into zebrafish based assays. In zebrafish embryos and larvae experiment conducted, it was reported that 2.5% concentration of DMSO was well tolerated [36].

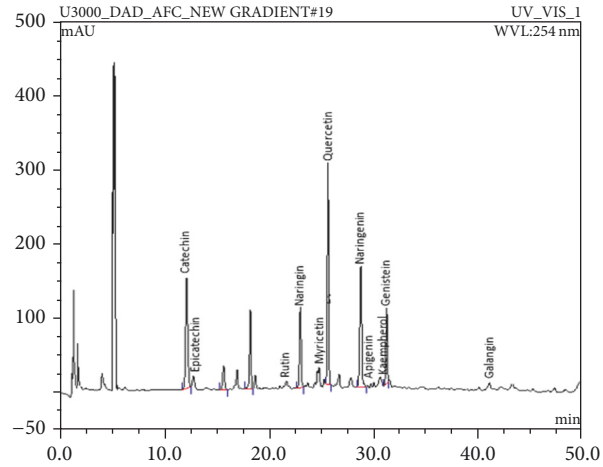

Figure 1: HPLC chromatogram of *Curcuma longa* rhizome extract at wavelength detection of 254 nm and 1.0 mL/min flow rate at different elution time for individual flavonoids detected.

2.8. C. longa Extract Fish Embryo Acute Toxicity (FET) Test on Zebrafish. Zebrafish embryos and larvae exposure to the extract were carried out in 24-well plate according to method described in [OECD. Test No. 236, 2006]. At 6-hour postfertilization (6hpf), selected healthy embryos were washed and examined under the microscope and fertilized embryos were selected for subsequent experiments. 12 fertilized eggs (n=12) at 6hpf for each concentration treatment were treated with the extract of *C. longa* and the experiment was performed in 3 independent replicates in a 24-well plate containing 2 mL of embryo media with 0.1% DMSO containing 125 μg (*C. longa*). It was serially diluted via 2-fold serial dilution to produce 5 different concentrations of extract *C. longa*. The control (untreated group) was exposed to 5mL of E3M containing only 0.1% DMSO. All the treated groups and control were repeated three times. The development endpoints that were evaluated on both embryos and larvae upon five-day exposure were egg coagulation, absence of heart beat in larvae, mortality of embryos and larvae, somites, tail detachment, otolith, eyes, and skeletal deformities were recorded each day for five days of exposure (Table 1). The larvae and embryos were subsequently examined with the aid of an inverted microscope (Nikon Eclipse TS 100) to check for malformation of body in each extract concentration for a period of five-day exposure. The malformed images of larvae and embryos were captured with Canon Digital camera (power shot A2300 HD). A minimum of 5 different concentrations of *C. longa* were tested for embryotoxic and teratogenic effects on the development of zebrafish embryos and larvae. Among the toxic effects assessed were egg coagulation, hatching, and heartbeat while developmental deformities in somites, tail detachment, otolith, blood circulation, heartbeat, motility, and skeletal mal-formation were the end of development evaluated for a time period of 5 days (120 hours) (Table 1).

Table 1: Morphological characteristics evaluated as measures for the teratogenic potency of *C. longa* at different time point.

Life Stage	Embryotoxicity	Developmental endpoints evaluated	Time point for observation of normal development. (normal = Score 0, abnormal = Score 1				
			24hr	48hr	72hr	96hr	120hr
Zebrafish Egg	Egg Coagulation		√	√	√	√	√
		Somites	√	√	√	√	√
		Tail detachment	√	√	√	√	√
		Otolith	X	√	√	√	√
		Eyes	X	√	√	√	√
		Heartbeat	X	√	√	√	√
		Blood Circulation	X	√	√	√	√
Hatching (Zebrafish larvae)	Larvae alive				√	√	√
		Hatch rate	X	√	√	√	√
		Skeletal deformities	X	√	√	√	√
		Motility	X	√	√	√	√

√, observation of normal development
X, no observation/no development
(i) Embryotoxic effect/time point: % of embryos with score 1 for motility at each time of observation
(ii) Teratogenic effect/time point: % of larvae with score 1 for any of the developmental endpoints at each time point of observation

2.8.1. Evaluations of Zebrafish Embryos Hatch Rate. The zebrafish embryos hatch rate was determined for five days at different concentration of *C. longa* (0–125 μg) extracts. The hatching of embryos was taken as the rupture of the chorion for the release of larvae using the inverted microscope.

2.8.2. Evaluations of Zebrafish Larvae Heart Beats. The heartbeat of larvae at five days treatment of *C. longa* extract (0–250 μg) was examined in this experiment. The heart beat counting was done by direct visual observation of the zebrafish larval cardiac ventricles using an inverted microscope connected with a computer and camera device. With a stop watch the heart rate was counted per minute.

2.9. Therapeutic Index (TI) Evaluations. Method described by Selderslaghs et al. (2009) was used for the data evaluation. At time points 24, 48, 72, 96, and 120hpf, mortality/embryotoxicity and morphological changes of the embryos were assessed using inverted microscope (Nikon Eclipse TS 100). Scores were assigned for each characteristic in a binominal manner ('1' was assigned for abnormal characteristics and '0' was assigned for normal). Based on the score assigned for particular characteristics, an overall score for percentage effect was created for each treatment in the experiment. An embryo is thought-out to either be normal (all score = 0), malformed, or dead for surviving animal (score = 1). In addition, effects were taken as a function of time.

When an increase in mortality is recorded at later time points, malformations incidences were determined as the addition of the incidence at the previous time point for dead larvae/embryos and the incidence for living embryos/larvae at that time. Hence every individual in the experiment was assigned scores for both malformation and mortality at a particular time points. This led to the determination of effective percentage for each concentration at each time point. The embryo toxicity percentage was determined as the ratio of dead embryos and/or larvae over the number of total embryos (12 fertilized eggs) at the exposure start time. Moreover, malformation percentage for 24, 48, 72, 96, and 120 hpf was determined as the ratio of malformed embryos and/or larvae over embryos number that were alive at 24 hpf. Therefore, the resulting output was made up of the cumulative percentage for each time point for observed individual that were dead or malformed.

2.10. Dose-Response Analysis. Using Graph Pad prism, version 5.0, the resulting data from minimum of three independent experiments (n=3) each with twelve (12) replicates (1 embryo per well) per concentration, concentration-response curves for malformed, and mortality for each time point was created. The variable shape obtained from the sigmoidal curves adequately fitted the data. The bottom and top curve were set to 0 and 100, respectively, with the requisite that percentage near 0 and 100 for effects falls within the concentration range. This concentration-response curve was used in determining the EC_{50} (teratogenic effect) and LC_{50} (lethal/Embryotoxic effects) values. These were derived from four parameter equation describing the curve as follows:

$$Y = \text{Bottom} + \left(\text{Top} - \frac{\text{Bottom}}{1} + 10^{\exp.\left(\log EC_{50} - X\right) \times \text{Hill slope}}\right) \quad (1)$$

where

Y is response (percentage of death or malformed individual).

X is log of concentration of the test substance.

Table 2: Quantified flavonoids in the rhizome extracts of *C. longa* using gradient ration of 2% acetic acid (aqueous) to acetonitrile detected at 254 nm.

Standards	Sample Concentrations (μg/mL)										
	Apigenin	Catechin	Epicatechin	Genistein	Kaempherol	Myricetin	Naringenin	Naringin	Quercetin	Rutin	Galangin
C. longa	151.46	3531.34	688.70	63.22	101.61	76.50	523.83	3.01	9.43	112.96	6.54

Table 3: LC_{50}, EC_{50} (mean values of 3 independent experiments) and TI values as derived from the concentrations-response curves for *C. longa*.

	C. longa (n=3)		
	LC_{50} (μg)	EC_{50} (μg)	TI(LC_{50}/EC_{50})
24 hpf	92.415	85.205	1.09
48 hpf	79.196	72.870	1.09
72 hpf	68.316	62.846	1.09
96 hpf	56.677	55.600	1.01
120 hpf	55.895	55.396	1.00

Note: hpf, hours postfertilization

Using calculated LC_{50} and EC_{50} values, a teratogenic index (TI) was calculated as the ratio of LC_{50}/EC_{50} for each time point. The higher the TI values are, the more the teratogenic effect of the extract tested is specific compared to overall embryotoxicity, as measured by the organism mortality.

2.11. Data Analysis. Results are presented as mean values ± SEM (n=12) from minimum of 3 independent experiments. With t-test, one-way of ANOVA, the statistical significance was determined and then Turkey's post hoc test was applied using the GraphPad Prism ver.5. Differences were considered significant at $p<0.05$.

3. Results

3.1. HPLC Analysis of C. longa Extract. The results revealed the presence of certain flavonoids and their concentrations in *C. longa* (Table 2). Catechin, epicatechin, and naringenin were the three most abundant flavonoid compounds detected with concentrations of 3,531.34, 688.70, and 523.83 μg/mL, respectively. Meanwhile, the least three detected flavonoids were naringin, galangin, and quercetin with amount of concentration of 3.01, 6.54, and 9.43 μg/mL, respectively (Table 2).

3.2. Morphological Characteristics Evaluated as Measure for Toxicity Potency of C. longa Extract on Zebrafish Larvae and Embryos. At 24-hour postfertilization (hpf), the embryos were incubated with *C. longa* extract at various concentrations; there was no observable effects at this time point and no hatching of embryo was observed. At 48 hpf, hatching of embryos was observed but no observable effect was noticed in 7.80, 15.63, and 31.25 μg/mL concentrations while, at 62.50 μg/mL, bend trunk was observed in some of the group and unhatched darkened embryos were observed in 125.0 μg/mL. At 72hpf, dead hatched larvae were observed at 125.0 μg/mL and morphological deformity such as stunted growth and bend trunk were seen at 62.50 μg/mL concentration. At 96 and 120hpf, kink and bend tail were observed respectively. Dead unhatched embryos were also discovered (Figure 2). For all the concentrations of extract tested, the toxicity effect on each individual was concentration-dependent. Using the percentage of the affected individual (malformation for any observed characteristics) for each concentration, concentration-response curve was produced for each time point (Figure 3). The LC_{50} (for embryotoxic effects/lethality) and EC_{50} (for particular teratogenic effects) data were obtained for the concentration-response curves for all time evaluated based on a minimum of 3 separate experiments (Table 3). The distance between the embryotoxicity and malformation concentration-response curves is taken as a measure of the specific teratogenicity of *C. longa* extract at the time points evaluated. This is also demonstrated by the therapeutic Index (TI) values which are calculated as the ratio of LC_{50}/EC_{50} (Table 2). In addition, mortality was observed as a shift to left (lower concentration) as a function of time (Figure 3).

3.3. The Effects of C. longa Extract Concentrations on the Embryos Hatch Rate. The hatching rate of zebrafish embryos exposed to varying concentrations of *C. longa* extract displayed delayed hatching at higher concentration of 62.50 μg/mL while no hatching was observed at 125.0 μg/mL as a result of embryos mortality (Figure 2). At 48 hpf, 80% of the embryos were hatched in 15.63 and 31.25 μg/mL concentrations while 100% hatching rate was observed in 7.80 μg/mL which is similar to what was obtained in the control group (Embryos medium, EM) (Figure 4).

3.4. The Effect of C. longa Extract on the Heartbeat of Zebrafish Larvae. The heartbeat of hatched larvae exposed to different concentrations of *C. longa* extract shows no significant difference in the mean heartbeat rate of the control larvae in the concentration range of 7.80, 15.63, 31.25, and 62.50 μg/mL (Figure 5). On the other hand, there was no heartbeat

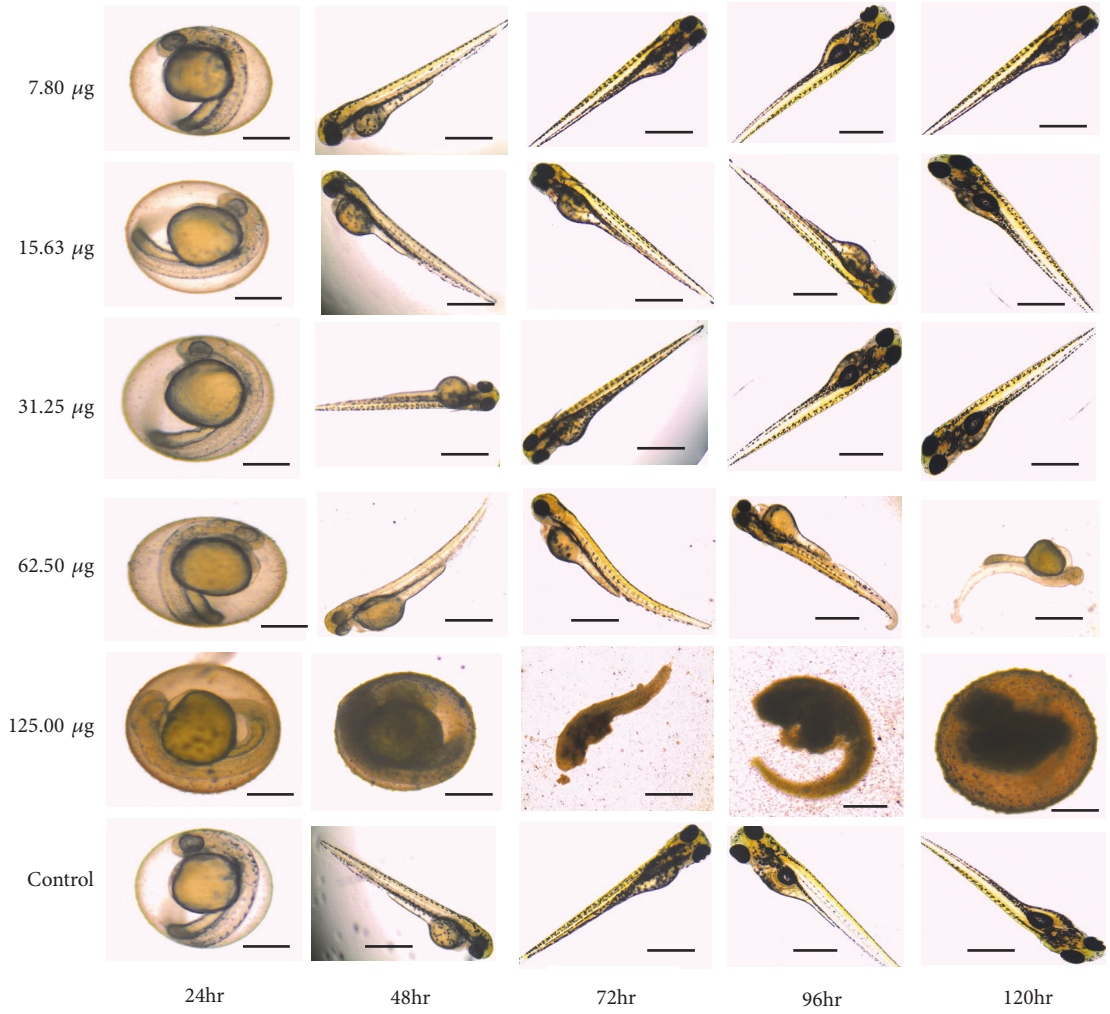

FIGURE 2: Morphological characteristics assessed as a measure for zebrafish embryotoxicity and teratogenicity of *C. longa* extract at different time point. At 125 μg the embryos are shown inside the chorion because they died during development and did not reach the stage corresponding to the control.

observed at higher concentration range from 125.0 μg/mL above due to mortality of embryos and larvae (Figure 5).

4. Discussion

Fetal development is a highly organized process in which complex changes are coordinated sequentially in time and changes at the molecular and cellular levels are integrated to enable manifestation of a particular phenotype in the whole organism. Assessing the embryotoxic and teratogenic toxicity of therapeutic plants on the development of the foetus is important as several products derived from herbal plants claimed to have pharmacological effects are gaining popularity in the global health market without information on their toxicology profile.

This research reveals the detection and concentration of some flavonoids such as Apigenin, Catechin, Epicatechin, Genistein, Kaempherol, Myricetin, Naringenin, Naringin, Quercetin, Rutin, and Galangin in the extract of *C. longa* (Table 2) by HPLC analysis. This set of detected flavonoids has been reported to possess some health benefits like antioxidant [37], antifungal, and antileishmanial [38]. Kaempherol was reported by Choi et al., [39] to inhibit thrombosis and platelet activation while rutin isolated from *Dendropanax morbifera* L. was also discovered to have antithrombotic effect [40]. Furthermore, dietary flavonoids have also been implicated in the amelioration of cataract induced by sugar [41]. Also, the effects of *C. longa* extract on the development of zebrafish embryos and larvae were investigated. The effect of curcumin at different concentrations on zebrafish embryo and larvae had been previously studied by [42] and their findings show a dose-dependent toxic effect of curcumin exposure. At 15 μM of curcumin, all the embryos were reportedly dead within 2 days of incubation and all larvae died at 10 μM of curcumin. They further investigated the safety of other polyphenolic compounds such as resveratrol, quercetin, and rutin. Unlike curcumin, no toxicity or teratogenic effect was observed in all the polyphenolic compounds tested suggesting that

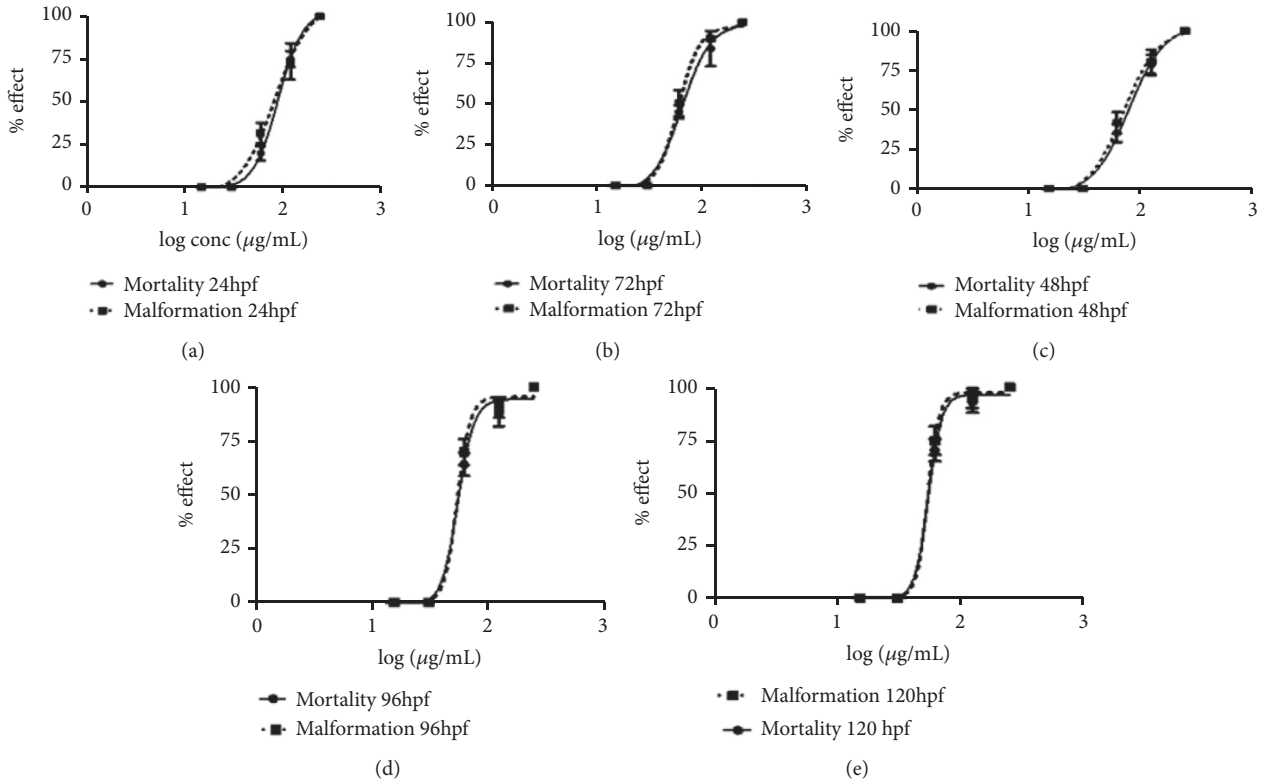

Figure 3: (a-e). Concentration-response curves for malformation and mortality of zebrafish embryos and larvae at different hours of postfertilization (hpf) in different *C. longa* extract concentrations (15.63, 31.25, 62.50, 125.0, and 250.0 μg/mL).

the embryotoxic and teratogenic effects observed in this study may not have been caused by the detected flavonoid compounds in the *C. longa* extract.

However, the findings of Chen et al. [43] reported that synthetic flavonoids such as 7-hydroxyflavone, 6-methoxyflavone, 7-methoxyflavon, 7-aminoflavone, and Kaempherol exerted more toxicity on zebrafish larvae as compared to flavone. This suggests that synthetic flavonoids might be toxic at higher concentrations; therefore caution should be taken when consuming them. The toxicity assessment of methanol extract for *C. longa* reveals embryotoxic effect on the zebrafish embryo at higher concentration of 125.0 μg/mL coupled with physiological malformation of larvae development as seen in Figure 2. The deformities were observed to be concentration-dependent (higher concentrations) and increase as the days of exposure increase. The fertilized embryos were exposed to different concentrations of *C. longa* extract ranging from 7.80 ug/mL to 125.0 ug/mL. At 24 hpf no hatching occurred and there was no observable toxicity effect on embryos in all concentrations when compared with the control group. Meanwhile, at 48 hpf hatching of embryo was observed in all concentrations and control group except for 125.0 ug/mL which shows delayed hatching or morbidity of embryos. This suggests possible embryotoxic effect of methanol extract of *C. longa* at higher concentrations. Curcumin has been experimentally reported as the most active and abundant compound present in *Curcuma longa* [44]. Dose-dependent toxicity effects of curcumin exposed to zebrafish were previously observed and the results showed mortality in embryos at third day of incubation at a concentration of 7.5μM of curcumin and producing deformities in zebrafish larvae [45], which is similar to what is reported in this study. This could possibly be explained that as the exposure of the extract is prolonged with increase in days of exposure, there is an increase in the accumulation of the extract until it reaches a concentration that can induce toxicity in the embryos and larvae. The result from this study is similar to the findings of [46]; they reported that natural state turmeric exhibited toxicity at higher concentrations on developing embryos.

Also, at higher concentration of 62.50 μg/mL teratogenic effects in the form of deformities in body development were recorded, displaying malformations such as kink tail, bend trunk, physiological curvature, and yolk sac edema after 48hpf. The findings of [47] reported slight toxicity at oral consumption and moderate toxicity at intraperitoneal administration of essential oil extracted from oil of *C. longa* cultivated in South western Nigeria in a model mice whereas at lower concentrations of 7.80 ug/mL–31.25ug/mL no observable malformation was seen (Figure 2) confirming the safety of *C. longa* extract on zebrafish larvae development at lower concentrations [48]. This finding evidenced a significant increase in toxicity effect after hatching at 48hpf resulting in reduction in survival rate, physiological malformation, and delayed rates of hatching.

At the concentration of 125 ug/mL (Figure 2), an increase in embryo toxicity was observed to be dependent on the time of exposure to extract, and as the time of exposure increases, a decrease in the survival rate of embryo in the chorion

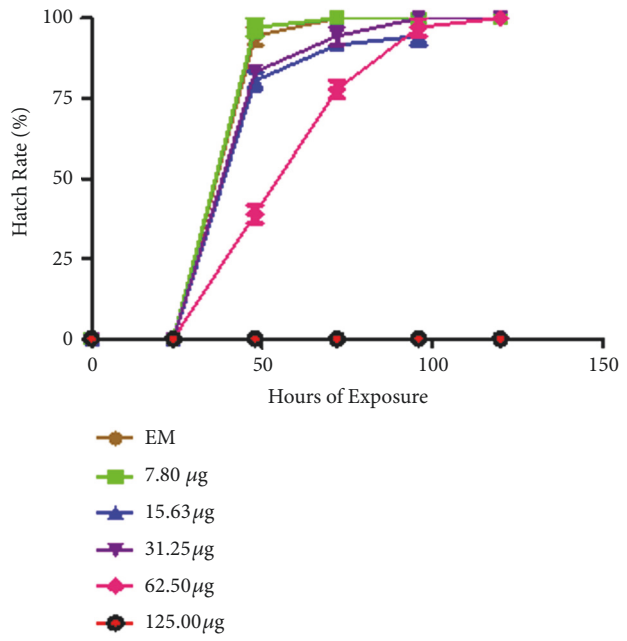

Figure 4: Hatching of zebrafish embryos on exposure to *Curcuma longa* extract.

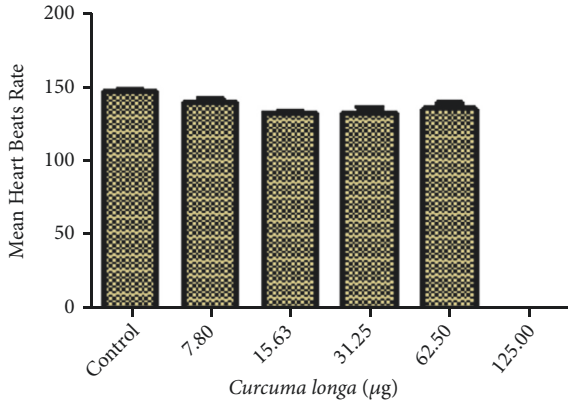

Figure 5: Effects of *Curcuma longa* extract on zebrafish larvae heartbeat. No significant difference at $p<0.05$ between the control and the tested concentrations group.

was observed. This result suggested that the accessibility of extract to embryo increases as the time of exposure prolongs, leading to the observed toxicity. This could be as a result of weakened or damaged embryo protective layer (chorion). In previous experiment conducted by [49], their findings show continuous changes in the protective layer of zebrafish embryo as the age of development advances. They concluded that this could be as a result of the changes in the profile of the chorion protein which might have caused an increase in the opening or widening of the chorion pore channel permitting greater influx of external solute. Furthermore, the effect of the extract on the heartbeat rate of the survive larvae shows no significant difference (Figure 5) when compared with the control and similar result was previously reported by [46], their finding revealed no significance difference in the heart rate of zebrafish embryos treated with raw turmeric and the control. However, the pure curcumin treated embryos demonstrated increased heart rate.

The toxicity effect of curcumin on the proliferation and embryonic development of mouse blastocyst had been previously investigated by [50]. They reported a 7.5-fold higher cell death in curcumin treated blastocysts relative to the control through the generation of ROS and Mitochondria-Dependent apoptotic signaling pathway. On the other hand, recent review on the bioavailability of curcumin and its effects on birth defects was reported by [51]. Their report described the role of curcumin as a scavenger of ROS, which was implicated by [50] as the cause of blastocyst death in mouse. The findings of [51] show that curcumin can help ameliorate the toxic effects of certain drugs with teratogenic effects prescribe during pregnancy due to their ability to scavenge ROS.

The concentration-response curve of malformation and mortality of zebrafish embryos and larvae at different time points plotted to obtain the EC_{50} and LC_{50}, respectively (Figure 3). The ratio of LC_{50}/EC_{50} produces the therapeutic index (TI) values for each day of treatment. The TI values are used for ranking the teratogenic effects of any toxic compound; i.e., the higher the TI value is, the greater the teratogenic potential a compound would display [52]. Hence, for this research, the TI values obtained for the 5-day treatment were in close range, suggesting the same teratogenic effects throughout the experiment. That is to say, once the deformities in the development are established it cannot be reversed.

5. Conclusion

This present research has shown that medicinal herb with potential therapeutic effect could still possess certain toxic effects on embryos and development of larvae especially at higher dosage. Since this extract is usually consumed in their crude form, other phytochemical compounds present in most medicinal plants could subdue the beneficial effect of the extract. Therefore, detailed toxicity assessment should be carried out to establish the safety of extract on embryos and their development as samples confirmed to be safe to organs could still exert toxic effects on the embryo.

Abbreviations

DMSO: Dimethyl sulfoxide
HPLC: High performance liquid chromatography
OECD: Organisation for Economic Cooperation and Development
FET: Fish
hpf: Hour of postfertilization.

Data Availability

We do not have any data from our research to be deposited in any public data repository. The tables, figures (photos), and graphs data used to support the findings of this study are included within the article.

Conflicts of Interest

No conflicts of interest are declared by the authors.

Authors' Contributions

All authors contributed equally to this work.

Acknowledgments

We acknowledge the staff of Chromatography Laboratory, Agro-Biotechnology Institute (ABI), Malaysia, for their HPLC technical support and, also, the staff of Taman Pertanian Universiti (University Agricultural Park) and the resident botanist of the Biodiversity Unit, Institute of Bioscience (IBS), Universiti Putra Malaysia. This research was funded by Universiti Putra Malaysia (Project no. GP-IPS/2016/9481300).

References

[1] P. D. Al-Snafi, "Beneficial medicinal plants in digestive system disorders (part 2): plant based review," *IOSR Journal of Pharmacy (IOSRPHR)*, vol. 06, no. 07, pp. 85–92, 2016.

[2] K. N. Venugopala, V. Rashmi, and B. Odhav, "Review on natural coumarin lead compounds for their pharmacological activity," *BioMed Research International*, vol. 2013, Article ID 963248, 14 pages, 2013.

[3] P. Mikaili, S. Maadirad, M. Moloudizargari, S. Aghajanshakeri, and S. Sarahroodi, "Therapeutic uses and pharmacological properties of garlic, shallot, and their biologically active compounds," *Iranian Journal of Basic Medical Sciences*, vol. 16, no. 10, pp. 1031–1048, 2013.

[4] T. Lavecchia, G. Rea, A. Antonacci, and M. T. Giardi, "Healthy and adverse effects of plant-derived functional metabolites: the need of revealing their content and bioactivity in a complex food matrix," *Critical Reviews in Food Science and Nutrition*, vol. 53, no. 2, pp. 198–213, 2013.

[5] C.-H. Cottart, V. Nivet-Antoine, and J.-L. Beaudeux, "Review of recent data on the metabolism, biological effects, and toxicity of resveratrol in humans," *Molecular Nutrition & Food Research*, vol. 58, no. 1, pp. 7–21, 2014.

[6] M. Kifayatullah, M. S. Mustafa, P. Sengupta, M. M. Sarker, A. Das, and S. K. Das, "Evaluation of the acute and sub-acute toxicity of the ethanolic extract of Pericampylus glaucus (Lam.) Merr. in BALB/c mice," *Journal of Acute Disease*, vol. 4, no. 4, pp. 309–315, 2015.

[7] N. A. Shah, M. R. Khan, and A. Nadhman, "Antileishmanial, toxicity, and phytochemical evaluation of medicinal plants collected from Pakistan," *BioMed Research International*, vol. 2014, 2014.

[8] T. Melchardt, T. Magnes, L. Weiss et al., "Liver toxicity during temozolomide chemotherapy caused by Chinese herbs," *BMC Complementary and Alternative Medicine*, vol. 14, no. 1, article 115, 2014.

[9] H. Nasri and H. Shirzad, "Toxicity and safety of medicinal plants," *Journal of Herbmed Pharmacology*, vol. 2, no. 2, pp. 21-22, 2013.

[10] M. S. Easmin, M. Z. I. Sarker, S. Ferdosh et al., "Bioactive compounds and advanced processing technology: Phaleria macrocarpa (sheff.) Boerl, a review," *Journal of Chemical Technology and Biotechnology*, vol. 90, no. 6, pp. 981–991, 2015.

[11] T. van Andel and L. G. Carvalheiro, "Why urban citizens in developing countries use traditional medicines: the case of Suriname," *Evidence-Based Complementary and Alternative Medicine*, vol. 2013, Article ID 687197, 13 pages, 2013.

[12] H. P. T. Ammon and M. A. Wahl, "Pharmacology of *Curcuma longa*," *Planta Medica*, vol. 57, no. 1, pp. 1–7, 1991.

[13] S. Dall'Acqua, M. Stocchero, I. Boschiero et al., "New findings on the in vivo antioxidant activity of Curcuma longa extract by an integrated 1H NMR and HPLC-MS metabolomic approach," *Fitoterapia*, vol. 109, pp. 125–131, 2016.

[14] K. Violet, F. Peter, and A.-W. Yasser, "In vitro modulation of pancreatic insulin secretion, extrapancreatic insulin action and peptide glycation by Curcuma longa aqueous extracts," *Journal of Experimental and Integrative Medicine*, vol. 4, no. 3, pp. 187–193, 2014.

[15] M. M. Salahshooh, S. M. R. Parizadeh, A. Pasdar et al., "The effect of curcumin (Curcuma longa L.) on circulating levels of adiponectin in patients with metabolic syndrome," *Comparative Clinical Pathology*, vol. 26, no. 1, pp. 17–23, 2017.

[16] B. Kocaadam and N. Şanlier, "Curcumin, an active component of turmeric (curcuma longa), and its effects on health," *Critical Reviews in Food Science and Nutrition*, vol. 57, no. 13, pp. 2889–2895, 2015.

[17] A. M. Neyrinck, M. Alligier, P. B. Memvanga et al., "*Curcuma longa* extract associated with white pepper lessens high fat diet-induced inflammation in subcutaneous adipose tissue," *PLoS ONE*, vol. 8, no. 11, pp. 1–10, 2013.

[18] S. S. Boyanapalli and A. T. Kong, "'Curcumin, the king of spices': epigenetic regulatory mechanisms in the prevention of cancer, neurological, and inflammatory diseases," *Current Pharmacology Reports*, vol. 1, no. 2, pp. 129–139, 2015.

[19] R. Uchio, Y. Higashi, Y. Kohama et al., "A hot water extract of turmeric (Curcuma longa) suppresses acute ethanol-induced liver injury in mice by inhibiting hepatic oxidative stress and inflammatory cytokine production," *Journal of Nutritional Science*, vol. 6, article e3, 2017.

[20] P. Dulbecco and V. Savarino, "Therapeutic potential of curcumin in digestive diseases," *World Journal of Gastroenterology*, vol. 19, no. 48, pp. 9256–9270, 2013.

[21] L. Azmi, S. K. Ojha, and C. V Rao, "Curcumin: boon for human being," *World Journal of Pharmacy and Pharmaceutical Sciences*, vol. 4, no. 6, pp. 239–249, 2015.

[22] M. M. Yallapu, S. Khan, D. M. Maher et al., "Anti-cancer activity of curcumin loaded nanoparticles in prostate cancer," *Biomaterials*, vol. 35, no. 30, pp. 8635–8648, 2014.

[23] G.-Q. Wu, K.-Q. Chai, X.-M. Zhu et al., "nti-cancer effects of curcumin on lung cancer through the inhibition of EZH2 and NOTCH1," *Oncotarget*, vol. 5, no. 18, 2016.

[24] S. M. Salama, M. A. Abdulla, A. S. AlRashdi, S. Ismail, S. S. Alkiyumi, and S. Golbabapour, "Hepatoprotective effect of ethanolic extract of Curcuma longa on thioacetamide induced liver cirrhosis in rats," *BMC Complementary and Alternative Medicine*, vol. 13, article no. 56, 2013.

[25] J. Trujillo, Y. I. Chirino, E. Molina-Jijón, A. C. Andérica-Romero, E. Tapia, and J. Pedraza-Chaverrí, "Renoprotective effect of the antioxidant curcumin: recent findings," *Redox Biology*, vol. 1, no. 1, pp. 448–456, 2013.

[26] P. R. Baldwin, A. Z. Reeves, K. R. Powell et al., "Monocarbonyl analogs of curcumin inhibit growth of antibiotic sensitive

and resistant strains of Mycobacterium tuberculosis," *European Journal of Medicinal Chemistry*, vol. 92, pp. 693–699, 2015.

[27] R. Ashok, A. Ganesh, and K. Deivanayagam, "Bactericidal effect of different anti-microbial agents on fusobacterium nucleatum biofilm," *Cureus*, vol. 9, no. 6, 2017.

[28] Y. Kim, Y. You, and H.-G. Yoon, "Hepatoprotective effects of fermented *Curcuma longa* L. on carbon tetrachloride-induced oxidative stress in rats," *Food Chemistry*, vol. 151, pp. 148–153, 2014.

[29] T. Ahmed and A. Gilani, "Therapeutic potential of turmeric in alzheimer's disease: curcumin or curcuminoids?" *Phytotherapy Research*, vol. 28, no. 4, pp. 517–525, 2014.

[30] L. Wang, T. Wu, C. Yang et al., "Network pharmacology-based study on the mechanism of action for herbal medicines in Alzheimer treatment," *Journal of Ethnopharmacology*, vol. 196, pp. 281–292, 2017.

[31] M. M. Donglikar and S. L. Deore, "Development and evaluation of herbal sunscreen," *Pharmacognosy Journal*, vol. 9, no. 1, pp. 83–97, 2017.

[32] BPFK, "Annual Report of the National Centre for Adverse Drug Reaction Monitoring," 2013.

[33] OECD, *Fish Embryo Acute Toxicity (FET)*, Test No. 236, OECD Publication, 2006.

[34] H. Misbah, A. A. Aziz, and N. Aminudin, "Antidiabetic and antioxidant properties of Ficus deltoidea fruit extracts and fractions," *BMC Complementary and Alternative Medicine*, vol. 13, 2013.

[35] A. Crozier, E. Jensen, M. E. J. Lean, and M. S. McDonald, "Quantitative analysis of flavonoids by reversed-phase high-performance liquid chromatography," *Journal of Chromatography A*, vol. 761, no. 1-2, pp. 315–321, 1997.

[36] J. Maes, L. Verlooy, O. E. Buenafe, P. A. M. de Witte, C. V. Esguerra, and A. D. Crawford, "Evaluation of 14 organic solvents and carriers for screening applications in zebrafish embryos and Larvae," *PLoS ONE*, vol. 7, no. 10, pp. 1–9, 2012.

[37] A. A. Alafiatayo, A. Syahida, and M. Mahmood, "Total antioxidant capacity, flavonoid, phenolic acid and polyphenol content in ten selected species of Zingiberaceae rhizomes," *African Journal of Traditional, Complementary, and Alternative Medicines*, vol. 11, no. 3, pp. 7–13, 2014.

[38] D. R. Alves, S. Maia De Morais, F. Tomiotto-Pellissier et al., "Flavonoid composition and biological activities of ethanol extracts of caryocar coriaceum Wittm., a native plant from caatinga biome," *Evidence-Based Complementary and Alternative Medicine*, vol. 2017, Article ID 6834218, 7 pages, 2017.

[39] J.-H. Choi, S.-E. Park, S.-J. Kim, and S. Kim, "Kaempferol inhibits thrombosis and platelet activation," *Biochimie*, vol. 115, pp. 177–186, 2015.

[40] J.-H. Choi, D.-W. Kim, S.-E. Park et al., "Anti-thrombotic effect of rutin isolated from Dendropanax morbifera Leveille," *Journal of Bioscience and Bioengineering*, vol. 120, no. 2, pp. 181–186, 2015.

[41] K. K. Patil, R. J. Meshram, N. A. Dhole, and R. N. Gacche, "Role of dietary flavonoids in amelioration of sugar induced cataractogenesis," *Archives of Biochemistry and Biophysics*, vol. 593, pp. 1–11, 2016.

[42] J. Wu, C. Lin, T. Lin, C. Ken, and Y. Wen, "Curcumin affects development of zebrafish embryo," *Biological & Pharmaceutical Bulletin*, vol. 30, no. 7, pp. 1336–1339, 2007.

[43] Y.-H. Chen, Z.-S. Yang, C.-C. Wen et al., "Evaluation of the structure-activity relationship of flavonoids as antioxidants and toxicants of zebrafish larvae," *Food Chemistry*, vol. 134, no. 2, pp. 717–724, 2012.

[44] E. Abdel-Lateef, F. Mahmoud, O. Hammam et al., "Bioactive chemical constituents of Curcuma longa L. rhizomes extract inhibit the growth of human hepatoma cell line (HepG2)," *Acta Pharmaceutica*, vol. 66, no. 3, pp. 387–398, 2016.

[45] R.-J. Shiau, P.-C. Shih, and Y.-D. Wen, "Effect of silymarin on curcumin-induced mortality in zebrafish (Danio rerio) embryos and larvae," *Indian Journal of Experimental Biology (IJEB)*, vol. 49, no. 7, pp. 491–497, 2011.

[46] R. E. Rajagopal, M. Balasubramanian, and S. Kalyanaraman, "Raw turmeric and pure curcumin: a comparison of embryonic cytotoxicity in zebrafish," *IJBCP International Journal of Basic & Clinical Pharmacology*, vol. 6, pp. 2020–2026, 2017.

[47] I. A. Oyemitan, C. A. Elusiyan, A. O. Onifade, M. A. Akanmu, A. O. Oyedeji, and A. G. McDonald, "Neuropharmacological profile and chemical analysis of fresh rhizome essential oil of Curcuma longa (turmeric) cultivated in Southwest Nigeria," *Toxicology Reports*, vol. 4, pp. 391–398, 2017.

[48] V. B. Liju, K. Jeena, and R. Kuttan, "Acute and Sub-chronic toxicity as well as mutagenic evaluation of essential oil from turmeric (Curcuma longa)," *Food and Chemical Toxicology*, vol. 53, pp. 52–61, 2013.

[49] M. K. Ali, S. P. Saber, D. R. Taite, S. Emadi, and R. Irving, "The protective layer of zebrafish embryo changes continuously with advancing age of embryo development (AGED)," *Journal of Toxicology and Pharmacology*, vol. 1, no. 2, 2017.

[50] C.-C. Chen, M.-S. Hsieh, Y.-D. Hsuuw, F.-J. Huang, and W.-H. Chan, "Hazardous effects of curcumin on mouse embryonic development through a mitochondria-dependent apoptotic signaling pathway," *International Journal of Molecular Sciences*, vol. 11, no. 8, pp. 2839–2855, 2010.

[51] A. Kumar and V. Bind, "Curcumin bioavailability issues and its effect on birth defects," *MOJ Bioequivalence & Bioavailability*, vol. 5, no. 2, 2018.

[52] I. W. T. Selderslaghs, A. R. Van Rompay, W. De Coen, and H. E. Witters, "Development of a screening assay to identify teratogenic and embryotoxic chemicals using the zebrafish embryo," *Reproductive Toxicology*, vol. 28, no. 3, pp. 308–320, 2009.

Hindawi
Evidence-Based Complementary and Alternative Medicine
Volume 2019, Article ID 4168126, 10 pages
https://doi.org/10.1155/2019/4168126

Research Article

Chinese Herbal Formula Feilin Vaginal Gel Prevents the Cervicitis in Mouse Model

Xin Mao[1], **Ronghua Zhao**[1], **Rongmei Yao**[1,2], **Shanshan Guo**[1], **Lei Bao**[1], **Yingjie Gao**[1], **Jing Sun**[1], **Yanyan Bao**[1], **Yujing Shi**[1] and **Xiaolan Cui**[1]

[1]*Institute of Chinese Materia Medica, China Academy of Chinese Medical Sciences, Beijing 100700, China*
[2]*College of Traditional Chinese Medicine, North China University of Sciences and Technology, Hebei 063210, China*

Correspondence should be addressed to Xiaolan Cui; cuixiaolan2812@126.com

Received 5 November 2018; Accepted 25 December 2018; Published 10 January 2019

Guest Editor: Arielle Cristina Arena

Cervicitis is a common sexually transmitted disease. In recent years, the abuse of antibiotic in the treatment of cervicitis results in the emergence of antibiotic-resistant bacteria; alternative strategies are needed to be developed. In this research, we investigated the effects of Feilin Vaginal Gel (FVG), a Chinese herbal formula, on the treatment of cervicitis. Two cervicitis models were optimized using BALB/c mouse; one *in vitro* model was established in HeLa cells. In *Chlamydia trachomatis*-induced cervicitis model, the high level of bacterial loads, the inflammation in tissue, and the cytokines in serum could be observed. With the administration of FVG, the bacterial loads in cervical mucus and cervix tissue could be significantly inhibited in dose-dependent manners. The pathological injury of cervix and vagina, as well as the levels of IL-2, IL-17, and MCP-1 in serum, could be mitigated by FVG. FVG reduced the number of inclusion induced by *C. trachomatis* in HeLa cells. In addition, the histological damage in *Escherichia coli* and *Staphylococcus aureus*-induced cervicitis model could be reduced by FVG. These results suggest that FVG is capable of treating cervicitis through the inhibition of pathogens and the regulation of host immune responses. FVG may contribute as an alternative agent for the treatment of cervicitis.

1. Introduction

Cervicitis is a common sexually transmitted disease with an inflammatory condition of the uterine cervix [1]. The infection of cervix starts from lower genital tract (vagina) and then develops into the pelvic inflammatory disease with ascending infection of the upper genital tract (uterus and fallopian tubes) and peritoneal cavity [2]. Cervicitis occurred frequently as an asymptomatic infection. Abnormal cervical or vaginal mucopurulent discharge and cervical ectopy may be the signs and symptoms of cervicitis in some patients [3]. However, serious cervicitis can lead to further infertility and ectopic pregnancy. Cervicitis is considered to be associated with the transmission of HIV infection and the development of cervical carcinomas [4].

Cervicitis can be induced by various pathogens such as *Chlamydia trachomatis*, *Neisseria gonorrhea*, *Mycoplasma genitalium*, *Mycoplasma hominis*, *Ureaplasma urealyticum*, *Trichomonas*, Herpes simplex virus, cytomegalovirus, and adenovirus [4]. *C. trachomatis* infection is reported to be the most frequent cause of cervicitis. More than 10% of women with cervicitis are diagnosed to be infected by *C. trachomatis* and the number of these infections continues to increase over the past decades [5]. *C. trachomatis* is Gram-negative obligate intracellular bacterium. Two forms of *C. trachomatis* can be found in its developmental cycle. Attachment of elementary bodies (EBs) to host cells mediates the invasion of *C. trachomatis*. Inside the host cells, *C. trachomatis* forms the reticulate bodies (RBs) and then RBs replicate within the cytoplasmic vacuole and finally form the inclusion [6].

Chlamydia can persist for a long time in uterine cervix without symptom. The infection may resolve spontaneously without treatment or may cause cervicitis. The clearance of *C. trachomatis* requires the responses of Th1 immunity [7, 8]. However, the responses of adaptive immunity may have a double-edged nature and bring tissue damage. The management of *C. trachomatis* infection is based on the treatment of the patients and their sexual partners with

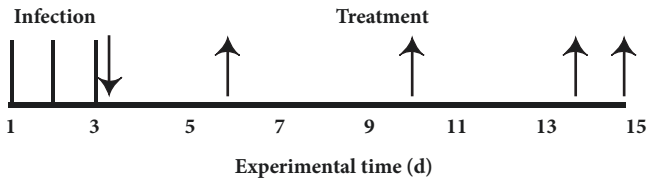

Figure 1: Schematic of the experimental timeline used to establish the cervicitis models.

macrolides. The abuse of antibiotic and false-positive diagnose may contribute to the emergence of antibiotic-resistant organisms. The antibiotic-resistant bacteria, on the other hand, lead to treatment failure [4, 5, 9]. After treatment with the antibiotic, 10%-20% of patients will suffer from reinfection within one year, which may be due to the absence of protective immunity against Chlamydia [10]. Considering these conditions, alternative strategies are needed to be developed.

Traditional Chinese Medicine (TCM) has a long history in treating gynecological diseases [11]. Feilin Vaginal Gel (FVG) is developed from a clinically used Chinese medicine formula that is used to treat the mucopurulent cervicitis. FVG consists of the following herbal medicines: Gentianae radix et rhizoma, Stemonae radix, Fraxini cortex, Paeoniae radix rubra, Dictamni cortex, and Glycyrrhizae radix et rhizome. According to the theory of TCM: FVG can be used to treat the accumulation of dampness and toxic materials induced abnormal vaginal discharge, such as profuse, fetid and yellowish leukorrhea, itching, and pain around the external genitalia [12]. The extraction, preparation, and quality control of FVG had been studied. The concentrations of gentiopicroside and paeoniflorin in FVG were analyzed to be approximately 5.90 mg/g and 8.96 mg/g, respectively [12].

In the present study, we tested the hypothesis that FVG could treat the cervicitis effectively. Mouse cervicitis models were established to evaluate the treatment of FVG. In the *C. trachomatis* infected mouse model, the bacterial loads, the pathological injury, and the levels of MCP-1, IL-2, and IL-17 in serum were evaluated. The inclusions in HeLa cells induced by *C. trachomatis* were enumerated *in vitro*. In addition, after being infected by the mixture of *Escherichia coli* and *Staphylococcus aureus*, the treatment of FVG was evaluated through the histological examination of the cervix.

2. Materials and Methods

2.1. Preparation of FVG. The six herbal medicines were extracted three times with boiling water and precipitated with alcohol to 70% (v/v) ethanol. The supernatant was concentrated with the rotary evaporator to a relative density of 1.30-1.35 (50°C) to get the Feilin extraction (FE, 5.62 g/g). The gel base was the mixture of carbopol 941 and xanthan gum. The extraction was mixed with the gel base to get FVG. The drug loading of FVG was 2.5 g/g, 1.25 g/g, and 0.625 g/g.

2.2. Bacterial Strains and Host Cell. Chlamydia trachomatis mouse pneumonitis strain Nigg II (ATCC® VR-123™), *Escherichia coli* (ATCC® 25922™), and *Staphylococcus aureus* (ATCC® 25923™) were obtained from American Type Culture Collection. *E. coli* and *S. aureus* were cultured in nutrient broth. Human cervix epithelial cell line HeLa (ATCC® CCL-2™) was purchased from Culture Collection of Chinese Academy of Medical Sciences and cultured in RPMI 1640 medium containing 10% FBS at 37°C in the presence of 5% CO_2. *C. trachomatis* N was propagated in HeLa cells. Before infection, infected HeLa cells (10^5 cells/mL) were disrupted and centrifuged. The supernatant was collected to get purified elementary bodies (EBs), which can be used to infect mice and HeLa cells directly.

2.3. Animal Infections and Treatment. 120 female BALB/c mice (18-20 g) were purchased from Charles River Laboratories China (Beijing, China). Animals were housed in a BSL2 barrier animal facility. All animal experimental procedures described here were by the permission of Institute of China Academy of Chinese Medical Sciences, Chinese Materia Medica, Ethic Committee. The ethic approval reference number is 20162019.

The cervix tissue of BALB/c mice was injured with angled needle under anesthesia. Mice were then inoculated with 50 μL of *C. trachomatis* N or the mixture of *E. coli* and *S. aureus* (10^9 CFU/mL). The mice were infected once a day and repeated for three days. 24 h after the last infection, the FVG was given into the mouse vagina using pipette (the volume of FVG was carefully controlled) at the dose of 2.2 g/kg, 1.1 g/kg, and 0.55 g/kg for 12 days. Policresulen suppositories (PS), as a positive control, was mixed with gel base and given at a dose of 16.5 mg/kg for 12 days. The control group and the model group were given an equal volume of gel base. On the 4^{th}, 8^{th}, and 12^{th} day of treatment, the cervical mucus was collected with the swab. On day 15, mice were anesthetized, blood samples were taken from aorta ventralis and the serum was separated. Mice were then killed by cervical dislocation under anesthesia and the cervix and vagina were removed. The schematic of the experimental time was shown in Figure 1.

2.4. ELISA Analysis of C. trachomatis N, IL-2, IL-17, and MCP-1. The swabs with cervical mucus were dispersed with an equal volume of PBS, the level of *C. trachomatis* N in PBS was analyzed with enzyme-linked immunosorbent assay (ELISA) kit (Meilian, Shanghai, China) according to the manufacturer's instruction (add 50 μL of sample and 50 μL of detection antibody to each well and incubate at 37°C for 1 hour; wash the wells, add 100 μL of HRP conjugate to each well, and incubate at 37°C for 0.5 hour; wash the wells, add 50 μL of chromogenic substrates to each well, and incubate

at 37°C for 0.5 hour; add 50 μL of stop solution to each well; read the absorbance of each well at 450 nm). The levels of IL-2, IL-17, and MCP-1in serum were determined by ELISA kit (Meilian, Shanghai, China) according to the manufacturer's instructions as described above.

2.5. RT-PCR Analysis of C. trachomatis N. Total RNA was extracted from the cervix using TRIzol (Invitrogen, California, USA); the expression of target genes was analyzed using One Step SYBR Prime Script RT-PCR Kit II (TaKaRa, Beijing, China) with Piko Real 96 (Thermo Fisher Scientific, Massachusetts, USA). The primers were used as follows: 16S rRNA forward primer, 5'-ACC CGT TGG ATT TGA GCG TA-3'; 16S rRNA reverse primer, 5'-GTT GAG CCC CGA GAT TTG AC-3'; GAPDH forward primer, 5'-GCT GAG TAT GTC GTG GAG T-3'; GAPDH reverse primer, 5'-GTT CAC ACC CAT CAC AAA C-3'. The relative expression of *C. trachomatis* N gene and mouse gene was calculated according to the $2^{-\Delta\Delta Ct}$ method.

2.6. Histological Examination. The tissues of mice were fixed with 10% formaldehyde, then embedded in paraffin and cut into slices for hematoxylin and eosin staining. The sections were visually evaluated by DMLB (Leica Camera AG, Wetzlar, Germany); two sections were prepared from each sample. The following criteria were applied for grading the pathological changes.

"-" Cervix and vagina epithelium show no hyperplasia and no inflammation and tissues are normal.

"+" Cervix and vagina epithelium have mild hyperplasia; connective tissue has mild segmental inflammation.

"++" Cervix and vagina epithelium have hyperplasia; connective tissue was infiltrated by inflammatory cells.

"+++" Cervix and vagina epithelium have significant hyperplasia and were infiltration of inflammatory cells; connective tissue was surrounded by diffuse inflammation and vascular congestion.

2.7. Host Cell Infection and Inclusion Stain. HeLa cells were seeded in 6-well plate with the density of 2×10^5 cells/well and cultured for 48 h. Then the cells were incubated with *C. trachomatis* N EBs contained medium. The plate was centrifuged at 32°C for 1h and continually cultured at 37°C in the presence of 5% CO_2 for 2h. The medium of infected cells was replaced with FE (500, 250, and 125 μg/mL) contained medium and incubated for another 48 h. After then, the cells were washed with PBS, fixed with methanol and stained with Giemsa. The inclusions in HeLa cells were captured by IX71 (Olympus, Tokyo, Japan) and enumerated.

2.8. Statistical Analysis. Statistical analyses were performed using GraphPad Prism v.6 (GraphPad Software, California, USA). All the data were normally distributed (Kolmogorov-Smirnov test). Inclusion number and histological scores were analyzed with the Mann-Whitney U test; others were analyzed with the unpaired t-test. A value of $p < 0.05$ was considered to be significant.

3. Results

3.1. FVG Inhibits the Level of C. trachomatis N in Cervical Mucus. EBs of *C. trachomatis* germinate and form the RBs after invading the host cells. The RBs begin to multiply after 7-21 days. Enzyme immunoassay is a commonly used nonculture method to diagnose the chlamydial infection [9]. We analyzed the level of *C. trachomatis* N in cervical mucus to evaluate the severity of mice infection.

At the early stage of *C. trachomatis* N infection, no significant change of the bacterial load was observed. 10 days after the first infection, the increase of *C. trachomatis* N in mice could be tested. On the 14th day, the level of the bacterial load was significantly higher than the control group (Figure 2(a)). With the successive treatment of FVG (2.2, 1.1, 0.55 g/kg), the level of *C. trachomatis* N in mice cervical mucus could be strongly inhibited in dose-dependent manners (Figures 2(c) and 2(d)).

3.2. FVG Inhibits the Load of C. trachomatis N in Cervix. In the diagnosis of chlamydial infection, the nucleic acid amplification technique including polymerase chain reaction (PCR) is more sensitive and specific than the enzyme immunoassay [13]. Hence, we further tested the load of *C. trachomatis* N in mice cervix with the RT-PCR method. On day 15, the expression of 16S rRNA of *C. trachomatis* N in mice was significantly higher than the control group (Figure 3). Treatment of FVG (2.2, 1.1 g/kg) for 12 days could strongly inhibit the load of *C. trachomatis* N in cervix (Figure 3).

3.3. FVG Diminishes the C. trachomatis N-Induced Cervicitis and Vaginitis. The infection of *C. trachomatis* in mice is an appropriate model for studying genital tract infections. The infection fails to induce severe upper tract genital pathology [14]. The pathology of cervix and vagina was analyzed to characterize the severity of *C. trachomatis* N infection.

As is shown in Figure 4, in the control group, the epithelial cells and connective tissue of cervix were normal, no hyperplasia or inflammation was observed. In the model group, cervix epithelial layers have hyperplasia and the inflammatory cells were infiltrated into the epithelium and connective tissue. After the treatment of FVG (1.1 g/kg), the pathological injury of cervix could be significantly reduced (Figure 4).

As is shown in Figure 5, in the control group, the vaginal epithelium was normal, no hyperplasia or inflammation was observed. In the model group, vaginal epithelium layers have hyperplasia and the inflammatory cells were infiltrated into the epithelium tissue. After the treatment of FVG (2.2, 1.1 g/kg), the injury of vagina could be significantly reduced (Figure 5).

3.4. FVG Reduces the Serum Cytokine Responses of C. trachomatis N Infection. The cytokines can be released by the epithelial cells and immune cells after the *C. trachomatis* infection, most of which come from Th1 cells. These cytokines contribute to the immune responses but induce the pathological damage [15]. The levels of cytokine in serum were tested

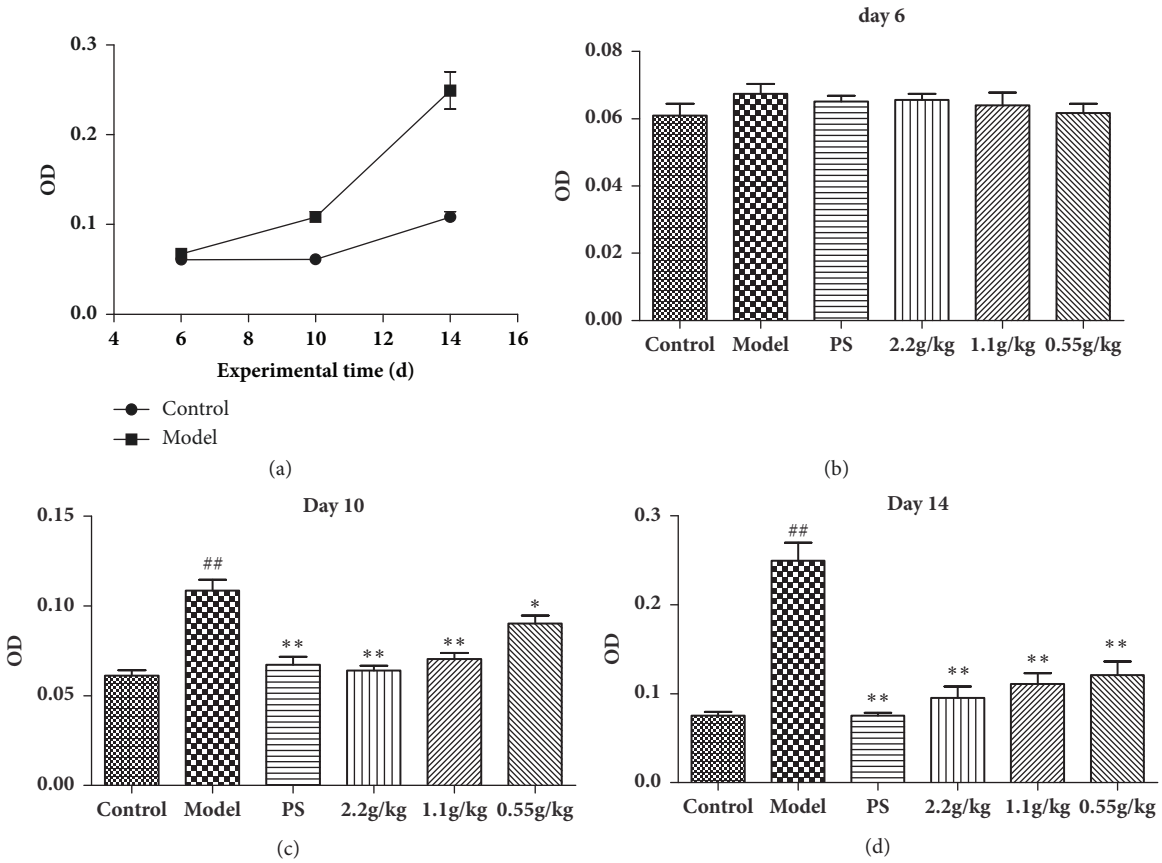

Figure 2: The FVG inhibit the level of *Chlamydia trachomatis* N in cervical mucus. (a) The level change of *C. trachomatis* N in the control group and the model group, (b-d) the effects of FVG on the level of *C. trachomatis* N on day 6 (b), day 10 (c), and day 14 (d). The results are mean±SEM, n=10, statistically significant $^{\#\#}p<0.01$: compared with control; $^{**}p < 0.01$ and $^{*}p < 0.05$: compared with model, determined by the unpaired t-test.

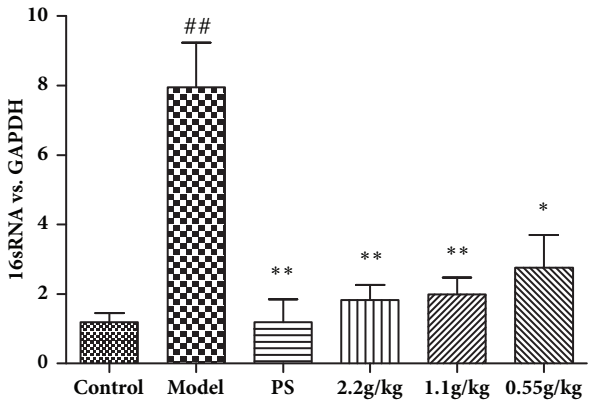

Figure 3: The FVG inhibit the load of *Chlamydia trachomatis* N in cervix. Relative level of *C. trachomatis* N in cervix tissues was assessed by RT-PCR. The results are mean±SEM, n=5, statistically significant $^{\#\#}p<0.01$: compared with control; $^{**}p < 0.01$ and $^{*}p < 0.05$: compared with model, determined by the unpaired t-test.

to support the histological examination results. On the 15th day, the levels of IL-2, IL-17, and MCP-1 were significantly upregulated (Figure 6). Three doses of FVG could effectively inhibit the release of IL-17 and MCP-1. The production of IL-2 could be downregulated by FVG at low doses (1.1 and 0.55 g/kg).

3.5. FVG Reduces the C. trachomatis N-Induced Inclusion Count In Vitro. The proliferation of *C. trachomatis* occurs in the host cells with the formation of RBs. Inclusion can be formed approximately 12 h after infection, which contains numbers of RBs [15]. The *in vitro* inhibition of FVG on the infection of *C. trachomatis* N was evaluated with the number of inclusion. After HeLa cells being incubated with *C. trachomatis* N for 48h, inclusions could be observed with the Giemsa stain. After treatment with FVG (FE), the number of inclusion was significantly downregulated in a dose-dependent manner (Figure 7).

3.6. FVG Reduce the Pathological Injury of Cervix Induced by E. coli and S. aureus. Even though *C. trachomatis* is reported to be the most common pathogen of cervicitis, anaerobes such as *E. coli*, *S. aureus*, and *Klebsiella pneumoniae* could be isolated in the cervicitis patients [5, 16]. A rat cervicitis model infected by the mixture of *E. coli*, *S. aureus*, and *N. gonorrhea* had been established in our previous work [17]. In the present

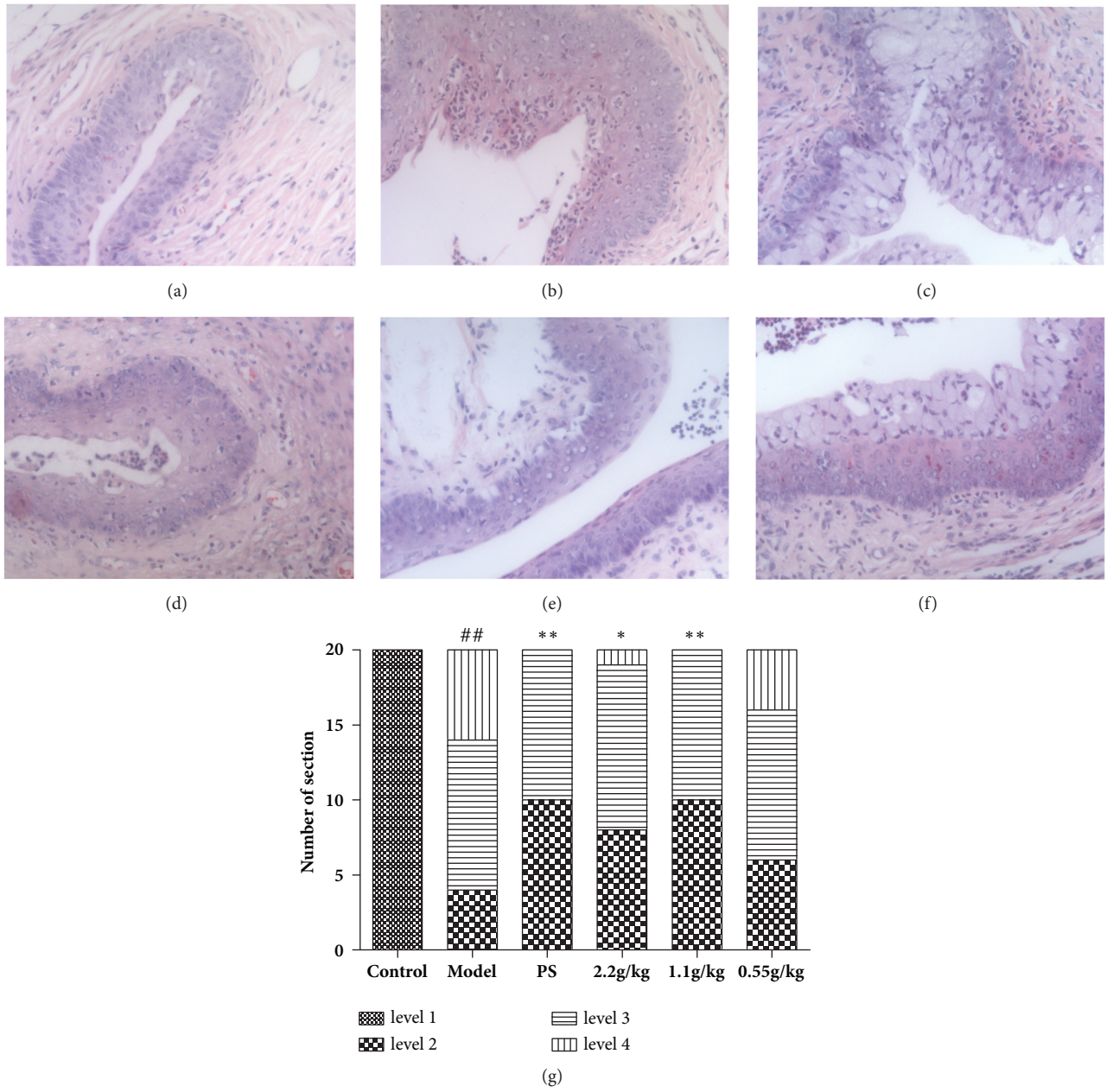

Figure 4: The FVG diminishes the *Chlamydia trachomatis* N-induced cervicitis. (a) Control group, (b) model group, (c) PS group, (d) FVG (2.2 g/kg) group, (e) FVG (1.1 g/kg) group, (f) FVG (0.55 g/kg) group, and (g) statistical analysis of histological examination. n=20, statistically significant $^{\#\#}p<0.01$: compared with control; $^{**}P < 0.01$ and $^{*}P < 0.05$: compared with model, determined by the Mann-Whitney U test.

research, a mice model infected by the mixture of *E. coli* and *S. aureus* was optimized. 14 days after the first infection, the cervix was proved to be severely infected.

In the control group, the cervical epithelium was normal and no hyperplasia or inflammation was observed. In the model group, inner layers of cervical epithelium have hyperplasia, and the inflammatory cells (neutrophil and eosinophil) were severely infiltrated into the epithelium tissue. After the treatment of FVG (2.2 and 1.1 g/kg), the inflammation of cervix could be significantly inhibited (Figure 8).

4. Discussion

The diagnosis of cervicitis is difficult due to the lack of the obvious symptom. In some patients, abnormal mucopurulent discharge and cervical ectopy could be observed [3]. Many mammal models of cervicitis had been established in the last decades. Macaques, rats, and mice could be used to establish the cervicitis model. Both bacteria (*C. trachomatis*) and chemical compounds (phenol, acetic acid) could be used to induce the cervicitis [17–20]. In this research, two mouse models were optimized. After infection with *C. trachomatis*

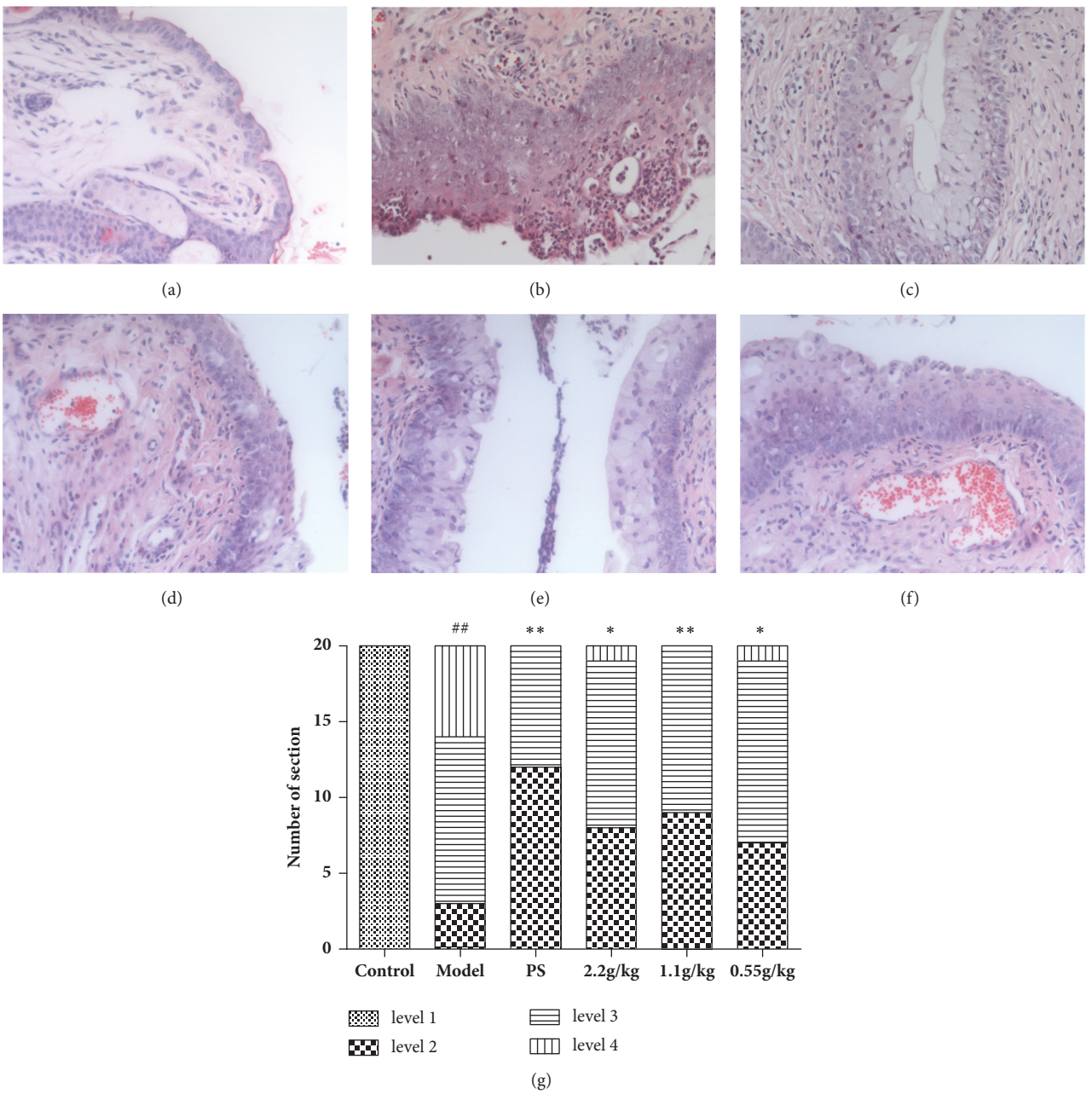

Figure 5: The FVG diminishes the *Chlamydia trachomatis* N-induced vaginitis. (a) Control group, (b) model group, (c) PS group, (d) FVG (2.2 g/kg) group, (e) FVG (1.1 g/kg) group, (f) FVG (0.55 g/kg) group, and (g) statistical analysis of histological examination. n=20, statistically significant $^{\#\#}p<0.01$: compared with control; $^{**}p < 0.01$ and $^{*}p < 0.05$: compared with model, determined by the Mann-Whitney U test.

N, the bacterial load of *C. trachomatis* N in cervical mucus was continuously raised over time. The *C. trachomatis* N infection could lead to the upregulation of cytokines in serum and the inflammation in the tissues of vagina and cervix. After infection with the mixture of *E. coli* and *S. aureus*, the injury of cervix could be detected in pathologic diagnosis.

Clinically, antibiotics were the first choice to treat cervicitis according to different pathogens. But the emergence of antibiotic-resistant such as the quinolone-resistant *C. trachomatis* and *N. gonorrhea*, methicillin-resistant *S. aureus*, and vancomycin-resistant *E. coli* becomes a serious problem worldwide due to the abuse of antibiotics [4, 5, 9]. The TCM may contribute alternative strategies for the treatment of cervicitis. The effects of FVG on cervicitis were tested in this research.

FVG is a vaginal gel, the gel base of which is the mixture of carbopol 941 and xanthan gum [12]. In recent years, many commercial vaginal gel preparations of Chinese herbal formula have been used to treat the cervicitis [21]. The vaginal drug delivery is a traditional mucosal drug delivery route, which can be used for the treatment of both local and systemic diseases [22]. Traditional preparations, such as

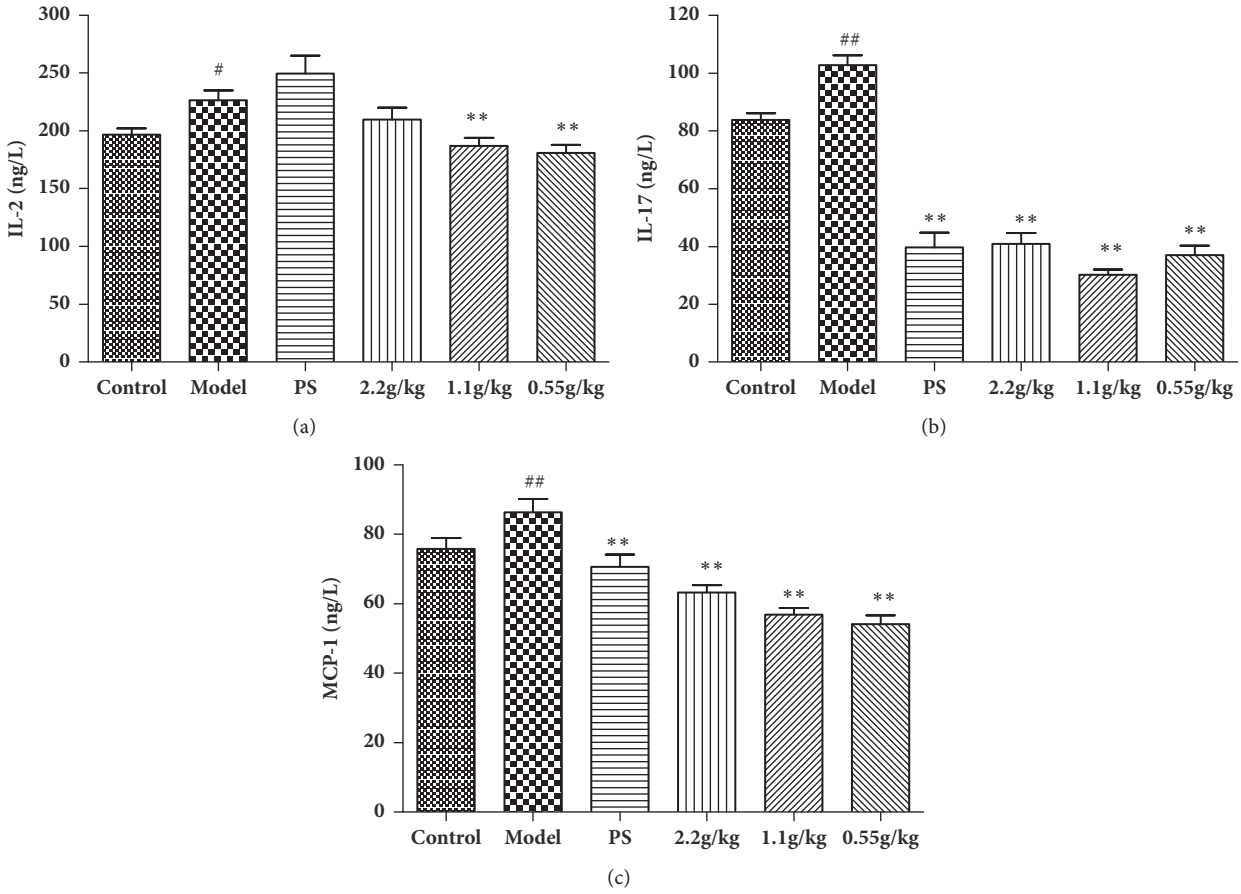

FIGURE 6: The FVG reduces the serum cytokine responses of *Chlamydia trachomatis* N infection. The levels of IL-2 (a), IL-17 (b), and MCP-1 (c) were measured by ELISA assay. The results are mean±SEM, n=10, statistically significant $^{\#\#}p<0.01$: compared with control; $^{**}p < 0.01$ and $^{*}p < 0.05$: compared with model, determined by the unpaired t-test.

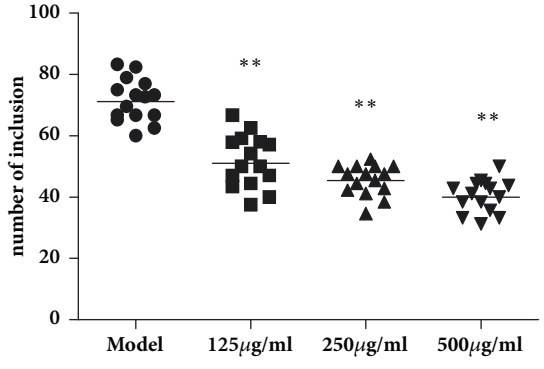

FIGURE 7: The FVG reduces the *Chlamydia trachomatis* N-induced inclusion count *in vitro*. The number of inclusion was enumerated after being stained by Giemsa. n=15, statistically significant $^{**}p < 0.01$: compared with model, determined by the Mann-Whitney U test.

suppositories, gels, tablets, vaginal films, irrigations, and pessaries can be used as vaginal formulations [22, 23]. As one of the most widely used drug delivery systems, vaginal gels have been used for the preparation of microbicides, contraceptives, labor inducers, and sex hormones. Comparing with other drug delivery systems, the vaginal gel is safer and has higher bioavailability [24].

All the six herbal medicines in FVG can be used in treating gynecological diseases in TCM [11]. According to the theory of TCM, in this formula, the Gentianae radix et rhizome is the "monarch drug" or "principal drug", the Stemonae radix and Fraxini cortex are the "ministerial drug" or "assistant drug", the Paeoniae radix rubra and Dictamni cortex are the "adjuvant drug", and the Glycyrrhizae radix et rhizome is the "guiding drug". The Gentianae radix et rhizome may contribute the most to the effects of FVG. Iridoids and total glucosides of peony are mainly isolated from Gentianae radix et rhizoma and Paeoniae radix rubra, respectively. These compounds show significant anti-inflammatory effects [25, 26]. Alkaloids and limonoids contribute to the antibacterial activity of Dictamni cortex [27]. The coumarins in Fraxini cortex and the flavones in Glycyrrhizae radix et rhizome show antibacterial and anti-inflammation effects [28, 29]. The alkaloids contribute to the insecticidal activity of Stemonae radix [30]. These bioactive compounds of these herbal medicines may support the treatment of FVG on cervicitis.

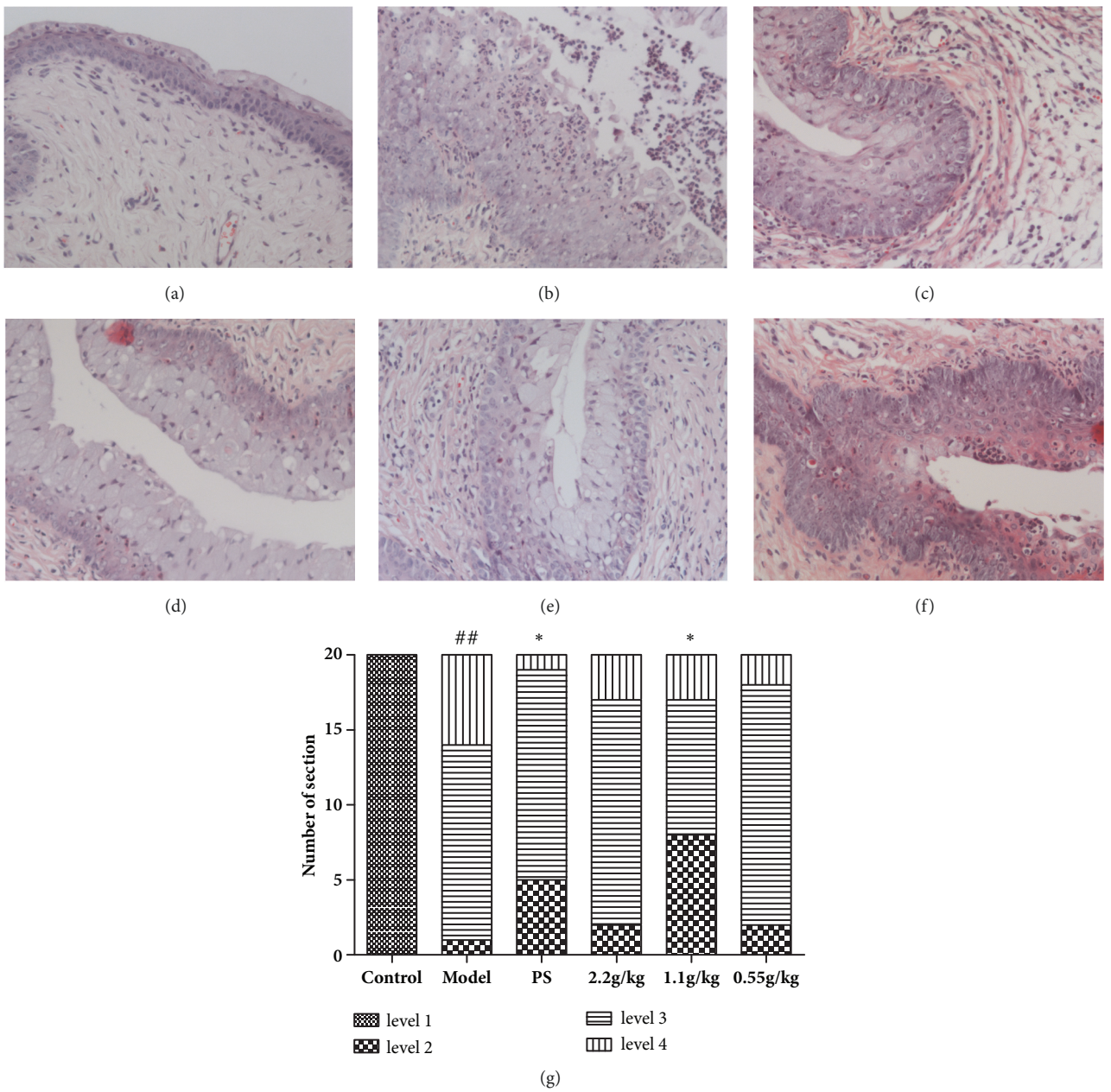

Figure 8: The FVG reduce the pathological injury of cervix induced by *Escherichia coli* and *Staphylococcus aureus*. (a) Control group, (b) model group, (c) PS group, (d) FVG (2.2 g/kg) group, (e) FVG (1.1 g/kg) group, (f) FVG (0.55 g/kg) group, and (g) statistical analysis of histological examination. n=20, statistically significant $^{\#\#}p<0.01$: compared with control; $^{**}p < 0.01$ and $^{*}p < 0.05$: compared with model, determined by the Mann-Whitney U test.

IL-17 is produced by Th17 cells characteristically. Clinically, the concentration of IL-17 in genital secretions of *C. trachomatis* infected patients is significantly higher than that of uninfected women [31]. The high level of IL-17 in the mouse cervicitis model was in agreement with the clinical result. The levels of IL-2 and MCP-1 are associated with the responses of Th1. IL-2 is secreted from Th1 cells and stimulates the production of cytokines. There is an inverse correlation between the level of MCP-1 and the Th1 responses. The inhibition of the MCP-1 can increase the production of IFN-γ [32, 33]. The FVG could downregulate the concentrations of IL-2, IL-17, and MCP-1. These results suggested that FVG could inhibit the cervicitis through the regulation of host immune responses.

Early in the *C. trachomatis* cycle of infection, type III secretion system enables the EBs to invade the host cells [34]. The internalization of *C. trachomatis* is followed by the development of RBs and inclusions. The inhibitor of type III secretion system could block the formation of inclusions [35]. The *in vitro* investigation demonstrated

that FVG could inhibit the number of inclusion in HeLa cells.

In conclusion, we successfully established two mouse cervicitis models with the infection of *C. trachomatis* N, *S. aureus*, and *E. coli*. We proved that FVG could significantly inhibit the cervicitis. FVG could downregulate the bacterial load, mitigate the pathological injury, and reduce the number of inclusion. The effects of FVG were associated with the inhibition of pathogens and the regulation of host immune responses. This research provides evidence that FVG could be used as a novel alternative agent that alleviates the problem of antibiotic-resistant during the treatment of cervicitis.

Data Availability

The data used to support the findings of this study are included within the article.

Conflicts of Interest

The authors do not have any conflicts of interest related to this work.

Authors' Contributions

Xin Mao and Ronghua Zhao contributed equally to this work.

Acknowledgments

This study was supported by the National Natural Science Foundation of China (nos. 81773977 and 81774204).

References

[1] J. M. Marrazzo, "Mucopurulent cervicitis: No longer ignored, but still misunderstood," *Infectious Disease Clinics of North America*, vol. 19, no. 2, pp. 333–349, 2005.

[2] J. Paavonen and V. V. Valtonen, "Chlamydia trachomatis as a possible cause of peritonitis and perihepatitis in a young woman," *The British Journal of Venereal Diseases*, vol. 56, no. 5, pp. 341–343, 1980.

[3] R. C. Brunham, J. Paavonen, C. E. Stevens et al., "Mucopurulent Cervicitis — The Ignored Counterpart in Women of Urethritis in Men," *The New England Journal of Medicine*, vol. 113, no. 1, pp. 1–6, 1985.

[4] L. M. Josephine and K. Pam, "Cervicitis: a review," *Current Opinion in Infectious Diseases*, vol. 21, pp. 149–155, 2008.

[5] A. M. Burnett, C. P. Anderson, and M. D. Zwank, "Laboratory-confirmed gonorrhea and/or chlamydia rates in clinically diagnosed pelvic inflammatory disease and cervicitis," *The American Journal of Emergency Medicine*, vol. 30, no. 7, pp. 1114–1117, 2012.

[6] Y. M. AbdelRahman and R. J. Belland, "The chlamydial developmental cycle," *FEMS Microbiology Reviews*, vol. 29, no. 5, pp. 949–959, 2005.

[7] W. M. Geisler, S. Y. Lensing, C. G. Press, and E. W. Hook, "Spontaneous resolution of genital chlamydia trachomatis infection in women and protection from reinfection," *The Journal of Infectious Diseases*, vol. 207, no. 12, pp. 1850–1856, 2013.

[8] A. J. Carey and K. W. Beagley, "Chlamydia trachomatis, a Hidden Epidemic: Effects on Female Reproduction and Options for Treatment," *American Journal of Reproductive Immunology*, vol. 63, no. 6, pp. 576–586, 2010.

[9] K. Manavi, "A review on infection with Chlamydia trachomatis," *Best Practice & Research Clinical Obstetrics & Gynaecology*, vol. 20, no. 6, pp. 941–951, 2006.

[10] R. C. Brunham, B. Pourbohloul, S. Mak, R. White, and M. L. Rekart, "The unexpected impact of a Chlamydia trachomatis infection control program on susceptibility to reinfection," *The Journal of Infectious Diseases*, vol. 192, no. 10, pp. 1836–1844, 2005.

[11] J. Zhou and F. Qu, "Treating gynaecological disorders with traditional Chinese medicine: a review," *African Journal of Traditional, Complementary and Alternative Medicines*, vol. 6, no. 4, pp. 494–517, 2009.

[12] P. D. Yang, *Study on Preparation and Quality Control for Feilin gel*, Guangdong Pharmaceutical University, 2015.

[13] E. Honey, C. Augood, A. Templeton et al., "Cost effectiveness of screening for Chlamydia trachomatis: A review of published studies," *Sexually Transmitted Infections*, vol. 78, no. 6, pp. 406–412, 2002.

[14] S. Vasilevsky, G. Greub, D. Nardelli-Haefliger, and D. Baud, "Genital *Chlamydia trachomatis*: understanding the roles of innate and adaptive immunity in vaccine research," *Clinical Microbiology Reviews*, vol. 27, no. 2, pp. 346–370, 2014.

[15] R. C. Brunham and J. Rey-Ladino, "Immunology of Chlamydia infection: implications for a *Chlamydia trachomatis* vaccine," *Nature Reviews Immunology*, vol. 5, no. 2, pp. 149–161, 2005.

[16] S. Saini, N. Gupta, A. Aparna et al., "Role of anaerobes in acute pelvic inflammatory disease," *Indian Journal of Medical Microbiology*, vol. 21, no. 3, pp. 189–192, 2003.

[17] S. Guo, Y. Gao, L. Bao et al., "Pharmacodynamics of Zijin Huadu Suppository in Treatment of Cervicitis," *Chinese Journal of Experimental Traditional Medical Formulae*, vol. 22, no. 5, pp. 115–122, 2016.

[18] D. L. Patton, Y. T. Cosgrove Sweeney, and W. E. Stamm, "Significant reduction in inflammatory response in the macaque model of chlamydial pelvic inflammatory disease with azithromycin treatment," *The Journal of Infectious Diseases*, vol. 192, no. 1, pp. 129–135, 2005.

[19] C. Mannari, S. Santi, M. Migliori et al., "Sucralfate modulates uPAR and EGFR expression in an experimental rat model of cervicitis," *International Journal of Immunopathology and Pharmacology*, vol. 21, no. 3, pp. 651–658, 2008.

[20] M. Tuffrey and D. Taylor-Robinson, "Progesterone as a key factor in the development of a mouse model for genital-tract infection with Chlamydia trachomatis," *FEMS Microbiology Letters*, vol. 12, no. 2, pp. 111–115, 1981.

[21] J. Liu, C. Zhai, and L. Chu, "Application Progress of Chinese Medicine Gel in Cervicitis," *Acta Chinese Medicine and Pharmacology*, vol. 39, no. 5, pp. 88–99, 2011.

[22] F. Acartürk, "Mucoadhesive vaginal drug delivery systems," *Recent Patents on Drug Delivery and Formulation*, vol. 3, no. 3, pp. 193–205, 2009.

[23] A. Hussain and F. Ahsan, "The vagina as a route for systemic drug delivery," *Journal of Controlled Release*, vol. 103, no. 2, pp. 301–313, 2005.

[24] J. das Neves and M. F. Bahia, "Gels as vaginal drug delivery systems," *International Journal of Pharmaceutics*, vol. 318, no. 1, pp. 1–14, 2006.

[25] L.-P. Dong, L.-H. Ni, Z.-L. Zhao, and J.-R. Wu, "Research progress on iridoids in Gentiana L.," *Chinese Traditional and Herbal Drugs*, vol. 48, no. 10, pp. 2116–2128, 2017.

[26] D.-Y. He and S.-M. Dai, "Anti-Inflammatory and Immunomodulatory Effects of Paeonia Lactiflora Pall., a Traditional Chinese Herbal Medicine," *Frontiers in Pharmacology*, vol. 2, no. 2, 2011.

[27] M. Lv, X. Ping, T. Yuan et al., "Medicinal uses, phytochemistry and pharmacology of the genus Dictamnus, (Rutaceae)," *Journal of Ethnopharmacology*, vol. 171, pp. 247–263, 2015.

[28] A.-Z. Nie, Z.-J. Lin, and B. Zhang, "Advance in studies on chemical constituents of Fraxini Cortex and their pharmacological effects," *Chinese Traditional and Herbal Drugs*, vol. 47, no. 18, pp. 3332–3341, 2016.

[29] H. Hosseinzadeh and M. Nassiri-Asl, "Pharmacological Effects of Glycyrrhiza spp. and Its Bioactive Constituents: Update and Review," *Phytotherapy Research*, vol. 29, no. 12, pp. 1868–1886, 2015.

[30] R. A. Pilli, G. B. Rosso, and M. D. C. F. De Oliveira, "The chemistry of Stemona alkaloids: An update," *Natural Product Reports*, vol. 27, no. 12, pp. 1908–1937, 2010.

[31] L. Masson, A. L. Salkinder, A. J. Olivier et al., "Relationship between female genital tract infections, mucosal interleukin-17 production and local T helper type 17 cells," *The Journal of Immunology*, vol. 146, no. 4, pp. 557–567, 2016.

[32] M. Akdis, A. Aab, C. Altunbulakli et al., "Interleukins (from IL-1 to IL-38), interferons, transforming growth factor β, and TNF-γ: Receptors, functions, and roles in diseases," *The Journal of Allergy and Clinical Immunology*, vol. 138, no. 4, pp. 984–1010, 2016.

[33] T. Darville, J. Andrews C.W., J. D. Sikes, P. L. Fraley, L. Braswell, and R. G. Rank, "Mouse strain-dependent chemokine regulation of the genital tract T helper cell type 1 immune response," *Infection and Immunity*, vol. 69, no. 12, pp. 7419–7424, 2001.

[34] K. A. Fields, D. J. Mead, C. A. Dooley, and T. Hackstadt, "Chlamydia trachomatis type III secretion: Evidence for a functional apparatus during early-cycle development," *Molecular Microbiology*, vol. 48, no. 3, pp. 671–683, 2003.

[35] S. Muschiol, L. Bailey, A. Gylfe et al., "A small-molecule inhibitor of type III secretion inhibits different stages of the infectious cycle of Chlamydia trachomatis," *Proceedings of the National Academy of Sciences of the USA*, vol. 103, no. 39, pp. 14566–14571, 2006.